THE SEPARATION OF MIXTURES OF FATTY ACID DERIVATIVES

BY

CONTINUOUS CHROMATOGRAPHIC REFINING

A Thesis Submitted

by

M. I. Howari, B.Sc., M.Sc.

to the

Faculty of Engineering

University of Aston in Birmingham

for the

Degree of Doctor of Philosophy

Department of Chemical Engineering

University of Aston in Birmingham

February 1980

TO MY PARENTS

AND

FRIENDS

ACKNOWLEDGEMENTS

The Author is indebted to the following:

Professor G. V. Jeffreys and the Department of Chemical Engineering for making available the facilities for research.

Professor P. E. Barker, who supervised the work, for his advice, guidance and encouragement.

Dr. G. Irlam for his advice on both theoretical and practical aspects of the research topic.

Fellow members in the Separation and Purification Research Group, for many invaluable discussions.

Mr. N. Roberts and other members of the departmental technical staff.

Mrs. Helen Turner and Miss N. P. Freeman for their diligence in typing this thesis.

THE SEPARATION OF MIXTURES OF FATTY ACID DERIVATIVES BY CONTINUOUS CHROMATOGRAPHIC REFINING

Mousa Ishaq Howari

A Thesis submitted for the Degree of Doctor of Philosphy 1980

Summary

A review is given of the factors affecting the performance and the scale up of chromatographic columns. The industrial separation of fatty acid derivatives and the application of G.L.C. as a possible separation method for fatty acids are also reviewed.

The design and construction of a sequential continuous chromatographic refiner (SCCR-2) for high temperature (up to 210°C) preparative scale G.L.C. separation is described. Counter-current operation was simulated by sequencing a system of inlet and outlet port functions around twelve fixed, 2.21 cm diameter and 61 cm long stainless steel columns.

The separation capabilities of the SCCR-2 unit have been investigated using mixtures of different fatty acid esters. The feed mixtures selected had separation factors in the range of 1.44-2.8 and required equipment operation in the range of 105-210°C, while using OV-275 (a cynosilicone liquid phase) on Chromosorb P, as chromatographic packing material.

Fatty acid derivatives; ethyl caprylate/ethyl caprate (separation factor (S.F.) 1.9, 105°C), ethyl caprate/ethyl laurate (S.F. 1.44, 160°C), ethyl laurate/methyl myristate (S.F. 1.54, 185°C) and methyl myristate/methyl stearate (S.F. 2.8, 206°C) were separated on the SCCR-2 unit. Purities of greater than 99% have been achieved for both product streams at feed rates of up to 80 $cm^3 h^{-1}$ and at an operating temperature of 105°C. Lower throughputs; 50, 25 and 20 $cm^3 H^{-1}$ at operating temperatures 160, 185 and 205°C respectively were used to retain the purity in excess of 98.0% for both products.

The experimental results of the separation of binary mixtures at different temperatures have been compared with the results of a plate model computation procedure. Results achieved from the theoretical study indicated partial agreement with the experimental findings.

Keywords

CHROMATOGRAPHY, CONTINUOUS, COUNTER-CURRENT, FATTY ACID ESTERS

TEMPERATURE

CONTENTS

LIST OF FIGURES

LIST OF TABLES

CHAPTER 1

INTRODUCTION

INTRODUCTION

Work presented in this thesis is part of an extensive research project in gas liquid, liquid/liquid and gel permeation chromatography. This programme was initiated by Professor P.E. Barker early in the sixties(1-18) and was continued in the Chemical Engineering Department at the University of Aston in Birmingham. The programme has been substantially sponsored by a series of grants from different sectors of industry.

A general and brief description of chromatographic methods may be summarized as follows. Chromatography is traditionally a batch wise separation technique, in which a given sample (solute) is distributed between a static solvent phase, normally of large surface area, and a mobile carrier phase according to a particular partition coefficient ratio. However, the separation of various solutes is achieved by differences in the partition coefficient for each solute between the two phases just mentioned. Although chromatographic methods have only been effectively used as a scientific tool for about 35 years, chromatography has become firmly established in all branches of science as a highly versatile means of obtaining anlytical identification of chemical compounds and mixtures. Of the various chromotographic methods, gas chromatography has become the most popular anlytical technique and is probably the most important single analytical tool in existence at this time (19). Elution gas/liquid chromatography is currently the most

useful method of gas chromatographic analysis.

A natural outgrowth of the impressive success of analytical gas chromatography is the desire to develop practical methods for the isolation of pure materials on a large scale. It has been estimated that preparative gas chromatography may be economically competitive with conventional processing techniques such as distillation, vacuum distillation, extraction, and crystallization for certain high purity, heat sensitive materials (20). Gas chromatography has several important advantages that makes it an interesting possibility for high purity separations.

- A high separation factor is available because the normal relative volatility differences between solutes are present and a highly selective partitioning phase may normally be chosen for a given separation.

- The short residence times in gas liquid chromotography compared to other mass transfer processes is a vital factor in processing heat sensitive materials.

- It is possible to collect a large number of high purity fractions or to isolate a trace component in a mixture.

However, there are certain disadvantages in using gas chromatography which limit its use to the types of separation where a great deal of difficulty is experienced by other separation process currently being used such as distillation and extraction.

- Solute and solvent concentrations within the column are quite low compared to other more conventional separation processes. The solute primarily moves through the column as a "low density" gas phase which is further diluted by an inert carrier gas fluid.

- Current column packing materials are costly and require replacement and reconditioning very frequently.

If proper equipment design and operation is achieved, gas chromatography may be expected to be competitive with conventional separation processes in certain purification problems in the chemical, food, fragrance and flavours, petrochemical, and pharmaceutical industries. Gas chromatography is not expected to replace conventional separation processes, where favourable solutes with relative volatilities and vapour pressures exist and where heat sensitive substances are not a particular problem.

Efficient preparative scale sample purification by gas chromatography can only be performed when the factors affecting the sample production rate are thoroughly understood. The difficulty of preparing large diameter columns without loss of efficiency is still of fundamental importance today, and several approaches have been attempted to overcome this problem. Golay (21) attributed the decrease in efficiency of large diameter columns to radial velocity fluctuations. Preparative work is dependent on achieving efficient sample separation under quite different (much higher) conditions of

solute concentrations. These higher concentrations cause changes in the separation factor and solute distribution coefficients. Also, the higher concentrations along with large diameters of preparative columns, cause heats of adsorption and desorption, and heat transfer rates to become important. When sizeable temperature changes and gradients occur, separation factors (SF) and distribution coefficients will be greatly influenced (21).

Abcor Ltd. (22) have developed a production scale G.L.C. process using large diameter columns (30-120 cm). Dupont Co. have reported a unit capable of separating a wide range of substances at high purity (23). Others have reported a success by smaller units (24,25).

Various schemes have been attempted to improve the column utilization and therefore the feed throughput of a production scale G.L.C. process. Of the many schemes that have been developed, the "repetitive injection" batch operated process, and the "continuous counter-current" schemes have attained the most success. In counter current schemes the mobile phase fluid (carrier gas), and stationary phase fluid are moved counter currently, whilst a continuous feed mixture is introduced at some point in the separating section. The feed components with the least affinity for the stationary phase fluid travel preferentially with the mobile fluid, whilst the more strongly adsorped components move in the opposite direction with the stationary phase.

Consequently, continuous product off take is possible. Since the early 1960's Barker and co-workers actively developed these processes (1-18, 26-34). Many of the units now being operated by Barker and co-workers for both gas liquid and gel permeation chromatographic separations are based on a concept developed by Barker and Deeble (12). This scheme is based upon counter-current movement which is simulated by sequencing a system of inlet and outlet port functions around a closed loop of columns. The first unit of this type was called the 'Sequential Continuous Chromatographic Refiner', SCCR-1. Its viability has been demonstrated by the continuous separation of 1.1.2-trifluoro-1.2.2-trichloroethane (Arklone-P) and 1.1.1-trichloroethane (Genklene) which was achieved at equivolume feed rates at up to 1400 cm^3 hr^{-1}. However, the use of the SCCR-1 unit to separate non-volatile materials was limited by the lack of any heating facilities and the air used as a carrier gas. The second unit SCCR-2, based on the same principle, was developed to work at temperatures of up to 210° C, and was the equipment used in this research. The SCCR-2 machine is made up of 12 stainless steel columns, each 61 cm long and 2.54 cm in diameter. The promising results of S. Liodakis (16) for separating organic mixtures such as methyl chloroacetate/ethyl lactate (separation factor (SF) 1.5, 105° C) using SCCR-2 equipment led to an attempt to perform a higher temperature separation in the range of 100-206° C. The work reported in this thesis was

initiated with the aim of achieving that goal using mixtures of industrial importance, such as fatty acid derivatives, with moderate to high boiling points. Besides the experimental programme a mathematical simulation was also to be part of this research programme.

CHAPTER 2

LITERATURE SURVEY

2.1 SCOPE

Following the work of James and Martin in 1952 (35) chromatography has developed into an accepted analytical and preparative technique. Although a large portion of the published work has been mainly devoted to analytical techniques, it is necessary to be restrictive in the summary of relevant literature. Hence, after the introduction of the basic terminology, whose origins inevitably lie in the analytical field, this survey will be concerned with the development of theoretical models of the column chromographic process.

Scale-up of the chromatographic process is next reviewed in two sections: batch chromatography, and continuous chromatography.

Finally, a review of fatty acid separations in industry and the future of gas chromatography, as an alternative technique will be discussed.

2.2 BASIC TERMINOLOGY

The following has been included to provide a basic understanding of the subject area. Further details may be found in several general texts (36,37).

2.2.1 The Basic Process

The principle of gas liquid partition chromatography (GLC) is that an inert carrier gas is passed through a column which is packed with solid support on which a liquid

stationary phase is impregnated. The mixture of solutes to be separated is usually introduced with the carrier as it enters the column as in the case of GLC analysis units and in conventional static bed preparative scale chromatographic units. It is the difference in the selective retardation of the compounds to be separated by the stationary liquid phase as they move in the column under column conditions that causes their bands to travel at different rates. Consequently they will be separated and are eluted in the order of least retarded first. Fig. 2.1 shows a typical elution curve for two fully resolved components 1 and 2.

The ordinate represents detector response and the abscissa represents either time or volume. The first sharp peak is obtained for unabsorbed gas, while the second and third peaks have undergone the chromatographic process.

Also t_m = "elution" or "retention time" for an unabsorbed component, which is a measure of the gas hold-up in the column (dead volume of column).

t_R = "elution" or "retention time" for a component.

$t'_R = t_R - t_m$ "adjusted retention time", which measures the effect of the chromatographic process of a component.

FIG. 2.1 ELUTION DIAGRAM

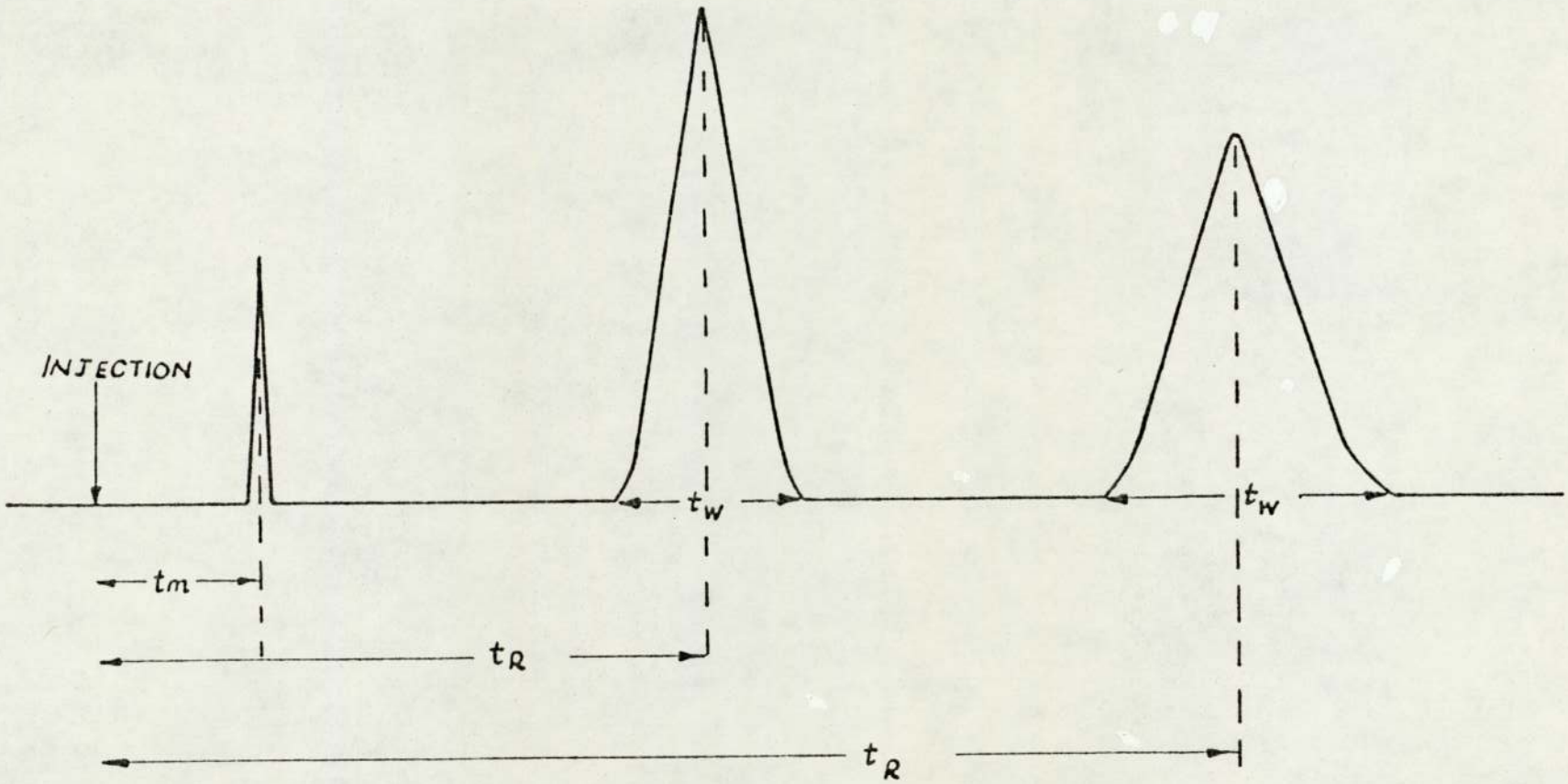

The "distribution" or "partiition coefficient", K, is defined as the equilibrium ratio of the solute concentration in the liquid solvent to the concentration in the gas phase and is a measure of the affinity of a solute for a solvent.

The ratio of "partition coefficient" of component 2, to that of component 1 defines the "separation factor", SF, of solutes 1 and 2.

Thus, $$SF = \frac{K_2}{K_1} \qquad (2.1)$$

and since the larger value of K is placed in the numerator, as the "separation factor", SF, approaches unity, the separation becomes more difficult.

Further definitions, relationships and theoretical aspects of the basic elution G.L.C. chromatographic theory, as well as for the other types of chromatography can be found in general texts (37,38).

In general, separation in elution chromatography is achieved through differences in migration rates of solutes, governed by thermodynamic equilibrium. However, the effectiveness of a separation is also dependent on the degree of overlap of the solute zones, which is governed by column dynamics. It is obviously desirable to keep the solute zones narrow to reduce or eliminate overlap.

Solute zone broadening theories involve factors that contribute to zone spreading and therefore are briefly reviewed in the following sections.

2.3 THEORY OF ZONE SPREADING

2.3.1 The Plate Model

The theoretical plate model was introduced into chromatography by Martin and Synge (39) because of its effectiveness in describing distillation processes. Their early work was later expanded by Mayer and Tompkins (40) and Glueckauf (41).

It is necessary to make a number of simplifying assumptions when the plate model is used, which may be listed as follows:

(1) the solute exchange process is thermodynamically reversible such that instantaneous equilibrium is achieved.

(2) the partition coefficient is constant throughout the column and independent of concentration; i.e. linear chromatography.

(3) longitudinal diffusion may be neglected.

(4) mobile flow is discontinuous. The flow is usually achieved by stepwise additions of volumes of mobile phase equal to the mobile phase volume per plate.

By reducing the plate volume to an infinitesimal value, Glueckauf (41) obtained a continuous model. The elution curve exhibited a Poisson distribution which approximated to a Gaussian distribution for greater than 100 plates. The standard deviation (σ) of the Gaussian distribution (a direct measure of zone spreading is given by:

$$\sigma = \sqrt{HL_M} \qquad (2.2)$$

where H is the height equivalent to a theoretical plate (HETP) and L_M is the distance migrated. Equation 2.2 shows that H varies directly with σ^2, and an important statistical property of σ^2 is that independent contributions to it are additive,

i.e. $$H = \frac{\sum\sigma^2}{L_M} \qquad (2.3)$$

Thus contributions to the plate height may be determined independently and summed to give an overall H value.

Although plate height is an empirical quantity, and plate theory does not deal with the mechanisms which determine it, such as partition phenomena, molecular diffusion and flow patterns through packed beds, it has considerable value in the comparison of the efficiency of chromatographic columns, and has gained almost universal acceptance in this area. In practice, H is used to describe the summation of all the contributions to peak dispersion (σ^2), which are generally caused by; finite mass transfer rates, longitudinal molecular diffusion and eddy diffusion caused by the heterogeneous nature of the packing (42).

The following section will deal with the various rate theories advanced to evaluate these effects.

2.3.2 Zone Broadening Rate Theories

2.3.2.1 Van Deemter Theory

Much theoretical work has been carried out to express the behaviour of a chromatographic column in terms of H.E.T.P. Lapidus and Amundson (43) were the first to introduce mass transfer and diffusion terms into a model, and their theory was developed by Van Deemter, Zuiderweg and Klinkenberg (44) who derived the following expression, relating the column parameters to the H.E.T.P.

$$H = 2.\lambda d_p + \frac{2\gamma' D_m}{u} + \frac{8}{\pi^2} \frac{K' d_f^2}{(1+K')^2 D_s} u \qquad (2.4)$$

λ = packing characterization factor for eddy diffusion such that eddy diffusivity, E, = $\lambda.u.d_p$

d_p = mean particle diameter

γ' = labyrinth factor to allow for toruous flow path

D_m = mobile phase molecular diffusivity

D_s = stationary phase molevular diffusivity

d_f = thickness of stationary phase liquid film

u = interstitial gas phase velocity

K' = $F_m/K.F_s$ = mass distribution coefficient

F_m = fractional volume of mobile phase

F_s = fractional volume of stationary phase

K = partition coefficient

The equation may be written in shortened form:

$$H = A + B/u + C_s u \qquad (2.5)$$

A, B, and C_s are the eddy diffusion, axial diffusion, and mass transfer resistance terms respectively, stationary phase mass transfer being assumed the controlling factor. Van Deemter (44) introduced a further term (C_m) to allow for resistance to mass transfer in the mobile phase. Equation 2.4 has been applied extensively to the field of gas chromatography and was responsible for the significant improvements obtained in column performance therein. It is shown graphically in Fig. 2.2 that at low gas velocities the axial diffusion term is significant and therefore high molecular weight carrier gases are desirable to minimize H. At higher gas velocities the dependence of H on $(\frac{B}{u})$ disappears and the mass transfer resistance terms become controlling.

2.3.2.2 Random Walk

The original Van Deemeter equation has been extended and modified by many workers (45-49). Considerable work has been carried out by Giddings on the mechanisms of zone broadening, details of which are given in his well known text (36). Using the individual molecular processes occurring in a chromatographic column he developed a "random walk" model (49). The basic concept of this model is that the solute molecules, although moving randomly have an equal chance of moving forward or backward. It is convenient to define an average (root mean square) step length ($\bar{\ell}$), although actual molecular displacements differ widely in length. This random molecular movement results in a statistical spread of the molecules in the form of a Gaussian curve. The variance

FIG. 2.2 GRAPHICAL REPRESENTATION OF THE VAN DEEMTER EQUATION

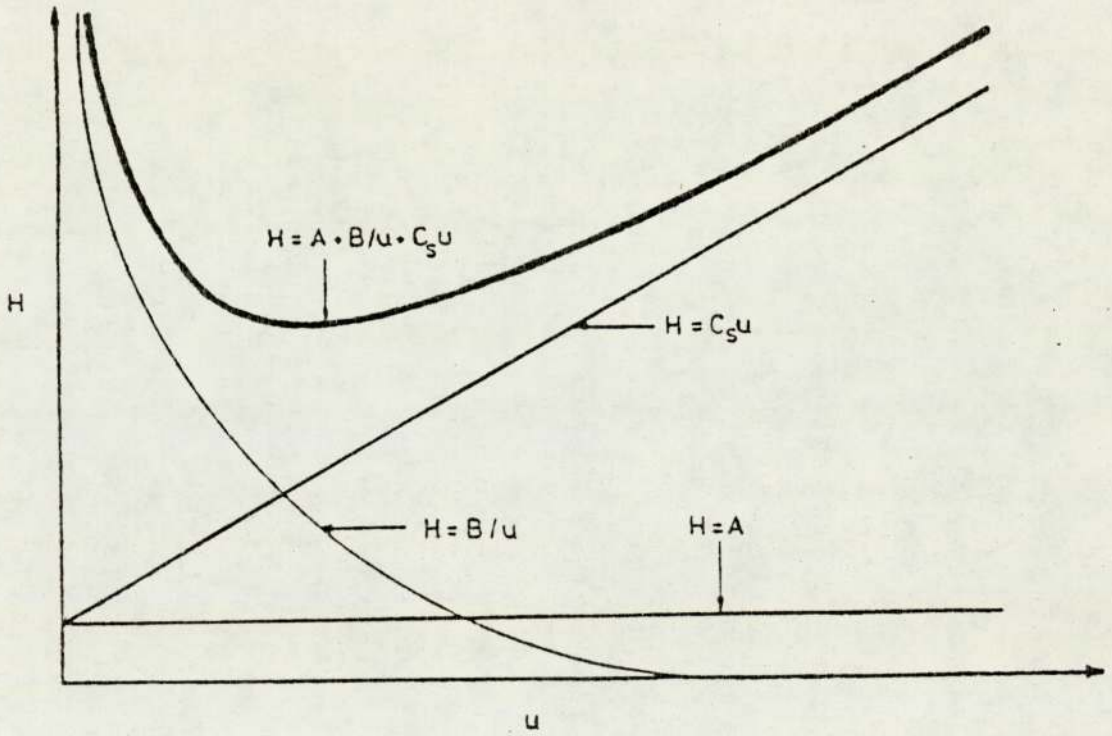

σ^2, is equal to ℓ' n', where n' is the number of steps taken. Each process occurring in the column has its own value of ℓ' and n' which may be summed to give a total variance:

$$\sigma^2_{Total} = \sum\sigma^2 = \sum\ell_i^{-2}n_i' = H \qquad (2.6)$$

Giddings (36) evaluates the contribution to plate height from longitudinal mobile phase diffusion as:

$$H = \frac{2\gamma' D_m}{u} \qquad (2.7)$$

By using the same Einsteinian relationship for diffusion (50) the stationary phase diffusion was calculated as

$$H = \frac{2\gamma_s . D_s}{u} \; \frac{(1-R)}{R} \qquad (2.8)$$

γ_s = obstructive factor within solid particles

R = retention ratio

Simple kinetic mechanisms describing the adsorption-desorption process can be formulated as a random walk and Giddings (36) obtained:

$$H = 2R(1-R) \; \frac{d_f^2 . u}{D_s} \qquad (2.9)$$

Diffusion processes occurring in the mobile phase are significantly more complex than those in the stationary phase. This is because of the complex nature of the flow channels, and the velocity inequalities, both transcolumn

and longitudinal occurring in the mobile phase itself. The mechanisms leading to this zone spreading within the mobile phase originate from.

1. Transchannel effects caused by a higher velocity in the centre of a channel than at the wall.

2. Long-range interchannel effects.

3. Transcolumn effects.

4. Transparticle effects caused by the stagnant mobile phase trapped in the porous solid support particles.

5. Short range interchannel effects.

The resulting mobile phase mass transfer term is:

$$H = \frac{W.d_p^{\,2}.u}{D_m} \qquad (2.10)$$

$W = \sum_c W_i$ (five values) $= W_\alpha^{\,2} W_\beta^{\,2}/2$

$W_\alpha =$ (distance between velocity extremes) d_p

$W_\beta =$ (distance between extreme and average velocity) u

The eddy diffusion contribution was determined by using the classical theory of solute molecules being locked in fixed stream paths, again consider the five mechanisms giving:

$$H = 2\lambda_i d_p \qquad (2.11)$$

$$\lambda_i = \sum_i W_\beta^{\,2}.W_\lambda/2 \qquad (2.12)$$

W_λ = structural parameter

Summing all the plate height contributions from the random walk approach we have:

$$H = 2\lambda d_p + \frac{2}{u}\left|\gamma' D_m + \gamma_s D_s \frac{(1-R)}{R}\right| + 2R(1-R)\frac{d_f^{\,2}.u}{D_s} + \frac{W.d_p^{\,2}.u}{D_m} \qquad (2.13)$$

or $$H = A + \frac{B}{u} + C_s u + C_m u \qquad (2.14)$$

This is of the same general form as equation 2.5 except for the inclusion of a mobile phase resistance to mass transfer term ($C_m u$). Giddings (36) has shown that the eddy diffusion and mobile phase mass transfer terms are not independent and therefore their variances not additive. Combining these two contributions in one term leads to the general equation

$$H = \frac{B}{u} + C_s u + \left(\frac{1}{A} + \frac{1}{C_m u}\right)^{-1} \qquad (2.15)$$

The value of the contribution to H of the coupled term is always less than that obtained from either of the component part (see Fig. 2.3).

A major criticism of the random walk model is that it is based on a fixed number of steps for all participating molecules, while in reality, particularly in reference to sorption-desorption kinetics, a variable number of steps are taken. Giddings (36) recognised the limitations of the random walk approach and developed the more powerful

FIG. 2.3 COMPARISON BETWEEN CLASSICAL AND COUPLED EQUATION FOR PLATE HEIGHT

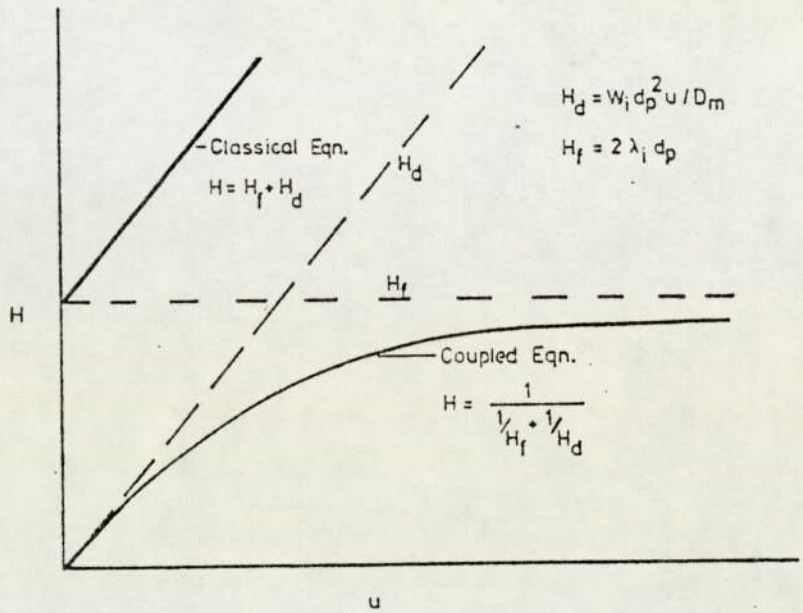

FIG. 2.4 COMPARISON BETWEEN ACTUAL AND EQUILIBRIUM COMPONENT ZONE CONCENTRATION PROFILES FOR NORMAL ELUTION CHROMATOGRAPHY

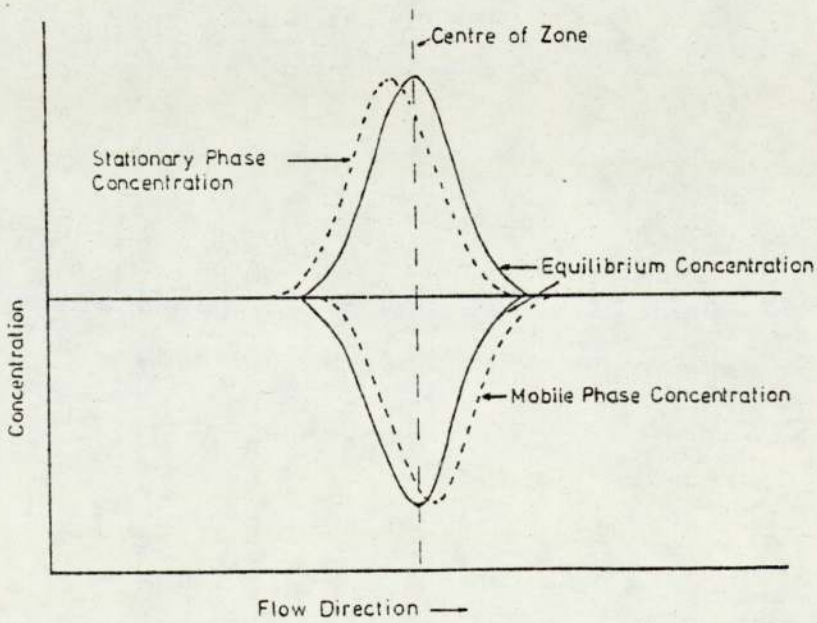

generalized non-equilibrium theory of zone broadening, which, unlike the microscopic random walk theory, considers bulk properties of the chromatographic system.

2.3.2.3 Generalized Non-equilibrium Theory

The non-equilibrium theory is based on the fact that sorption/desorption processes require a finite amount of time to occur. The theory, with a physical representation of non-equilibrium, is illustrated in Fig. 2.4 and shows the stationary phase concentration has a lag in its equilibrium value, whilst the mobile phase concentration will always be ahead of its equilibrium concentration. The degree of non-equilibrium, indicated by the gap between the related curve of Fig. 2.4, is a function of the rate of mass transfer between the phases and can be minimized by having the zone migrating slowly, thus preventing rapid concentration changes.

The generalized non-equilibrium theory is only used to calculate the C terms of equation 2.14 (36), which for practical chromatography, using high mobile phase velocities, are the most significant non-equilibrium contributions. (see Fig. 2.3). The stationary phase contribution may be represented in the following way for most stationary phases:

$$H = q' R\frac{(1-R).d^2.u}{D_s} \qquad (2.16)$$

q' = configuration factor dependent on the shape of the stationary phase layer.

The mobile phase diffusion expression is again a function of the five mechanisms discussed in the random walk theory (section 2.3.2.2) and if several simplifying assumptions are made equation 2.10 is again produced. However, the advantage of the non-equilibrium model lies in its ability to include various geometries, so a balance has to be made between the assumptions made and complexity of mathematics thereby involved. The final relationship for H derived from non-equilibrium theory becomes:

$$H = \frac{2\gamma'.D_m}{u} + q'R(1-R)\frac{d_f^{\,2}.u}{D_s} + \left|\frac{1}{2\lambda d_p} + \frac{D_m}{W.d_p^{\,2}.u}\right|^{-1} \quad (2.17)$$

The models outlined in the preceding text have provided a firm theoretical background for the molecular processes occurring in chromatographic columns.

Additional contributions to the plate height encountered in large diameter columns are reviewed briefly in the following section.

2.4 LARGE SCALE CHROMATOGRAPHY

In the previous sections, theories of chromatography have been reviewed. However, most of the theories are derived for analytical columns. Their applications in separations at the laboratory preparative or production scale level, are only possible if factors governing scale

up can be identified and accounted for. Hence, included in the following sections, is a survey of such factors. As studies on continuous chromatographic processes are extremely limited, findings for batch chromatographic processes are employed as a practical guide line to highlight the most important factors on scale-up.

2.4.1 Factors Affecting Scale-up

2.4.1.1 Flow Dynamics in Packed Columns

The random walk approach of Gidding (36) outlined in Section 2.2.3.2 indicates five mechanisms by which velocity inequalities may occur in packed columns. Of these the transcolumn term is of particular importance for production chromatography when large diameter columns are employed. This is because substantial velocity differences often occur between the central and outer regions of large diameter columns due to effects associated with the column wall. To account for such uneveness in flow velocity, an extra term H_c, is incorporated into the Van Deemter plate height equation 2.14:

$$H = (A + \frac{B}{u} + C_m u + C_s u) + H_c \qquad (2.18)$$

Giddings (51) used his non-equilibrium theory to evaluate a plate height contribution, based on a parabolic velocity profile, and found good agreement with experimental results for 0.6 cm and 5.1 cm diameter columns (52). The

contribution may be expressed as;

$$H_c = G_2 \frac{r_c^2 u}{(96.\gamma'.D_m)} \qquad (2.19)$$

G_2 = constant

Huyten (53) extended the study to columns with 7.5 cm diameter, similar observations being made by Friscone (54). A similar expression to equation 2.18 was obtained by Higgin and Smith (55) and Rijinders (56). In contrast, Hupe (57) and Volkov (58) have observed maximum zone velocities at the centre of their packed columns. This was attributed to the fact that the higher packed density in the central sections of a column leads to faster mass transfer rates. Bayer, Hupe and Mack (59) based their derivation on this observation and obtained an empirical expression for H_c as:

$$H_c = 2.83 \frac{r_c^{0.58}}{u^{1.886}} \qquad (2.20)$$

r_c = column radius

which gave good experimental agreement for columns between 1.3 cm and 10.2 cm diameter. The band spreading caused by the non-uniform velocity profile can be reduced by lateral diffusion. Littlewood (60) and Sie and Rijinders (61) described the lateral diffusion as being composed of molecular diffision (γD_m) and "convective" diffusion ($\alpha' d_p u$) arising from repeated mixing and separation of mobile phase streams. They obtained

$$H_c = \frac{0.5I' d_c^2 u}{\gamma D_m + \alpha' d_p u} \qquad (2.21)$$

α' = constant for packing geometry

I' = complicated double definite integral of the velocity profile gradient (62)

d_c = internal column diameter

All of these expressions, however, predict a fall-off in efficiency with increased diameter, differing only in degree. Pretorius and de Clerk (63) suspected these correlations and maintained that the 'wall effect' and the particle to column diameter ratio are the factors governing the velocity profile. The resultant profile they developed is of a 'w' shape with maximum velocity being experienced several particle diameters into the bed, and the plate height expression was found to be:

$$H_c = \frac{M' d_c^{\,2} u}{2 d_r . d_p} \qquad (2.22)$$

d_r = radial diffusion coefficient

where

$$M = \left(\frac{1}{100}\right) \exp\left(-\frac{d_c}{10 d_p}\right) \qquad (2.23)$$

This indicates that the plate height increases with d_c at constant $\frac{d_p}{d_c}$, reaches a maximum at $\frac{d_p}{d_c} = 0.5$, and then decreases with increasing d_c. The results of Spencer and Kucharski (64) and Knox (65) give support to the above hypothesis. This effect could be due to the fact that if the column diameter is so large that radial equilibrium is not achieved, the plate height becomes independent of diameter (51, 52). This 'infinite diameter' effect was

discussed by Knox and Parcher (66), who considered that adverse wall effects could be overcome by choosing a column of sufficient diameter that the sample was eluted before the solute had time to diffuse to the wall. The authors also suggest a technique whereby only the central portion of the eluted solute band is removed.

To summarise, the effect of column diameter on operating efficiency is still a debatable subject. However, the majority of opinion indicates a loss of efficiency when columns are scaled to the production level.

2.4.1.2 Temperature Effect

One of the accepted requirements for efficient analytical chromatographic operation, is a uniformly heated column. The same requirements have been assumed to be necessary for preparative or large scale chromatographic columns. This cannot be true in practice, because of the combined effects of the heat of solution of the larger samples and the finite rate of heat transfer across large diameter columns. The variation in temperatures of columns of diameter 2.5 cm and 50 cm. have been demonstrated by many workers (31, 57, 67-70). They conclude that the excess heat generation increases with increasing flowrate, sample size and decreasing partition coefficient values. The first two factors are believed to be of paramount importance in preparative and production chromatography. The results of Rose et al (68) indicated that heat transfer properties

could be of primary importance in the design of preparative and production columns.

The solute zone migration velocity was established to be dependent upon the local column temperature (51) which subsequently introduced a further plate height term (H_t) to allow for thermal fluctuations across the columns:

$$H_t = \alpha_t.(\Delta T) \frac{r_c^2.u^2}{900.D_m} \qquad (2.24)$$

αt = constant of value 0.004

ΔT = Temperature difference between the centre and wall.

2.4.1.3 Finite Concentration Effects

Feed concentration and band width are closely linked variables, and an increase in either leads to a marked reduction of the column efficiency in terms of the number of theoretical plates (70,71). Thus, in analytical chromatography the sample size is so small that the chromatographic process is conducted essentially at infinite dilution. In contrast, the large sample sizes used in preparative or production scale chromatography create finite solute concentrations in the column which in turn change the shape of the eluted peak and separation process, requiring a major change of the basic chromatographic theories discussed in section 2.3 (72).

Basically at finite solute concentration, chromatographic behaviour is affected by three major effects: the absorption isotherm, the sorption and enthalpic overloading effects.

2.4.1.3.1 Absorption Isotherm

This effect assumes that, if the partition coefficient is a function of solute concentration, i.e. non-linear isotherm, then the elution volume is given by (73)

$$V_R = V_M + V_S \cdot \left(\frac{\partial q}{\partial c}\right)_c \qquad (2.25)$$

V_R = retention volume of component

V_M = column mobile phase volume

q = solute concentration in stationary phase

c = solute concentration in mobile phase

V_S = column stationary phase volume

It is also assumed for the case of a linear absorption isotherm that the fundamental retention equation for a chromatographic system is:

$$V_R = V_M + KV_S \qquad (2.26)$$

K = equilibrium partition coefficient

Fig. 2.5 shows the effect of the three commonest types of isotherm on the shape of the solute peak. For the Langmuir isotherm, Fig. 2.5(b) the partition coefficient decreases with increasing concentration, resulting in a lower elution volume. The eluted band has a sharpened leading edge and a diffuse trailing edge. In contrast for anti-Langmuir types, Fig. 2.5(c), the partition coefficient increases with increasing concentration, resulting in a

FIG. 2.5 THE RELATIONSHIP BETWEEN THE SOLUTE ZONE BOUNDARY CONCENTRATION PROFILE AND THE TYPE OF PARTITION ISOTHERM

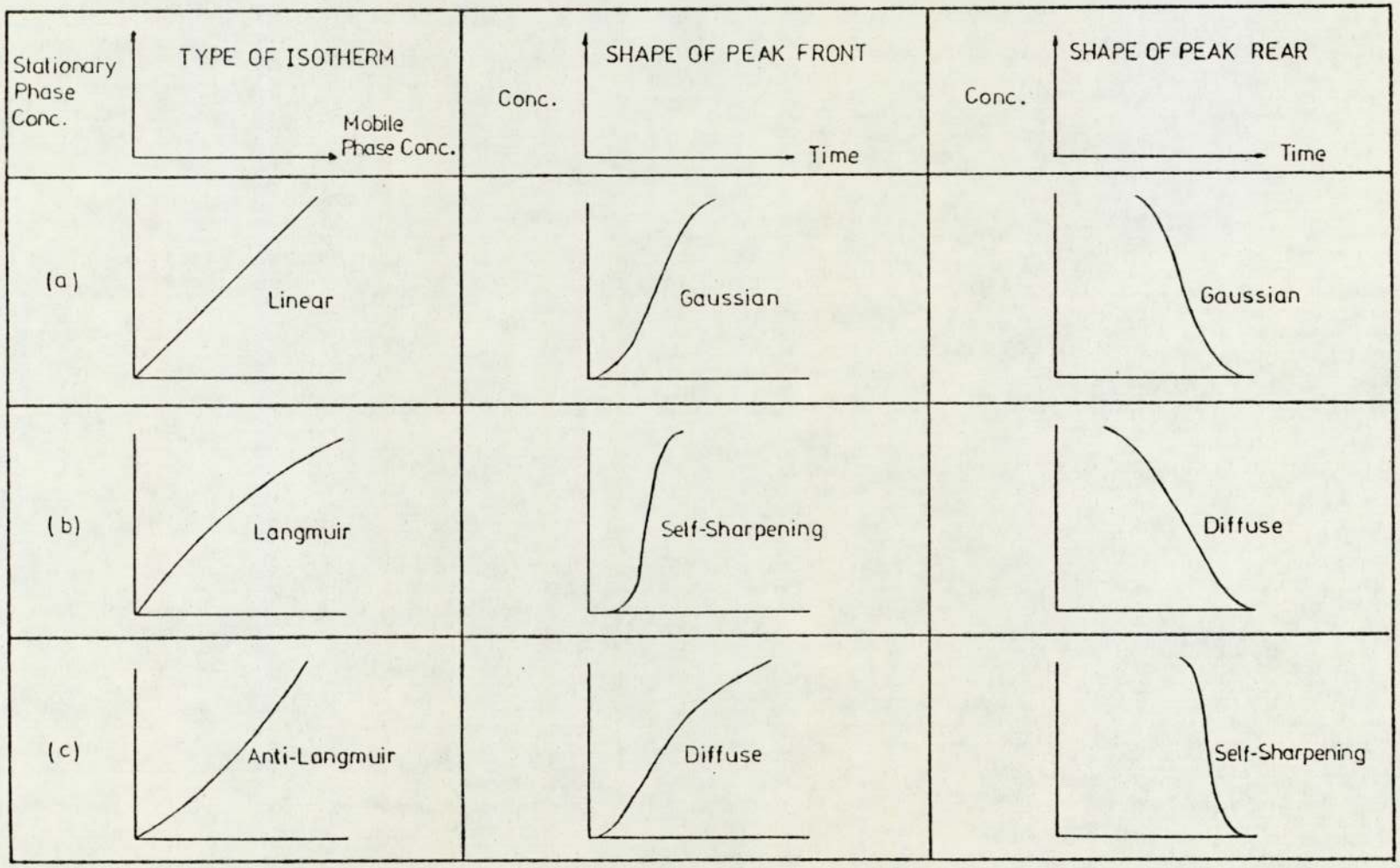

higher elution volume. This produces a diffuse front and sharpened trailing edge. The vast majority of chromatographic systems exhibit non-linear isotherms. Operation in the non-linear region requires an extra column length to compensate for the decrease in resolution. However, the gain in throughput obtained by operating at high solute concentrations in many cases outweights the detrimental effects of the peak skewing.

2.4.1.3.2 Sorption Effect

The influence of the variation in gas velocity with the shape of the chromatogram was described by Bosanquet (74,75). This results from the movement of molecules into or out of the gas phase as the solute boundary progresses. Conder and Purnell (76,77) modified equation 2.24 to include the sorption effect as follows

$$V_R = V_M + V_S\ (1-jY_o)\left(\frac{\partial q}{\partial c}\right)_c \qquad (2.27)$$

j = James and Martin gas phase compressibility factor where Y_o equals the mole fraction of the solute in the gas phase as measured at the column outlet. As the concentration increases the mobile phase flow increases giving a reduced retention volume. This effect tends to give a sharp forward front and diffuse tail to the elution peak as the solute zones of high concentration move faster than those at a lower level. The resultant effect of high concentration on band broadening is therefore dependent on whether the effects of the absorption isotherm and of sorption are naturally supporting or opposed. If opposed, a 'stationary

front' can be formed, the bandwidth becoming independent of column length (78).

2.4.1.3.3 Enthalpic Overloading

At finite solute concentrations, the heats of absorption and desorption of the solute in the stationary phase become significant, and general local temperature variations occur throughout the column due to the inability of the column to rapidly attain thermal equilibrium. These local temperature variations are particularly marked in large diameter columns because of the inherent low thermal conductivity of most packings and result in different isotherm characteristics between the column wall and interior regions (57,67). The resultant eluted peak will be distorted and broadened. This effect which was named by Higgins and Smith (55) as the 'enthalpic overloading effect'.

2.5 PRACTICAL SOLUTIONS TO THE SCALE-UP PROBLEM

2.5.1 Methods of Packing

The low efficiencies in large diameter columns are very often the result of a poor method of packing. Hence, many workers have sought to achieve a packing technique giving both high and reproducible column efficiencies. Dry packing is the conventional method in gas chromatography, and although disagreement exists concerning the best method such as 'mountain packing', fluidization, 'bulk packing', typical values of H.E.T.P. between 1 and 3 mm have been obtained (53-59).

To summarise, a gain in efficiency with careful packing of chromatographic columns is possible, but opinions differ on the best packing technique to use. More comprehensive reviews about packing methods may be found in the literature (64).

2.5.2 Use of Multiple Columns

Utilizing several columns in parallel has the obvious advantage of allowing each individual column to be of narrow bore, while the total quantity of solvent phase remains substantial. Thus, the previously discussed large scale column effects are avoided without reduction in capacity. However, the method of multiple columns has not gained wide acceptance because of the difficult and tedious effort involved in balancing the array of parallel columns. Difficulty is also experienced in even distribution of sample and gas flow through the inlet manifold. Hence, parallel columns have not found wide acceptance (64).

2.5.3 Repeated Feed Injections

In analytical elution chromatography, a small sample of feed is injected and eluted subsequently. As the solute bands only occupy a small part of the available column packing at any one time, column utilization is poor and unacceptable for preparation and production purposes.

To maximise column utilization, a repetitive method of sample feeding has been commonly employed. The batch samples are injected at as frequent time intervals as the total on-column width of the preceding sample permits without extensive overlap. In practice a limit must be made to the rate of injection if excessive overlap of successive samples is to be avoided, and considerable work has been carried out in this area. Two different approaches have been developed based on repetitive injection. The first where the eluted profiles are completely resolved and successive injections do not overlap, and second technique in which the solute bands are allowed to overlap and the central impure portion is 'cut out' and recycled (63). Gordon (79-81), indicated that significant gain in throughput may be obtained by the latest 'cut out' method when high purity products are required. Conder in his review (82) has reported that it is always preferable to overlap the component bands rather than to avoid the need for cutting by increasing column length and resolution, and that an optimum recovery value exists at 60% of the injected sample The remaining contaminated 40% is recyled. (83).

2.6 RECENT WORK ON PREPARATIVE AND PRODUCTION SCALE BATCH CHROMATOGRAPHY

Ryan (84) reported a design study for a gas chromatography plant capable of separating 50 million Kg/Yr, of a p-xylene/m-xylene mixture with 99% pure products. The

design was based on two 1.4 ft diameter, 14ft long columns operating with alternate feed injection and on a packing that had a separation factor of 1.3 for the isomers. With the aid of flow distributors within the column, Cavel et al (85) were able to successfully scale-up throughput in direct proportion to cross sectional area when increasing diameter from 1 to 30 cm. For the 30 cm diameter, a single injection of 1475 cm of a hydrocarbon mixture ($n-C_6, C_7, C_8$) was fully resolved. The column length was 2.44 m. ELF French petroleum company has reported the installation of ten batch units in Europe and the United States each with a capacity of 200 Tons/year (86,87).

2.7 CONTINUOUS CHROMATOGRAPHY

2.7.1 Introduction

The word continuous is used here to refer to the process of feed introduction and products withdrawal continuously. However, the main advantage in choosing a continuous operation over a batch type scheme is that it allows the utilization of the whole chromatographic column for the separation process, Fig. 2.6(a,b). Greater throughputs higher purities and lower costs are normally found in continuous mass transfer processes when compared with the equivalent batch processes.

Many workers have sought to design and perfect chromatographic systems capable of operating in a continuous

FIG. 2.6 CHROMATOGRAPHIC CONCENTRATION PROFILES OBTAINED FOR SEPARATION OF TWO COMPONENTS

(a) Repeated Batch Co-current Operation

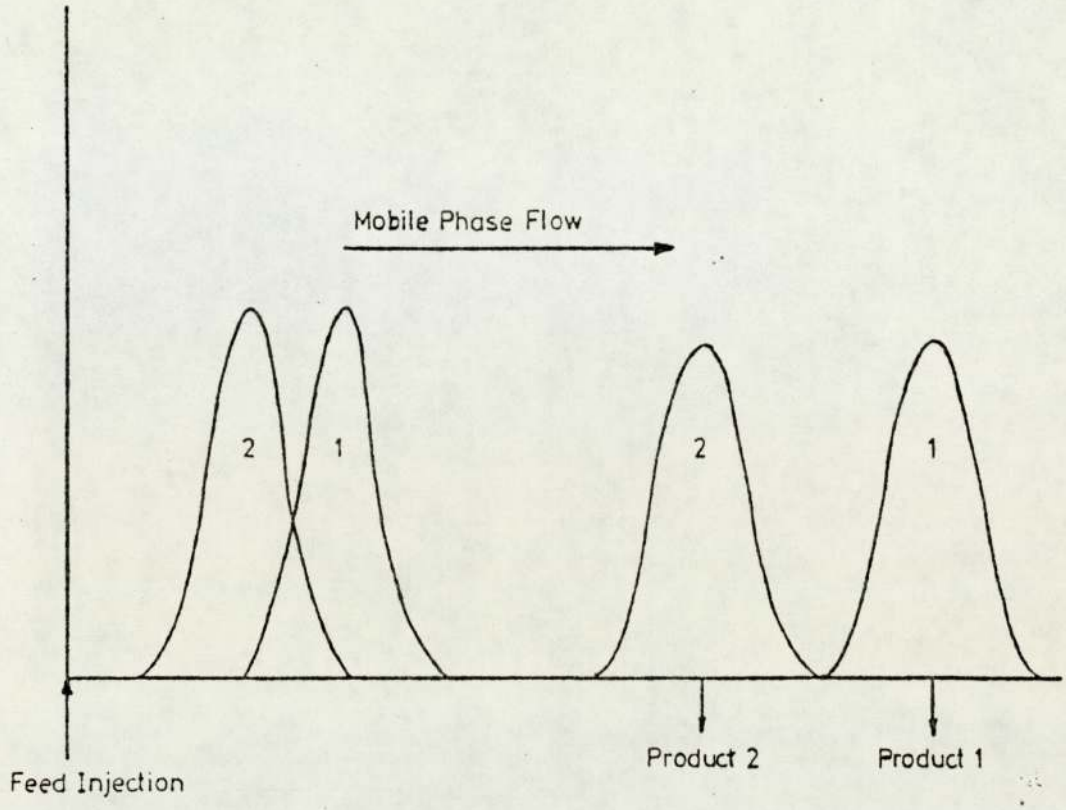

(b) Continuous Counter-current Operation

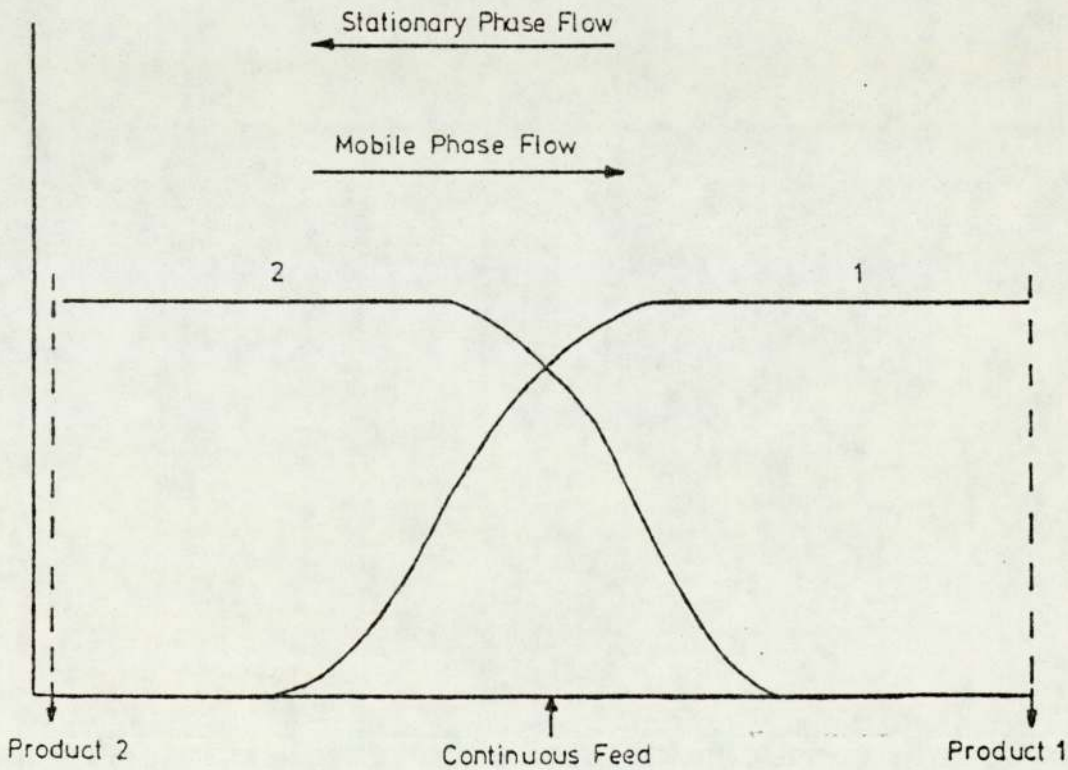

mode. The achievement of a mechanical system based on the principle of counter-current gas/liquid chromatography may be classified into fixed bed, moving bed, and simulated moving bed or pseudo moving bed (Fig.2.7). The following summary will be restricted to the moving bed systems. However, other systems have been covered as in recently pulbished reviews (29,30).

2.7.2 Moving Bed Systems

2.7.2.1 Counter Current Flow

The development of continuous chromatographic processes, based on this principle has taken place in three stages; moving packing, moving column, and pseudo-moving column or simulated moving bed.

2.7.2.1.1 Moving Packing

Counter-current movement in a chromatographic column can be achieved by having the packing move downwards under its own gravity against the mobile phase. A typical apparatus for moving packing was that used by Barker and co-workers (1-4,7,28) (Fig.2.8). A vertical copper column of 2.5 cm diameter was fed with solvent-coated solid support from a hopper (Fig. 2.8a). The solids flowed under gravity and the rate of flow was controlled by a rotating table at the column base. Vibration of the column wall ensured steady flow of packing. The feed mixture was introduced somewhere near the middle of the column. The

FIG. 2.7 CONTINUOUS MODES IN CHROMATOGRAPHY

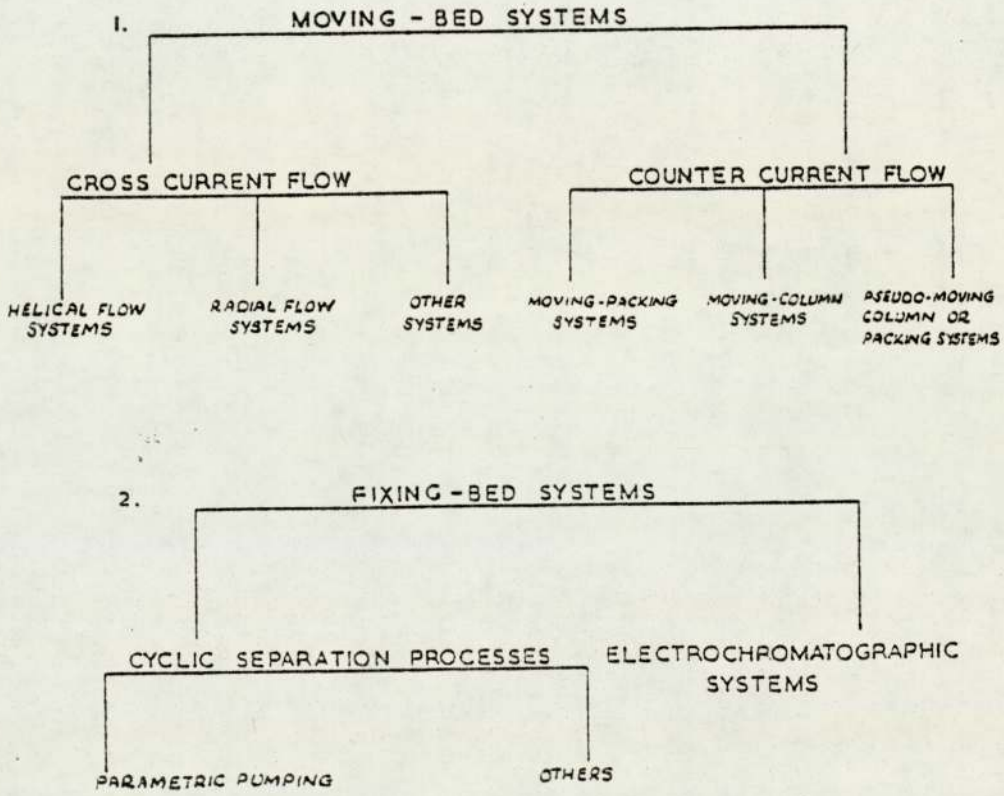

FIG. 2.8 COUNTER-CURRENT FLOW SCHEMES

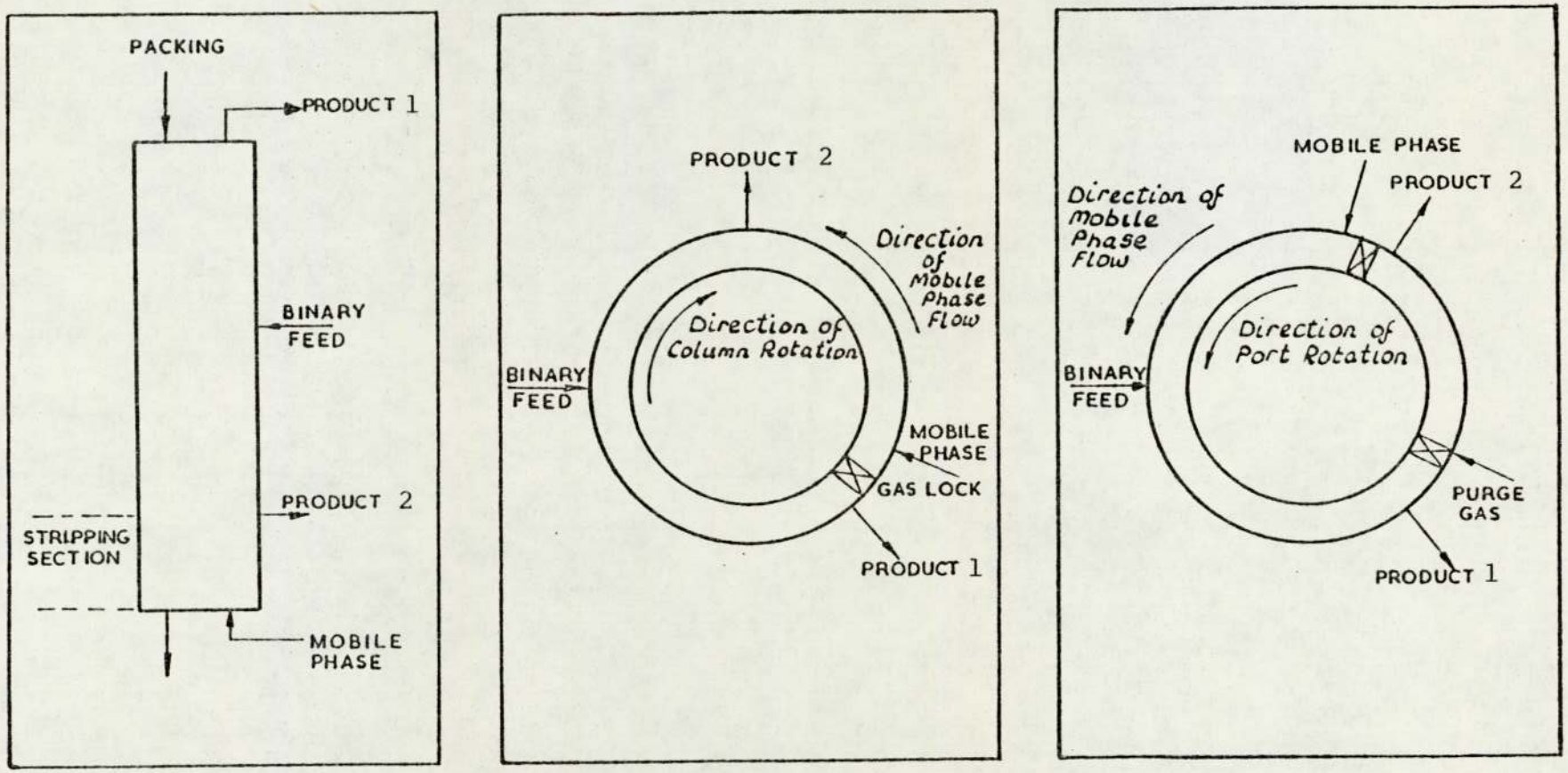

(a) PRINCIPLE OF MOVING-PACKING SYSTEMS

(b) PRINCIPLE OF MOVING-COLUMN SYSTEMS

(c) PRINCIPLE OF THE BARKER AND DEEBLE PROPOSED PSEUDO-MOVING COLUMN SYSTEM (11)

relative flowrates of the phases (packing and the carrier gas) could be adjusted to let the strongly adsorbed feed component travel with the packing into the heated stripping section, to be removed at the product 2 off take. The least strongly adsorbed component was removed at the product 1 port.

Barker and co-workers successfully used this equipment to achieve the separation of several binary mixtures involving benzene, cyclohexane and methylcyclohexane. With air as a carrier gas and operating the separating section at ambient temperature, high separated product purities were obtained at throughputs of up to 30 cm^3 h^{-1}. Various other moving bed schemes have been reported on smaller diameter units (88-93). The Philips Petroleum Co. (94) report the construction of a unit of 15 cm diameter and 2.5 m long for the separation of a 30% cyclohexane and 70% benzene mixture at 225 cm^3 min^{-1}.

An industrial unit has been developed by the Union Oil Co., Los Angeles, California using activated carbon adsorbent, flowing down through a streamof hydrogen gases (95,96). Even packing densities and accurate solid flow control proved difficult to achieve. To overcome such problems, a new approach based on the rotation of a circular column past fixed inlet and outlet ports was developed.

2.7.2.1.2 Moving Column Systems

One of the solutions to the above mentioned problems is to let the mobile phase flow in the opposite direction to the rotation of the columns Fig. 2.9. Three novel mechanical designs were set up by various workers. The schemes differ in the flow direction in the stripping/purging sections and the means of controlling the flow direction generally within the column. In the designs of Pichler (97), Gulf Research and Development Corporation (98), Luft (99), and Glasser (106), the carrier gas flow rates within the column were controlled by pressure drop. Barker (6) removed the restrictions by placing cam-operated locks between the carrier gas inlet port and the product 1 off-take. As the gas flow was unidirectional, the length of the packed column stripping section was kept to a minimum.

A prototype machine was constructed by Barker and Huntington (8-10), and consisted of eight 3.8 cm square cross-section chambers linked through external valves to form a circle of diameter 1.5m. The gas flow in and out of the columns was through 180 gas passages equally spaced over the chamber face, and automatic self-sealing valve controlling each one of these passages. Gas sealing was achieved by means of 'O' rings, set in the torroid face. The 'O' rings were sealed against the face by means of spring loaded plates. The performance and the operating characteristics of this prototype machine appeared in

FIG. 2.9 MOVING COLUMN SCHEMES FOR CONTINUOUS G.L.C.

(a) Scheme of Pichler and Schultz (97)

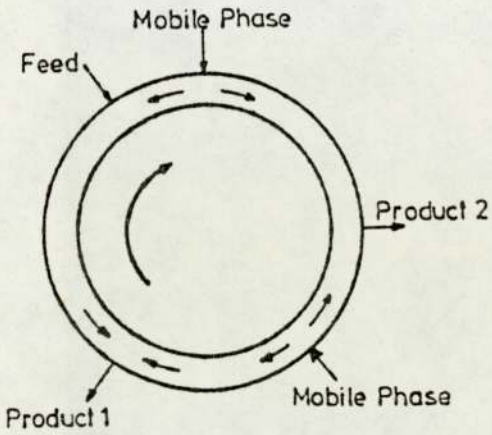

(b) Scheme of Luft (99)

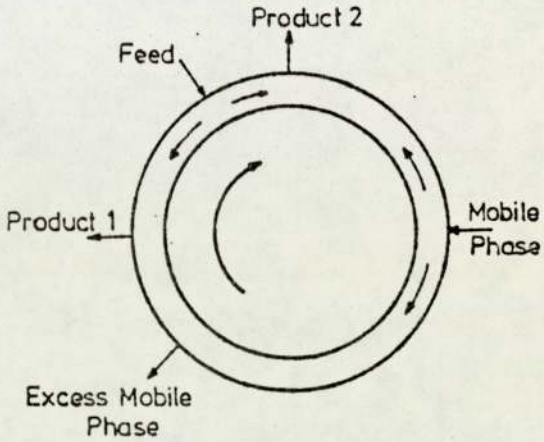

(c) Scheme of Glasser (100)

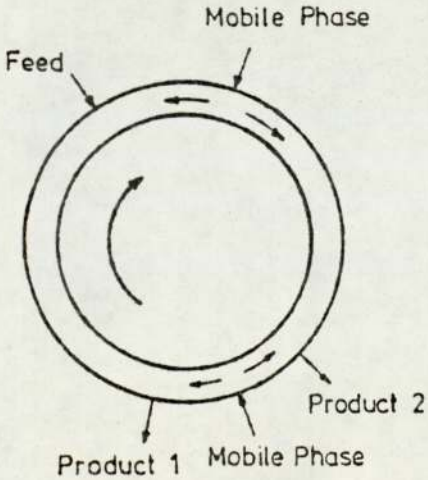

(d) Scheme of Barker (6)

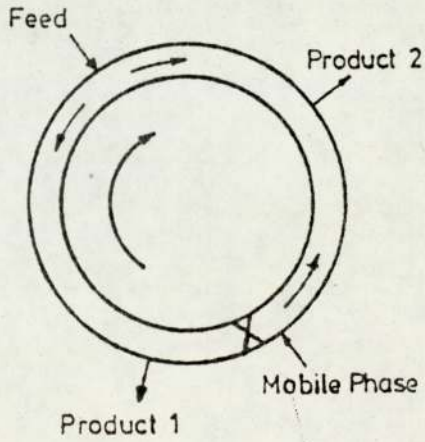

several publications (8-10).

The limited separating power of this prototype machine led Barker, in collaboration with Universal Fisher Group, Ltd., Guilemin (101) to construct a new compact circular chromatograph. The machine consisted of a cylindrical net of 44, 2.5 cm diameter by 22.8 cm long, stainless steel tubes linked alternately at top and bottom to give a closed loop. The tube bundle rotated at speeds between 0.2 and 2.0 r.p.h. The transfer of gas between tubes was controlled by cam operated poppet valves.

Several publications give experimental performance data which showed a marked improvement of the separating power of this machine (26,27,32). One of the main disadvantages of compact circular chromatography is the difficulty of sealing at high temperature.

2.7.2.1.3 Pseudo Moving Bed or Simulated Moving Bed

The problems and the difficulties which have already been outlined in moving bed/fixed port circular chromatographic machines, were dealt with by many workers and research projects. Universal oil producs has developed a pseudo-moving bed, counter flow, continuous chromatographic group of processes that are beginning to find significant industrial application. Generally known as Sorbex (102, 103), individual variants include Molex for recovering n-paraffins from light napthas, Parex used to separate p-xylene from other C_8 hydrocarbons, and Olex which

separates n-olefins from olefin n-paraffin mixtures. The processes use molecular sieve adsorbents and operate in the liquid phase. Several other workers designed various units working on similar principles for different typesof separations (104-106).

Barker et al, have also achieved counter current movement by using a programmed sequencing of selenoid valves (11-14,107), or pneumatic valves (15,16,33). The sequential type of gas chromatography has undergone two stages of development. These are reflected in the SCCR-1 unit (11,14,31) and the SCCR-2 unit (15,16,33), the equipment was used in these research studies. This equipment will be described in more details later. The SCCR-1 machine performance and mode of operation has been described in a series of publications (11-14,31).

Simulated moving-bed units are by no means limited to gas liquid chromatographic separations. Barker et al have reported the design and operation of various types of equipment for liquid solid chromatographic separations. These units in operation include, a unit for continuous fractionation of a dextran polymer by gel-permeation chromatography (18,34,108) and L.S.C. (Liquid Solid Chromatography) for the separations and purification of carbohydrates (109).

2.7.2.2 Cross Current Flow Systems

In cross-current flow systems, the chromatographic bed moves perpendicular to the direction of the mobile phase flow within the bed. This system may be classified into two distinct forms, helical and radial.

2.7.2.2.1 Helical Flow Columns

Martin (110) suggested this type of column and provided a theoretical analysis for its operation, which is based on an annular packed column. The feed enters at the top and the paths travelled by different components are in the form of helices. Denelli (111, 112) converted this concept to a working unit.

Several other working units based on this principle have been reported; for the gel permeation chromatographic separation of dextran (108), and a gas liquid chromatographic application in separating volatile organic compounds (113-115).

2.7.2.2.2 Radial Flow

In this type of column, the feed travels from the centre to the circumference of an annular packing. This scheme was initially proposed by Moiser (116) and developed by Sussman and his co-workers (117,118). By relative rotation of the packing and the feed inlet, the paths taken by different components of the feed will be different, depending on the retention volume of the component, and so

continuous separations can be achieved. In this system either the feed injection and collection system can be rotated and the feed system static, this method being preferred. Sussman et al used this latter scheme for gas liquid chromatographic separation of binary hydrocarbon mixtures at throughputs up to 18.9 cm^3 h^{-1} (117,118).

CHAPTER 3

SEPARATION OF FATTY ACIDS

3.1 INTRODUCTION

A very important application of gas chromatography is the analysis of fatty acids. The best illustration of the importance of this application is the fact that the first paper on Gas Chromatography, by James and Martin (35) dealt with such a problem. One year later, Cropper and Heywood (119) extended the use of gas chromatographic separation to include the methyl esters of the fatty acids. Many researchers followed these pioneers and by 1958 more than fifty papers dealt with the analysis of fatty acids and their esters by gas chromatography. Thus, the background of GLC methods applicable to fatty acids can be found in any of several books on the GLC technique (90, 120-122).

The following treatment will be dealing briefly with the problems arising from the analysis of free fatty acids and their esters, in addition to the industrial separation of these compounds.

3.2 ANALYTICAL SEPARATION OF FATTY ACIDS

3.2.1 The Analysis of Free Fatty Acids and the Problems Arising

Gas liquid chromatography was first applied to unesterified aliphatic fatty acids of 1-12 carbon atoms, using DC-550 silicone fluid as a stationary phase. Difficulties were found in getting a good resolution. The

tailing effect was one of the major problems, and it was solved by adding stearic or phosphoric acid to the liquid phase. Beerthuis et al. (123) eliminated the tailing effect by increasing the column temperature.

During the early times of chromatography, no specific liquid phases such as Silicone or Apiezone grease were used. Thus, the introduction of the polyester liquid phases in 1958 by ORR and Callen (124, 125) were an important step in giving the necessary separation efficiency. However, other phases have been introduced with different physical and chemical properties (126-133), but the problems facing the separation of unesterfied fatty acids remain intact. These problems include; adsorption of the acids in the chromatographic bed, dimerization of the acids in the liquid phase, the relative low volatility of unesterfied fatty acids and the long elution times of the acids. Although, several methods have been proposed to minimize the effect of these problems, such as deactivation of the support material by acid washing, injecting a low concentration of formic acid in the carrier gas, or the addition of a non-volatile acid into the liquid phase, but the major problems have still not been solved (134-137).

Separation of free fatty acids has been limited by the high boiling points of the acids and by many other unsolved difficulties some of which are mentioned above.

These problems have resulted in poor peak shapes, and are more pronounced when it comes to high molecular weight fatty acids. Generally the solution put forward has been to convert the fatty acids to their methyl or ethyl esters. This allows the elution at lower temperatures, as the boiling points of the esters are usually (20-30°C) less than those of the free acids (138).

3.2.2 G.L.C. of Fatty Acid Esters

While the separation of free fatty acids was achieved in the early works of James and Martin (139, 140), probably the earliest report relevant to the usual practice of separation of methyl esters was that of Cropper and Heywood (141,142). James and Martin (143) soon showed a reasonable separation of the C_1-C_{18} saturated esters of related iso and anteiso acids, and of some unsaturated esters on Apiezon grease.

Many reports soon followed, and with the introduction of polar stationary phases, the separation of various isomers was achieved (124, 132, 144-146). However, polyesters are the principal phases for use with fatty acid esters, and EGS, DEGS and BDS, probably find greatest use (133). While a wide range of modified polyesters are offered by different manufacturers, the polar siloxanes phases have found some use, and at the present time this would seem to be the principal area of development, especially

where isomer separation is involved.

The cyanoethyl polysiloxanes were used by Litchfield et al. (147) for the partial separation of the C_{18} isomers. Scholfield and Dutton (148) using the same phase also reported the separation of fatty acid esters. A range of organosilicone polymers liquid phases were reported by Supina (149) under different trade names, with a variety of physical and chemical properties.

In 1974, the most polar Cynoalkyl Siloxane (OV-275) appeared, and is reported to be stable up to 275°C (133). This material is variously suggested to be a di-β-Cyanoethyl polysiloxane or a co-polymer with γ-Cyanopropyle groups. No information was available either in the literature or direct from the dealers and the manufacturer.

Ottenstein et al. (150), who extensively studied the separation of methyl elaidate/methyl oleate esters have shown that OV-275 is superior to other liquid phases in terms of resolution. This phase was used to pack the columns in the SCCR-2.

3.3 INDUSTRIAL SEPARATION OF FATTY ACIDS

Methods of separating and isolating fatty acids are extremely important, for many of the key industries, such as food, pharmaceutical, paints, paper, etc.

The following summary will be devoted to the common methods of separation such as distillation, crystallization and the future of chromatographic methods for fatty acid separations.

3.3.1 Distillation

One of the most important processes in making Commercial fatty acids is by distillation. A fatty acid mixture of known composition and acids of high purity could be made in this way (151).

The most widely used distillation procedure in this field, is the fractional distillation of methyl esters under reduced pressure. Even under these conditions high temperatures are required $\approx 200^{o}C$ causing many fatty acids to under go polymerization, cylization and other intra and inter molecular reactions (151). Unsaturated fatty acid esters are the most susceptible, since they contain highly reactive double bonds (152-154). An extensive review of the industrial separation and processing of fatty acid esters was published by Muckerheide (153).

3.3.2 Crystallization

Solvent processes such as liquid-liquid extraction have been used without success in the fatty acid industry, since the mutual solubility of mixed fatty acids in solvents usually results in an inefficient separation (155).

In contrast, crystallization is considered as a classical procedure for the separation of fatty acids, particularly for the acids having very close boiling points (acids with the same chain length and different degree of unsaturation).

Several procedures have been applied to the specific problems in fatty acids separation such as, crystallization of lead salts, crystallization of lithium salts and low temperature crystallization (152, 154-156). However, the latter method is the most popular in the fatty acids industry.

The efficiency of fatty acid separation by crystallization methods is subject to three limiting factors, namely:

- the separation is not always so complete
- dissolved acids act as excellent solvents for those which crystallize, cooled solutions come to equilibrium very slowly and must be held at the crystallizing temperature for several hours.
- complete separation of mother liquor from crystals is incomplete even after thorough washing with cold solvent.

However, fatty acids can be separated by several other methods of very limited application to the industry

such as counter-current distribution (153, 157) and urea fractionation (158).

3.4 THE FUTURE OF CHROMATOGRAPHIC METHODS FOR LARGE SCALE FATTY ACIDS SEPARATION

The most important advances in separation procedures are concerned with chromatographic methods. Gas liquid, and liquid-liquid chromatography are the main interest of development since their introduction by James and Martin. These interests vary from the analytical laboratory scale, to the production scale.

There have been many attempts to extend the analytical potential of gas chromatography to the production scale by many workers. Rose et al. (159, 160) have reported the use of a batch G.L.C. unit for the separation of fatty acid esters at production rates of up to 100 cm^3h^{-1}. Another batch unit to separate saturated from unsaturated fatty acid esters was reported by Scholfield (161).

On the industrial scale ELF Co. (French Petroleum Company) as previously mentioned (section 2.6) has reported the installation of ten batch units in Europe and the United States for the separation of essential oils and fatty acids, with a capacity of 200 Tons/year (86, 87).

Recently, Szepsey et al. (105) reported a continuous preparative unit for the separation of higher boiling

saturated and unsaturated fatty acid esters (C_{16}-C_{22}) at a feed rate of 5 cm^3h^{-1}.

Fatty acid separation has been studied on a continuous G.L.C. system by Barker et al., and some results have already been published (15, 16, 33), while more recent results are recorded in this thesis from Chapter 7 onwards.

A direct comparison between the conventional purification methods and chromatography is difficult at the moment through lack of economic and technical data. The chromatographic techniques show promise, however, in the separation of fine chemicals, especially those that do not lend themselves to conventional purification methods.

CHAPTER 4

THE DESIGN AND OPERATION OF THE SEQUENTIAL CONTINUOUS CHROMATOGRAPHIC SEPARATOR SCCR-2

4.1 PRINCIPLE OF OPERATION

Fig. 4.1a shows the distribution of a binary mixture within the system soon after start up. The carrier fluid enters the column and flows through the solvent coated packing. The least strongly sorbed, component 1 is preferentially moved towards the product 1 off take, P1. A discrete section of closed loop is isolated by locks B1 and B2, these locks advancing concurrently with the carrier gas (Fig. 4.1b). The rate of port-advancement is less than the velocity of the less strongly sorbed component through the packing, but greater than that of the more strongly sorbed component 2. Consequently component 2 is being held preferentially on the solvent coated packing while component 1 is continually removed with the carrier fluid from P1. A separate gas supply is required to desorb the slower moving species, component 2 and thereby regenerate the section of stationary phase packing between locks B1 and B2 issuing from P2.

Fig. 4.1c shows the fully established operating condition where the locks B1 and B2 now containing component 2 is being purged to give product 2 and regenerate the packing ready to receive the advancing component 1, at present issuing from P1. It can be seen that the position of the feed is advanced by the same distance around the loop so that it is still diametrically opposite the isolated loop.

FIG. 4.1 ILLUSTRATION OF THE OPERATING PRINCIPLE OF THE SCCR-2 UNIT

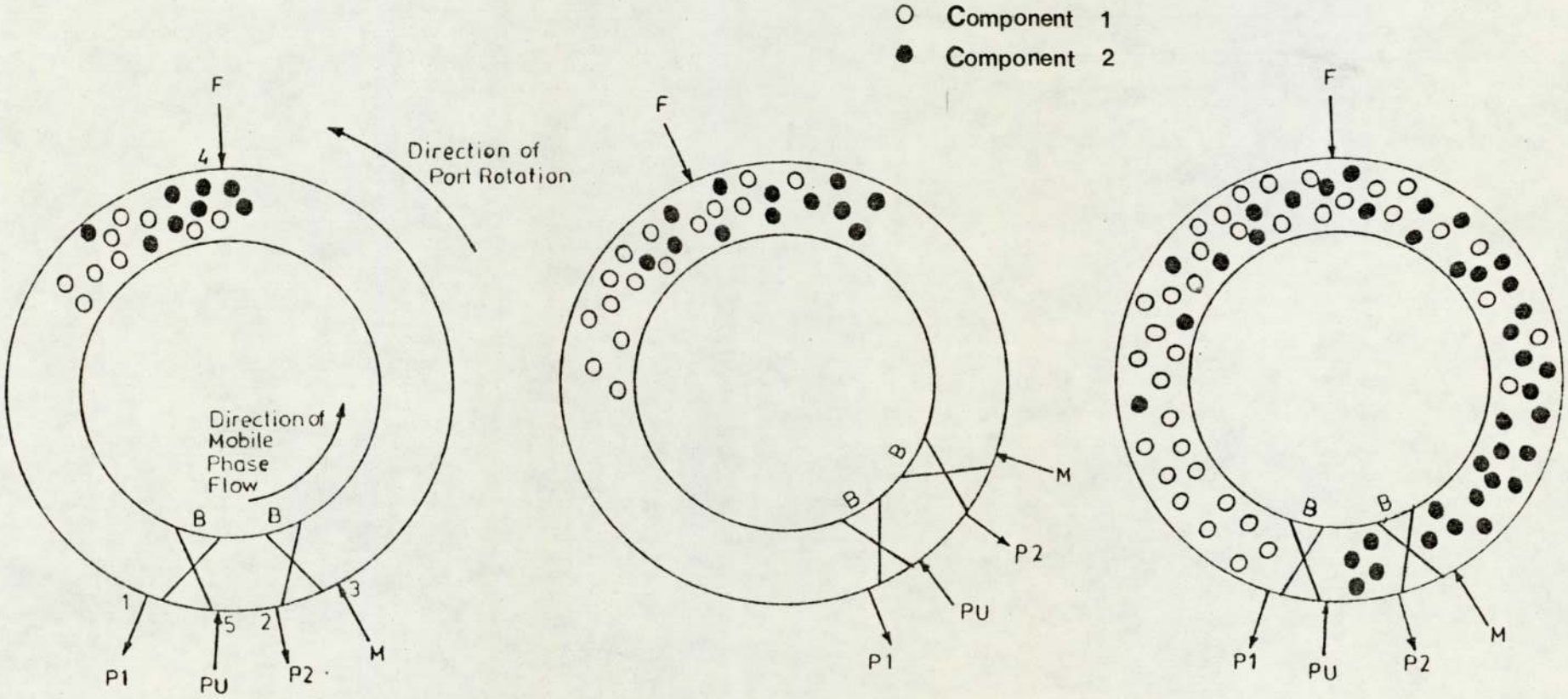

F Feed M Mobile Phase P1 Product 1 P2 Product 2 PU Purge B Transfer Valve Lock

4.2 DESIGN AND CONSTRUCTION

The development of the Sequential Continuous Chromatographic Refiner (SCCR), has been well documented in previous publications (1-18, 26-31). The SCCR-2 machine used in this research was built to overcome the temperature/corrosion limitations in the SCCR-1 machine used by Deeble (13) and Bell (31). The SCCR-2 equipment was initially used by Liodakis (16) to separate a mixture of relatively volatile fatty acid esters.

The SCCR-2 equipment consists of twelve stainless steel columns (61 cm in length, 2.54 cm O.D) packed with 15% OV-275 (a Cyno Silicon liquid phase), coated on 40/60 mesh chromosorb P-AW-DMCS as a support. The columns are housed in an oven operating up to 220°C. A control box controls the opening and closing of the stainless steel and PTFE air operated diagram poppet valves at preset time intervals.

A full design specification of the chromatograph has been given by Liodakis (16). The following brief description is a precise of the above specifications highlighting the major characteristics of the Sequential Continuous Chromatographic Refiner.

4.2.1 The Column

The SCCR-2 has twelve stainless steel columns of

2.54 cm O.D, 2.21 cm internal diameter and 61 cm long. The columns were evenly spaced on a pitch circle diameter of 75 cm. This provides a distance between column centres of 19.8 cm. Two stainless steel end flanges were silver soldered to the outer wall of each tube. A support for the packing inside the column was provided by a fine stainless steel gauze, of 76 mm (200 B.S Mesh) aperture size, silver soldered on both ends of the flanges of the tubes. A PTFE gasket was fitted between the end flange of the tube and the end fittings to prevent gas leakage. Fig. 4.2 shows the end fittings made from stainless steel which were designed to reduce the internal dead volume. A "¼ in B.S.P." parallel male stud stainless steel coupling was silver soldered into the centre of the top of the end fittings to receive the 0.64 cm O.D line from the appropriate transfer valve. To permit connection within the respective inlet/outlet gas diaphragm valves, two stainless steel tubes 2.8 cm long and 0.64 cm O.D, were silver soldered into the cylindrical surface of the end fitting. Midway along the columns a "⅛ in B.S.P." male stud stainless steel coupling was silver soldered to accommodate the feed diaphragm valve, via a 0.32 cm O.D stainless steel tube as close as possible to the column. A capillary tube was mounted inside the 0.32 cm O.D tube in order to reduce the feed hold up in the line between the column and feed valve. A "$\frac{1}{6}$ in B.S.P." stud coupling

FIG. 4.2 THE END FITTINGS

scale (1:1)

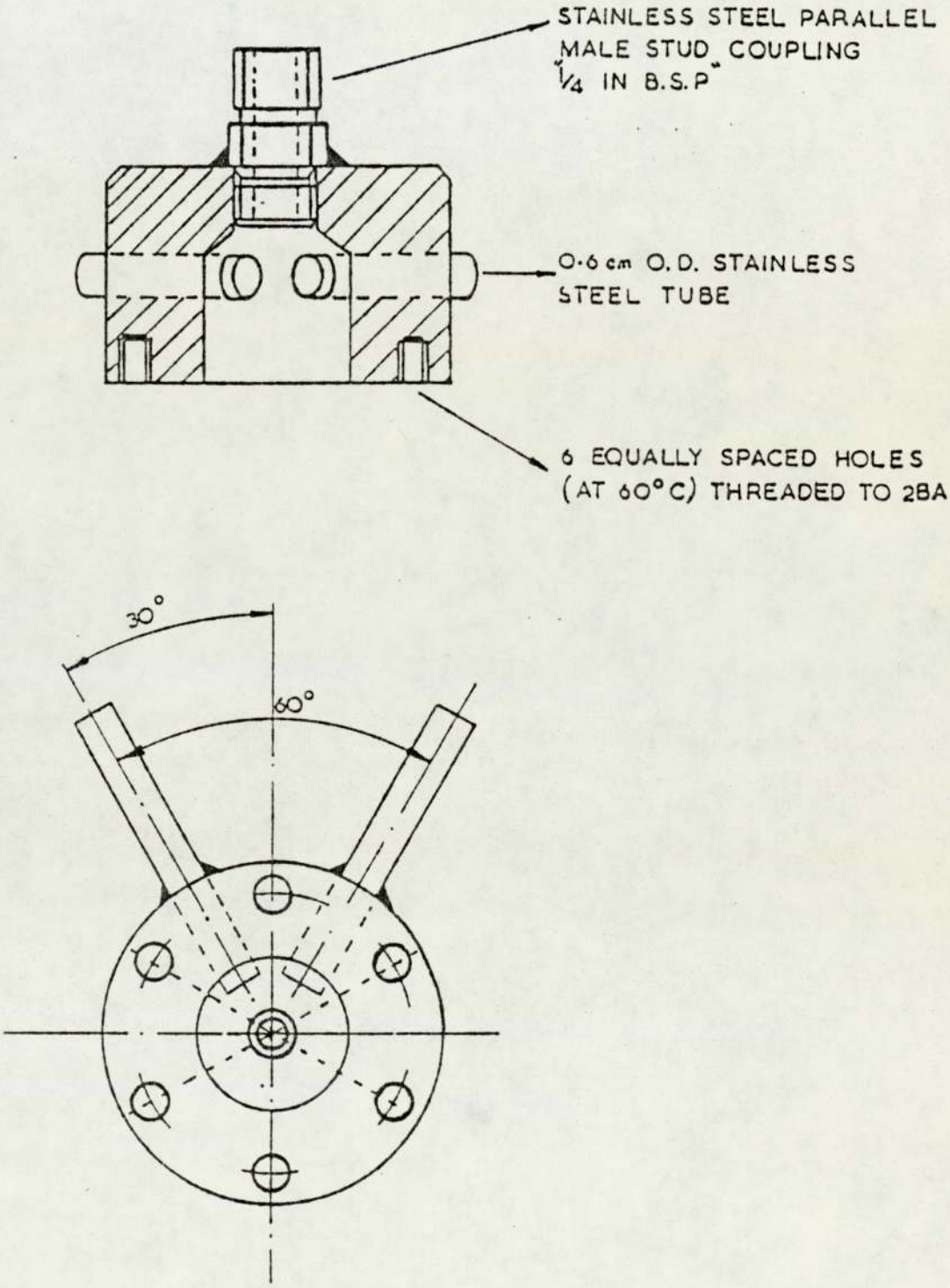

was soldered onto the bottom end fitting of each alternate column, this making the total number of sampling points 6. The samples were drawn off the column from these sampling points through 0.05 cm I.D. capillary tube connected to the sampling valve.

4.2.2 The Packing

Much work has been conducted into the most suitable method for packing preparative columns (54, 55, 101, 162, 163). A modified version of the shake-turn and pressurize method (S.T.P) (163) was employed for packing the SCCR-2 columns. The coated support was gradually added to the column under nitrogen pressure while the column was periodically tapped with a heavy metal bar. The vibration plus the presence of the nitrogen pressure resulted in an increase in the packing density in the peripheral region of the column. The exact weight of packing material used for each column is shown in Table 4.1.

After many runs to recover the γ- linolenic acid from "fungal oil", six of the columns were re-packed, and the remainder were topped with 1.0 gram of fresh packing. The topping of some of the columns was necessary because some of the packing in the columns settled to give a dead volume 2-3 cm at the end of the columns.

4.2.3 The Pneumatic Valves

In the design of the Sequential Chromatograph, SCCR-2,

Table 4.1

Quantity of Chromatographic Packing Material used for the SCCR-2 Unit

15% OV-275 on 353-251 μm Chromosorb P - AW-DMCS	
Assigned Column Number	Weight of Packing (gram)
1	112.2
2	112.1
3	114.5
4	113.4
5	113.8
6	117.0
7	112.5
8	114.0
9	112.4
10	112.5
11	113.5
12	115.0
Total Weight(g)	1362.9
Average Weight per Column	113.57
Total Weight of liquid phase (g)	204.43

careful selection of the valves was necessary as they must remain fully closed when operating against a back or forward pressure possibly in excess of the 446 kN m^{-2}. A two-way pneumatic diaphragm operated poppet valve was chosen; it was designed by Dr. B. Jones (164). This diaphragm valve, essentially consisted of two sections. The pneumatic control section, made out of brass, and the process fluid section made out of stainless steel. By applying air pressure on the pneumatic section of the valve, the stainless steel diaphragm was deflected causing the poppet to move downwards, thus allowing flow to proceed (Fig. 4.3) otherwise, the valve was normally closed.

0.3 cm orifices "⅛ in B.S.P." ports were used for the twelve feed valves to reduce the dead volume of the liquid held up in each valve after closure. Sixty gas valves were required to control the carrier and purge gas inlet and outlet functions. The valve construction and specification are illustrated in Fig. 4.3, Table 4.2 and Plate 4.1.

Each column in the SCCR-2 required 6 valves to provide the necessary operating function, which makes the total number 72 for the twelve columns used in the SCCR-2. Fig. 4.4 and Plate 4.2 shows the arrangement of 12 chromatographic columns in the SCCR-2 unit.

FIG. 4.3 DIAPHRAGM VALVE DESIGN

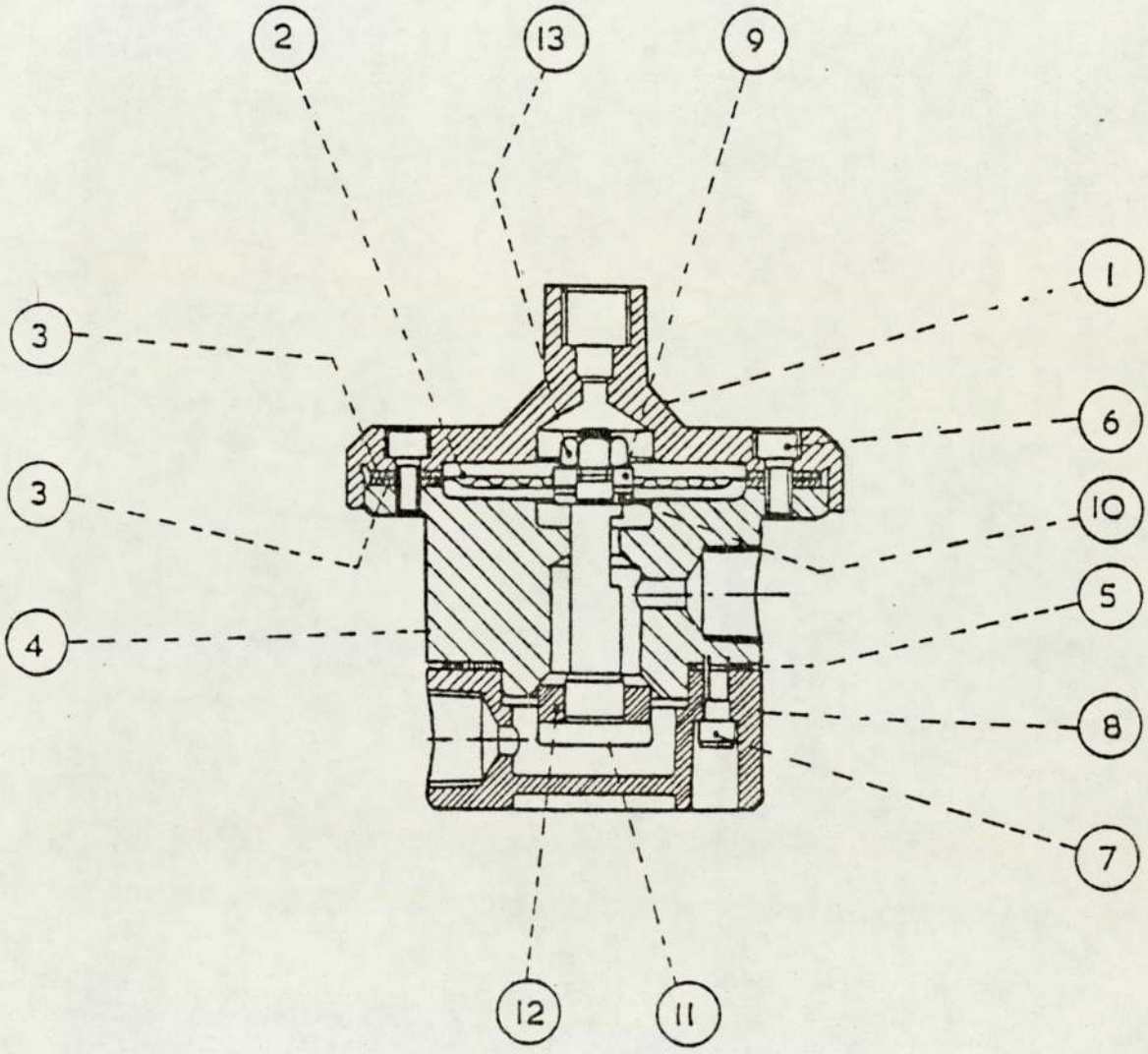

Table 4.2

VALVE PARTS LIST

ITEM NUMBER	PART NAME	MATERIAL	REMARKS	DESIGN DIMENSIONS IN CMS
1	VALVE CAP	BRASS	FEMALE PORT "$\frac{3}{16}$ IN B.S.P."	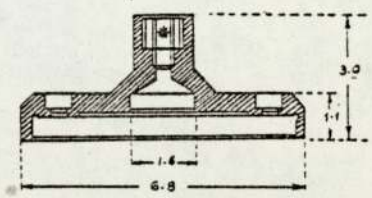
2	DIAPHRAGM	STAINLESS STEEL		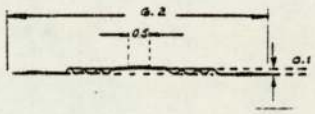
3	DIAPHRAGM SEALING RING	P.T.F.E.		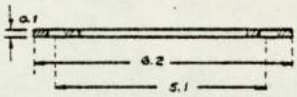
4	VALVE BODY	STAINLESS STEEL	FOR GAS VALVES IS A "¼ IN BSP" FEMALE PORT, WHILE FOR THE FEED VALVES IS"⅛ IN BSP". A P.T.F.E RING WAS INSERTED IN THE PORTS OF THE FEED VALVES TO REDUCE THE DEAD VOLUME	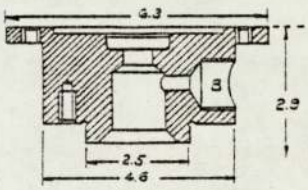
5	BODY SEALING	P.T.F.E.		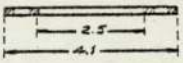
6	VALVE CAP SCREWS	STAINLESS STEEL	4 BA × 0.8 CM LONG N° REQUIRED: 6	
7	VALVE BODY SCREWS	STAINLESS STEEL	4 BA × 1.3 CM LONG N° REQUIRED: 6	

Table 4.2

VALVE PARTS LIST CONTINUED

ITEM NUMBER	PART NAME	MATERIAL	REMARKS	DESIGN DIMENSIONS IN CMS
8	VALVE LOWER CHAMBER	STAINLESS STEEL	B "¼ IN BSP" AND "⅛ IN BSP" FEMALE PORT FOR THE GAS VALVES AND FEED VALVES RESPECTIVELY. A P.T.F.E. RING WAS INSERTED IN THE PORTS OF THE FEED VALVES TO REDUCE THE DEAD VOLUME	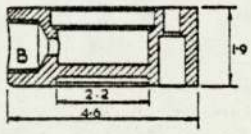
9	VALVE WASHER	STAINLESS STEEL		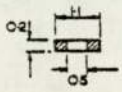
10	VALVE SHIM	STAINLESS STEEL		AS ABOVE
11	POPPET VALVE	STAINLESS STEEL		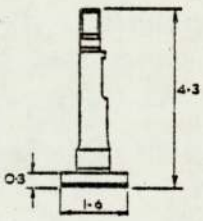
12	VALVE SEATING RING	P.T.F.E.		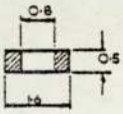
13	DIAPHRAGM NUT	STAINLESS STEEL	2 BA	

PLATE 4.1 THE DIAPHRAGM VALVE

AV = assembled valve

D = diaphragm

N = diaphragm nut

P = poppet

PSR = P.T.F.E. sealing ring in valve cap

VB = valve body

VBS = valve body sealing

VC = valve cap

VLC = valve lower chamber

W = washer

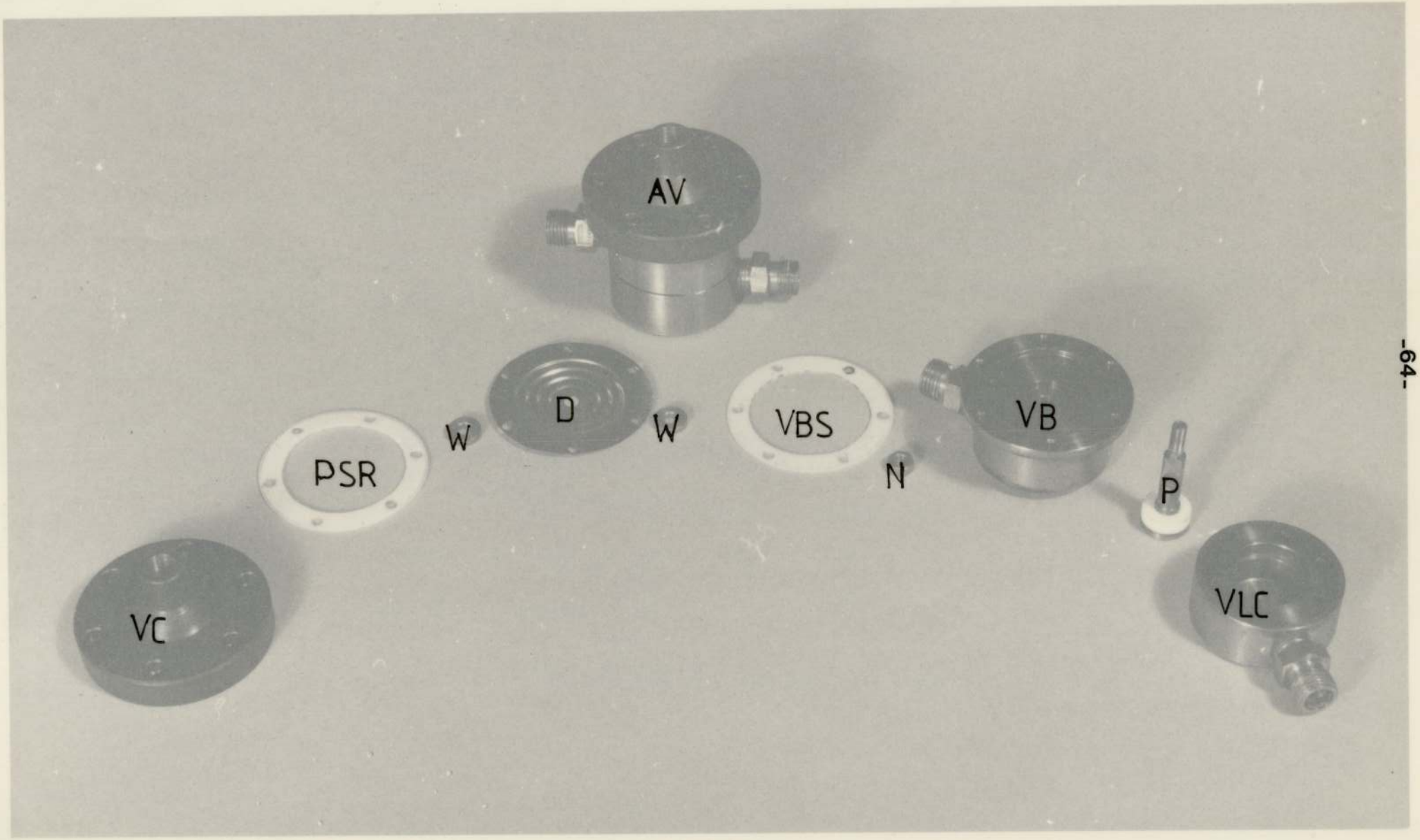
AV
D
W
W
PSR
VC
VBS
N
VB
P
VLC

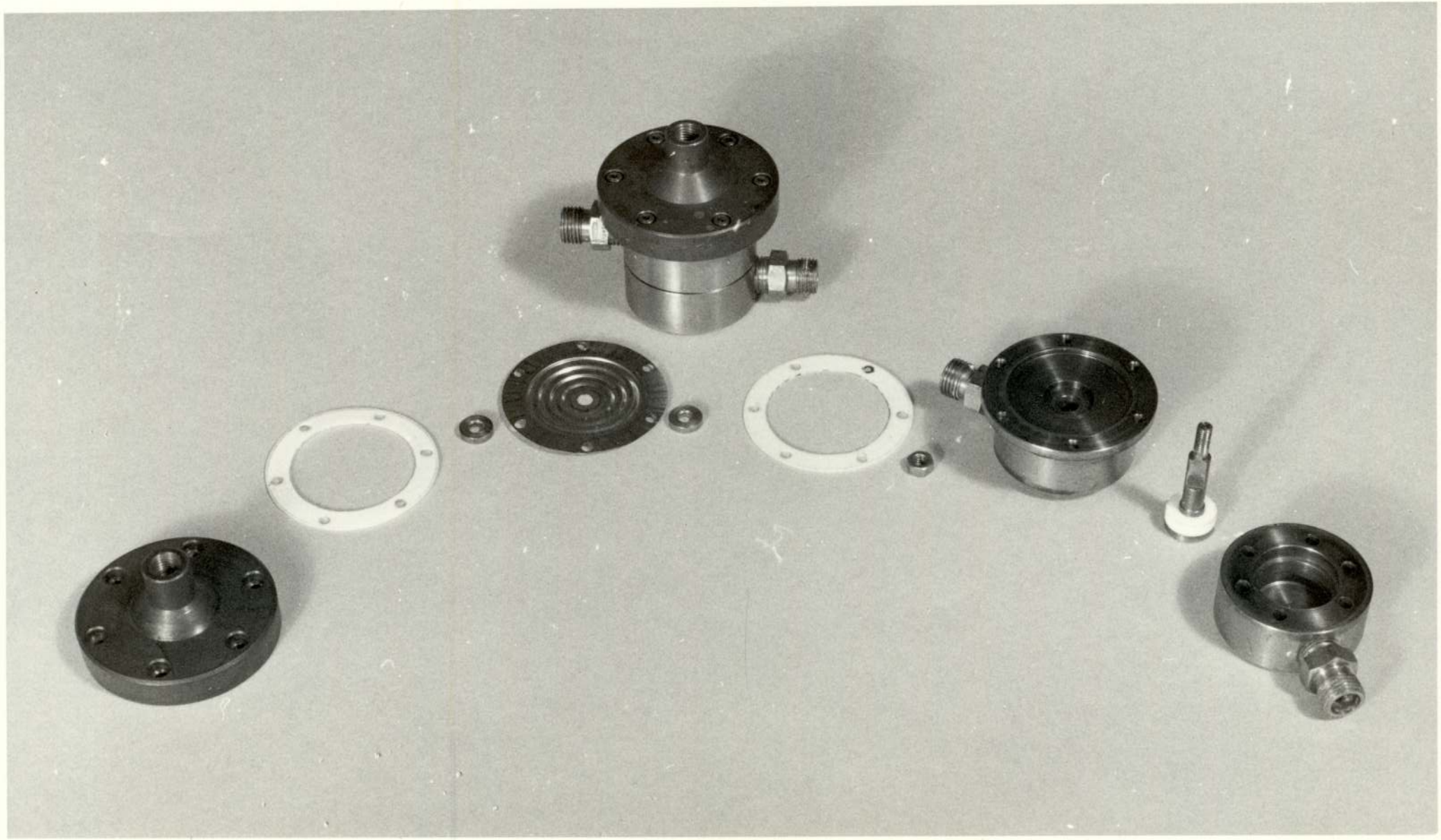

FIG. 4.4 SCHEMATIC DIAGRAM SHOWING THE POSITION OF DIAPHRAGM VALVES ON CONSECUTIVE COLUMNS

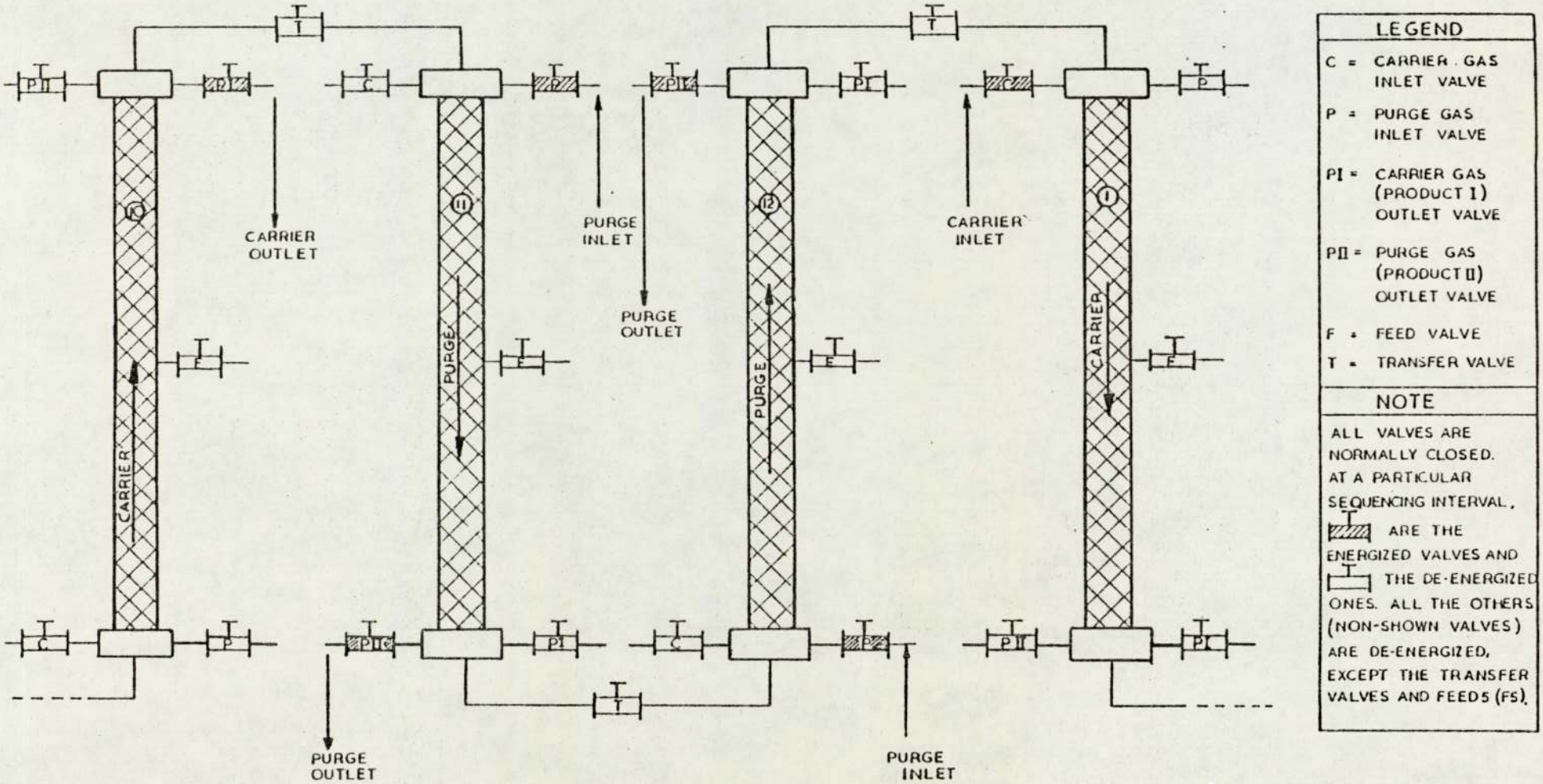

PLATE 4.2 THE ARRANGEMENT OF DIAPHRAGM VALVE

BT = brass tube to the pneumatic section of diaphragm valve

CC = chromatographic column

C,P = carrier/purge inlet valves

P1,P2 = product 1/product 2

ST = stainless steel tube to the flow process section of diaphragm valve

T = transfer valve

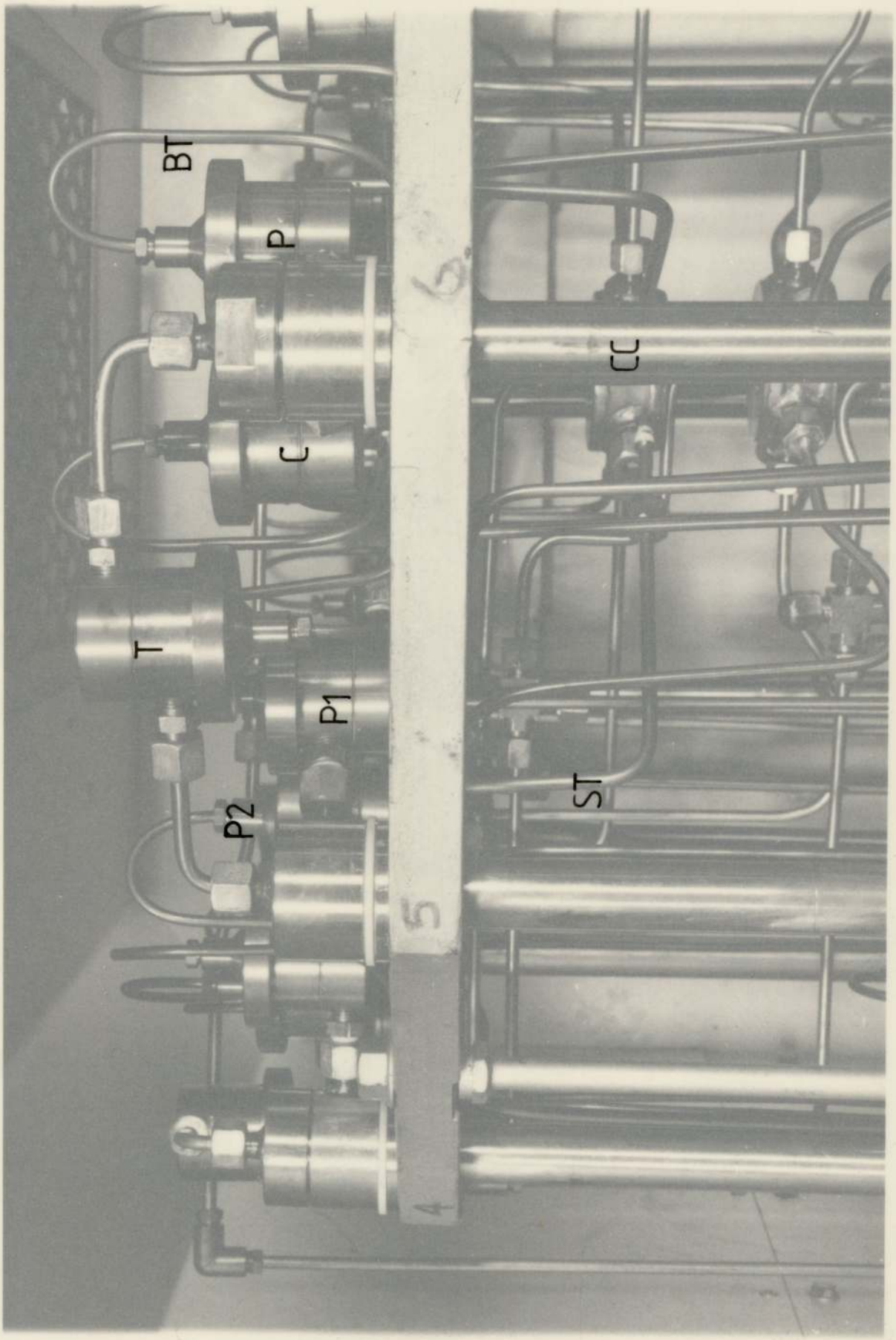
BT
P
C
T
P1
P2
CC
ST

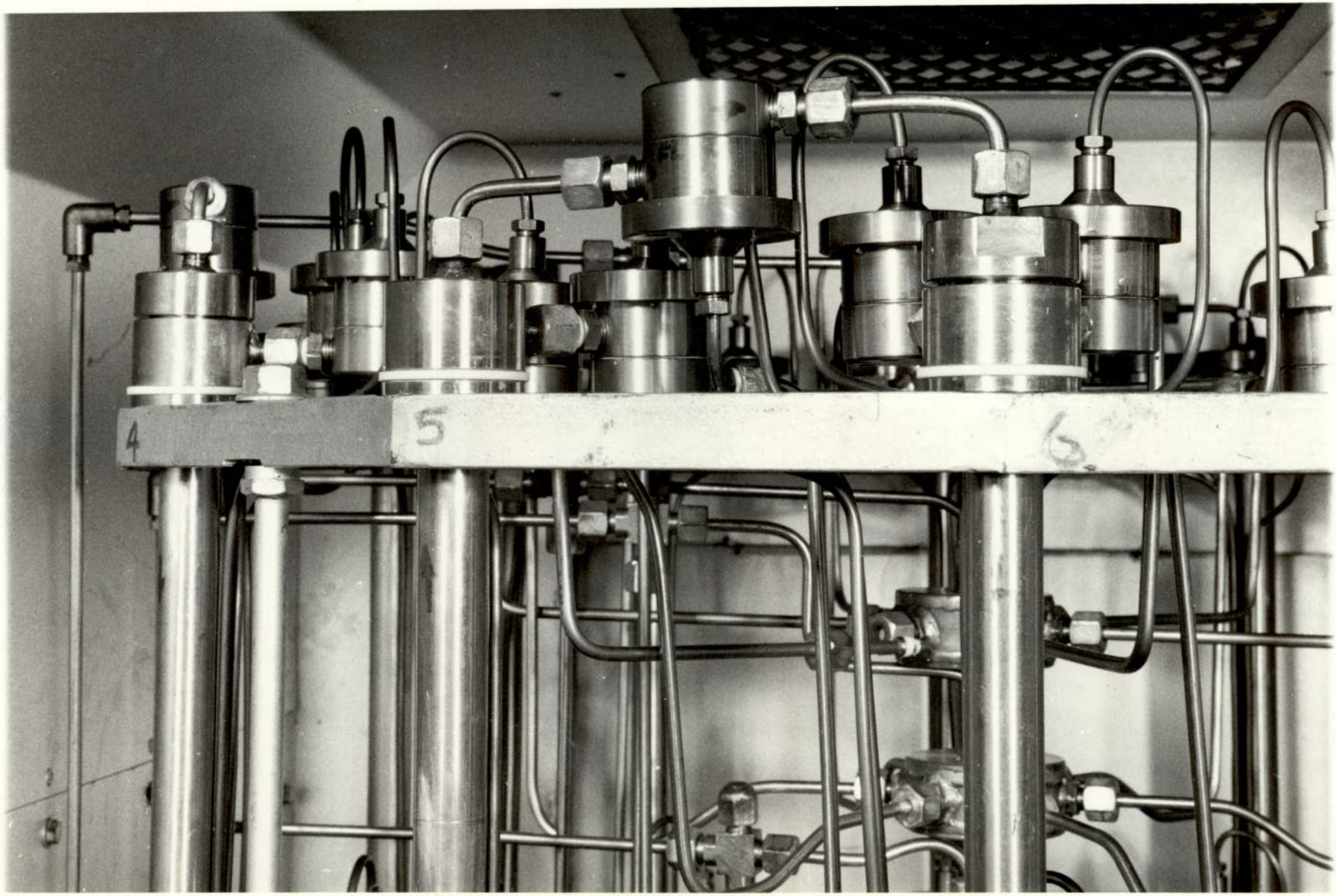
4
5
6

4.2.4 The Central Distribution Network

Fig. 4.5 shows a schematic diagram for the gas lines, and the product streams around the chromatograph. The symmetrical nature of the SCCR-2 can be seen from the Fig. 4.4, in which the four inlet/outlet ports alternate between the top and bottom of adjacent columns. Therefore, for each gas inlet or product outlet line two distributors were required, each supplying six columns. Each gas distributor was constructed from a stainless steel closed cylinder 3.5 cm in height and 7.7 cm in diameter with six "¼ in B.S.P." parallel male stud stainless steel couplings, silver soldered and evenly spaced on its cylindrical surface, Fig. 4.6. The eight distributors were set vertically on the axis of the cylinder formed by twelve columns (Plate 4.3).

4.2.5 The Oven

The oven of internal dimension (0.915m× 0.915m ×0.915m) was supplied by Hedinair Limited, and it is an electrically heated oven with forced air circulation. It has an internal volume of 0.766 m^3. The heat was provided by Incolloy sheathed mineral insulated rod elements located in ducts along both sides of the oven walls. The air was partially recirculated through the oven at least ten times per minute by a centrifugal fan.

FIG. 4.5 FLOW DIAGRAM OF THE SCCR-2 UNIT

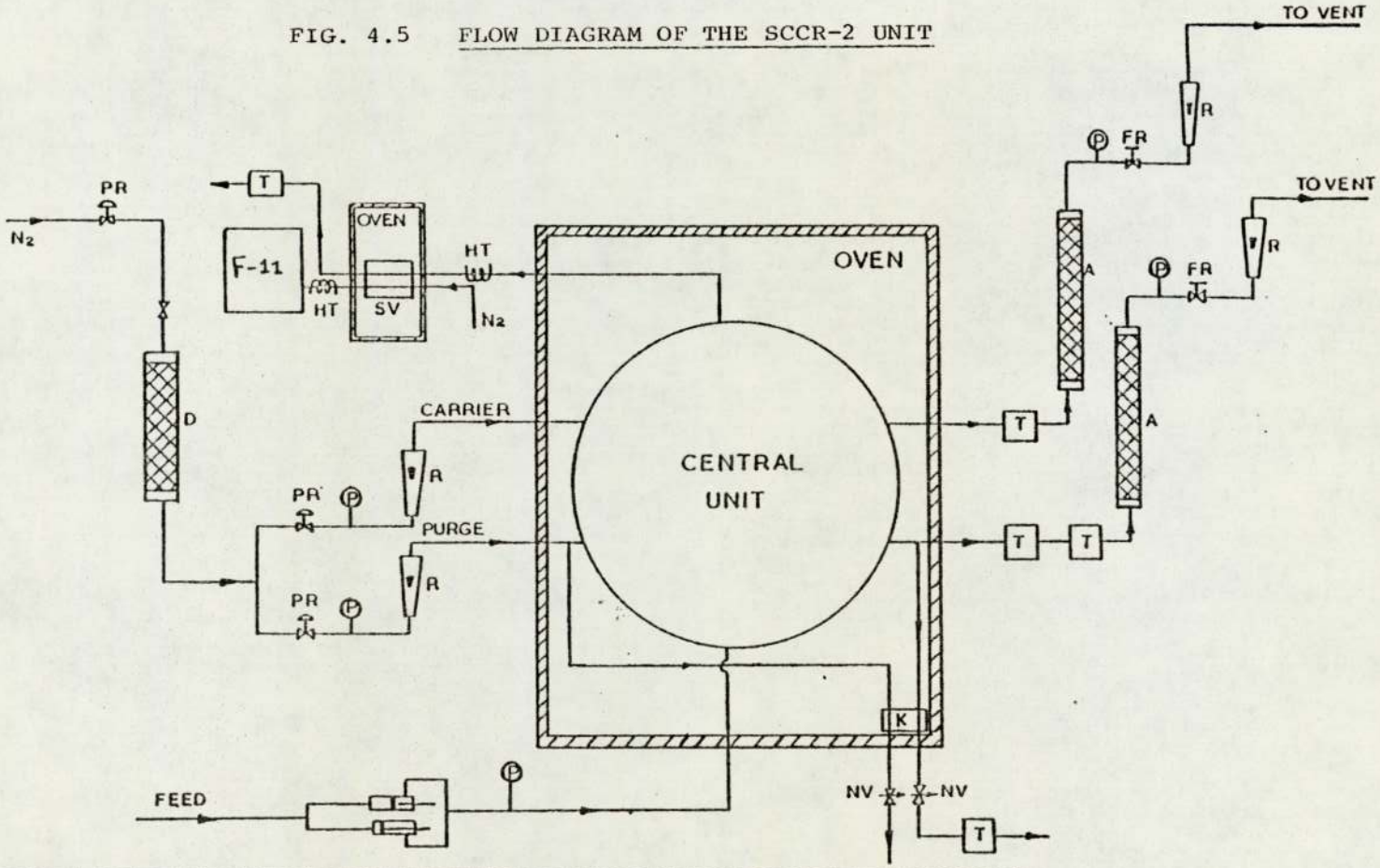

FIG. 4.6 THE GAS DISTRIBUTOR

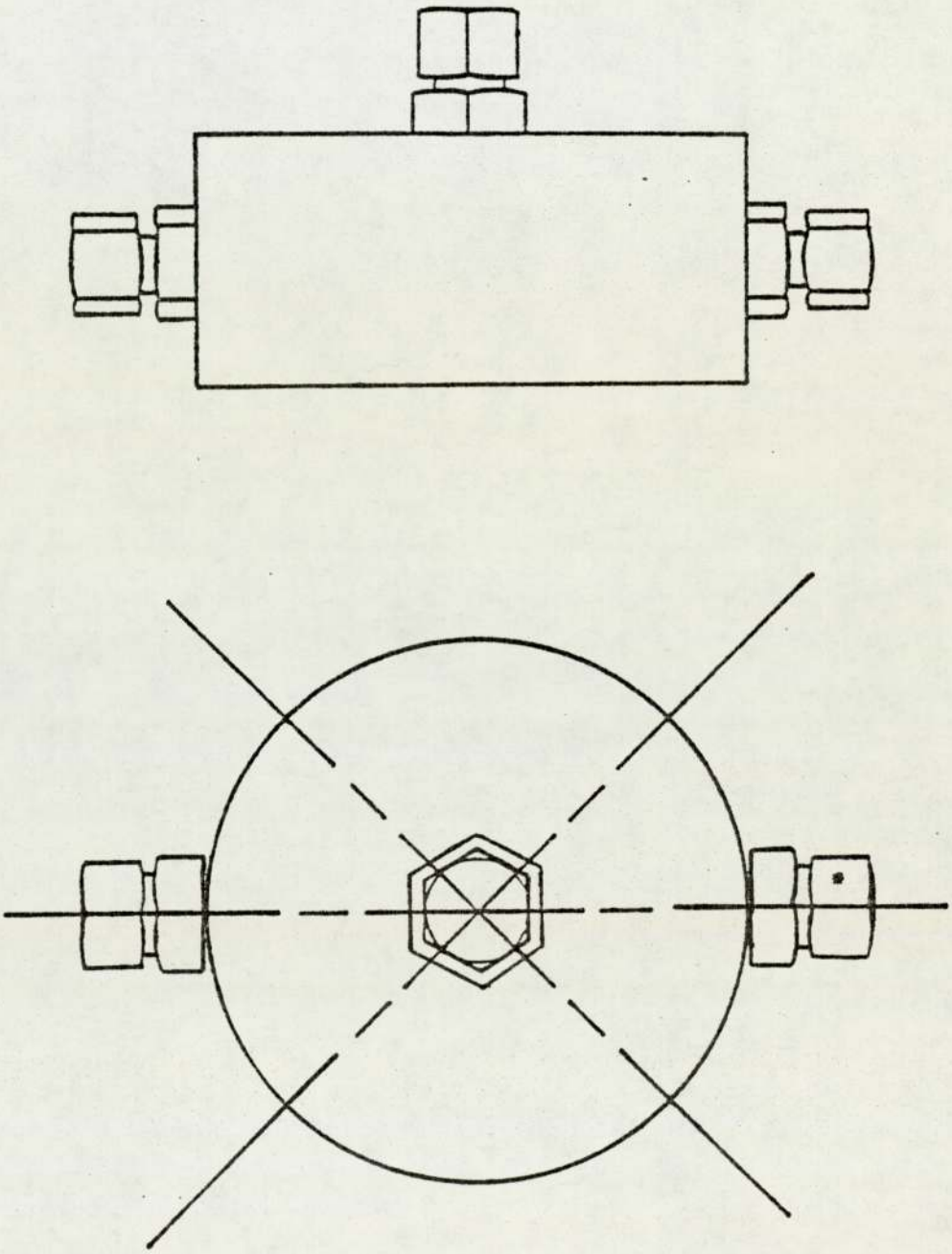

* NOTE 6 STAINLESS STEEL PARALLEL MALE STUD COUPLINGS "1/4 IN B.S.P."

PLATE 4.3 THE CENTRAL DISTRIBUTION NETWORK

C = carrier gas inlet

F = feed valve

P = purge gas inlet

P1 = product 1 outlet

P2 = product 2 outlet

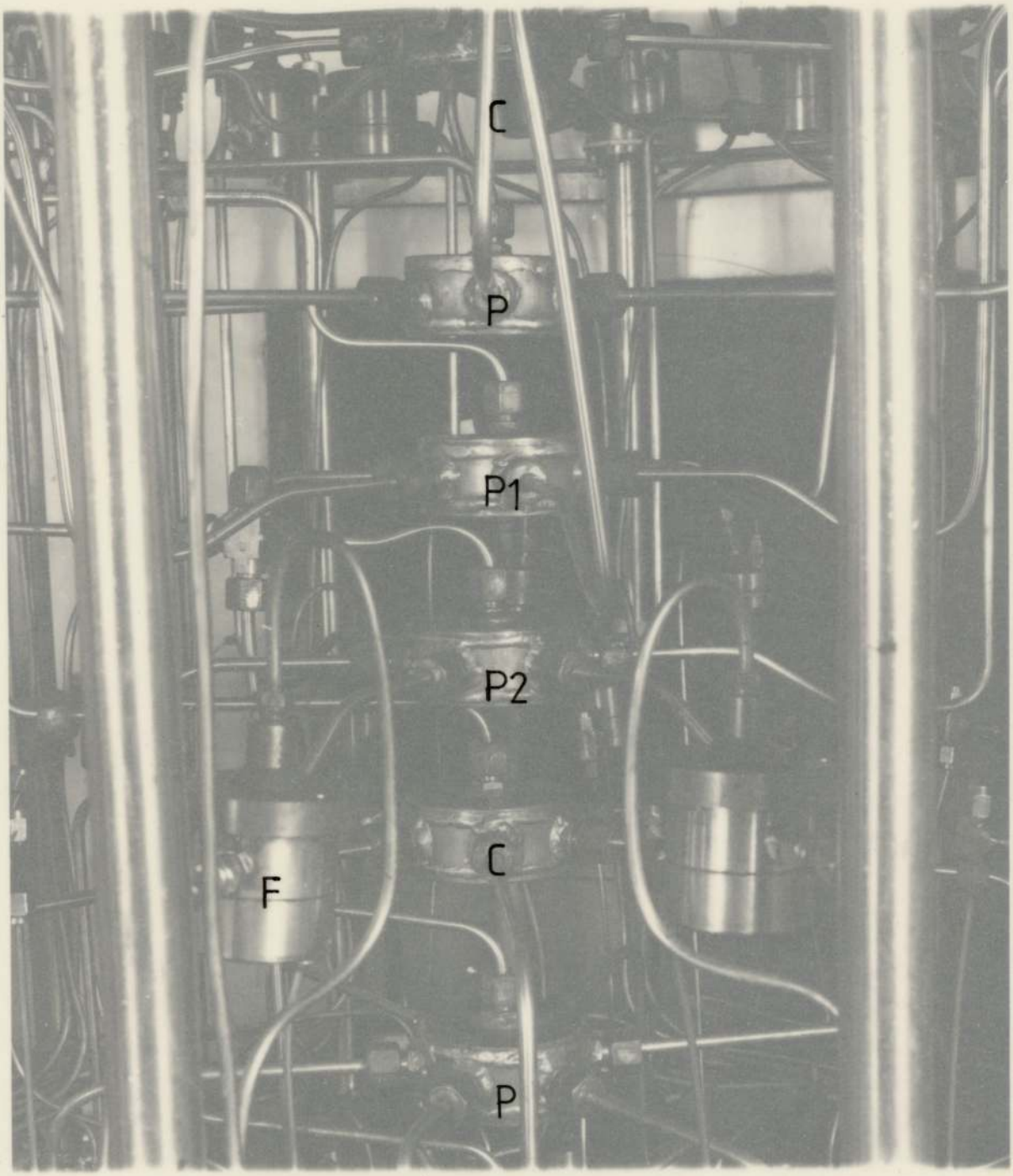
C
P
P1
P2
C
F
P

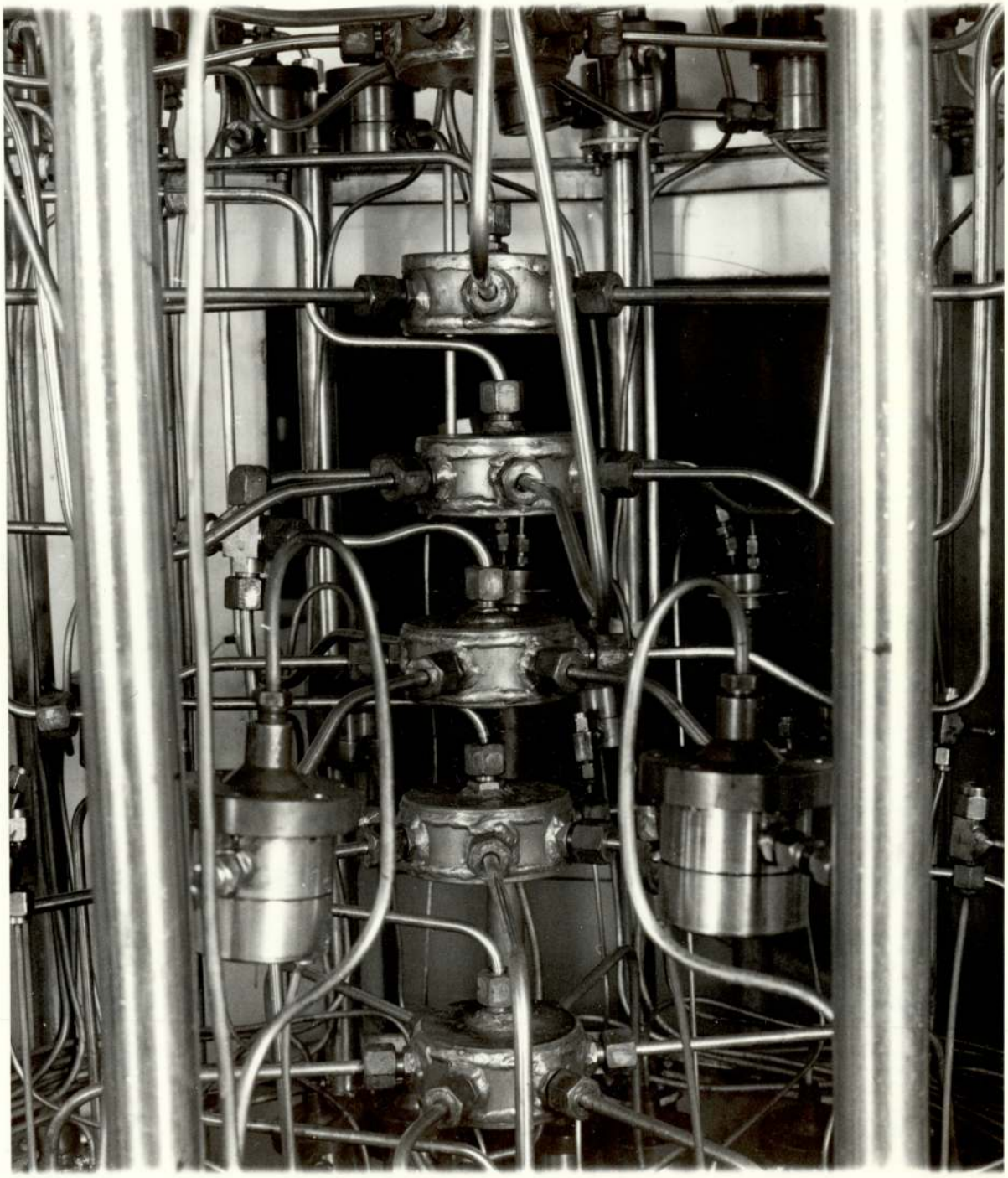

The walls and doors of the oven were made out of sheet steel and the thermal insulation was provided by mineral wool 7.62 cm thick.

The oven could provide a maximum operating temperature of 300°C, with a maximum energy consumption of 13 Kw, and is capable of maintaining the temperature with an accuracy of ±5°C.

A large exhaust vent was fitted on the oven with a setting quadrant for manual control to enable evacuation of fumes to take place.

The ovens original design was modified by placing a 0.61m × 0.61m explosion relief/access door in the centre of the rear wall.

4.3 CONTROL, MEASURING AND PERIPHERAL FUNCTIONS

4.3.1 The Pneumatic Control Unit

Plate 4.4 clearly shows the pneumatic control unit supplied by Festo Pneumatic Limited which controls the operation, and the sequencing of the valves at appropriate times.

The pneumatic control unit consisted of a cam belt unit operating on twenty on/off 3-way valves. The cam belt shaft was driven by a synchromesh gear motor which could be regulated in the torque range of 1-10 r.p.m..

PLATE 4.4 THE CENTRAL UNIT

C = central distributor

CC = chromatographic Column

F = feed valve

G = gas inlet/outlet valve

OL = output line circuit from the control unit

SF = support frame

T = transfer valve

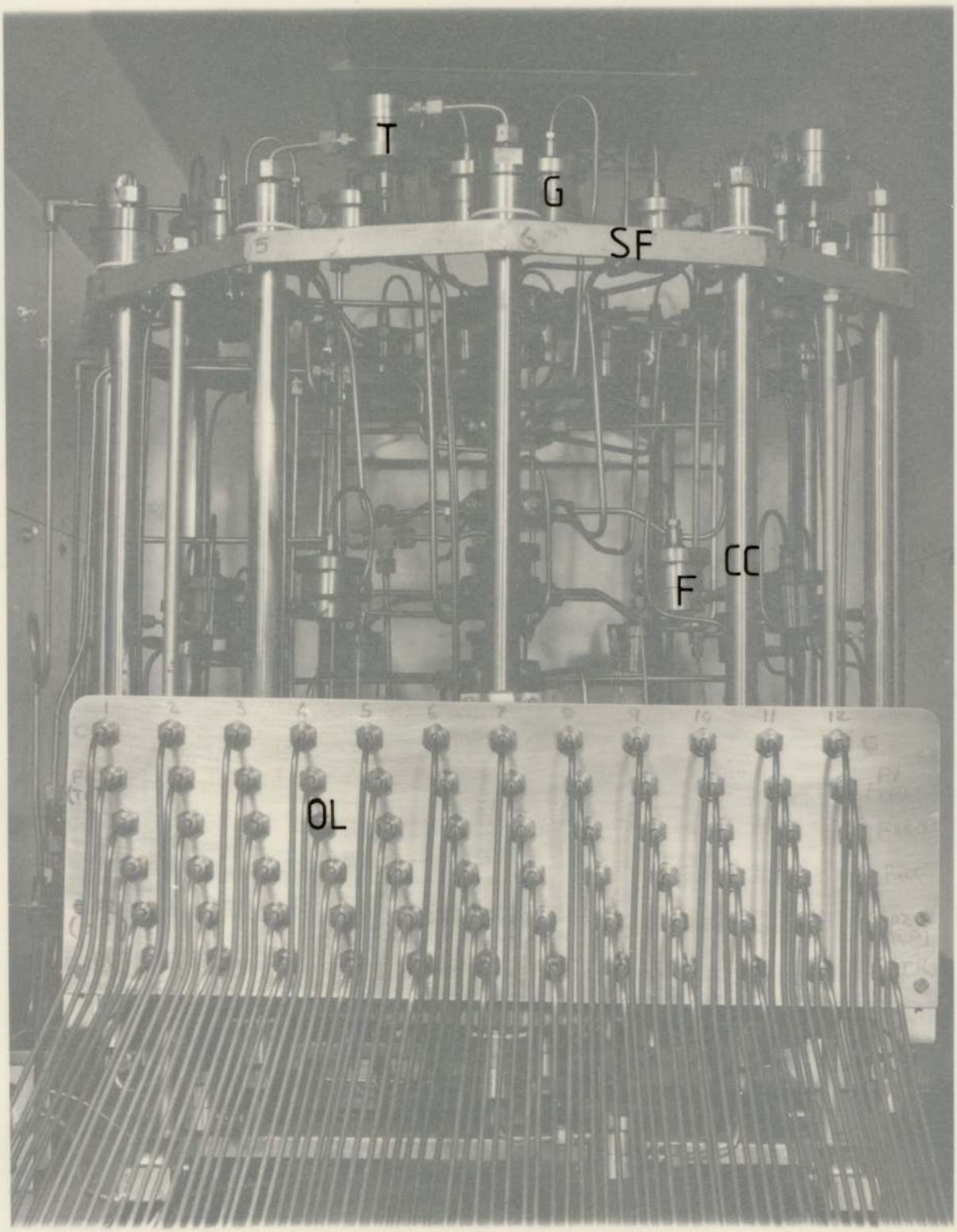
T
G
SF
CC
F
OL

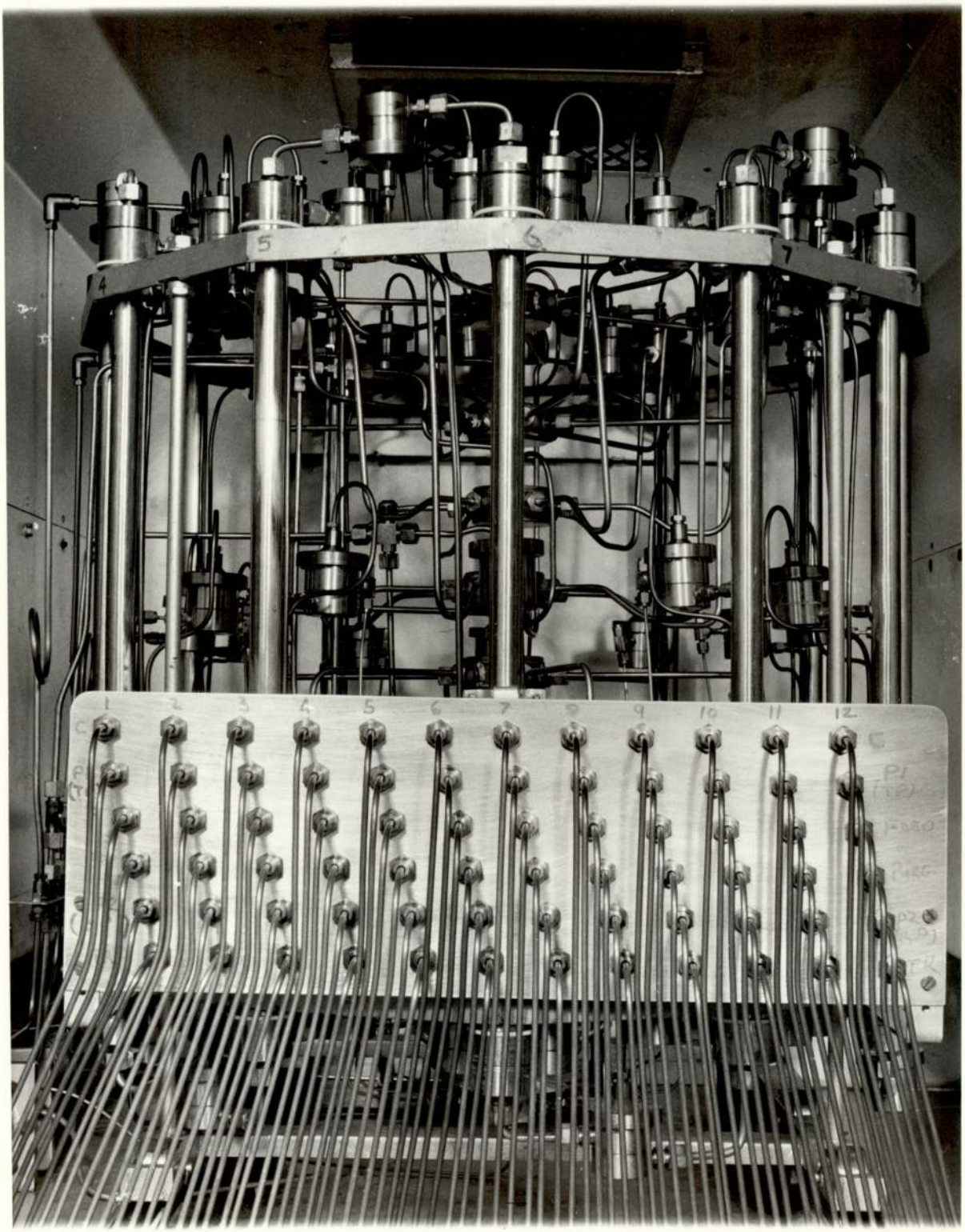
5
6
7
4
1
2
3
4
5
6
7
8
9
10
11
12

These torques were transmitted to the cam belt shaft via a pair of gear wheels. Thus, revolution times of the cam belt varying from 9 seconds to 24 hours could be obtained. The cam belt shaft consisted of 48 links and each of them could accommodate up to 12 cams. For the operation of the SCCR-2 unit, 12 links were employed, each one having a set of 5 cams.

A set of cams in contact with the appropriate 3-way pneumatic valves, energized them for a period of time controlled by a digital timer (Fig. 4.7a). After a selected time interval the motor was energized bringing into contact the next set of cams with the 3-way pneumatic valves. In the meantime the digital timer was automatically reset to zero. By the time the new set of pneumatic valves had been energized, the motor was automatically de-energized. With the pneumatic valves there was only one communal connection to the air supply which was required to have a minimum pressure of 377 KN m^{-2}. The first 12 pneumatic valves (Fig. 4.7b) connected to the transfer valves were normally open. The next 6 pneumatic valves (Fig. 4.7b) reserved for the other sixty diaphragm valves via a secondary circuit of valves, were normally closed. The secondary circuit consisted of two types of pneumatic valves. The type ZK-PK3-6/3 (Fig. 4.8), consisted of 3 single pneumatic valves, each with two inputs X and Y and one output A. The type OS-PK3-6/3 (Fig. 4.8) also consisted

FIG. 4.7a THE DIGITAL TIMER CIRCUIT

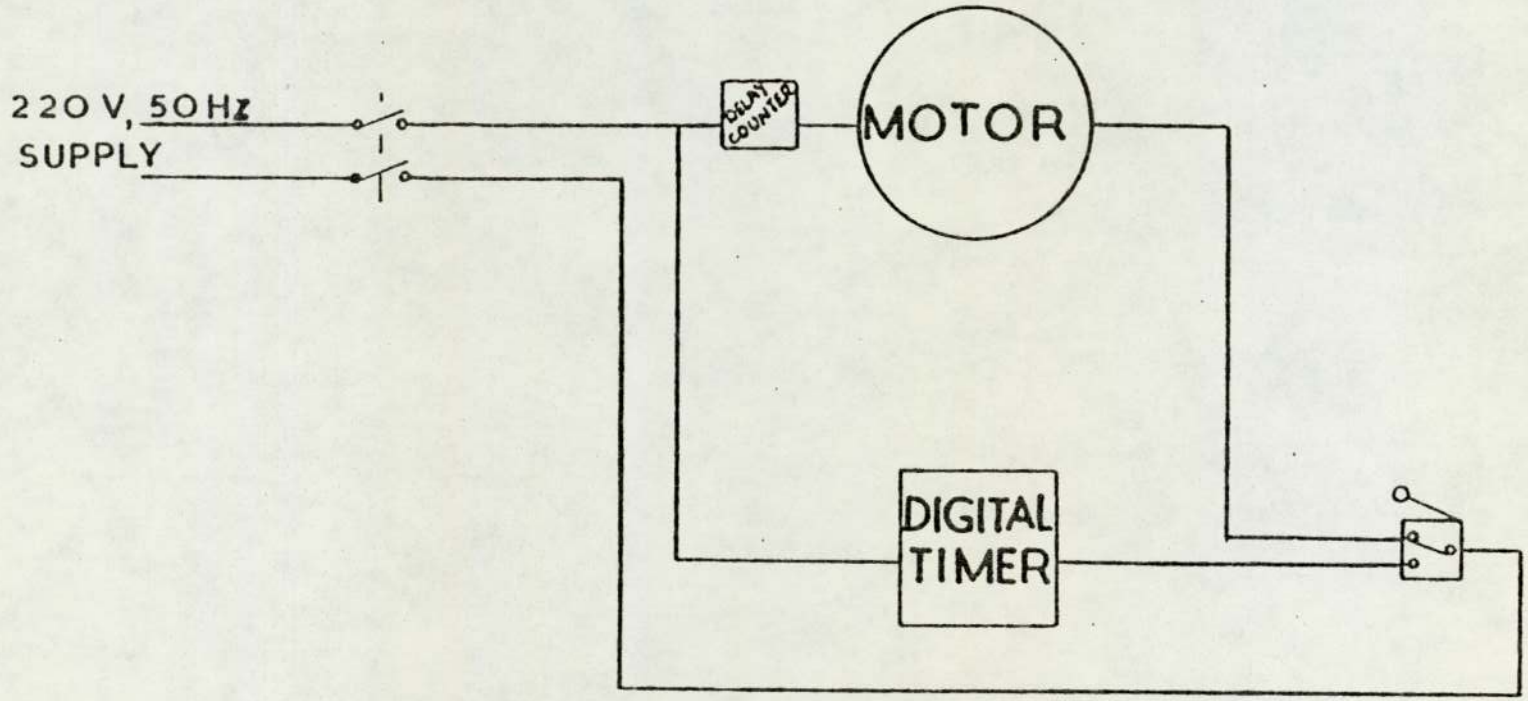

NOTE THE DELAY COUNTER IS A PNEUMATICALLY OPERATED CONTROL DEVICE GIVING INFORMATION FOR THE TIME PERIOD WHICH THE DIGITAL TIMER IS OFF

FIG. 4.7b DIAGRAMATIC PRESENTATION OF CONTROL UNIT

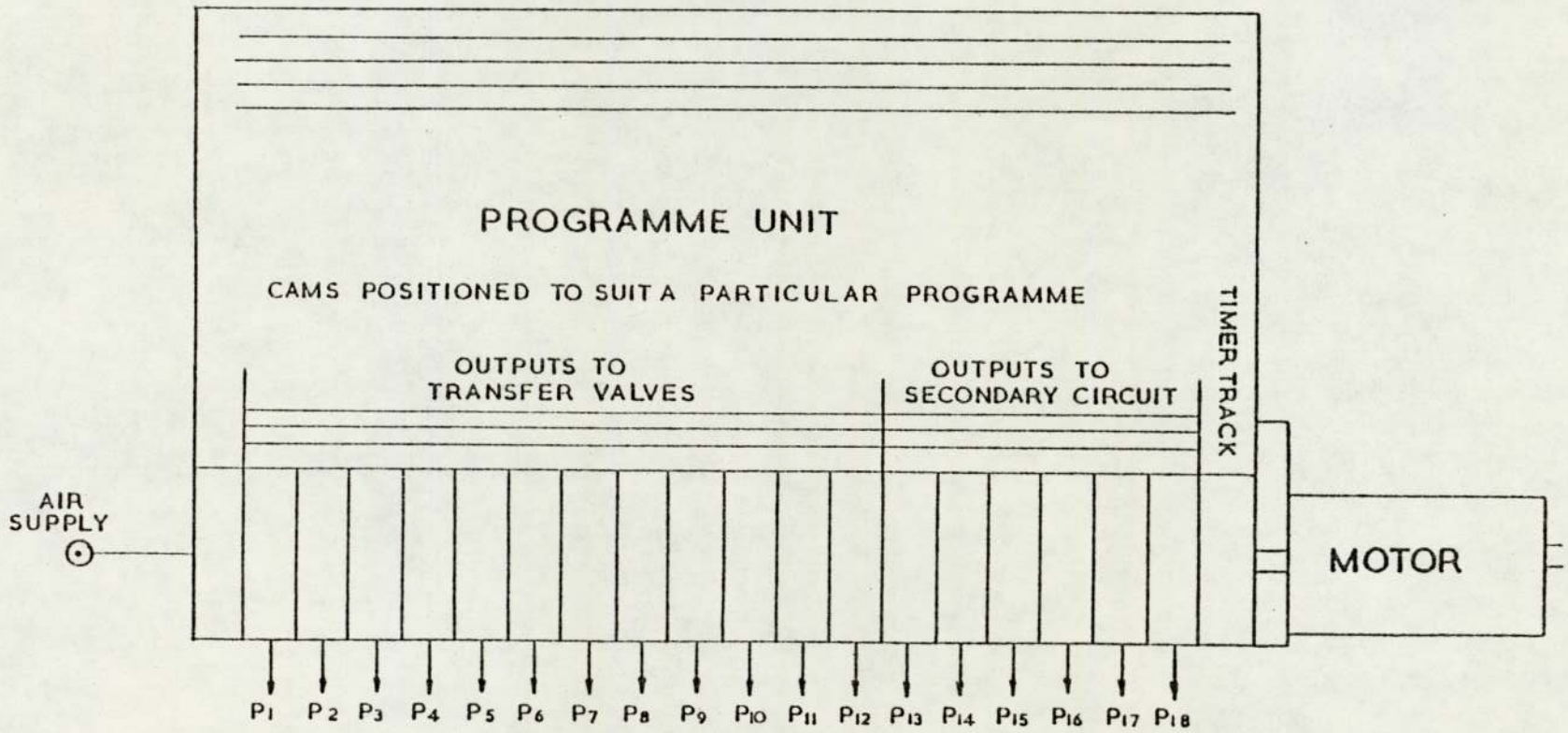

FIG. 4.8 THE SECONDARY PNEUMATIC CIRCUIT

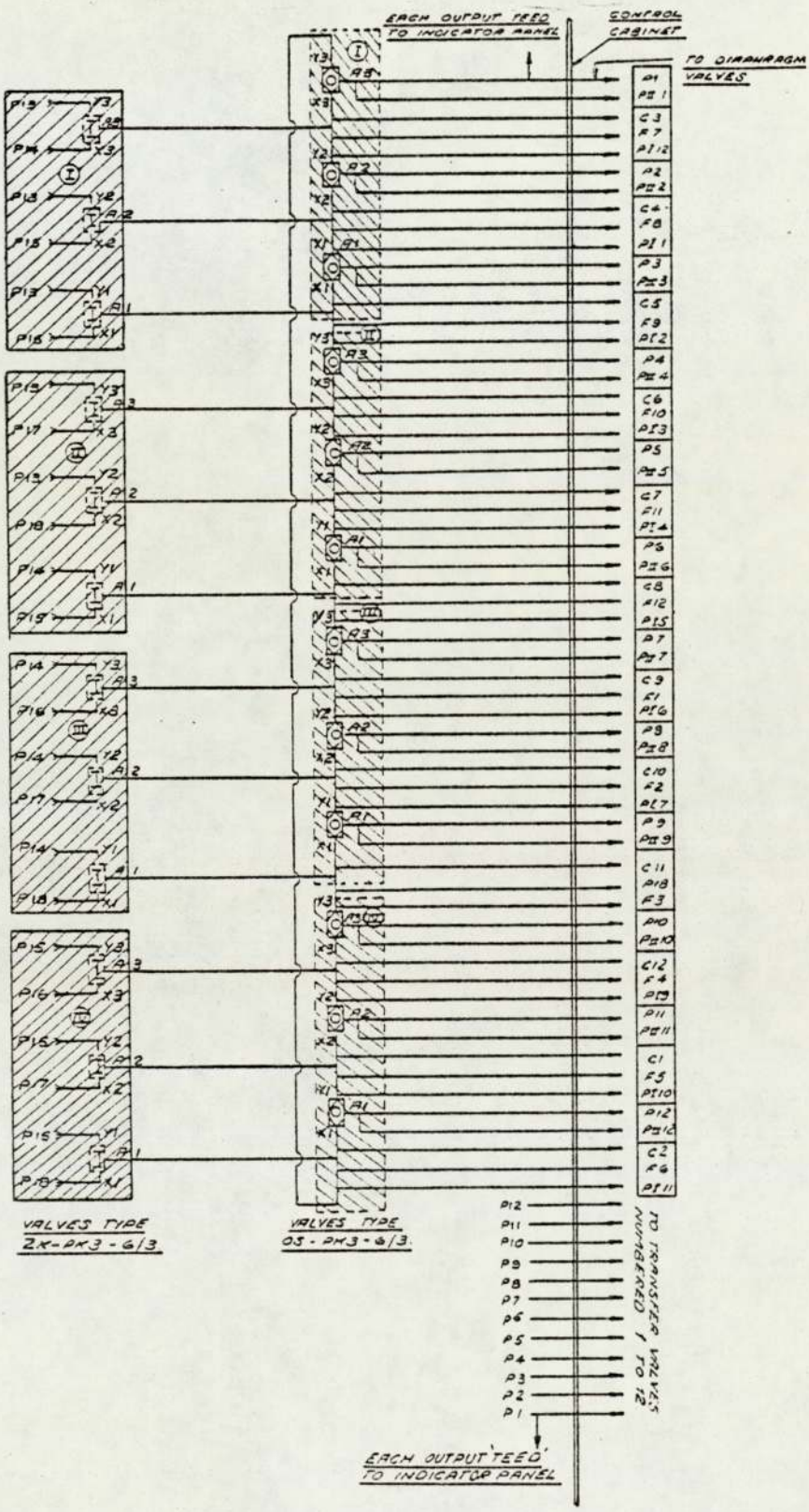

of 3 single pneumatic valves each with 2 inputs X, Y and one output A. If one or both of the inlet ports were under pressure, the output A was exhausted. The connection pattern of the various sets of diaphragm valves to the pneumatic valves of the control unit is demonstrated in Table 4.3.

4.3.2 Inlet and Outlet Gas Control

A schematic diagram (Fig. 4.5) shows the distribution of the inlet nitrogen (carrier gas fluid) and outlet product streams around the chromatographic refiner (SCCR-2).

Nitrogen was supplied from cylinders initially regulated to a pressure of 515 KN m^{-2}, and then passed through a silica gel bed (5.5 cm I.D. and 51 cm long) for drying.

All regulators used in regulating the purge and carrier gas are of the "Norgen" two diaphragm type regulators. The pressure gauges employed are of the same type.

The individual gas flow rates were also monitored by two "Brooks 1100" rotatometers.

4.3.3 Feed Mixture Supply

The feed enters the chromatographic unit through the pneumatic valves positioned at the column mid-points.

Table 4.3

The Sequencing of Energized Valves According to the SCCR-2 Operating Requirement

	COLUMNS ISOLATED (Assigned Numbers)	1,2	2,3	3,4	4,5	5,6	6,7	7,8	8,9	9,10	10,11	11,12	12,1
PNEUMATIC CONTROL	MAIN PNEUMATIC VALVES ENERGIZED Type : RS-3	P_{12} P_1 P_2 P_{13} P_{14}	P_1 P_2 P_3 P_{13} P_{15}	P_2 P_3 P_4 P_{13} P_{16}	P_3 P_4 P_5 P_{13} P_{17}	P_4 P_5 P_6 P_{13} P_{18}	P_5 P_6 P_7 P_{14} P_{15}	P_6 P_7 P_8 P_{14} P_{16}	P_7 P_8 P_9 P_{14} P_{17}	P_8 P_9 P_{10} P_{14} P_{18}	P_9 P_{10} P_{11} P_{15} P_{16}	P_{10} P_{11} P_{12} P_{15} P_{17}	P_{11} P_{12} P_1 P_{15} P_{18}
	SECONDARY PNEUMATIC VALVES ENERGIZED Type: ZK-PK-3	IA_3	IA_2	IA_1	IIA_3	IIA_2	IIA_1	$IIIA_3$	$IIIA_2$	$IIIA_1$	IVA_3	IVA_2	IVA_1
	Type: OS-PK-3	IA_3, IA_2	IA_2, IA_1	IA_1, IIA_3	IIA_3, IIA_2	IIA_2, IIA_1	IIA_1, $IIIA_3$	$IIIA_3$, $IIIA_2$	$IIIA_2$, $IIIA_1$	$IIIA_1$, IVA_3	IVA_3, IVA_2	IVA_2, IVA_1	IVA_1, IA_3
DIAPHRAGM VALVES	TRANSFER VALVES ENERGIZED (Directly Controlled)	T3 T8 T4 T9 T5 T10 T6 T11 T7	T4 T9 T5 T10 T6 T11 T7 T12 T8	T5 T10 T6 T11 T7 T12 T8 T1 T9	T6 T11 T7 T12 T8 T1 T9 T2 T10	T7 T12 T8 T1 T9 T2 T10 T3 T11	T8 T1 T9 T2 T10 T3 T11 T4 T12	T9 T2 T10 T3 T11 T4 T12 T5 T1	T10 T3 T11 T4 T12 T5 T1 T6 T2	T11 T4 T12 T5 T1 T6 T2 T7 T3	T12 T5 T1 T6 T2 T7 T3 T8 T4	T1 T6 T2 T7 T3 T8 T4 T9 T5	T2 T7 T3 T8 T4 T9 T5 T10 T6
	INLET/OUTLET VALVES ENERGIZED (Indirectly Controlled)	F7 C3 PI 12 P1 P2 PII 1 PII 2	F8 C4 PI 1 P2 P3 PII 2 PII 3	F9 C5 PI 2 P3 P4 PII 3 PII 4	F10 C6 PI 3 P4 P5 PII 4 PII 5	F11 C7 PI 4 P5 P6 PII 5 PII 6	F12 C8 PI 5 P6 P7 PII 6 PII 7	F1 C9 PI 6 P7 P8 PII 7 PII 8	F2 C10 PI 7 P8 P9 PII 8 PII 9	F3 C11 PI 8 P9 P10 PII 9 PII 10	F4 C12 PI 9 P10 P11 PII 10 PII 11	F5 C1 PI 10 P11 P12 PII 11 PII 12	F6 C2 PI 11 P12 P1 PII 12 PII 1

Stainless steel tubing connected these feed valves to a central feed distributor (Fig. 4.9). A stainless steel "tee fitting" was placed in the line immediately precedeing the valve to enable all air to be displaced from the feed lines before start-up. The vertical stem of the "tee" was capped with a silver soldered stainless steel nut "¼ in B.S.P.".

The feed distributor was supplied by a positive displacement metering micropump series two, supplied by Metering Pumps Limited. Prior to the pump a large glass cylindrical reservoir was attached to a 100 cm^3 burette in which the feed was stored and its flow was monitored. A calibration chart for the pump is given in Appendix 1. The pressure in the distributor was monitored by a stainless steel/P.T.F.E. (101-515 KN m^{-2}) pressure gauge supplied by Bristol Automation Limited. It was connected to the feed line before entering the oven.

4.3.4 Monitoring the Solute Level by a Katharometer

Monitoring the product streams was useful for observing the onset of pseudo-equilibrium within the sequential chromatograph SCCR-2. This was done by using a (Gow-Mak) model 10-454 katharometer. The katharometer was installed in the SCCR-2 oven, inside a mild steel box filled with fibre glass to dampen the temperature fluctuations of the oven, Fig. 4.5. The katharometer was

FIG. 4.9 THE FEED DISTRIBUTOR

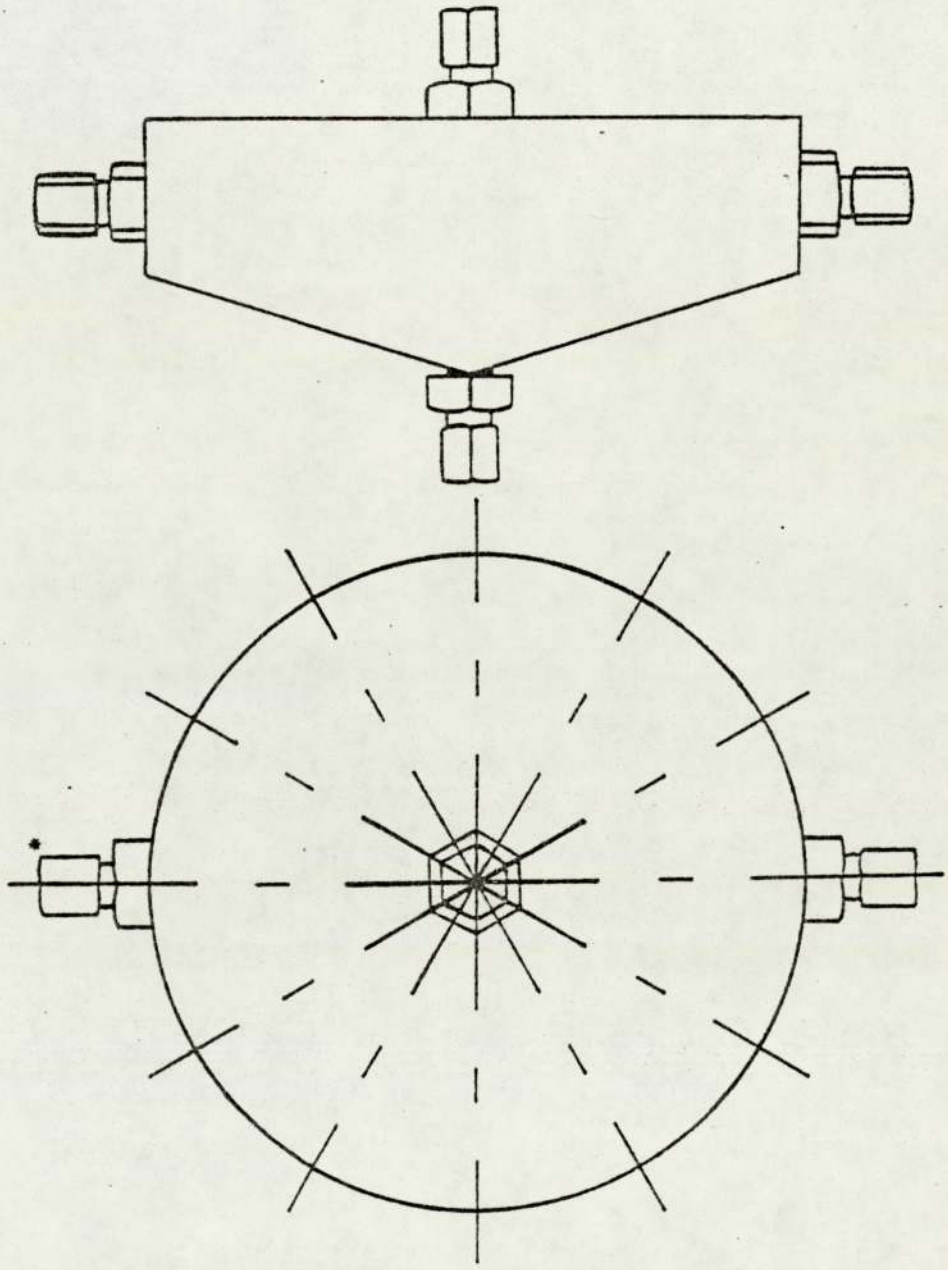

*NOTE 12 STAINLESS STEEL PARALLEL MALE STUD COUPLINGS "1/8 IN B.S.P."

capable of monitoring one product stream only at a time. The trace produced by a katharometer gave no quantitative indications of the composition of a stream.

4.3.5 Measuring the Temperature

The temperature effect on the distribution coefficient is a very significant factor to consider it in the gas chromatographic process. Thus, 6 thermocouples, supplied by Pyrotenax Limited, were fitted around the SCCR-2 to measure the following temperatures:

- the column's temperature (three thermocouples were fitted in columns 4, 8 and 12).
- the purge inlet temperature.
- the temperature of the carrier gas inlet.
- the oven temperature.

All thermocouples were finally connected via a selector switch to an Ether compensated temperature indicator. A calibration chart for the thermocouples is given in Appendix 1.

4.3.6 The Pre-Heaters

Two identical pre-heaters were installed on the purge and carrier nitrogen streams. The design was similar to that of a shell and tube heat exchanger. The heat was

provided by three 300 W steel jacket heaters to replace the tube bundle normally employed in heat exchangers. Inside the chamber, ten mild steel baffles, each 0.32 cm thick and 6.3 cm in diameter were arranged to be 2.5 cm apart and supported by three tie rods. The baffles were used to divert the flow over the heaters. These pre-heaters were installed to pre-heat carrier and purge gas streams to the temperature of the oven before entering the separation chromatographic process. By using the pre-heaters, nearly complete stripping of the more soluble component from the purge section was ensured.

4.3.7 Product Collection

Rectangular stainless steel traps (of dimensions 12 cm height, 4.9 cm wide and 4.9 cm long with a sloping base plate) were connected to the product off take lines of the SCCR-2 unit, Fig. 4.5. Although the design of the traps was dictated by economics and simplicity, a trapping efficiency of better than 70% was obtained.

4.4 SAFETY

Several safety devices were built into the SCCR-2:

- an explosion relief door at the mid-rear wall of the oven.
- an exhaust vent in the oven, was connected to an outside extractor fan to ensure continuous purge of the air within the oven.

- outlet product lines and the solute gas streams from the katharometers and sampling valve, were all connected to the extractor fan system.

- outlet lines from the traps were connected to two charcoal adsorption beds and then to the extractor fan system. The glass column charcoal filled beds were enclosed in thick perspex boxes.

- the pre-heaters were fitted with a safety cut-out system.

All these safety devices were built into the unit to ensure that any emergency could be handled.

CHAPTER 5

EXPERIMENTAL TECHNIQUES

5.1 SELECTION OF THE CHEMICAL SYSTEMS

The chemical systems chosen for this study were limited by many factors:

- the thermodynamic compatibility of the feed components with the stationary phase.
- the availability of pure components at a reasonable cost.
- the chemical stability of the feed components under the operating conditions of the Sequential Continuous Chromatographic Refiner (SCCR-2).

Hence, the following discussions will deal briefly with these factors.

5.1.1 Pre-Investigation of the Chemical System

The thermodynamic compatibility of the systems is related to the partition coefficient on OV-275 columns. The partition coefficient of the selected chemicals had to be relatively low on the OV-275 phase in order to reduce the elution time, and consequently the loss of the carrier gas (N_2).

Thermodynamic measurements of various solutes on OV-275 analytical columns have shown that the following chemicals are favourable for this study (see Section 6.1.1);

ethyl caprylate/ethyl caprate (S.F. 1.9, 105°C), ethyl caprate/ethyl laurate (S.F. 1.44, 160°C), ethyl laurate/ methyl myristate (S.F. 1.54, 185°C), and methyl myristate/ methyl stearate (S.F. 2.8, 205°C). However, another chemical system, ethyl acetate/ethyl butyrate (S.F. 2.3, 60°C) was processed on SCCR-2 as a commissioning system for the re-packing of the columns with OV-275 because it is relatively cheap.

These chemical systems provided a combination of a wide range of fatty acids C_8-C_{18}, with different degrees of difficulty in each system. The degree of difficulty of the system is not only related to the separation factor, but also to the vapour pressure of both components, and their physical states at ambient temperature. Although under the experimental conditions of the SCCR-2 machine, the feed should be liquid at ambient temperature, the methyl myristate and methyl stearate system which is solid at room temperature has to be dissolved in ethyl acetate as a solvent.

These chemicals were acquired in a high state of purity. Private communication with Aldrich Chemical Company (the supplier) and GLC analytical checking revealed that the total level of impurities in the 'as-sold' products did not exceed 0.5 - 1%. However the methyl stearate used in this study was exceptionally impure (≈ 95%+) because of

the very high costs involved in the manufacture of ultra pure methyl stearate.

Since the fatty acids involved in this study have reactive sites which might be affected through the process of separation in SCCR-2 at high temperatures pre-investigation experiments were carried out to investigate this point. Thus, a glass tube 12 cm long and 1 cm in diameter was fitted with a double surface reflux condenser. A capillary tube (for bubbling N_2 through) was fitted to the end of the condenser and its length was adjusted to suit the combined length of the condenser and the glass tube. The sample was placed in the glass tube with the packing and stainless steel chips to simulate the stainless steel columns used on the rig. A stream of nitrogen was passed through for one hour, at ambient temperature to ensure oxygen free atmosphere. An oil bath was used to heat the sample to the required temperature under a nitrogen blanket. The duration of each experiment was about one hour during which the temperature was maintained as near as possible to the suggesting operating temperature of the SCCR-2 (see Table 5.1). The samples were cooled under the nitrogen blanket and analysed immediately.

To confirm the stability of the chemical systems throughout the separation process, the samples were analysed by infra-red spectroscopy using a Perkin Elmer Grating

Table 5.1

Reflux Experimental Conditions

Sample Name	Experiment Temperature °C	Comment
Methyl aceto acetate	110-115	
Ethyl acetate	120-125	
Ethyl chloro acetate	120-125	
Ethyl lactate	125-130	
Roswood oil	140-145	Essential oil
Citral oil	145-150	Essential oil
Ethyl caprate	160-165	
Ethyl caprylate	160-165	
Ethyl laurate	180-185	
Fungal oil	200-205	Mixture of fatty acids
Methyl linolenate	200-205	
Methyl myristate	200-205	
Methyl stearate	200-205	
Duration of each experiment : 1h		

spectrophotometer before and after the reflux experiments. The infra red technique was chosen because of its potential in elucidating any change in the main functional groups of the chemical structure, and for its simplicity (165).

To support the IR analysis, analytical gas liquid chromatography was used to test for any foreign material. The fatty acids chosen for this study also satisfied the strict safety requirements required, being comparatively non-toxic and non-inflammable at the operating temperature.

The relevant physical properties, the experimental reflux conditions, and the vapour pressure at different temperatures are given in Tables 5.1 and 5.2 and Fig. 5.1 respectively. In addition, two IR spectra are also given in Figs. 5.2 and 5.3. Fig. 5.2 shows that ethyl laurate remained stable after the reflux treatment. In contrast Fig. 5.3, which refers to citral oil, indicates some change had taken place because of the appearance of a new peak at 1715 cm^{-1} (ν4.28μ). Since the chemical structure of citral oil (3,7 - dimethyl - 2, 6 - octadienal, geranial, neral; $(CH_3)_2C = CHCH_2CH_2C(CH_3) = CHCHO$) is a mixture of cis and trans, then stereomutation and transfer from one geometrical shape to the other are the most probable changes to occur.

Table 5.2

Properties of Selected Chemicals

Name	Synonym and Formula	Density	Boiling Point	Molecular Weight	Supplier	Purity
		$g\ cm^{-3}$	^{o}C			%
Ethyl acetate	$CH_3CO_2C_2H_5$	0.9003	77.06	88.12	AIDRICH CHEM.CO.	99+
Ethyl butyrate	$CH_3CH_2CH_2CO_2C_2H_5$	0.8785	121.6	116.16	"	99+
Ethyl caprylate	$CH_3(CH_3)_6CO_2C_2H_5$	0.8693	208.5	172.27	"	99+
Ethyl caprate	$CH_3(CH_2)_8CO_2C_2H_5$	0.8650	241.5	200.33	"	99+
Ethyl laurate	$CH_3(CH_2)_{10}CO_2C_2H_5$	0.8618	273	228.38	"	99+
Methyl myristate	$CH_3(CH_2)_{12}CO_2C_2H_5$	0.8573	295	256.43	"	99+
Methyl stearate	$CH_3(CH_2)_{16}CO_2C_2H_5$	0.8498	442.3	298.52	"	95+

FIG. 5.1 PLOT OF LOG p^o VERSUS I/T FOR SOME FATTY ACIDS (184)

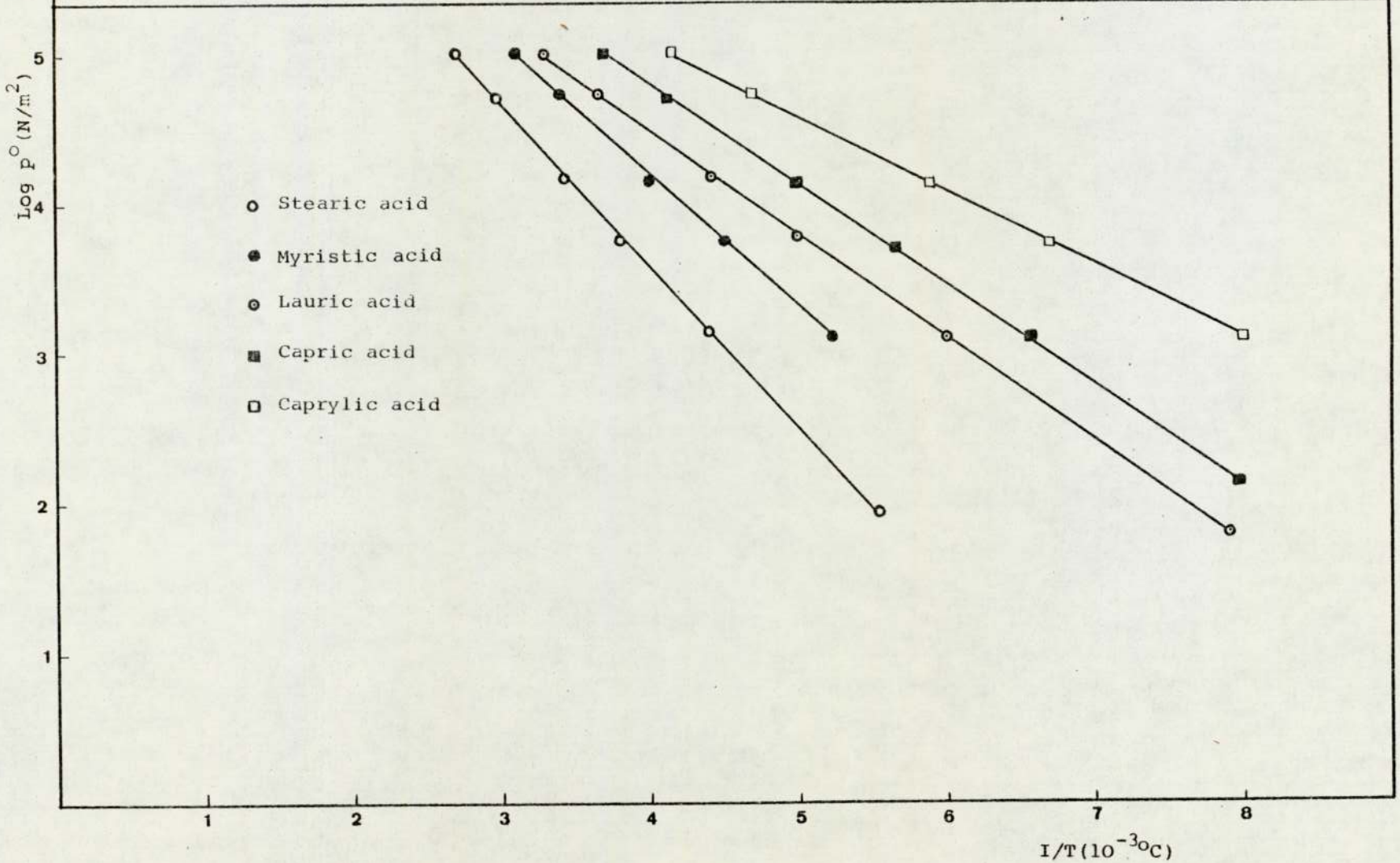

FIG. 5.2 INFRA-RED SPECTRA FOR ETHYL LAURATE BEFORE AND AFTER THE REFLUX EXPERIMENT

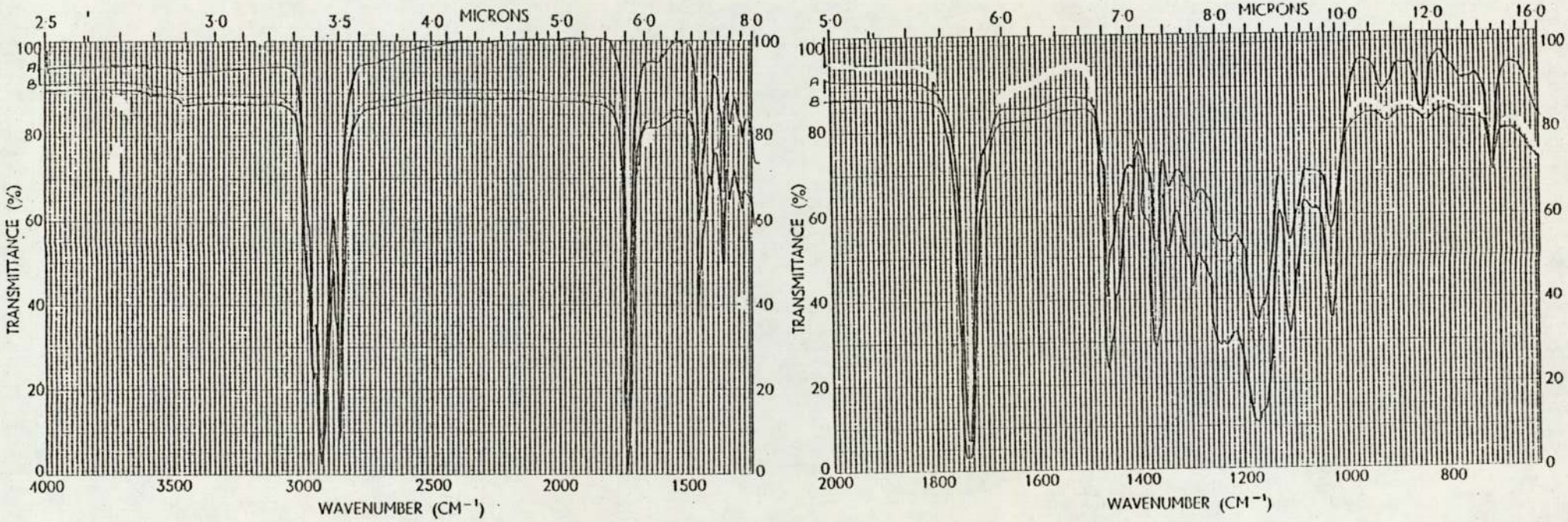

SAMPLE Ethyl laurate A:Before treatment B:After treatment	SOLVENT -	SCAN SPEED M	OPERATOR M.I.Howari
	CONC. Neat	SLIT N	DATE -
	CELL PATH Nacl	REMARKS No new peak appeared	
ORIGIN Pure	REFERENCE Air		

No

FIG. 5.3 INFRA-RED SPECTRA FOR CITRAL OIL BEFORE AND AFTER THE REFLUX EXPERIMENT

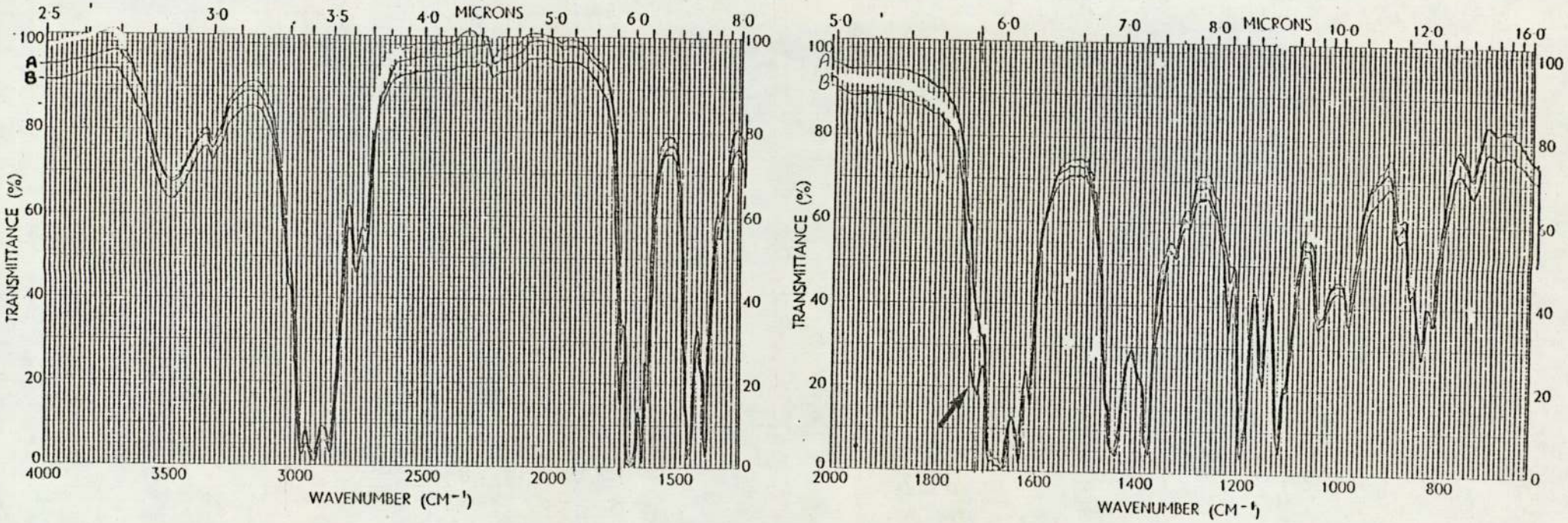

SAMPLE Citral oil A: Before treatment B: After treatment	SOLVENT -	SCAN SPEED M	OPERATOR M.I.Howari
	CONC. Neat (Thin Film)	SLIT N	DATE -
	CELL PATH Nacl	REMARKS New peak between 1800 - 1600 cm^{-1}	
ORIGIN Pure	REFERENCE Air		

No.

5.2 ANALYTICAL EQUIPMENT

5.2.1 Introduction

The analytical unit was used for the following three main purposes:

- determination of the partition coefficient using the flame ionization detector.
- determination of column to column concentration profile in the SCCR-2.
- continual monitoring of the solute concentration level in the product streams using the Gow-Mak katharometer.

Basically the GLC analytical unit used was a Perkin-Elmer F-11 chromatograph equipped with a twin Flame Ionization Detector (FID) system. The GLC (F-11 Chromatogram) and the Gow-Mak katharometer were connected to a Perkin-Elmer/Hitachi, model 159 recorder, and to a Hewlett-Packard series 3370B integrator.

5.2.2 Development of the Analytical GLC Unit

The original design of the FID detector in the Perkin-Elmer chromatograph was developed to perform the non-volatile fatty acid analyses, since the original design was not capable of performing this difficult analysis with the required efficiency.

The following modifications were made to the basic design:

1. the indirect injecting head Fig. 5.4 was changed to a direct column injection head, Fig. 5.5.
2. the space in the oven was adjusted to accommodate the Pye-Unicam glass column ("¼ B.S.P) Fig. 5.6a,b).

The above mentioned modifications were thought to be necessary, because of the problems faced in the analysis of the non-volatile fatty acids. The main problem was that the sample had to stay a long time in the injection head before getting onto the packed colum. In which case bad resolution, very severe tailing effect and distorted peaks were obtained.

5.3 THE KATHAROMETER

A Gow-Mak, model 10-454 katharometer was used in this work. The katharometer was installed in the SCCR-2 oven, inside a mild steel box filled with fibre glass, to monitor the product 2 stream, Fig. 4.5. This katharometer consisted of four hot rhenium-tungsten filaments connected to a Wheatstone bridge circuit. Two of the rhenium-tungsten filaments were fitted in the sample stream and the other two in a similar reference stream of the nitrogen carrier gas.

The flow rates through the katharometer blocks were regulated by two stainless steel needle valves and were

FIG. 5.4 PERKIN-ELMER INJECTION SYSTEM FOR THE F-11 CHROMATOGRAPH

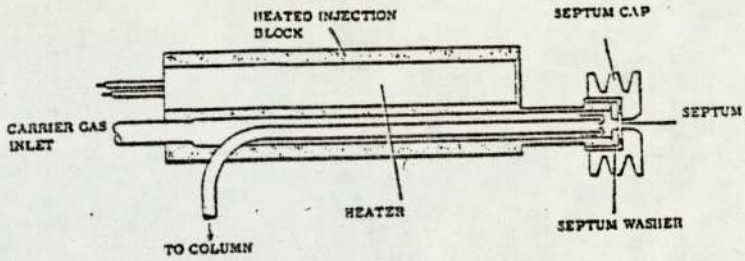

FIG. 5.5 PYE-UNICAM INJECTION SYSTEM

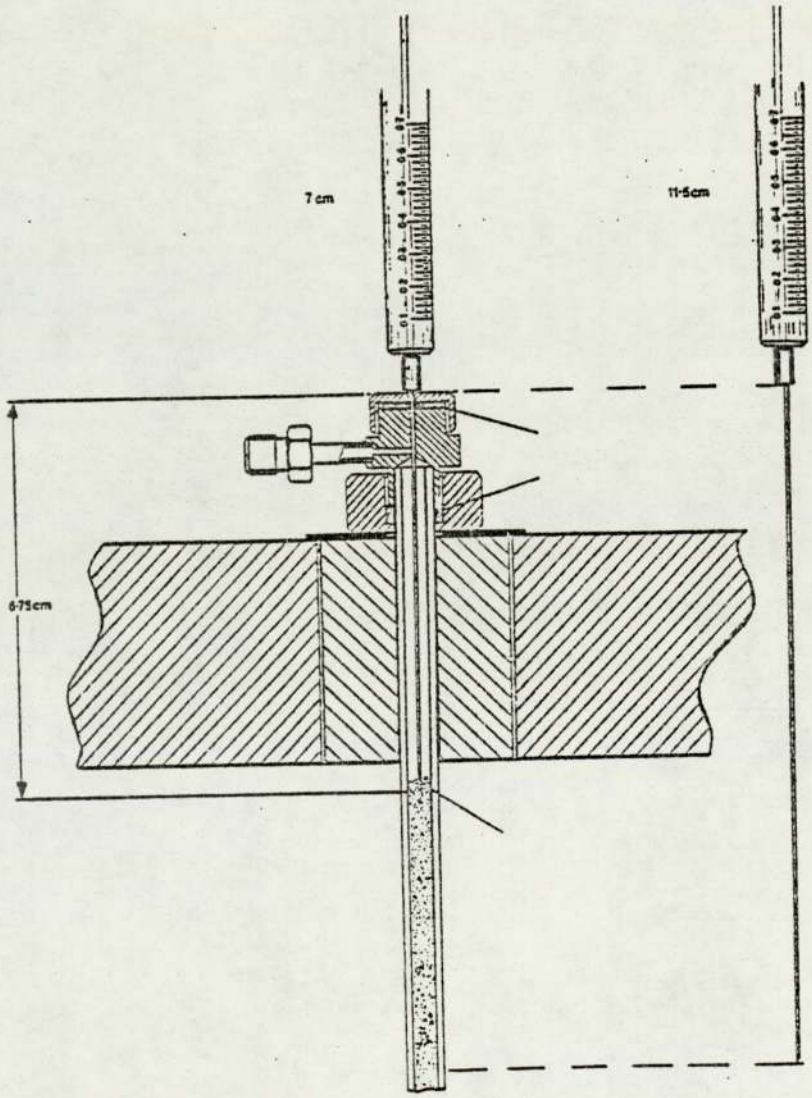

FIG. 5.6a COLUMN MOUNTING ARRANGEMENT FOR PYE-UNICAM THE 104 SERIES CHROMATOGRAPH

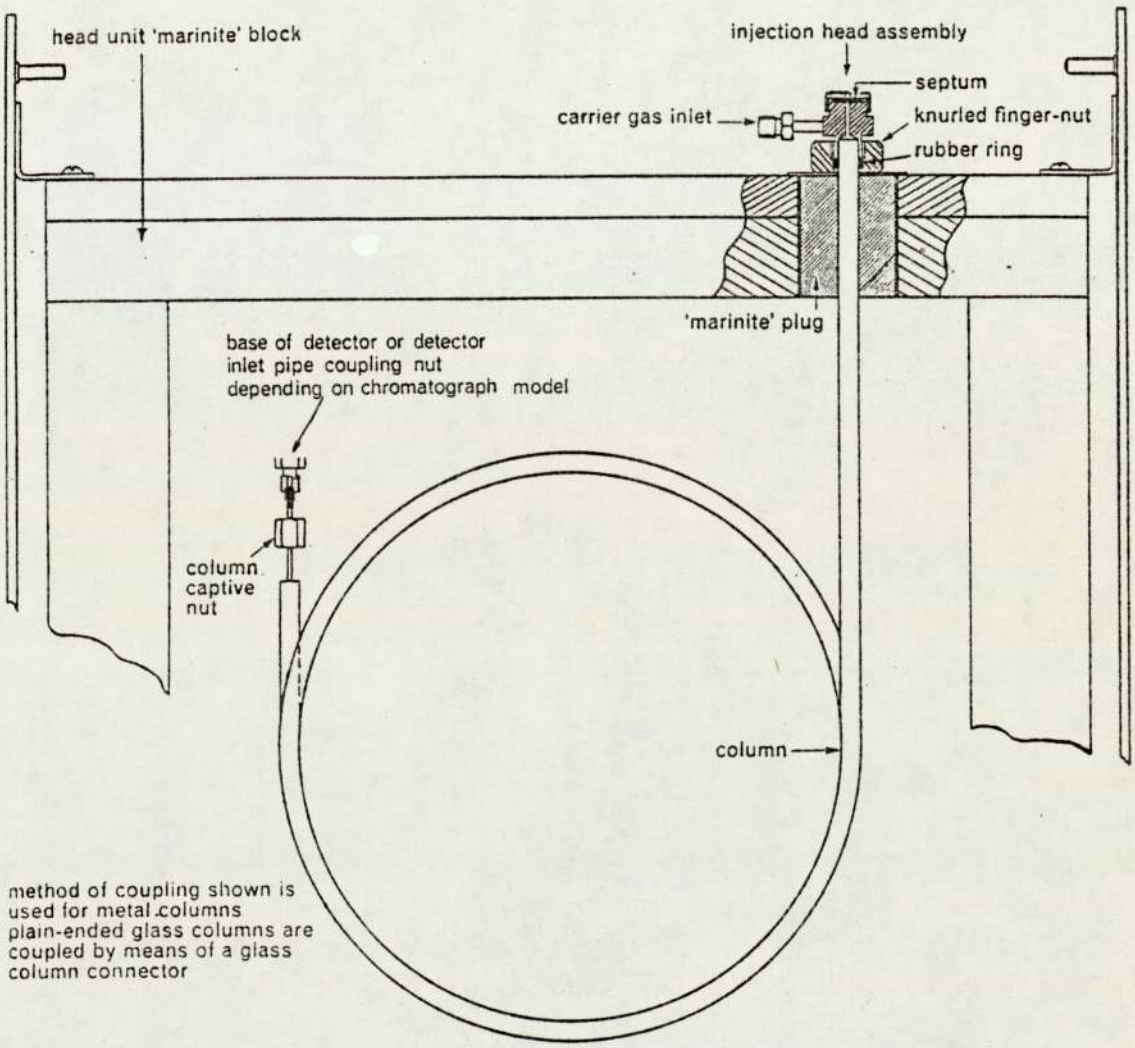

FIG. 5.6b GLASS COLUMN CONNECTOR ASSEMBLY

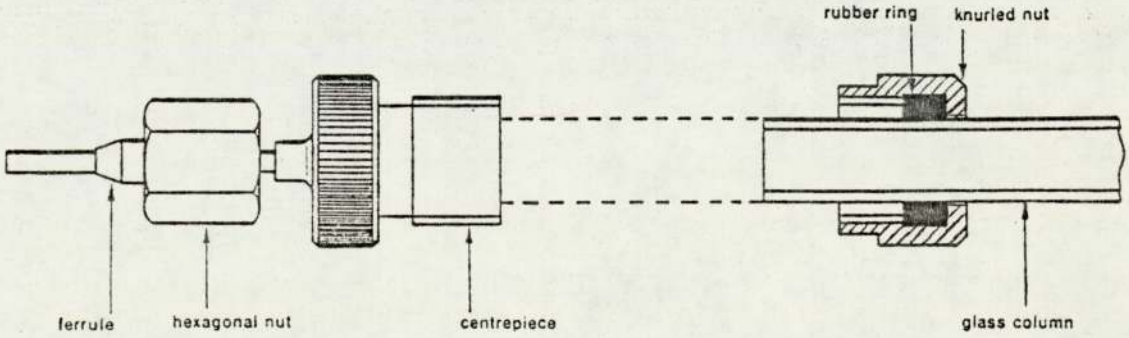

normally set at about 5 cm^3s^{-1}.

The katharometer traces obtained in the recoder were used to indicate the pseudo-steady state in the SCCR-2 unit and also any change in the feed pump or significant flow fluctuation in the purge section.

Upon recording the traces at 160-205°C the condensation problem severely affected the judgement that a pseudo-steady state had been reached. So, the alternative was to monitor the product stream's purity for two consecutive cycles as a criterion for pseudo-steady state.

5.4 THE FLAME IONIZATION DETECTOR

5.4.1 Mechanism

Quantitative analysis to obtain the concentration profile in the sequential unit was carried out using a modified Perkin-Elmer F-11 gas chromatograph (Section 5.2.2) linked to a Hewlett Packard 3373B integrator.

The detector consists of a diffusion type hydrogen burner, so that the flame is burning between two electrodes of potential difference 100-300V. The effluent gas from the column is mixed with an accurately controlled hydrogen stream. When the column effluent contains organic substances these will burn in the hydrogen flame of the detector and produce ions causing a change in the conductivity of the flame. This will consequently change

intensity of the ion current which can be recorded after an appropriate amplification.

5.4.2 Calibration of the FID Detector

Calibration of the FID detector involved relating the weight of a component in the injected sample to its peak area, as measured by the Hewlett-Packard integrator.

In this respect, for all the fatty acid esters used in this study, hexane solutions of several dilutions ranging from 1% to 10% V/V were prepared. Adequate volumes of these solutions were injected by a Hamilton 1.0 mm^3 liquid syringe into the F-11 chromatograph to determine the detector response to the respective solute weight. Calibration charts such as the one in Fig. 5.7 were constructed. A linear relationship was found to exist between concentration and peak area.

5.4.3 The Analytical Column

For the analysis of all the fatty acid esters used in this study, a glass column 182.9 cm long and 0.6 cm O.D. packed with 12.05 g of 149-125 μm chromosorb P-AW-DMCS support was used. This packing was coated with 10.06% by weight OV-275 liquid phase.

Before the analytical column was packed, it was thoroughly washed with acetone and dried by blowing

FIG. 5.7 CALIBRATION OF F.I.D. DETECTOR

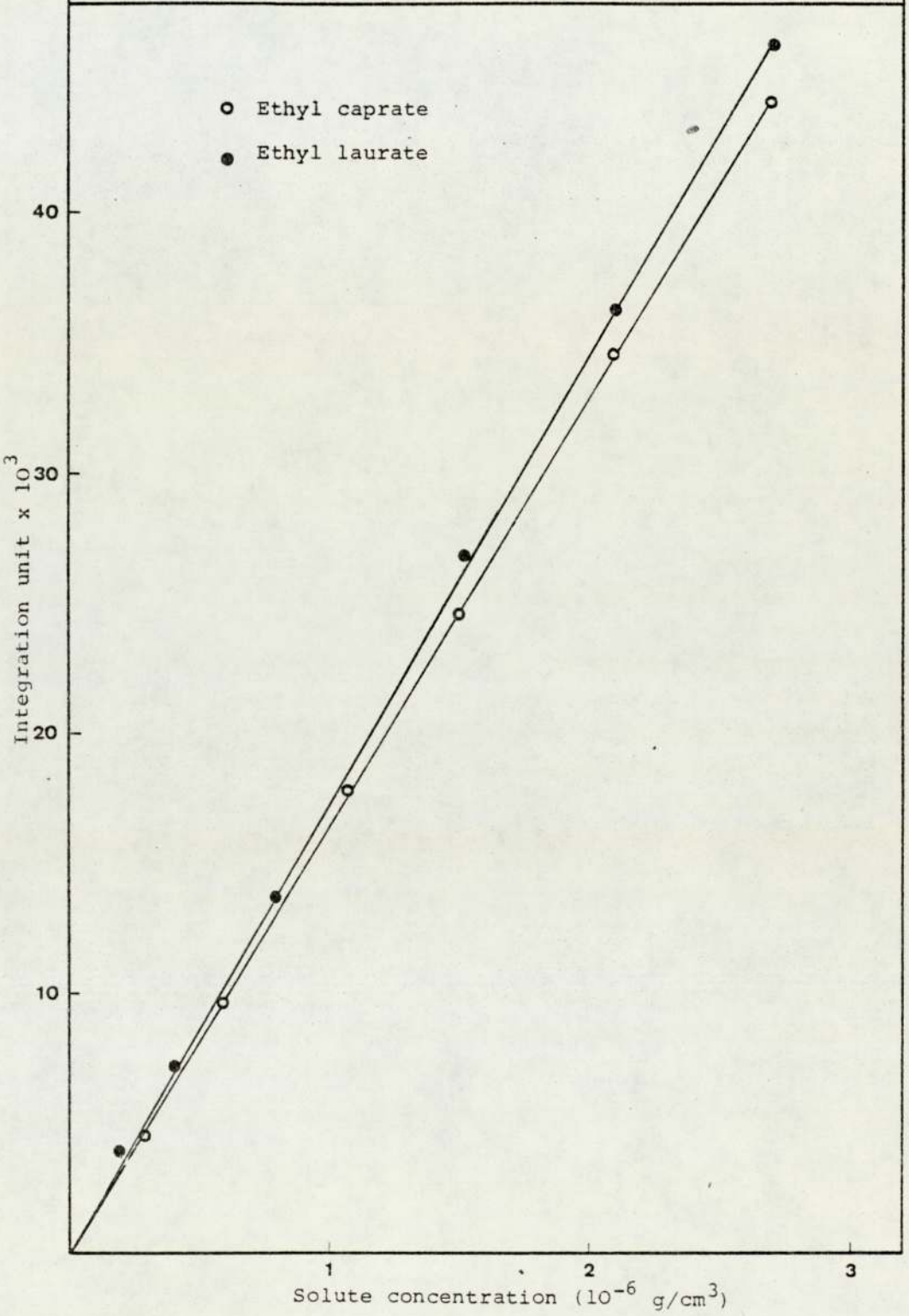

nitrogen through it. It was packed using a standard packing method S.T.P. (37). The packed column was conditioned at a temperature 20°C higher than the proposed operating temperature with nitrogen passing through the column for 20-24 hours before being used.

CHAPTER 6

OPERATIONAL MODE OF THE SCCR-2

6.1 PREDICTION OF THE OPERATING CONDITIONS

The selection of experimental conditions for the continuous fractionation of a binary feed mixture by using the SCCR-2 was based on the theory outlined by Barker and Lloyd (29, 166).

If, as with the SCCR-2, the packing is moved counter-currently to the mobile phase flow G, then the correct setting of the rate of packing movement L can make the slowest moving component travel with the packing whilst the faster moving component travels with the mobile phase. Fig. 6.1 illustrates schematically the operating conditions of the SCCR-2 unit, where the packing movement is simulated by the pneumatic valve sequencing action. The fast moving component will exit with the mobile phase at the product 1 outlet, and the slower moving components with the greater affinity for the stationary phase will be preferentially carried with the packing and exit with the purge gas at the product 2 outlet.

Mathematically, the preferential movement of component 1 in the mobile phase will be when:

$$G.\ c_1 > L.\ q_1 \qquad (6.1)$$

$$\text{i.e. } \frac{G}{L} > \frac{q_1}{c_1} \qquad (6.2)$$

where $\frac{q_1}{c_1} = K_1$ (Partition coefficient)

FIG. 6.1 SCHEMATIC DIAGRAM OF THE SCCR-2 UNIT

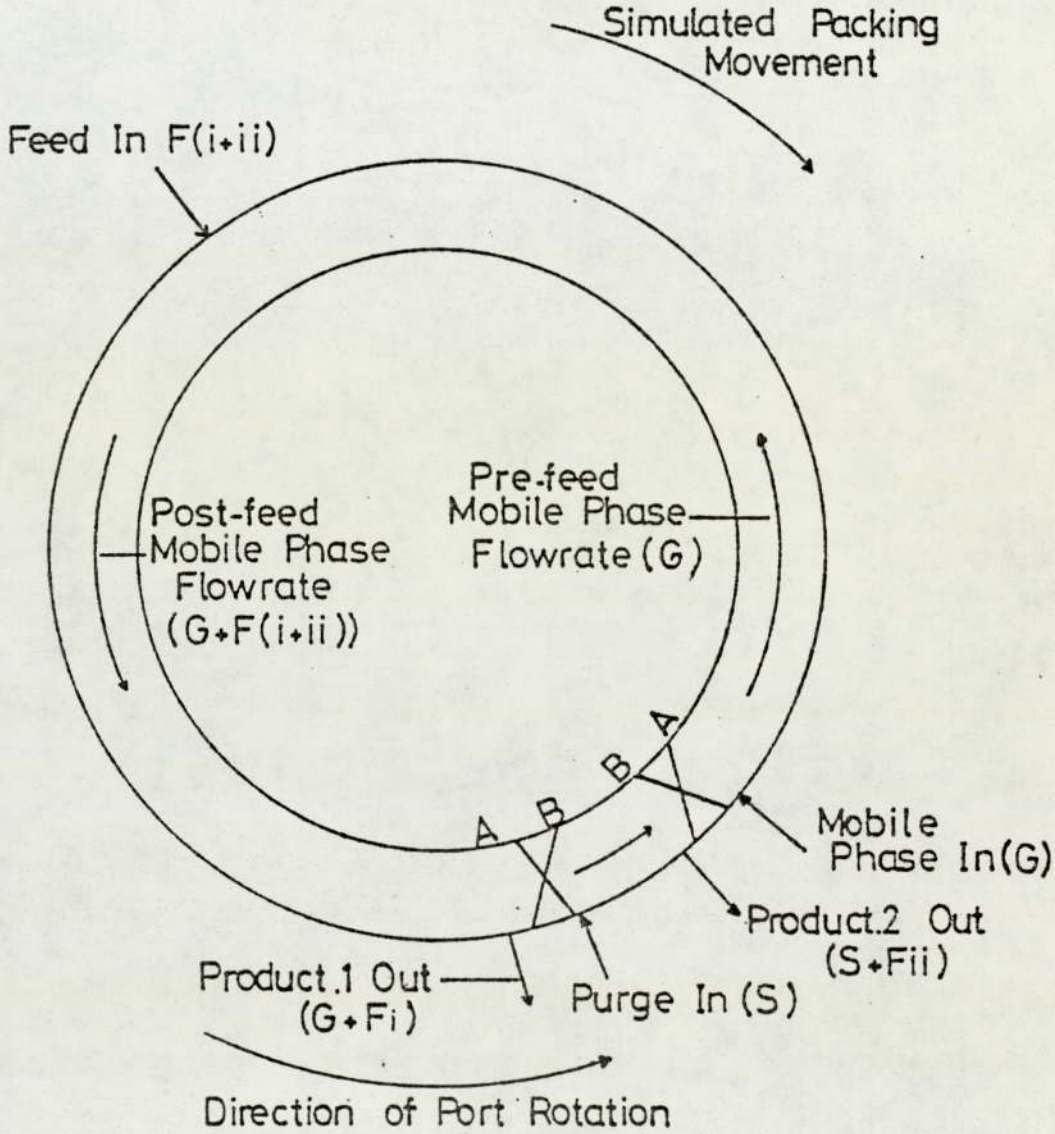

A-A Separating Section
B-B Purge Section

or $\frac{G}{L} > K_1$ (6.3)

Here c_1 and q_1 are the concentrations of component 1 in the gas and liquid phase respectively.

Similarly for component 2 to travel preferentially with the stationary phase

$$\frac{G}{L} < K_2 \quad (6.4)$$

Theoretically a separation will be achieved counter-currently when

$$K_1 < \frac{G}{L} < K_2 \quad (6.5)$$

where G/L is the ratio of volumetric mobile phase flow rate to the apparent liquid phase flow rate. Also component 2 will be completely purged from the isolated column if

$$\frac{S}{L} > K_2 \quad (6.6)$$

where S is the volumetric gas flow rate in the purge section of the SCCR-2 unit.

Equations 6.5 and 6.6 provide a basis for the selection of operating conditions. However, several factors have not been considered in the derivation of equation 6.5, and these are the following:

- finite concentration effect on partition coefficients
- finite feed flow rate

- mobile phase compressibility
- finite column length
- the sequential nature of operation
- chromatographic zone of operation
- the effect of temperature fluctuations.

Barker and Deeble (14) have shown that; to account for all these effects the inequality relation equation 6.5 becomes

$$(K_1^{\infty}+\Delta K_1+\sigma_1+\sigma_1'+S_1) < \frac{G_{min}}{L'} < \frac{G_{max}}{L'}(K_2^{\infty}+\Delta K_2-\sigma_2-\sigma_2'-S_2) \qquad (6.7)$$

while equation 6.6 becomes;

$$\frac{S}{L} > (K_2^{\infty}+\Delta K_2+\sigma_2+\sigma_2'+S_2) \qquad (6.8)$$

where

L' : the apparent volumetric stationary phase movement in the sequential unit (total volume of the liquid phase in columns/cycle time (sec)).

G_{min}, G_{max} : the volumetric mobile phase flow rates at the column inlet and outlet respectively.

K_1^{∞} : the partition coefficient of the less soluble component at infinite dilution.

K_2^{∞} : the partition coefficient of the more soluble component at infinite dilution.

ΔK_1, ΔK_2 : factors accounting for the effect of finite concentrations on the partition coefficient.

σ, σ' : factors to account for the finite column length and solute zone broadening respectively.

S_1, S_2: factors to account for the effect of the sequential nature of operation.

Equation 6.7 provides the limits for complete separation of components 1 and 2. The use of the equation requires a detailed knowledge of all the parameters involved, which requires a detailed practical and theoretical study. Many parameters in equation 6.7 are interactive, therefore definitions based purely upon experimental data are impossible. A theoretical model in Chapter 8 permits the study of the individual factors in isolation using the operational data from the SCCR-2 unit. Although it is not possible to give numerical values to many parameters in equation 6.7, but an accurate determination of the partition coefficient at infinite dilution K^{∞} is possible.

6.1.1 Determination of the Partition Coefficient

The partition coefficient K at infinite dilution may be calculated by the following equation:

$$K^{\infty} = \frac{F\left(\frac{T_c}{T_a}\right) . \left(\frac{P_o}{P_a}\right) . j . (t_R - t_m)}{V_L} \qquad (6.9)$$

where

F = carrier gas flow rate at ambient conditions

T_c = column temperature (K^o)

T_a = ambient temperature (K^o)

P_o = column inlet pressure (N/m^2)

P_a = ambient pressure (N/m^2)

t_R = retention time for absorbed component (seconds)

t_m = retention time for unabsorbed component (seconds)

V_L = volume of the liquid phase impregnated on the solid support (g/cm^3)

j = James and Martin (35) compressibility factor

$$= 1.5(P_{io}^2-1)/(P_{io}^3-1) \qquad (6.10)$$

where P_{io} = ratio of inlet to outlet column pressures (N/m^2)

Several restrictions were imposed on the application of equation 6.9. These are the following:

a - the partition coefficient is independent of concentration

b - the carrier gas ideality is assumed

c - the volume of the solute in the gas phase must not make a significant contribution to the retention volume.

d - there is no liquid or solid surface absorption.

Measurement of the partition coefficient at infinite dilution was carried out using a 0.6 cm O.D. glass column (see section 5.4.3). The small sample sizes used satisfied restrictions (a) and (c), whilst treatment (see section 5.4.3) of the analytical column to saturate

any active sites overcame restrictions (b) and (d).

In summarising the results, the partition coefficients for several fatty acid esters used in this study were determined over the temperature range 100 - 206°C and are recorded in Table 6.1. The solvent phase used in the analytical column was the same as that used in the SCCR-2 unit, namely OV-275.

The plot of $\log K_i^{\infty}$ against the reciprocal of absolute temperature gave a straight line as predicted by the thermodynamic equilibrium theory (167), Fig. 6.2.

6.1.2 Determination of the Apparent Gas to Liquid Ratio

G/L' in equation 6.7 serves as a practical guide for the experimental setting of the SCCR-2 unit. The value of G/L' was generally chosen to lie midway between the two partition coefficients of the solutes being separated.

As the carrier gas expands during its passage through the chromatograph, G/L' changes between G_{min}/L' and G_{max}/L'. Therefore it is desirable to arrange for G_{min}/L' and G_{max}/L' to be equidistant from the mid-point of the two partition coefficients. This is achieved by first redefining the G/L' ratio so that G becomes the gas flow rate at mean column pressure, G_{mc}, and secondly by using the James and Martin compressibility factor:

Table 6.1

K^{∞} Data of Some Fatty Acid Esters on OV-275 at Various Temperatures

Fatty Acid Esters			Fatty Acid Esters			Fatty Acid Esters			Fatty Acid Esters			Fatty Acid Esters		
Column Temp.	K^{∞}		Column Temp.	K^{∞}		Column Temp.	K^{∞}		Column Temp.	K^{∞}		Column Temp.	K^{∞}	
K^{o}	Ethyl acetate	Ethyl butyrate	K^{o}	Ethyl caprylate	Ethyl caprate	K^{o}	Ethyl caprate	Ethyl laurate	K^{o}	Ethyl laurate	Methyl myristate	K^{o}	Methyl myristate	Methyl stearate
331.2	59	136	381.7	58	111	433.2	74	107	443.2	80	131	453.2	42	129
341.2	40	93	393.2	46	85	440.2	69	97	453.2	52	84	463.2	41	121
351.2	32	60	403.2	39	71	447.2	63	89	458.2	40	63	467.2	40	117
374.2	17	30	414.2	30	53	465.2	55	75	461.2	38	58	478.2	37	106

FIG. 6.2 PLOT OF LOG K^{∞} VERSUS I/T FOR FATTY ACID ESTERS ON OV-275

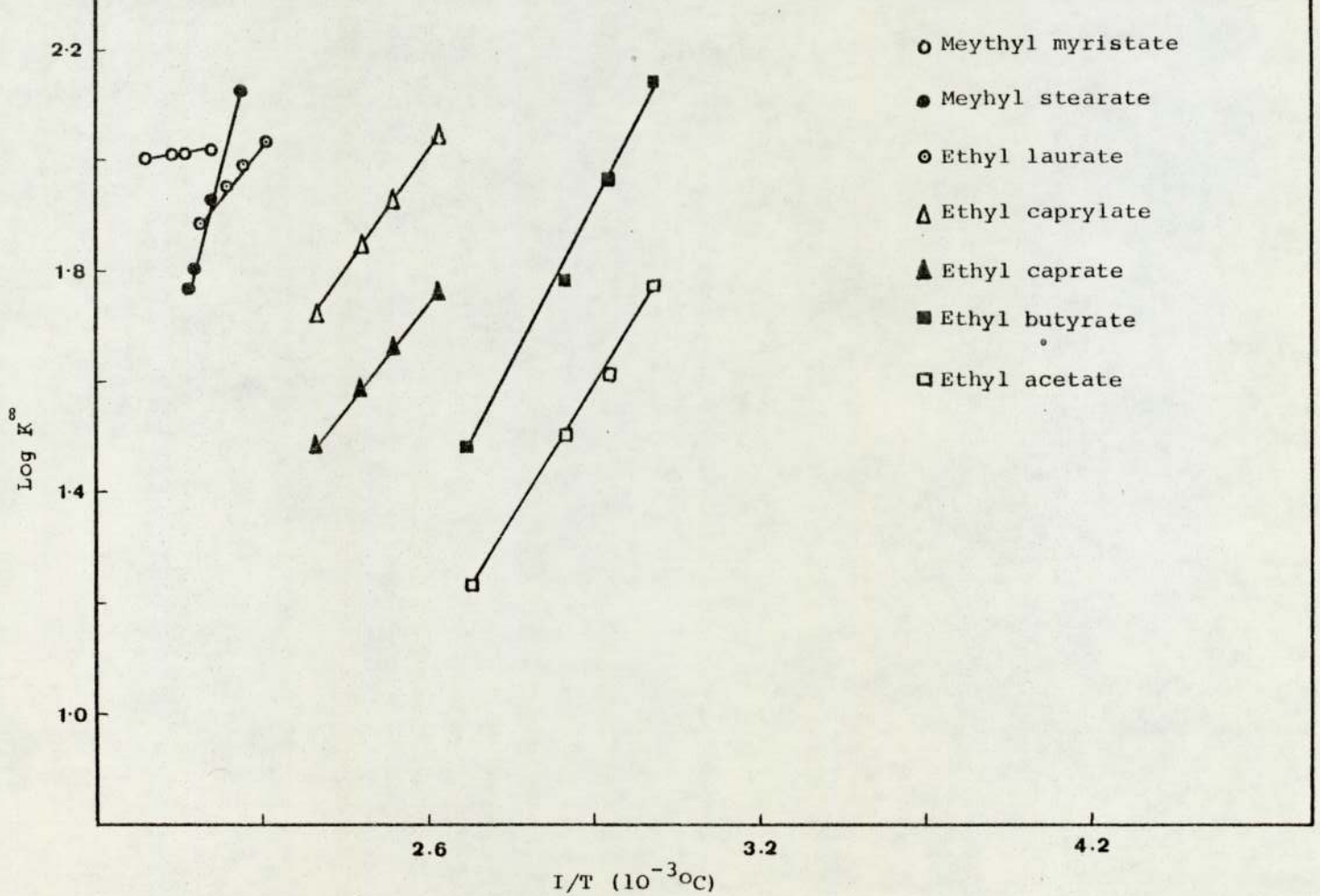

$$G_{mc}/L' = \frac{G_a \times P_a/P_o \times j}{L'} \qquad (6.11)$$

where G_a is the gas outlet flow rate measured at atmospheric pressure.

The experimental value of G_{mc}/L' tended to be higher than the theoretical mid-point value discussed above. This could be attributed to the fact that the real value of G_{mc}/L' is not the calculated value, since many effective parameters (section 6.1) were neglected in the calculation of G_{mc}/L' (eqn. 6.7). The setting of a mean column gas flow rate by adjustment of the inlet pressure and outlet flow rate requires trial and error and experience.

An example of the calculation of G_{mc}/L', S_{mc}/L' and L' are given in Appendix 2.

6.2 EXPERIMENTAL PROCEDURE AND ANALYSIS

6.2.1 "Start Up" Procedure

The following 'start up' procedure was used:

(a) the traps were thoroughly cleaned by successive washing with acetone and hexane.

(b) the SCCR-2 unit was tested for external leaks by use of a soap solution.

(c) leaks in the valves were tested for by applying nitrogen pressure in the purge section. With the carrier

gas inlet pressure regulator fully closed. The presence of gas in the separating section or in the feed distributor indicated leakage across a closed diaphragm valve. Location of the exact faulty valve was assisted by manually 'skipping' the isolated column around the cycle, depressurizing the carrier section between each sequencing step, and observing the effect on the leak rate. Appropriate action was taken to eliminate any malfunctioning valves.

(d) to test the feed valves, nitrogen pressure was applied to the feed distributor and all the feed valves were checked by a soap solution while closed and disconnected from the columns.

(e) having checked that the unit was operating correctly, the feed could be introduced. Air was completely displaced from each feed line via the open vertical arm of the tee-connection immediately preceding the closed diaphragm valve. Thus when liquid issued from the "tee" it was firmly capped with a stainless steel silver soldered nut.

(f) the oven takes 2-3 hours before the start of a run in order for a steady temperature to be established around the 12-column system. During that period, nitrogen was flowing through separating and purge sections of the SCCR-2 unit to purge out any chemicals from previous

experiments and to recondition the packing.

(g) the gas flow rates of purge and separating section were adjusted to the values selected according to the procedure in section (6.1.2). Meanwhile, the feed diaphragm valves were kept closed by disconnecting the appropriate air lines from the pneumatic control box, until with continued pumping the liquid feed pressure becomes approximately equal to the mid-pressure of the separating section. This precaution was taken to avoid surging from, or 'blow-back' into, the feed distributor network.

(h) finally the digital timer in the control box was adjusted to the selected sequencing time interval and a fine adjustment of the feed throughput was made by the micrometer setting on the pump head (Appendix 1).

(i) the 'shut down' procedure was basically the reverse of the 'start up' technique, namely:

1 - switch-off the feed pump and the oven electric heater.

2 - disconnect the traps and empty the feed distributor.

3 - although at this stage feed stock was no longer entering the unit, solute present in the chromatograph continued to circulate for many cycles and therefore is was necessary to purge out

continuously for 2-3 hours. Once the oven temperature cooled to room temperature, all the electrical switches function and the main gas supply were shut off.

6.2.2 Column to Column Concentration Profile

True steady state could not be achieved within the SCCR-2 due to the fact that it is semi-continuous in its operation. However, a point is eventually reached where the dynamic profile for the unit is reproduced from one cycle (12-sequences) to another. This on-set of 'pseudo-steady-state' was observed by the two following methods:

1. by the katharometer traces, which were not very reliable due to the condensation problem in the lines at an operating temperature of 160°C and above, and
2. by monitoring the purity level of the product streams in two consecutive cycles.

In general the unit was allowed to function a further 2-3 cycles after equilibrium was reached before any samples were taken.

Gas samples were taken from the sequential unit (SCCR-2) from a fixed sampling point for quantitative analysis. This was achieved by absorbing the gas stream from the column

through a short capillary sampling line into two glass tubes (20 cm long, 0.6 cm O.D.) connected together in series by a stainless steel capillary tube. Each tube contained 8 ml of ethyl acetate maintained at $4^{o}C$. The sampling time was timed at 30-50 seconds after the sequencing action for a period of 100 seconds.

The method proved to be suitable by having three glass tubes in series and by monitoring the traces of product collected in each of them (Section 7.6). The samples were capped in sample bottles and analysed immediately. The resultant profile from this method of sampling was equivalent to sampling all twelve columns at the same instant. Sampling for more than one cycle in this manner confirmed that the unit had reached and remained in a steady-state of operation.

Gas flow through the sampling line was measured using a soap bubble flow meter (1-100 cm^3) and it was corrected to the ambient conditions. Injection of the sample into the flame ionization detector produced a peak area expressed in integrator units, and from the appropriate calibration charts, the injection solute mass was calculated.

A standardised concentration has been adopted for comparison of experimental results consisting of the

the analysed solute mass divided by the sample volume corrected to atmospheric pressure.

Each successful experimental run is characterised with a unique title which includes the four main operating variables; the operating temperature (^{o}C), the feed rate ($cm^{3}h^{-1}$), the ratio of the mean column gas flow rate to the apparent liquid rate, and the sequencing rate (s).

Fig. 6.3 gives an example of the results taken during a separation run of the SCCR-2.

Basic programs were used to compute the run condition (flow chart - Fig. 6.4, listing - Appendix 3), and the concentration profile (flow chart - Fig. 6.5,listing - Appendix 3).

FIG. 6.3 EXAMPLE OF RECORDED DATA FOR AN EXPERIMENTAL RUN

RUN DESCRIPTION

System: 50/50 V/V-Ethyl caprylate/ Ethyl caprate

Temperature
- Oven : 105°C
- Purge in : 125°C
- Carrier in: 120°C

Ambient conditions
- Pressure : 101.3 kPa
- Temper. : 24°C

G_{mc}/L' : 95

Switching rate: 150 s

Feed rate : 30 $cm^3 h^{-1}$

Separating section
- Pin : 274 kPa
- Pout: 177 kPa
- Ga : 17.2 $cm^3 s^{-1}$

Purge section
- Pin : 198 kPa
- Pout: 130 kPa
- Sa : 124 $cm^3 s^{-1}$

ANALYSIS DESCRIPTION

Katharometer
- Gas flow : 4.1 $cm^3 s^{-1}$
- Bridge current: 115 mA
- Bridge voltage: 18 V
- Sensitivity : 9.7

Sampling valve
- Temperature : ambient
- Pressure in Sample loop : ambient
- Sample volume : 0.26 cm^3 (corrected to N.T.P.)

- Pressure H_2 : 225 kPa
- Pressure O_2 : 265 kPa
- Flow N_2 : 0.7 $cm^3 s^{-1}$
- Sensitivity 1×10^4
- Column temper: 108°C
- Chromat. Column Specific: 182.9cm long and 0.6cm O.D glass column with 12.05 g packing, 10.06% of OV-275 on chromosorb P-AW

CONCENTRATION		PROFILE		ANALYSIS	
The samples were taken from column 12, 100 sec after sequencing action on the 8th cycle					
Isolated Columns	Distance of sample point from product 1 outlet (cm)	Integrator units		Concentration (std)	
		Product 1	Product 2	Product 1 $\times 10^{-6} g\ cm^{-3}$	Product 2 $\times 10^{-6} g\ cm^{-3}$
1	61	8411	<100	41.9	0.0
2	122	13610	<100	67.9	0.0
3	183	20220	462	100.9	1.9
4	244	21820	3004	108.9	13.0
5	305	22220	3928	110.9	17.0
6	366	6608	5546	32.9	24.0
7	427	400	9244	1.9	40.0
8	488	400	8088	1.9	35.0
9	549	<100	8551	0.0	37.0
10	610	<100	6433	0.0	30.0
11	671	<100	924	0.0	3.9
12	732	<100	462	0.0	1.9

FIG. 6.4 FLOWCHART FOR THE COMPUTATION OF RUN CONDITIONS

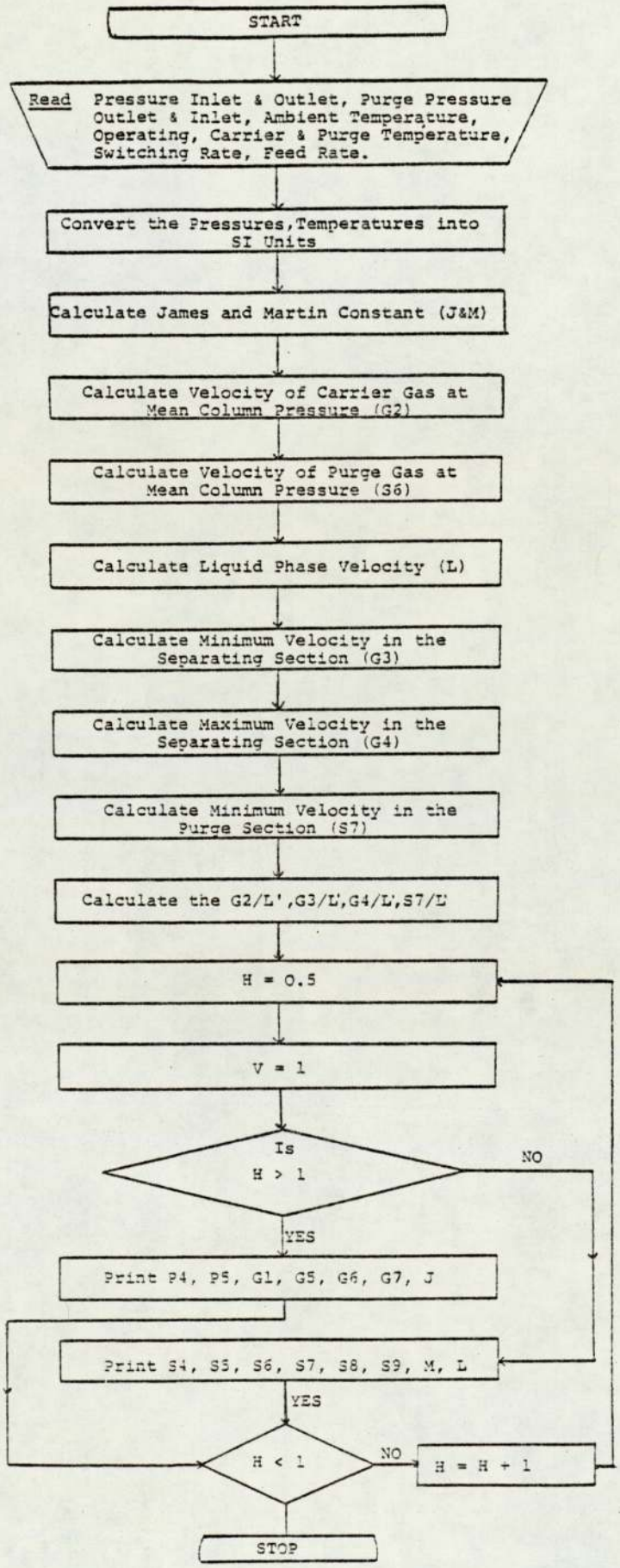

FIG. 6.5 FLOWCHART FOR THE COMPUTATION OF THE SOLUTE(S) CONCENTRATION PROFILES

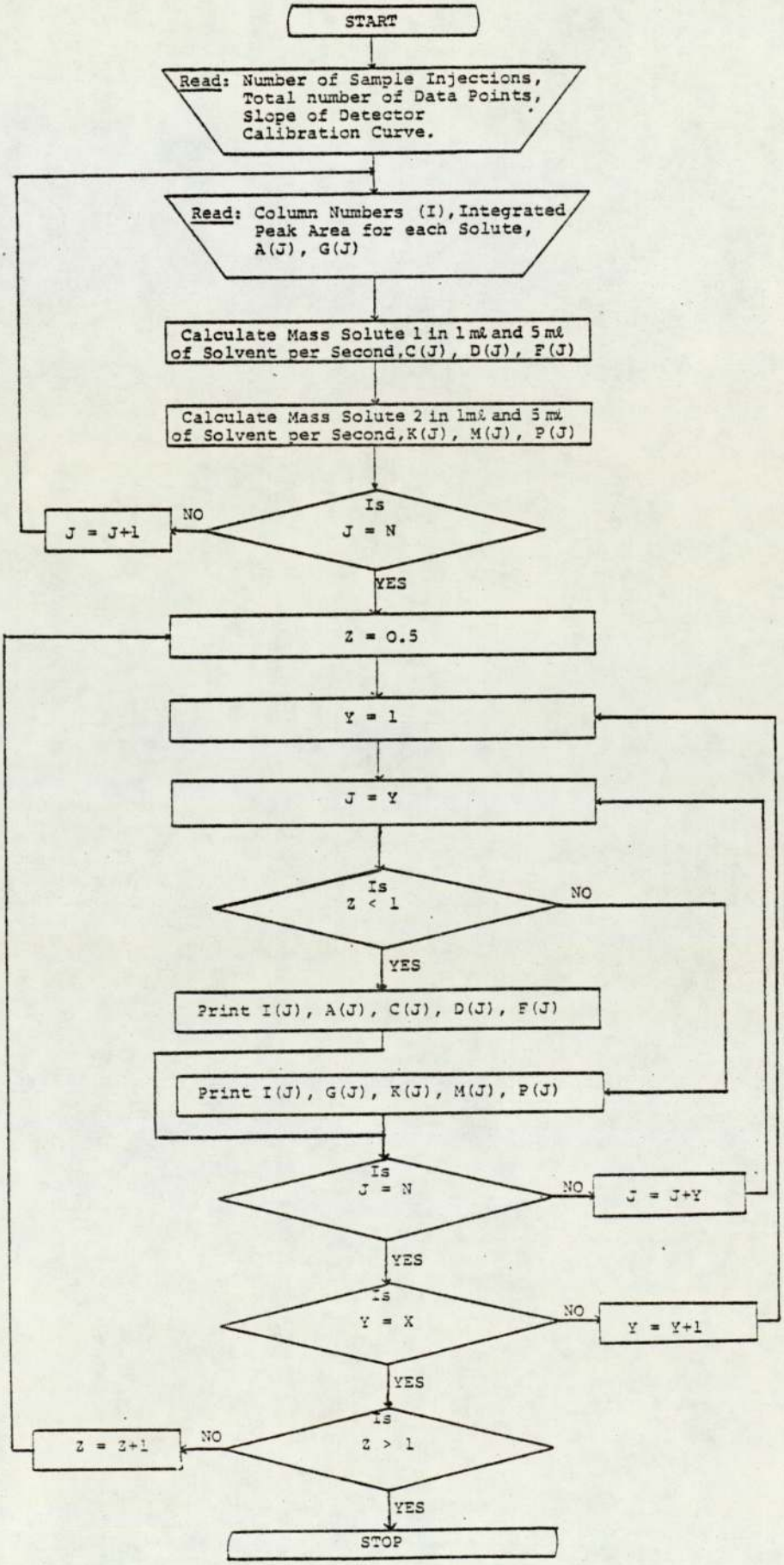

CHAPTER 7

SEPARATION STUDIES ON THE SCCR-2 UNIT

7.1 INTRODUCTION

Several separations were performed on the SCCR-2 unit. The objectives of these experimental studies were to determine the separating capabilities of the unit at higher temperatures than previous workers (13,16,31).

For this reason the separation of binary chemical mixtures of different separation difficulty and volatility were studied on the SCCR-2 equipment. The systems were selected with separation factors ranging from 1.45 to 2.3, and these required an operating temperature in the range of 105-205°C. The chemical mixtures used in this study and their physical properties are summarised in Table 5.2.

A 50:50 mixture of the component chemicals was used for all systems except for the mixture of ethyl laurate and methyl myristate, which was 70:30 respectively, because of the high price of methyl myristate. Also, ethyl acetate was used as a solvent to prepare the feed stock for the (50:50 W/W) methyl myristate/methyl stearate system, since methyl stearate is a solid at room temperature. Ethyl acetate constituted 25% of the total feed mixture.

Initially, the efficiency in terms of HETP of four randomly chosen columns in the SCCR-2 unit was obtained. A chemical mixture of ethyl acetate/ethyl butyrate was used as a commissioning system. This was followed by

increasingly more difficult mixtures of fatty acid esters such as; ethyl caprylate/ethyl caprate, ethyl caprate/ethyl laurate, ethyl laurate/methyl myristate and methyl myristate/ methyl stearate.

The performance of the SCCR-2 equipment in the separation of these mixtures was recorded as column to column concentration profiles and product purities except for the mixture of methyl myristate/methyl stearate. This was because condensation problems in the sampling lines and the associated loss of material prevented the construction of an exact concentration profile.

7.2 H.E.T.P. MEASUREMENTS AT DIFFERENT TEMPERATURES AND FOR DIFFERENT SOLUTES

7.2.1 Introduction

The conventional column performance term in chromatography is the H.E.T.P. which essentially relates the width of the eluted peak to the column length. However, the size and shape of the peak is mainly determined by the chromatographic process occurring within the column. Despite the empirical nature of the H.E.T.P. and the inability of the plate theory to relate some solute zone broadening mechanisms to it (partition phenomena, molecular diffusion and flow patterns through packed beds), H.E.T.P. has a considerable value for comparing the efficiency of chromatographic columns.

In this work, the Sternberg theory (168) was employed which takes into account the above mentioned factors. According to this theory the H.E.T.P. is given by the following equations:

$$H = \frac{\ell . |(\sigma_t)^2_{r.o} - (\sigma_t)^2_{r.i}|}{|(t_{r.o.c.} + \bar{t}_{r.o}) - (t_{r.i.c.} + \bar{t}_{r.i})|^2} \qquad (7.1)$$

where ℓ = column length (cm)

σ_t^2 = time based 2nd moment or variance (seconds)

$\bar{t}_{r.o}, \bar{t}_{r.i}$ = peak mean or 1st moment in seconds for the recorded outlet and injection profiles respectively.

$t_{r.o.c}, t_{r.i.c}$ = time (seconds) from injection to commencement of recording the outlet and injection profiles respectively.

Also $$\bar{t}_{r.o}, \bar{t}_{r.i} = \frac{S_1}{S} = \frac{\sum_{J=1}^{N'} |F(J).I.J|}{\sum_{J=1}^{N} F(J)}$$

$$(\sigma_t)^2_{r.o} \text{ or } (\sigma_t)^2_{r.i} = \frac{S_2}{S} \sum_{J=1}^{N'} \frac{|F(J).(I.J - \frac{S_1^2}{S})|}{\sum_{J=1}^{N} F(J)}$$

hence

I = time interval between data points (seconds)

F(J) = profile heights in order of recording (cm)

N' = number of profile height data points.

The H.E.T.P. values of four randomly chosen chromatographic columns of the SCCR-2 machine, were experimentally determined under various operating conditions such as gas flow rate, and column temperature. The aim of this part of the work can be summarised as follows.

(a) To compare the efficiency of the columns at temperatures ranging from 100 - 200° C in terms of the number of plates for different solutes.

(b) To investigate the effect of the carrier gas flow rate and the nature of the solutes on the efficiency of the columns.

7.2.2 Experimental Procedure

Fig. 7.1 diagrammatically represents the arrangement for the determination of H.E.T.P. Basically one column was isolated from the sequential unit and a constant inlet gas pressure applied. A 0.1 cm^3 sample of each solute was injected directly into the gas stream flowing into the column at (A) in Fig. 7.1. The profile was monitored by the katharometer in conjunction with the pen recorder.

For each injection and outlet profile the respective $t_{r.i.c}$ and $t_{r.o.c}$ times were measured by a stop watch. In addition for each profile the values of peak heights at equal time increments were read on the calibrated recorder chart. The time increment was chosen to give between 30-50 values of peak height for statistical

FIG. 7.1 THE ARRANGEMENTS OF SCCR-2 FOR HETP DETERMINATIONS

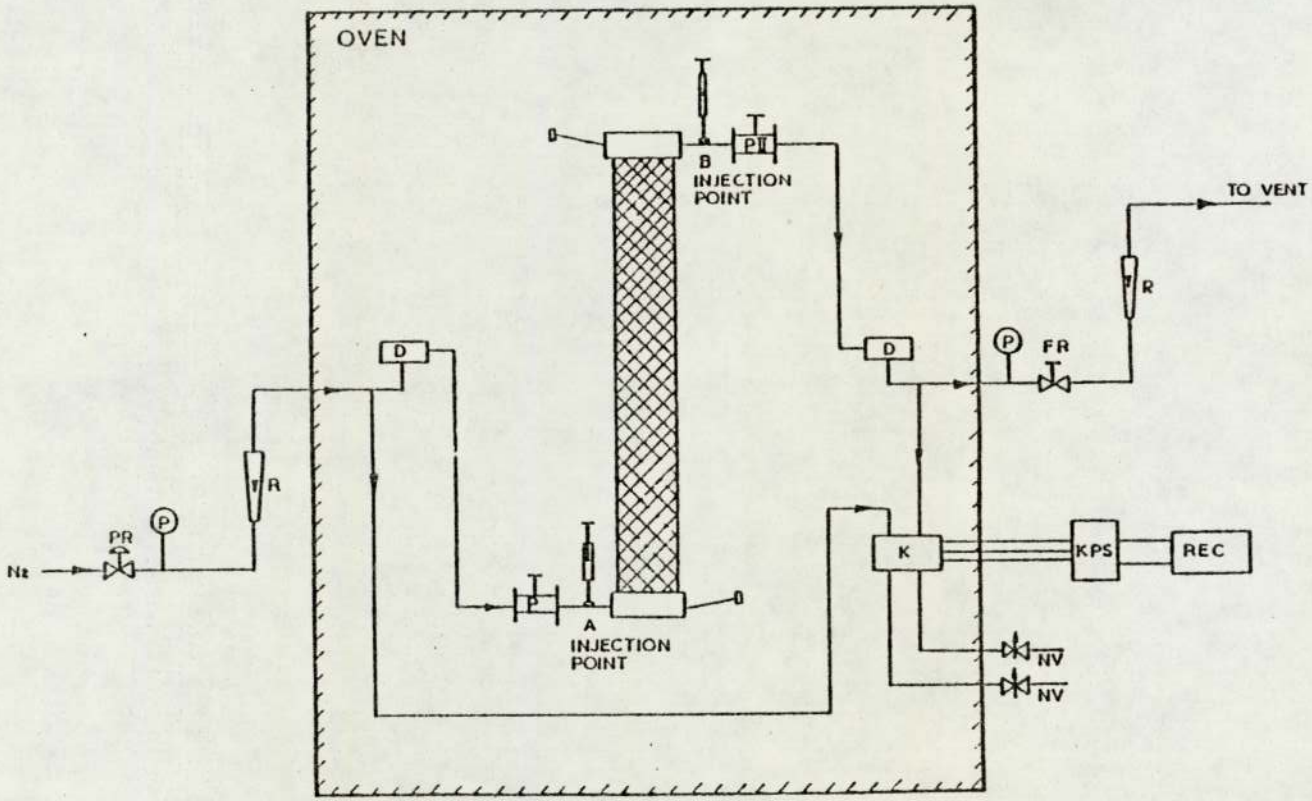

LEGEND			
	P - PRESSURE GAUGE	D - DISTRIBUTOR	K - KATHAROMETER
	R - ROTAMETER	P - PURGE DIAPHRAGM VALVE	KPS - KATHAROMETER POWER SUPPLY
	NV - NEEDLE VALVE	PII - PRODUCT II DIAPHRAGM VALVE	R - RECORDER

significance. The data taken for a pair of injection and outlet profiles were then applied to equation 7.1 for the H.E.T.P. determination.

7.2.3 Results

The number of theoretical plates calculated for a small sample injection, in which peak distortion is not present, is dependent on the carrier gas flow rate and the column temperature. Table 7.1 and Fig. 7.2 illustrate the number of theoretical plates in four columns using a 0.1 cm^3 sample of ethyl caprate and a column temperature of 100°C for various nitrogen carrier gas flow rates. The results indicate that the maximum number of theoretical plates per column occurred at a carrier gas flow rate of about 1.5 cm^3 sec^{-1}. Carrier gas flow velocities lower than about 1.5 cm sec^{-1} resulted in a rapid decrease in the number of theoretical plates. However, the variation from column to column is the result of the variation in the packing, a similar phenomena being reported by Deeble (13), Bell (31) and Liodakis (16). Fig. 7.3 and Table 7.2 show a comparison between the number of theoretical plates of columns obtained from the sample peaks of 0.1 cm^3 injections of three fatty acid esters at various column temperatures. It is apparent that column resolution decreases with increasing temperature, and varies with the chemical nature of the injected sample.

Table 7.1

Summary of the H.E.T.P. Determination for the SCCR-2 Unit

Mean Carrier Gas Velocity	Number of Theoretical Plates			
$cm\ s^{-1}$	Column 4	Column 6	Column 8	Column 12
0.6	38	33	26	36
0.8	44	36	30	40
1.18	49	43	38	47
1.7	53	41	36	47
2.3	42	33	23	37
3.0	23	21	18	20

Table 7.2

Summary of the H.E.T.P. Determinations at Different Temperatures

Column Temperature	Number of Theoretical Plates			Note
^{o}C	Ethyl caprate	Ethyl laurate	Methyl myristate	
110	36	44	54	1. Carrier
115	28	32	40	Gas Velocity
160	20	25	33	$2.0\ cm\ sec^{-1}$
190	14	21	29	2. Sample
200	13	19	27	size $1.0\ cm^{3}$

FIG. 7.2 VARIATION OF THE NUMBER OF THEORETICAL PLATES WITH CARRIER GAS FLOW RATE

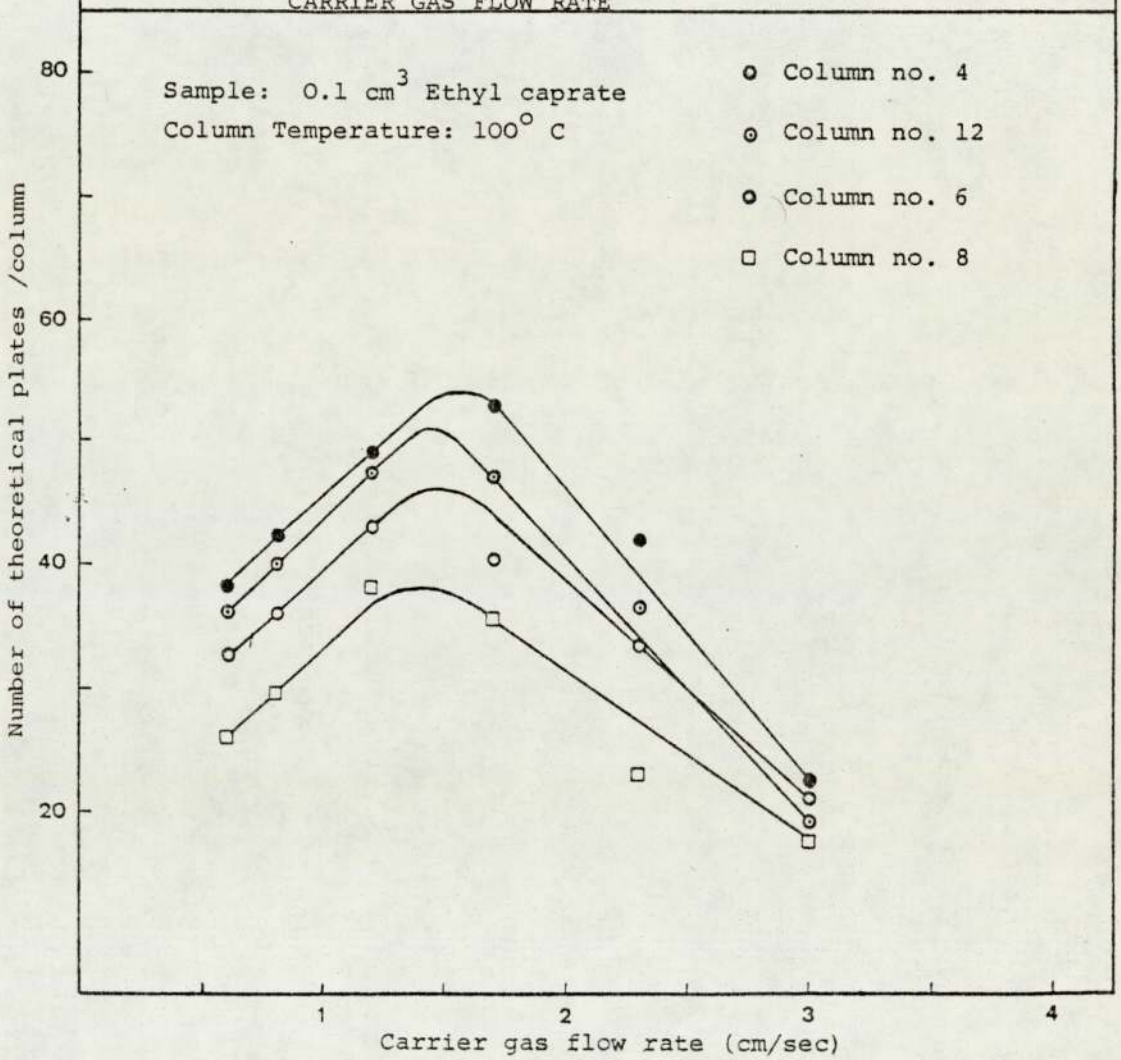

FIG. 7.3 VARIATION OF THE NUMBER OF THEORETICAL PLATES WITH COLUMN TEMPERATURE

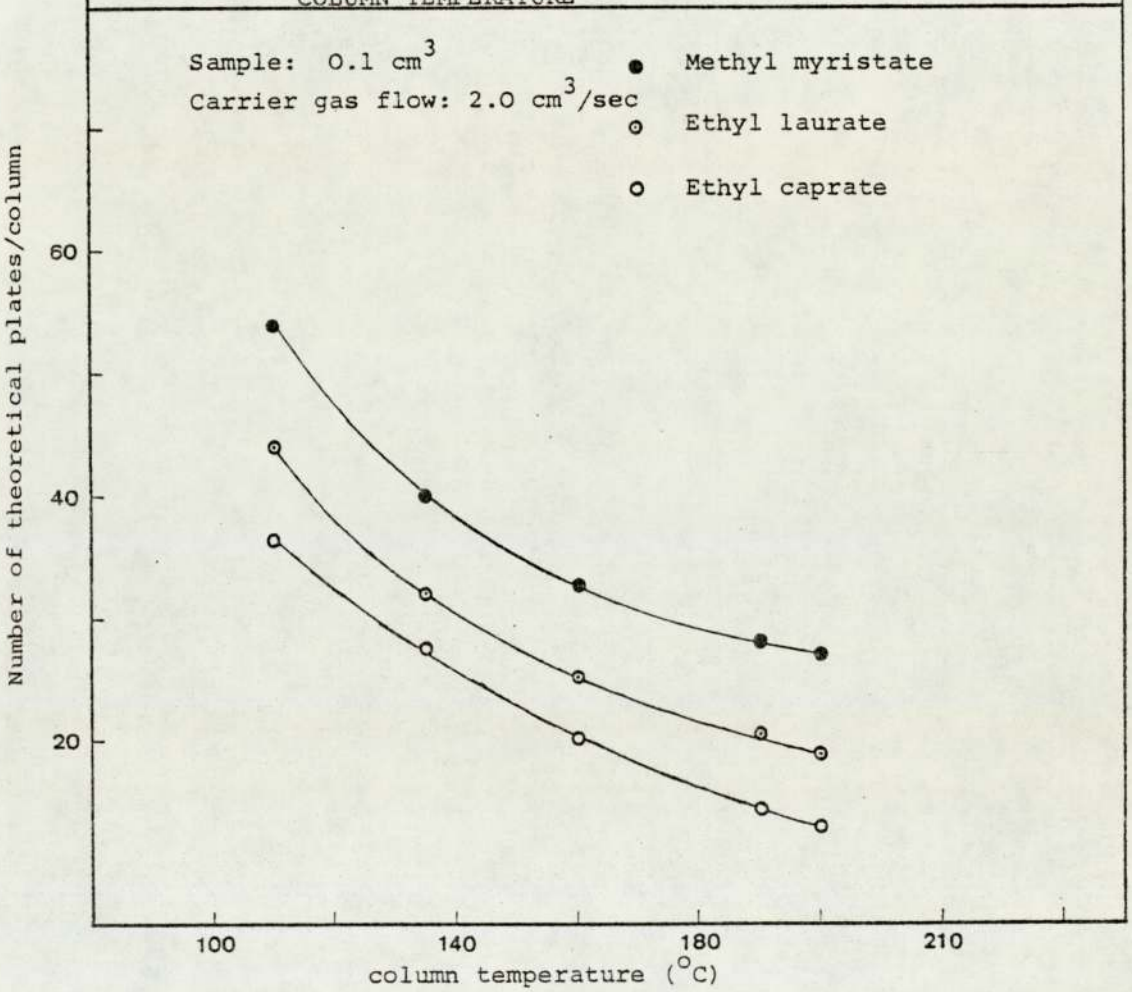

7.2.4 Discussion

From the results in Fig. 7.2 (Table 7.1) the variation from column to column appears to affect the SCCR-2 unit in the separating mode. This variation is probably the result of the difference of carrier gas velocity between the columns. Non-uniform carrier gas flow in large diameter columns has been reported (52) as a result of the point to point difference in diameter of the support particles, which also differs between columns irrespective of the uniformity and the care with which the column is packed. However, in the SCCR-2 unit, 10 columns are linked to form the main separating section. Thus in sequencing through the cycle the variation in the total number of plates in the separating section at any time is considerably reduced. Further, as the unit is to be operated at high solute concentrations it is to be expected that with the consequent further decrease in the number of plates the column to column variation would diminish. Experimental observations by Deeble (13) proved that the number of plates per column gradually decreases as the solute concentration in the solvent increases with increased throughput.

The results in Fig. 7.3 (Table 7.2) suggest that the maximum efficiency of the columns under investigation occurs at low column temperatures. However, the selection of the proper column operating temperature has been shown to be an especially important variable because the sample separation

efficiency varies greatly with the column temperature. At a relatively low column temperature for a given sample the separation factor is large and sample loading may be quite high per unit area of column bed. Such high sample loading results in peak distortion and wide sample bands. The results also indicate the dependence of the number of plates in the column on the type of solute used (Fig. 7.3).

Although the H.E.T.P. measurement is implicitly affected by many pronounced physical parameters such as the flow rate, the sample size, pressure drop ... etc., it is also affected by the chemical nature of the solutes. The interaction between the solutes and the solvents affects to a certain extent zone broadening and consequently the H.E.T.P.

The experimental comparison of the individual column characteristics emphasised the importance of the packing technique in large-scale chromatography. A small number of plates coupled with variation in column to column characteristics, represents a limitation on the separating potential of the SCCR-2 unit with very difficult separations of S.F 1.2 and less. However, the variation in column characteristics is minimized in operation as explained above.

On the basis of the above results, the theoretical

plate concept predicts that maximum resolution for the sample mixture under investigation occurs at relatively low column temperatures and a low carrier gas flow rate. It is a broad generalisation to assume that the same operating conditions apply to this work, since the H.E.T.P. measurements were made in the batch mode, while in practice the separation process which takes place in the SCCR-2 is semi-continuous. Therefore, the H.E.T.P. measurements have only qualitative value in comparing the column to column variations in the SCCR-2. Further tests on the performance of the SCCR-2 unit after the overhaul servicing was made by separating an easy mixture of ethyl acetate/ ethyl butyrate at 60° C.

7.3 ETHYL ACETATE AND ETHYL BUTYRATE SEPARATION AT 60°C WHICH WAS USED FOR COMMISSIONING THE SYSTEM

7.3.1 Results

Three separation runs are presented her, details of the operating conditions being given in Table 7.3. The three runs cover a range of throughputs of 20-40 cm^3 h^{-1}, the carrier gas and sequencing rates being maintained approximately constant.

Each experimental run is denoted by a combination of the four main operating variables, the operating temperature (C^{o}), the feed rate (cm^3 h^{-1}), the ratio of the mean column gas flow rate to the apparent liquid rate, and the sequencing rate (s). Thus, in the present

study the runs 60 - 20 - 143 - 60, 60 - 30 - 146 - 200, and 60 - 40 - 140 - 200 show the effect of increasing the throughputs.

The mean column purge gas rate, S_{mc}, was always set such that S_{mc}/L' was substantially in excess of the partition coefficient of ethyl butyrate at infinite dilution, thereby ensuring regeneration of the isolated column.

The product purities quoted in Table 7.3 are simply a chromatographically measured ratio of the two feed components trapped at the end of the run. However, the column to column concentration profile was considered earlier as the main record of performance of the SCCR-2 machine. Samples were taken close to the end of a sequencing interval using a gas sampling valve connected to the SCCR-2 and the analytical GLC unit. The reproducibility of the concentration profile was tested by comparing profiles obtained during different sequencing cycles from a fixed sample point (Figs. 7.4 - 7.6).

7.3.2 Discussion

For the duration of a sequencing interval the main separating section operates as a conventional frontal elution chromatographic system. The progress of the respective components through the column was followed by plotting the standardised concentrations for two consecutive cycles. Both solutes travel towards the product 1 exit

Table 7.3

The Separation of Ethyl Acetate/Ethyl Butyrate

Run Title	Temperature			Ambient Conditions		Solute Mixture Feedrate	I_s	L'	Separating Section					Purge Section				
	Opera-tion	Carrier Inlet	Purge Inlet	θ_a	P_a				G_a	P_{in}	P_{out}	J_3^2	G_{mc}/L'	S_a	P_{in}	P_{out}	J_3^2	S_{mc}/L'
θ-f-G_{mc}/L'-I_s	°C	°C	°C	°C	KP_a	cm^3h^{-1}	s	cm^3s^{-1}	cm^3s^{-1}	KP_a	KP_a	-	-	cm^3s^{-1}	KP_a	KP_a	-	-
60-20-143-200	60	65	68	21	101	20	200	0.08	21.25	239	183	0.86	143	183	205	183	0.79	1130
60-30-146-200	60	64	67	21	101	30	200	0.08	21.7	239	182	0.86	146	183	205	183	0.79	1130
60-40-140-200	60	63	65	21	101	40	200	0.08	21.25	243	186	0.86	140	183	205	183	0.79	1130

Summary of Results

Run Title	K^∞		Separating Section		Purge Section	Total Time of run	Total No. of Cycles	Time to Pseudo Steady State	Concentration Profile Analysis			
	Ethyl acetate	Ethyl butyrate	G_{min}/L'	G_{max}/L'	S_{min}/L'				Time to Analysis	Figure	Product Purities	
θ-f-G_{mc}/L'-I_s	-	-	-	-	-	h	-	h	h	-	%E.Ac.	%E.B.
60-20-143-200	57	134	129	166	1307	9	11	2	3.0	7.4	99.5	99.4
60-30-146-200	57	134	131	170	1307	9	11	2	3.0	7.5	99.5	99.2
60-40-140-200	57	134	126	163	1307	9	11	2	3.0	7.6	99.3	99.0

FIG. 7.4 CONCENTRATION PROFILE FOR RUN 60-20-143-200

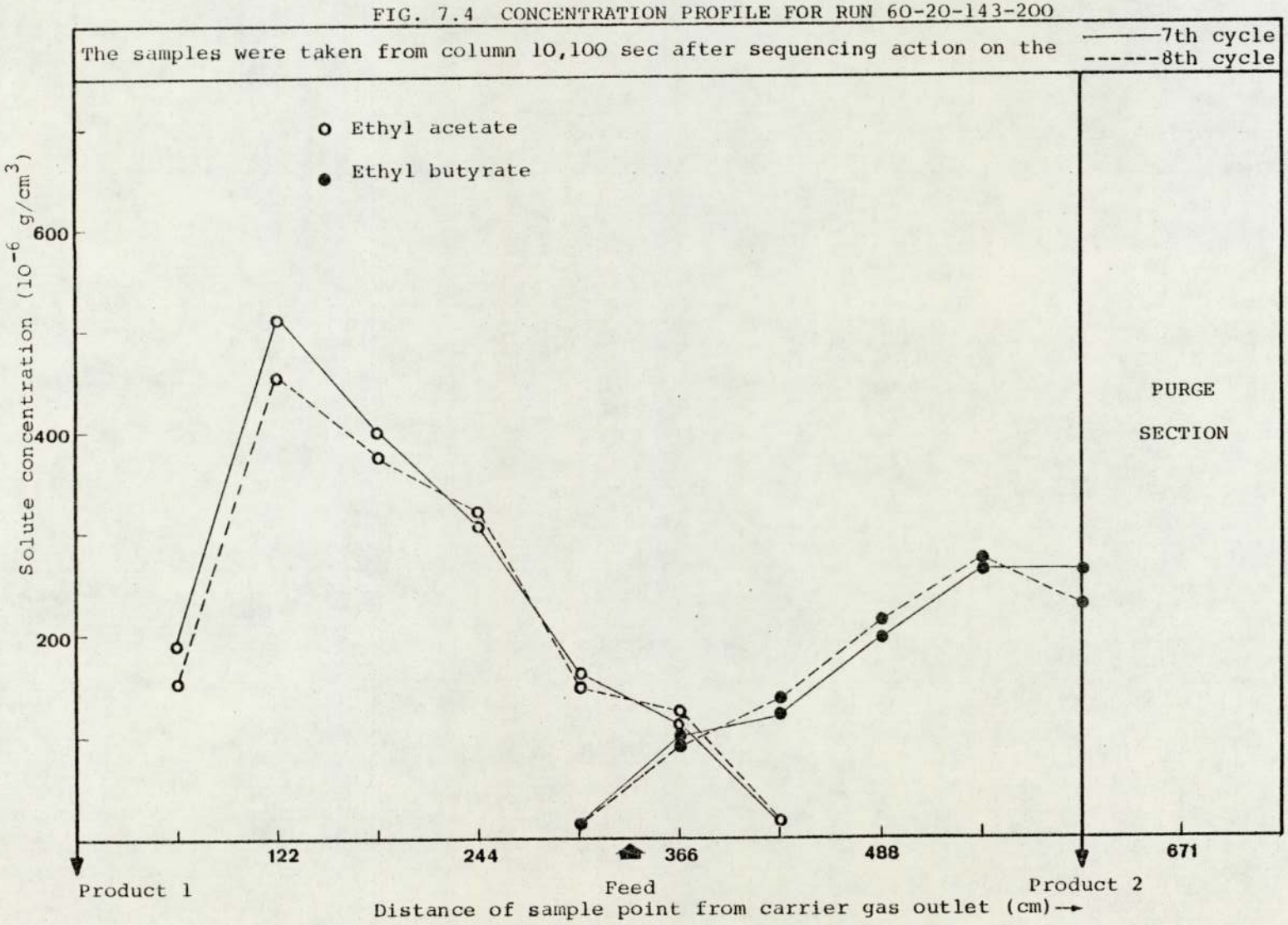

FIG. 7.5 CONCENTRATION PROFILE FOR RUN 60-30-146-200

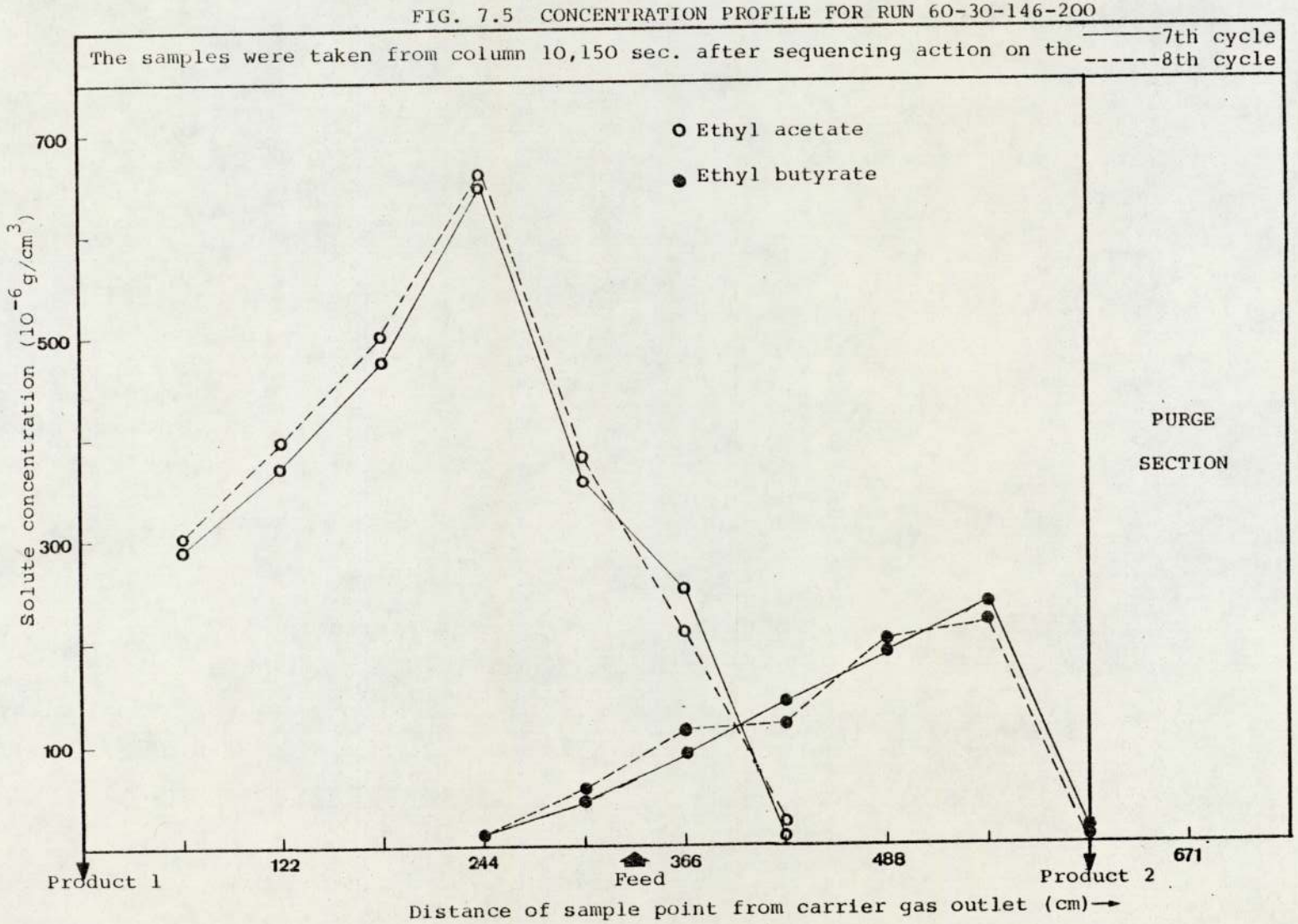

FIG. 7.6 CONCENTRATION PROFILE FOR RUN 60-40-140-200

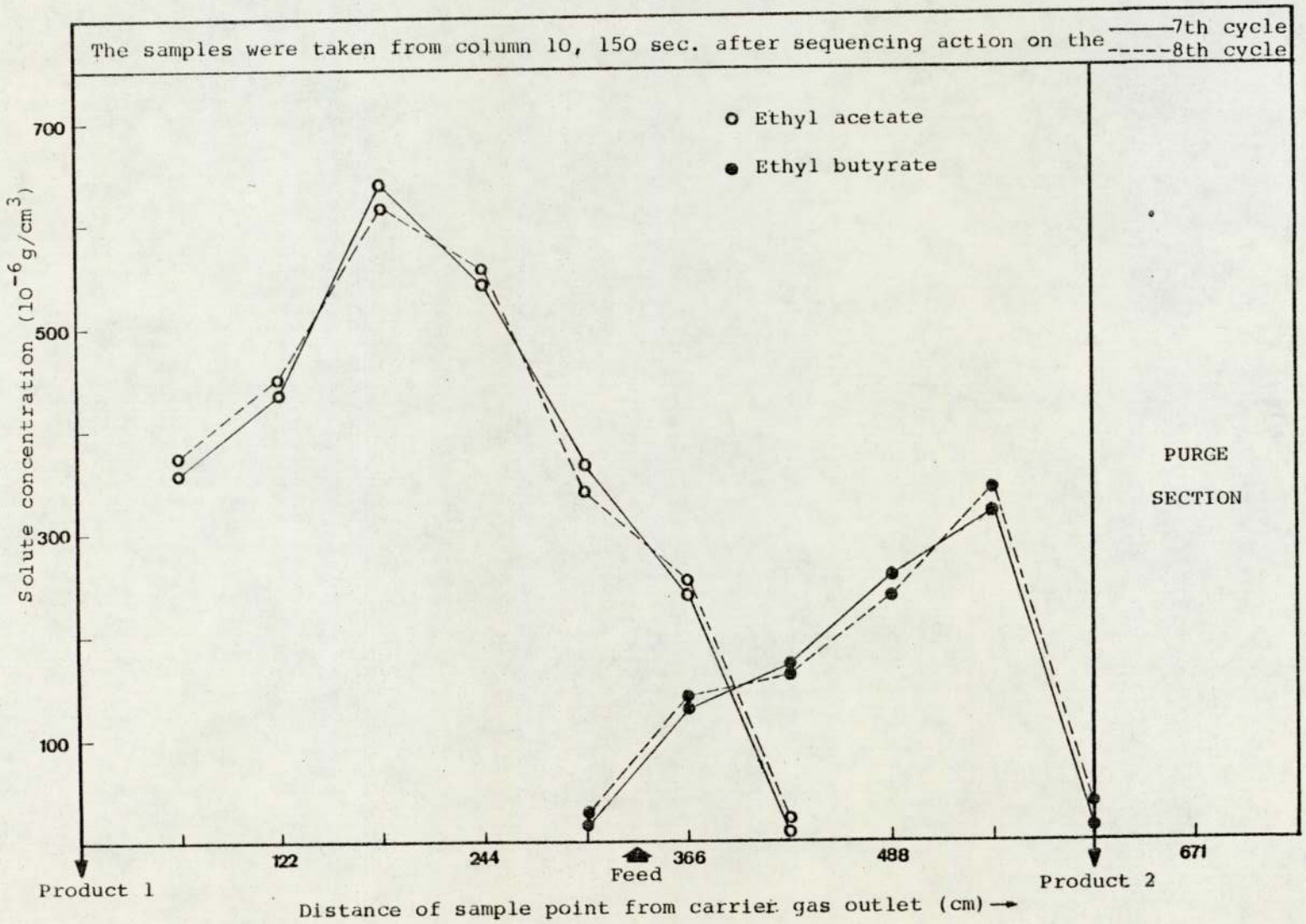

under the influence of the flowing carrier gas, with the advancement of the ethyl acetate profile being greater than that of the ethyl butyrate, in keeping with their respective partition coefficients. With the increase in throughput from 20 to 40 in steps of 10 $cm^3 h^{-1}$, Fig. 7.4 - 7.6, the feed area in which both solutes are present, is also increased. However, the feed point position was moved towards the product 2 exit more significantly in run 60 - 40 - 140 - 200. Since the number of columns involved in the separation remained almost the same in run no. 60 - 20 - 143 - 200 as in run no. 60 - 40 - 140 - 200, then the throughput could be increased without the risk of losing the purity of both products.

Throughout these experiments, the recorded profile for ethyl butyrate did not extend beyond column 5 (244 - 305 cm from the carrier gas outlet).

No attempts were made to find the maximum feed throughout for a successful separation in order to avoid stripping the liquid phase from the packing.

In conclusion, it can be said that the SCCR-2 was functioning normally after its extensive service. Hence, more difficult separations at higher temperatures could be attempted. It was decided to begin the study at 105°C (cf Liodakis (16)), and the ethyl esters of caprylic and capric acids were chosen for separation at this temperature.

7.4 ETHYL CAPRYLATE AND ETHYL CAPRATE AT 105°C

7.4.1 Results

The conclusions of Bell (31) and Liodakis (16), that the efficiency of separation was increased at sequencing rates below 200-seconds, served as an experimental guideline in the investigation of this system. A sequencing rate of 150-seconds was chosen along with reduced gas flow rate to give a $G_{m.c}/L'$ ratio in the range of 95 to 99. Details of the experimental runs 105 - 30 - 95 - 150, 105 - 50 - 97 - 150 and 105 - 80 - 99 - 150, which record the effect of feed throughput on the performance of the sequential unit, are presented in Table 7.4, (Figs. 7.7 - 7.10). These runs were carried out at a solute feed rate of 30, 50 and 80 $cm^3\ h^{-1}$ respectively, with all the operating conditions approximately constant. The sequencing rate was reduced to 100-seconds in run 105 - 80 - 97 - 100 detailed in Table 7.4 and Fig. 7.10, and it was thought that this would improve the poor purity obtained in run 105 - 80 - 99 - 150. However, the improvement was not significant in the product purity of product 2 as shown in Table 7.4.

7.4.2 Discussion

A comparison of the concentration profiles in Figs. 7.7 to 7.10, shows several well-defined trends. As the feed rate is increased from 30 to 80 $cm^3\ h^{-1}$ the general level of the gas phase concentration for ethyl caprylate rises accordingly. The trailing edge of the ethyl caprylate

Table 7.4

The Separation of Ethyl Caprylate/Ethyl Caprate

Run Title	Temperature			Ambient Conditions		Solute Mixture Feedrate	I_s	L'	Separating Section					Purge Section				
	Opera-tion	Carrier Inlet	Purge Inlet	θ_a	P_a				G_a	P_{in}	P_{out}	J_{32}	G_{mc}/L'	S_a	P_{in}	P_{out}	J_{32}	S_{mc}/L'
θ-f-G_{mc}/L'-I_s	°C	°C	°C	°C	KP_a	cm^3h^{-1}	s	cm^3s^{-1}	cm^3s^{-1}	KP_a	KP_a	-	-	cm^3s^{-1}	KP_a	KP_a	-	-
105-30-95-150	105	120	125	24	101.3	30	150	0.1	17.2	274	177	0.77	95	124	198	130	0.78	945
105-50-97-150	105	122	130	23	101.3	50	150	0.1	17.5	274	174	0.76	97	121	201	130	0.77	910
105-80-99-150	105	122	133	25	101.3	80	150	0.1	18.0	274	179	0.78	99	117	198	132	0.79	882
105-80-97-100	105	122	133	25	101.3	80	100	0.15	21.0	205	157	0.86	97	117	198	132	0.79	882

Summary of Results

Run Title	K^∞		Separating Section		Purge Section	Total Time of run	Total No. of Cycles	Time to Pseudo Steady State	Concentration Profile Analysis			
	Ethyl caprylate	Ethyl caprate	G_{min}/L'	G_{max}/L'	S_{min}/L'				Time to Analysis	Figure	Product Purities	
θ-f-G_{mc}/L'-I_s	-	-	-	-	-	h	-	h	h	-	%E.C.Y.	%E.C.
105-30-95-150	60	114	83	123	835	9	9	3	2.0	7.7	99.6	99.6
105-50-97-150	60	114	85	128	810	10	8	3	2.0	7.8	99.4	99.0
105-80-99-150	60	114	87	127	800	8	9	3	2.0	7.9	98.5	98.0
105-80-97-100	60	114	90	112	800	7	10	3	2.0	7.10	98.5	98.2

FIG. 7.7 CONCENTRATION PROFILE FOR RUN 105-30-95-150

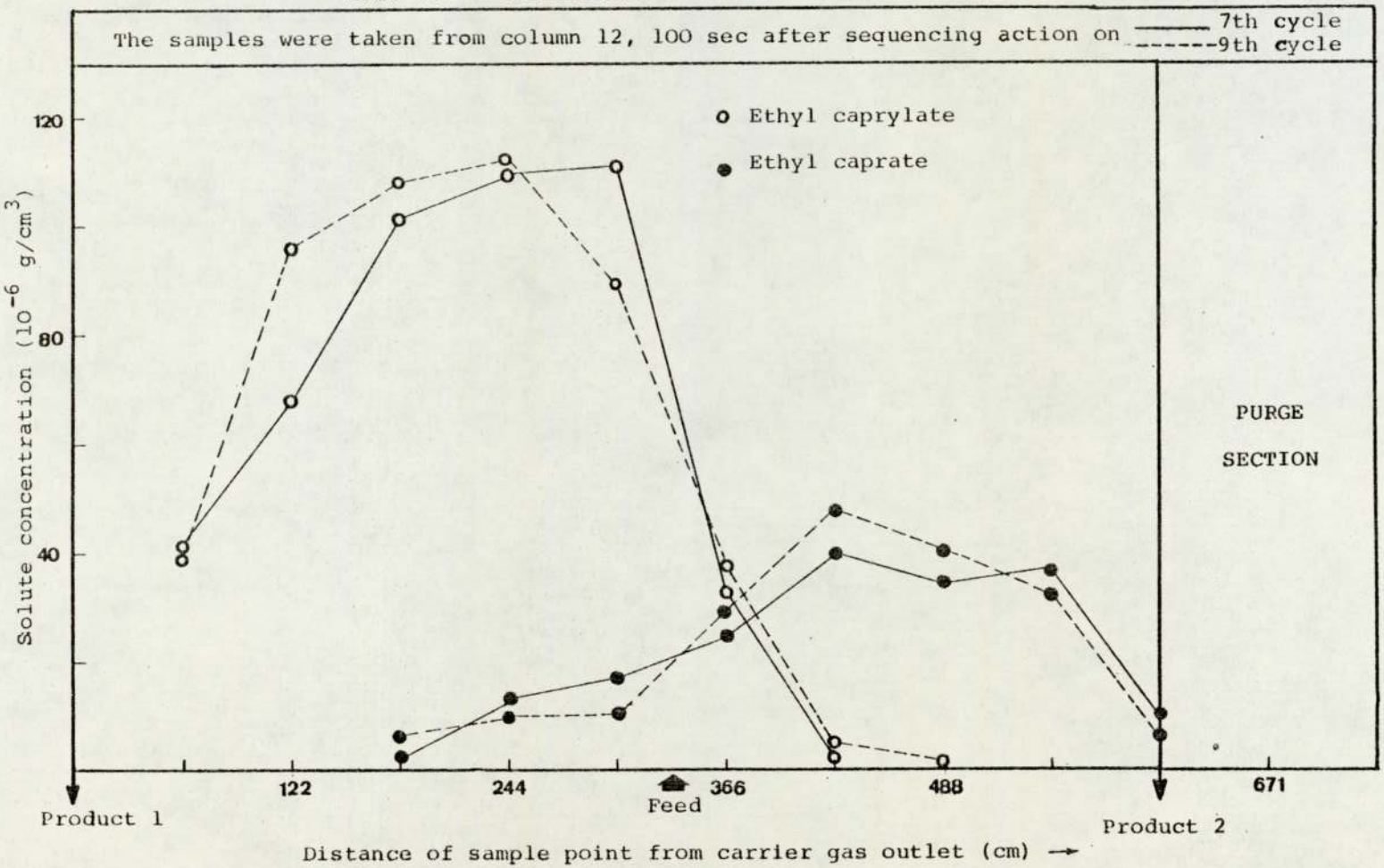

FIG. 7.8 CONCENTRATION PROFILE FOR RUN 105-50-97-150

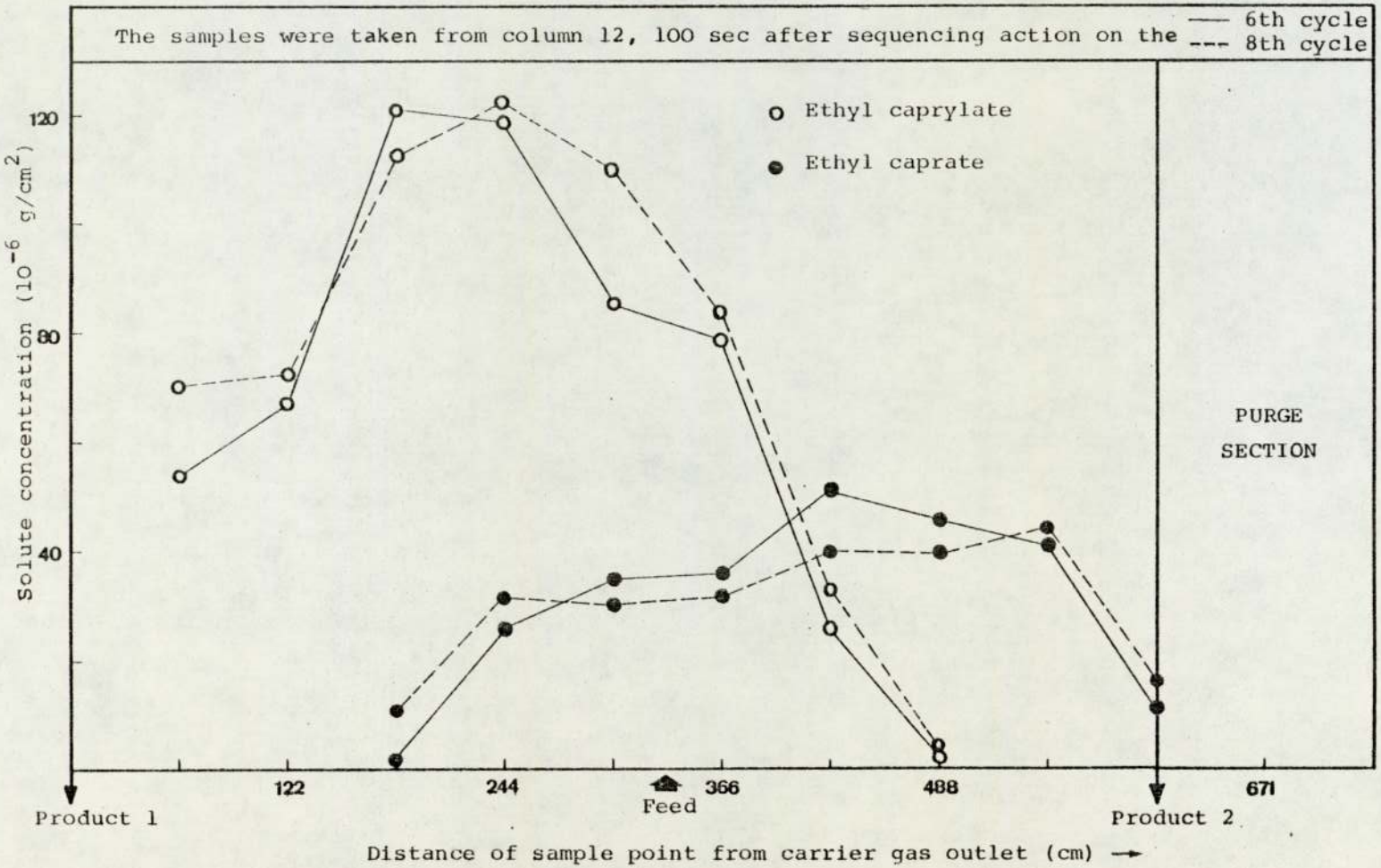

FIG. 7.9 CONCENTRATION PROFILE FOR RUN 105-80-99-150

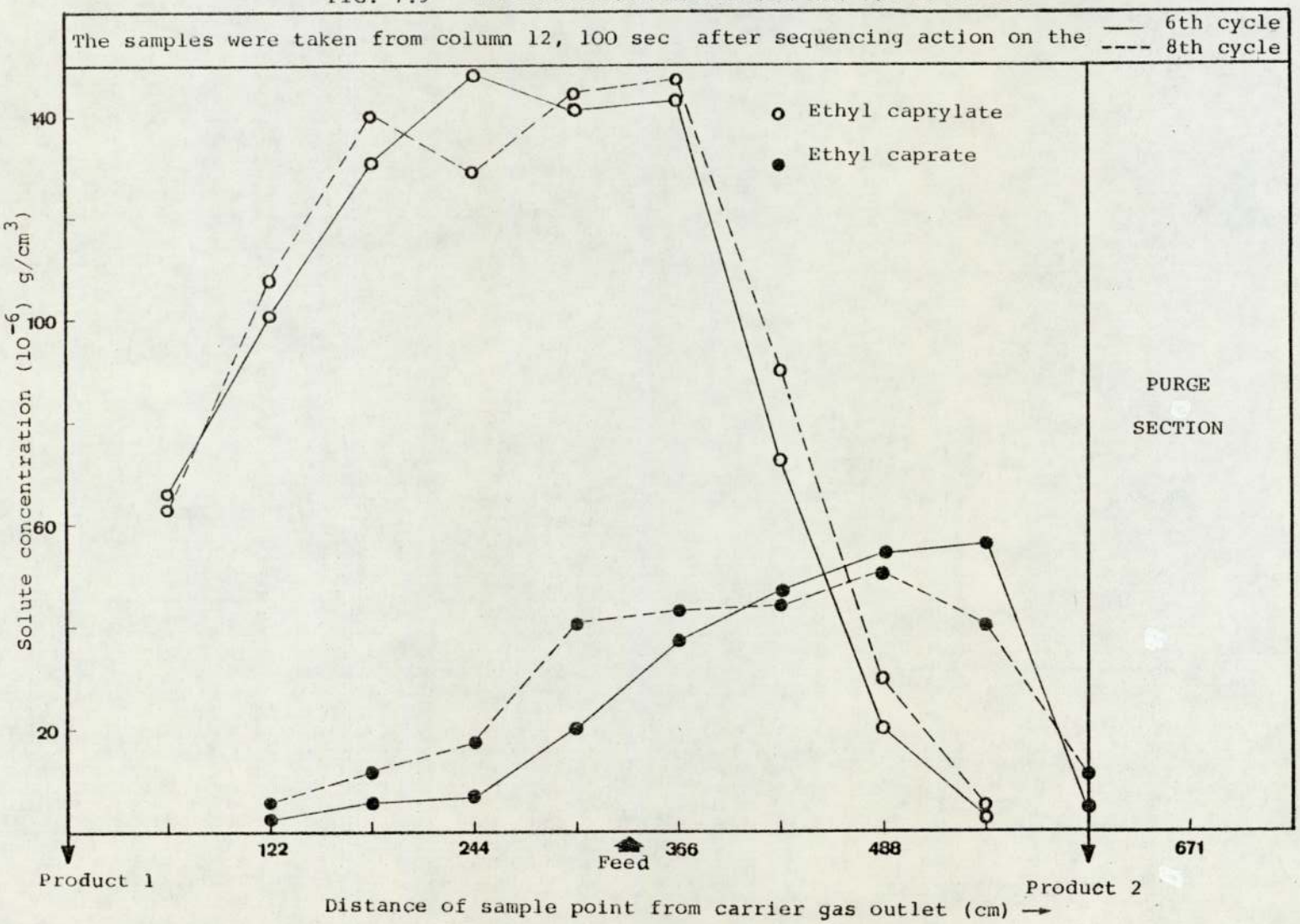

FIG. 7.10 CONCENTRATION PROFILE FOR RUN 105-80-97-100

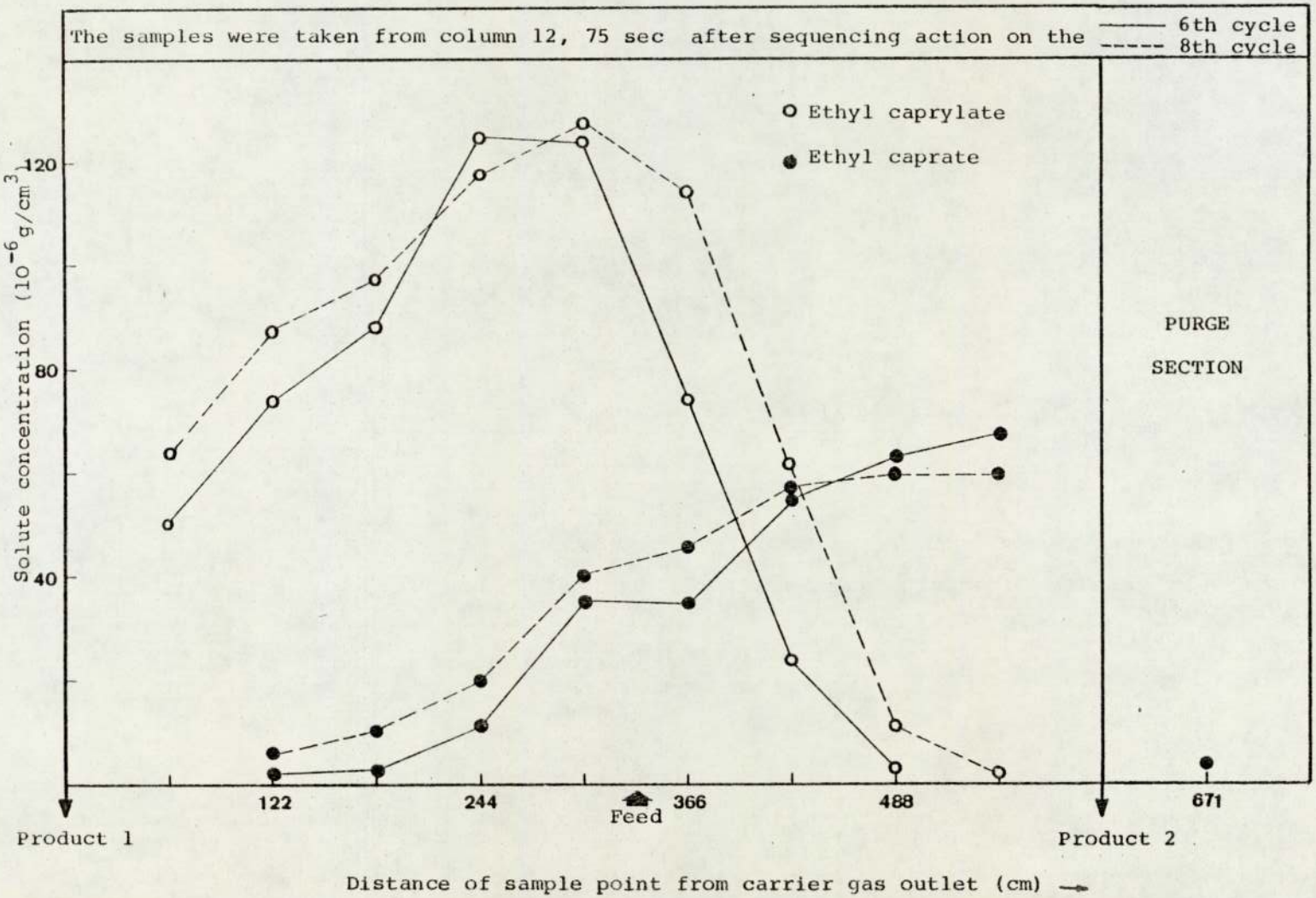

peak gradually extends in the direction of the isolated column, until in run 105 - 80 - 95 - 150, the ethyl caprylate begins to contaminate the product 2 stream. The tendency of ethyl caprylate to move towards the isolated column is consistent with an anti-Langmuir adsorption isotherm for which the preference of the solute for the solvent phase increases with increasing concentrations.

The concentration profile of ethyl caprate is somewhat more difficult to describe. In runs 105 - 30 - 95 - 150 and 105 - 50 - 97 - 150 the profile extends 2 columns (122 cm) in front of the feed point. This observation indicates that ethyl caprylate purity would be very high for the two runs (99.6% and 99.4% as shown in Table 7.4).

Further increase in the feed rate as in run 105 - 80 - 99 - 150 resulted in the ethyl caprate (product 2) profile extending up to 4 columns (244 cm) in front of the feed point. In this case the purity of products 1 was reduced to 98.5% and the purity of product 2 to 98% as a result of the extended profile of product 1. The conclusion that can be drawn from these observations is that the purging process was not so successful at high feed rates even though the purge gas flow rate was substantially higher than the flow rate needed to satisfy the relation $S_{min}/L' > (K^{\infty})$Ethyl caprate. With the present mechanical design limitations, and under the condition of this separation, no further increase in the purge flow rate was possible.

Hence if the purge rate was increased further, then the pressure drop will be very high and will have a very serious determintal effect on the whole separation process.

The concentration level of ethyl caprate is of particular interest since its level is well below the concentration level of ethyl caprylate. Averaging 50×10^{-6} g cm^{-3} for run 105 - 30 - 95 - 150, the gas phase concentration does not change appreciably for any run up to 80 cm^3 h^{-1}, at which point the feed rate has doubled. The general level of the ethyl caprate gas phase concentration, however was expected to rise with increasing feed rate, as was the case with the ethyl caprylate.

In attempting to explain this paradoxical situation, that the gas phase concentration for ethyl caprate was independent of its own feed rate, the possibility that all of the ethyl caprate liquid feed stock was not being varpourised was investigated.

Once, the partial pressure of ethyl caprate approaches the saturated vapour pressure value, further increase in the level of gas phase concentration is impossible. Calculations of the partial pressures of ethyl caprate showed that these were well below the value for the saturated vapour pressure. However, the cooling effect caused by the passage of carrier gas N_2 through the feed zone may have reduced the saturated vapour pressure, so that the maximum permissible gas phase

concentration may not be large enough to ensure that all ethyl caprate entering the unit as liquid is evaporated. Bell (31), in his extensive investigation of the cooling effect in the chromatographic beds of a similar unit (SCCR-1), showed that carrier gas temperature was low enough to prevent total vapourisation of the feed stock with the greatest affinity for the liquid phase, as is the case with ethyl caprate.

The unexpected results concerning the ethyl caprate concentration profile could be better interpreted by the following argument. Firstly, the apparent independence of the gas phase concentration can be explained by the fact that it was saturated with ethyl caprate owing to the low temperature. Secondly, advancement of the ethyl caprate profile in the direction of carrier gas flow would be unlikely as the partition coefficient would be significantly increased because of its inverse relationship with the absolute temperature.

The incomplete purging process at the high feed rate of 80 cm^3 h^{-1} (Figs. 7.9 and 7.10) could be explained by the fact that only the ethyl caprate absorbed in the liquid phase would have to be removed but also a quantity of unvapourised feed. Evaporation and desorption are both endothermic processes, and would tend to cool the purge beds. Thus, if the temperature drop was sufficient then the value of the partition coefficient for ethyl caprate

may increase so that K^{∞} becomes nearer or equal to S_{min}/L' and complete purging becomes impossible.

Unevaporated ethyl caprylate is also a possibility, and it may be that the advancement of the ethyl caprylate profile in the direction of the isolated column is not only due to the effect of an anti-Langmuir absorption isotherm but also to liquid ethyl caprylate being transferred in that direction after every sequencing interval of the unit. Any feed not evaporated within the unit will contain a much higher proportion of ethyl caprate, as ethyl caprylate has a higher saturated vapour pressure and will therefore preferentially vapourise. Purely from experimental observations it was decided that increased efficiency could be achieved at a lower sequencing rate and that a further run (105 - 80 - 97 - 100) in which the switching time was reduced to 100-seconds was required. To maintain a constant $G_{m.c}/L'$ ratio, a corresponding increase in carrier gas flow rate is required, as the sequencing interval is shortened. This attempt failed to improve the purities of both products appreciably. From a theoretical standpoint it seems logical to assume that an optimum sequencing interval exists. In section 2.3.2.1 it was shown that an optimum carrier gas flow rate occurs giving a minimum value for H.E.T.P. and it would be a relatively simple matter to determine this flow rate and therefore the switching time required to achieve it.

In practice however, factors such as pressure drop and dilution of products influence the choice of carrier gas flow rate and only very rarely are chromatographs operated at the flow rate giving minimum H.E.T.P. (36).

For this system, the maximum throughput of 80 cm^3 h^{-1} could be increased significantly if the feed rate was introduced as a vapour. In this case no hold-up of the solutes will occur apart from condensation problems in the column which are unlikely to be significant.

The successful separation of ethyl caprylate/ethyl caprate at 105° C was sufficiently encouraging to proceed to further separations at higher temperatures, which have not been achieved before with this type of equipment (SCCR). A mixture of ethyl caprate and ethyl laurate was selected for the next step of this research, which was to be performed at 160° C.

7.5 ETHYL CAPRATE AND ETHYL LAURATE AT 160° C

7.5.1 Results

The separation of ethyl caprate/ethyl laurate at 160° C represents a significant advancement in the use of the SCCR-2 unit for this type of separation. It is also a more difficult separation than the previous mixture of ethyl caprylate/ethyl caprate, since ethyl caprate and ethyl laurate have close vapour pressures. Several experimental runs were performed at an operating temperature of 160° C

and an average $G_{m.c}/L'$ of about 114, which was kept constant for all the runs reported in Table 7.5 and Figs. 7.11 - 7.15.

Starting at a feed rate of 25 cm^3 h^{-1} in run 160 - 25 - 114 - 300, the feed rate was increased in 25 cm^3 h^{-1} intervals to a maximum of 75 cm^3 h^{-1} in runs 160 - 50 - 114 - 300 and 160 - 75 - 113 - 300. In an attempt to improve the poor product purities in run 160 - 75 - 113 - 300, the switching rate was reduced to 200 and 150 seconds in run numbers 160 - 75 - 101 - 200 and 160 - 75 - 113 - 50 respectively.

The problem of sampling to enable the construction of the concentration profile was the most difficult problem with this high temperature separation. However, the absence of the sampling valve because of the condensation problem was solved by using two glass tubes connected in series and filled with ethyl acetate (see section 6.2.2).

The effectiveness of the sampling method was tested in a series of experiments. Two sampling tubes connected in series gave a similar result as three sampling tubes connected in series, Figs. (7.16, 7.17). However, cooling the sampling tubes resulted in an even better absorption effect than without cooling (Figs.(7.18, 7.19).

The effectiveness of the purge process in the column was tested by a technique in which the column was fed with the feed mixture under the same conditions of feed rate,

Table 7.5

The Separation of Ethyl Caprate/Ethyl Laurate

Run Title	Temperature			Ambient Conditions		Solute Mixture Feedrate	I_s	L'	Separating Section					Purge Section				
	Operation	Carrier Inlet	Purge Inlet	θ_a	P_a				G_a	P_{in}	P_{out}	J_3^2	G_{mc}/L'	S_a	P_{in}	P_{out}	J_3^2	S_{mc}/L'
θ-f-G_{mc}/L'-I_s	°C	°C	°C	°C	KP_a	cm^3h^{-1}	s	cm^3s^{-1}	cm^3s^{-1}	KP_a	KP_a	-	-	cm^3s^{-1}	KP_a	KP_a	-	-
160-25-114-300	160	166	170	21	101.3	25	300	0.051	10.8	308	239	0.87	114	137	198	129	0.78	2425
160-50-114-300	160	167	174	21	101.3	50	300	0.051	10.8	308	239	0.87	114	134	198	129	0.78	2361
160-75-113-300	160	168	171	24	101.3	75	300	0.051	10.8	308	239	0.87	113	131	205	130	0.77	2235
160-75-101-200	160	190	195	22	101.3	75	200	0.08	14.8	308	256	0.91	101	121	184	125	0.80	1496
160-75-113-150	160	185	192	22	101.3	75	150	0.10	21.5	308	242	0.88	113	154	198	129	0.78	1351

Summary of Results

Run Title	K^∞		Separating Section		Purge Section	Total Time of Run	Total No.of Cycles	Time to Pseudo Steady State	Concentration Profile Analysis			
	Ethyl caprate	Ethyl laurate	G_{min}/L'	G_{max}/L'	S_{min}/L'				Time to Analysis	Figure	Product Purities	
θ-f-G_{mc}/L'-I_s	-	-	-	-	-	h	-	h	h	-	%E. C.	%E.L.
160-25-114-300	74	107	103	131	2079	12	10	3	7	7.11	99.4	99.3
160-50-114-300	74	107	103	131	2042	11	9	3.5	5	7.12	99.4	98.4
160-75-113-300	74	107	103	130	1910	11	9	4	6	7.13	94.2	91.2
160-75-101-200	74	107	100	112	1376	10	9	3	5	7.14	95.1	94.8
160-75-113-150	74	107	108	129	1211	10	9	3	4	7.15	93.7	92.8

FIG. 7.11 CONCENTRATION PROFILE FOR RUN 160-25-114-300

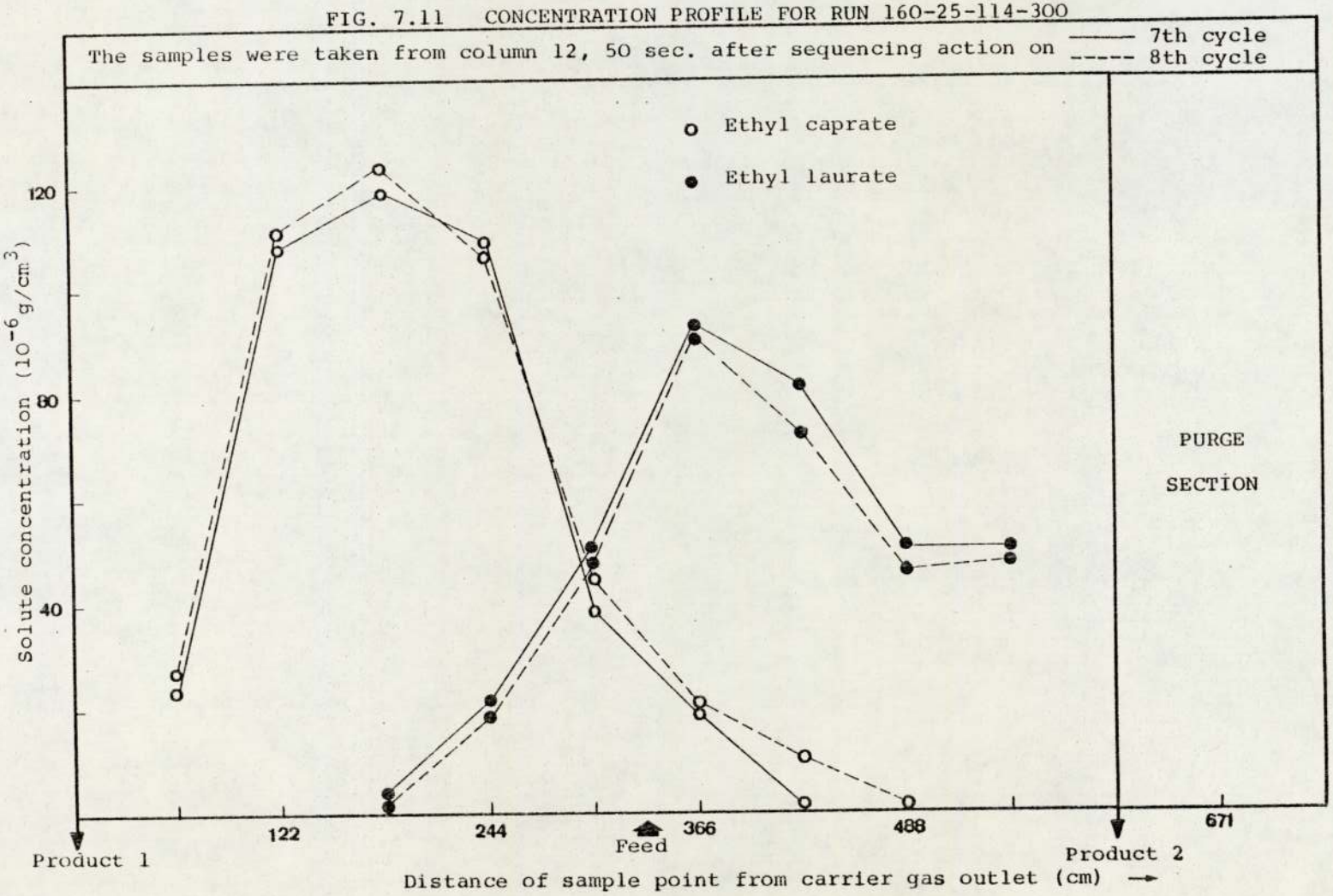

FIG. 7.12 CONCENTRATION PROFILE FOR RUN 160-50-114-300

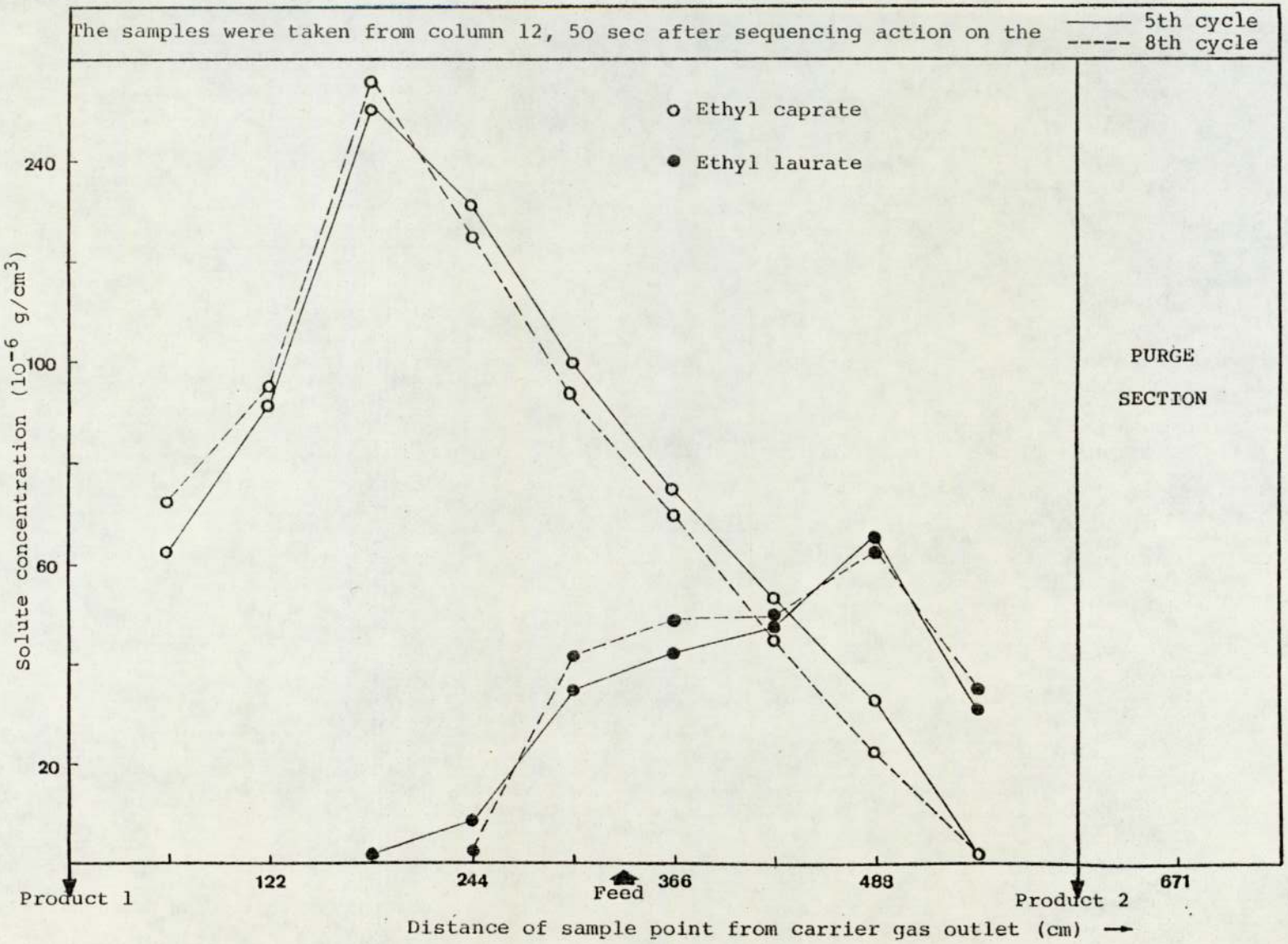

FIG. 7.13 CONCENTRATION PROFILE FOR RUN 160-75-113-300

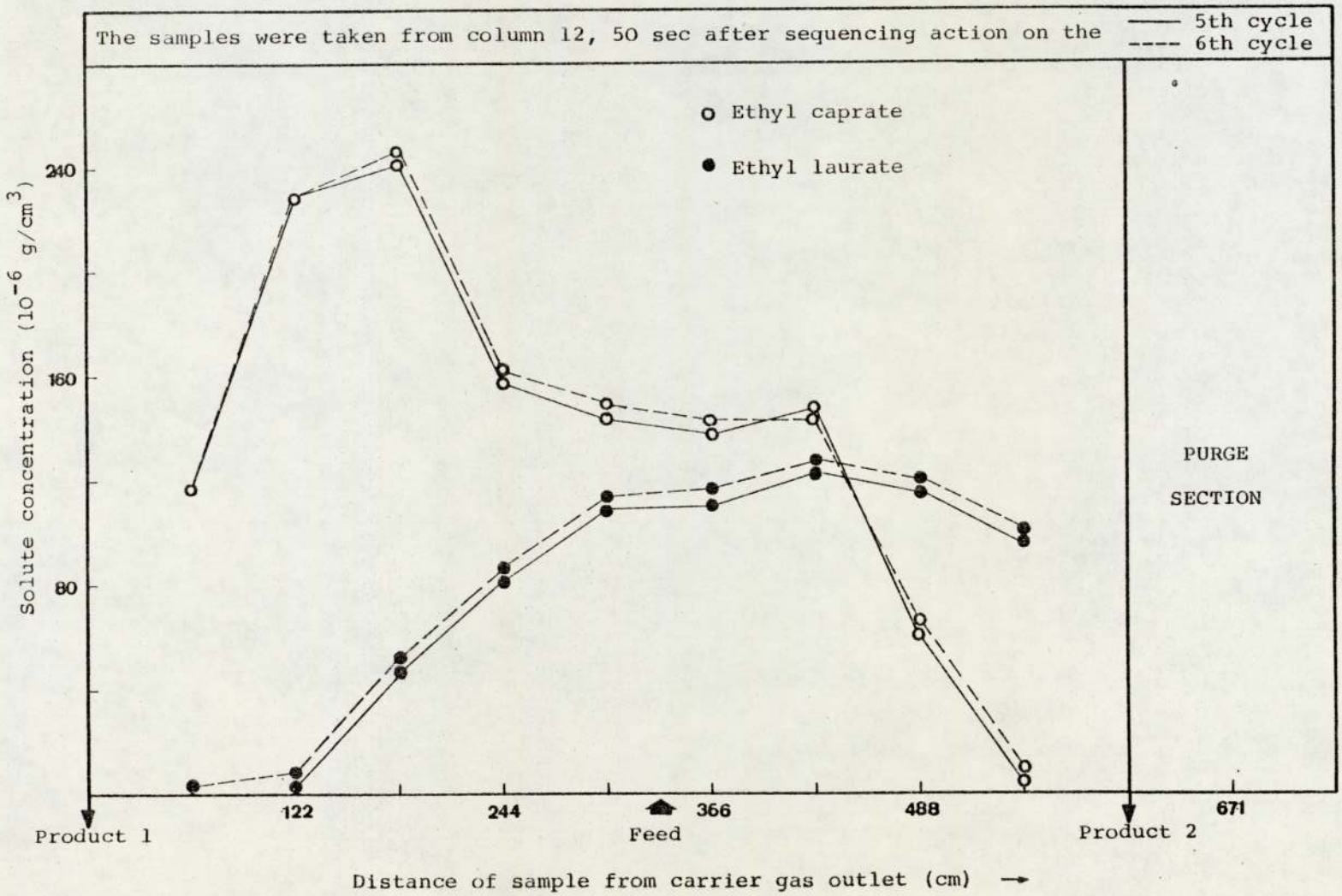

FIG. 7.14 CONCENTRATION PROFILE FOR RUN 160-75-101-200

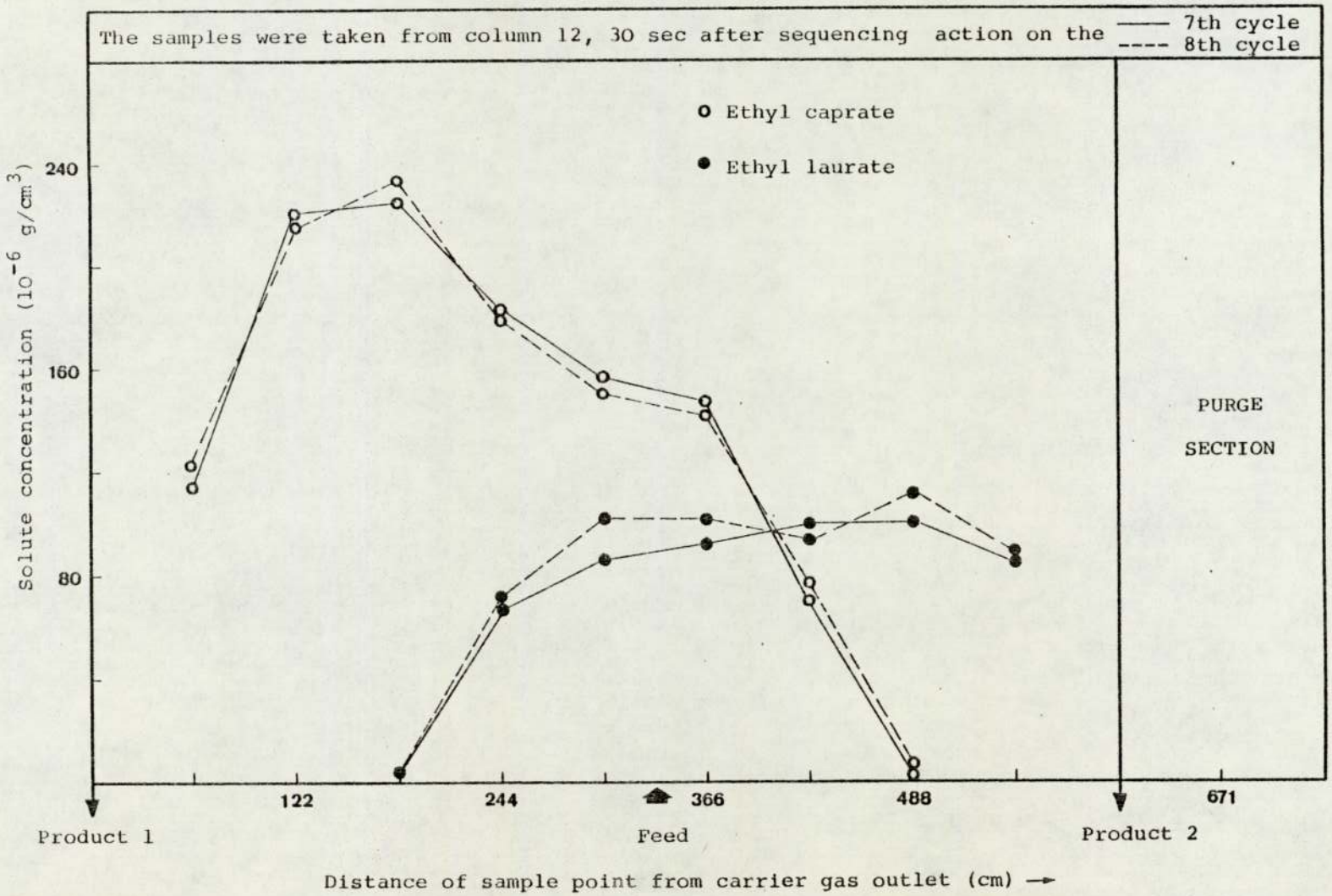

FIG. 7.15 CONCENTRATION PROFILE FOR RUN 160-75-113-150

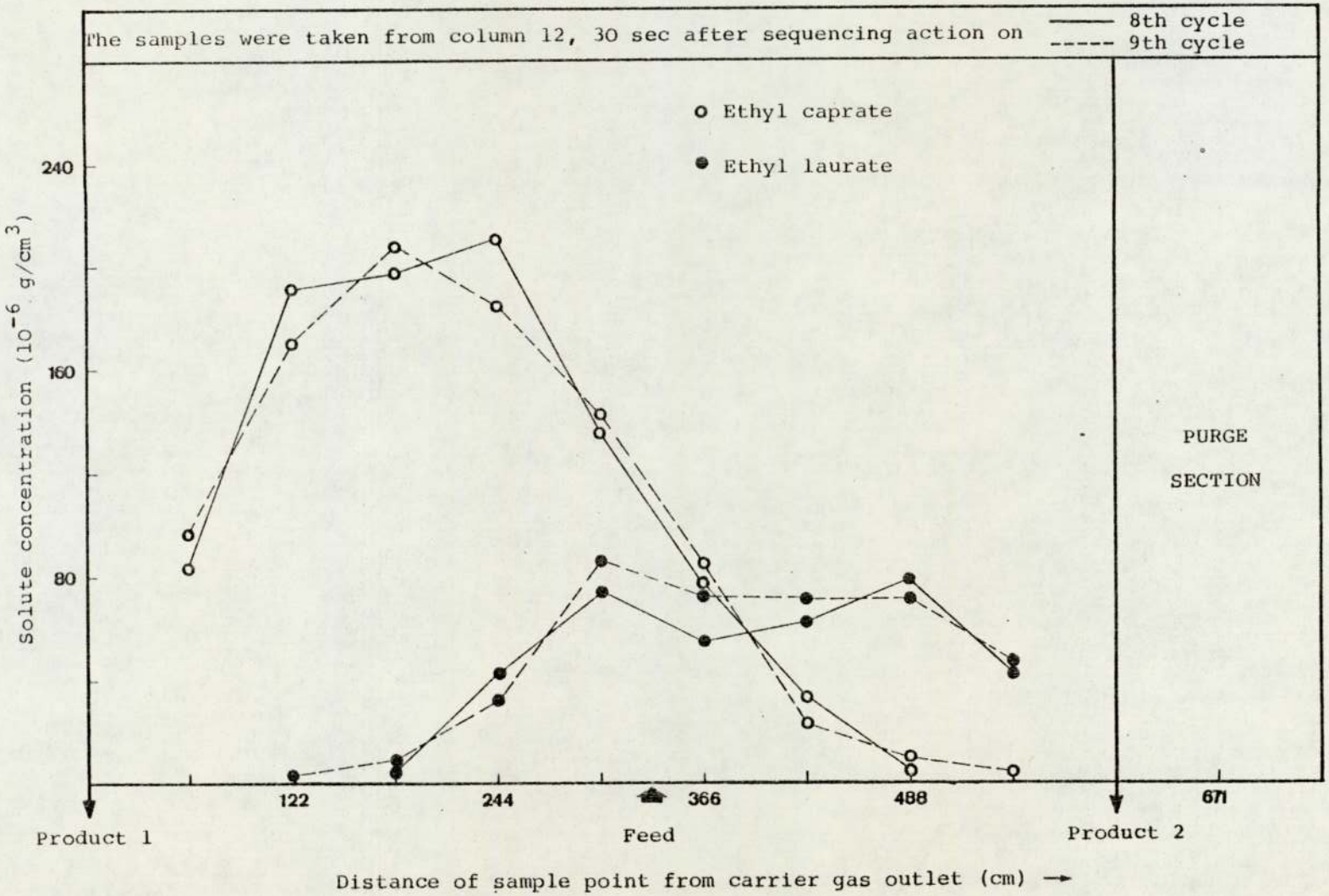

FIG. 7.16 THE EFFICIENCY OF THE SAMPLING METHOD FOR RUN 160-25-114-300

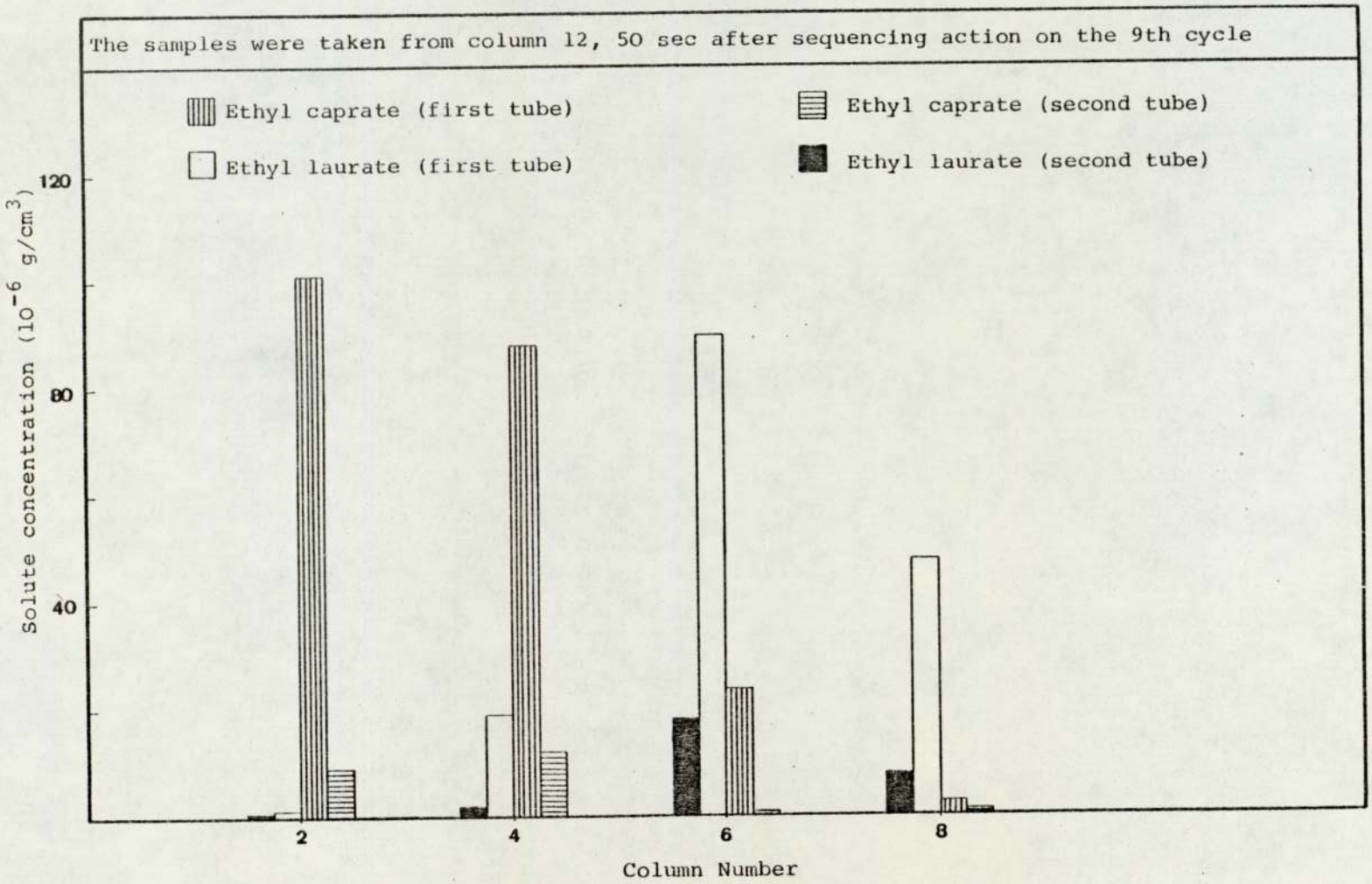

FIG. 7.17 THE EFFICIENCY OF THE SAMPLING METHOD WITH PRE-COOLED SAMPLING TUBES FOR RUN 160-25-114-300

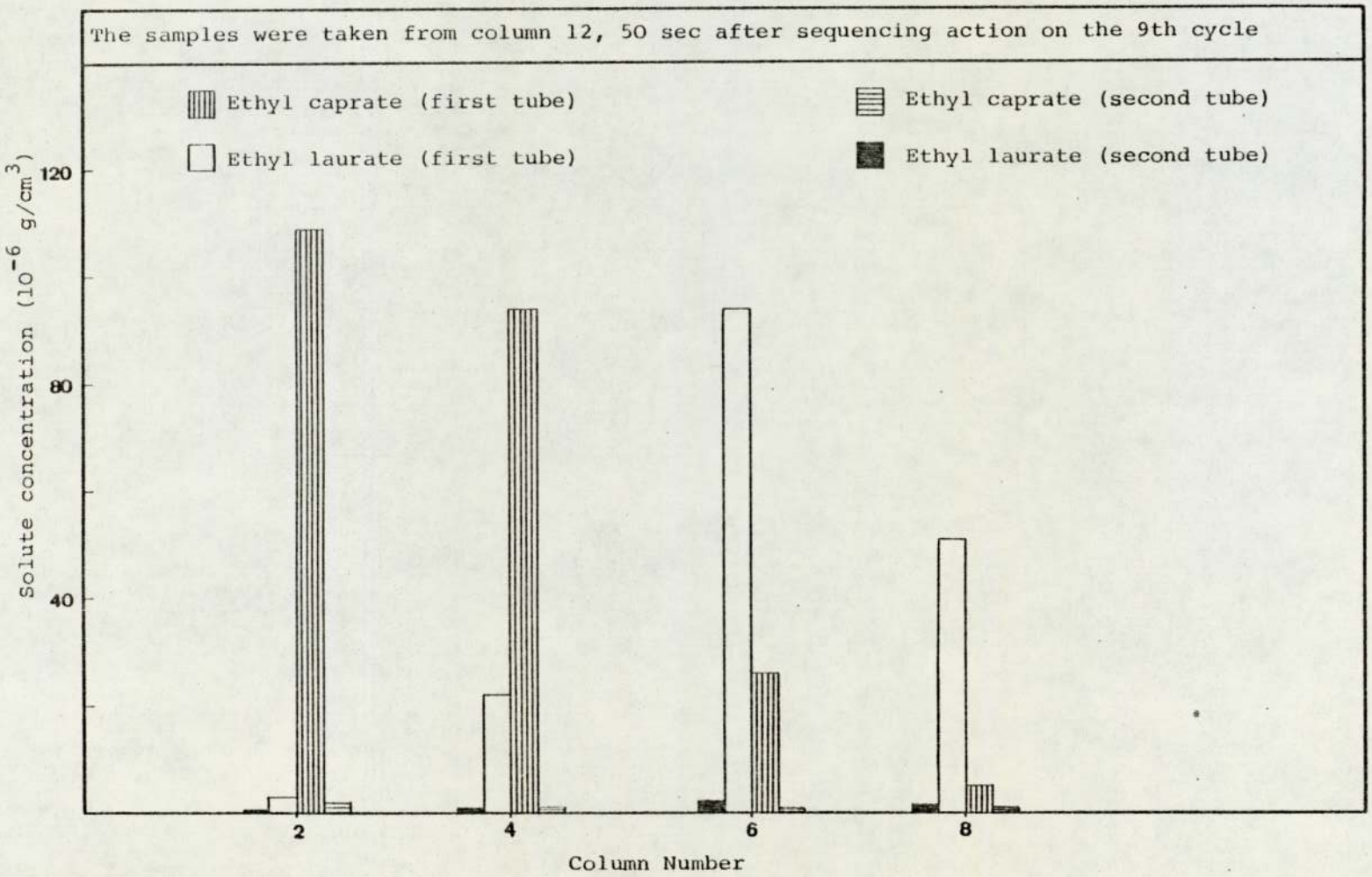

FIG. 7.18 THE EFFICIENCY OF THE SAMPLING METHOD WITH THREE TUBES FOR RUN 160-50-114-300

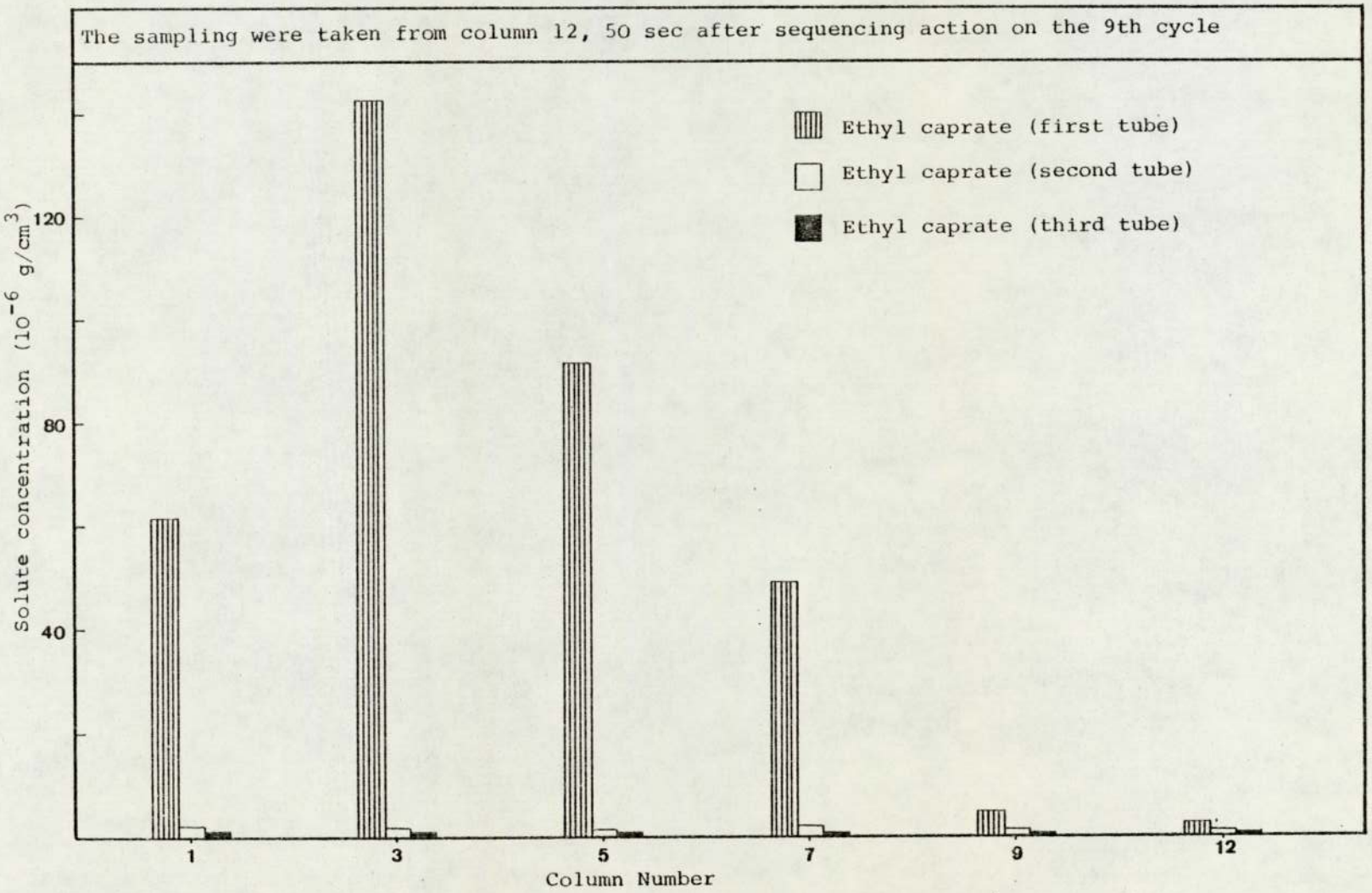

FIG. 7.19 THE EFFICIENCY OF THE SAMPLING METHOD WITH THREE TUBES FOR RUN 160-50-114-300

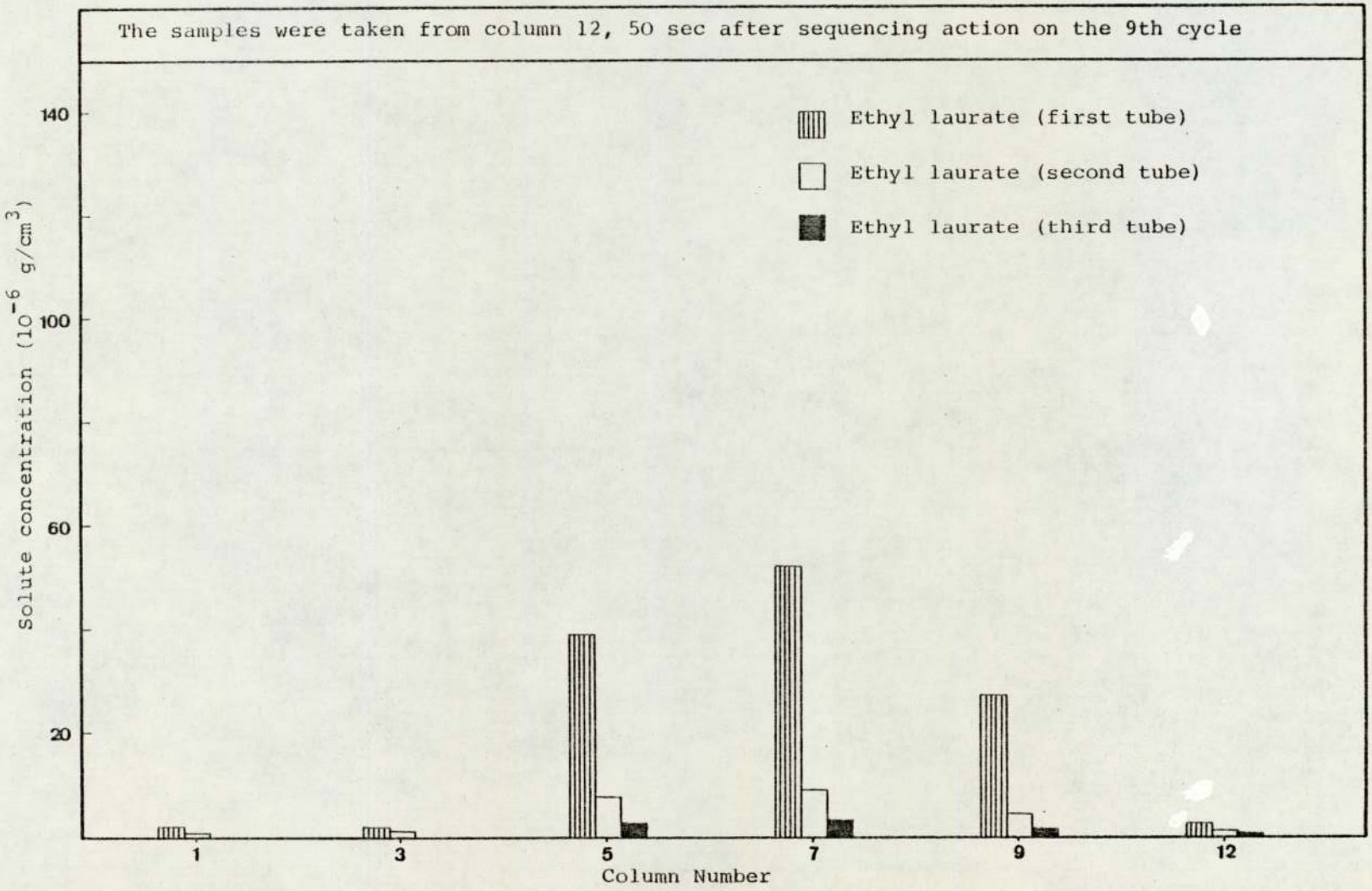

switching rate and flow rate of purge and carrier gas, as in an actual run. The purge flow was transferred manually from the control box and then gas samples were taken for one hour. The results are summarised in Figs. 7.20 - 7.22.

Finally, with the problems involved in the use of the katharometer to monitor the attainment of pseudo-steady state conditions, it was only possible to measure the product purity over 2 - 3 consecutive cycles. The results are summarised in Table 7.6.

7.5.2 Discussion

The successful separation of ethyl caprate and ethyl laurate, the fatty acid derivatives of caproic and lauric acids respectively, was performed on the SCCR-2 machine at a temperature of 160° C. Product purities of around 99% at throughput of 50 cm^3 hr^{-1} were obtained. Increasing the feed rate by a further 25 cm^3 hr^{-1} resulted in a severe reduction of the purity of product 2 and, to a lesser extent, of product 1. (See Table 7.5).

Although the operating temperature was 160° C, and the solutes are different from the previous system (ethyl caprate and ethyl caprylate) discussed in section 7.4, the general patterns are still the same. However, the product 2 (ethyl laurate) concentration was nearly the same as that of product 1 (ethyl caprate), but still lower than expected in run 160 - 25 - 114 - 300. In keeping with the partition coefficients the rate of advancement of ethyl caprate was

FIG. 7.20 THE EFFICIENCY OF THE PURGE PROCESS FOR RUN 160-25-114-300

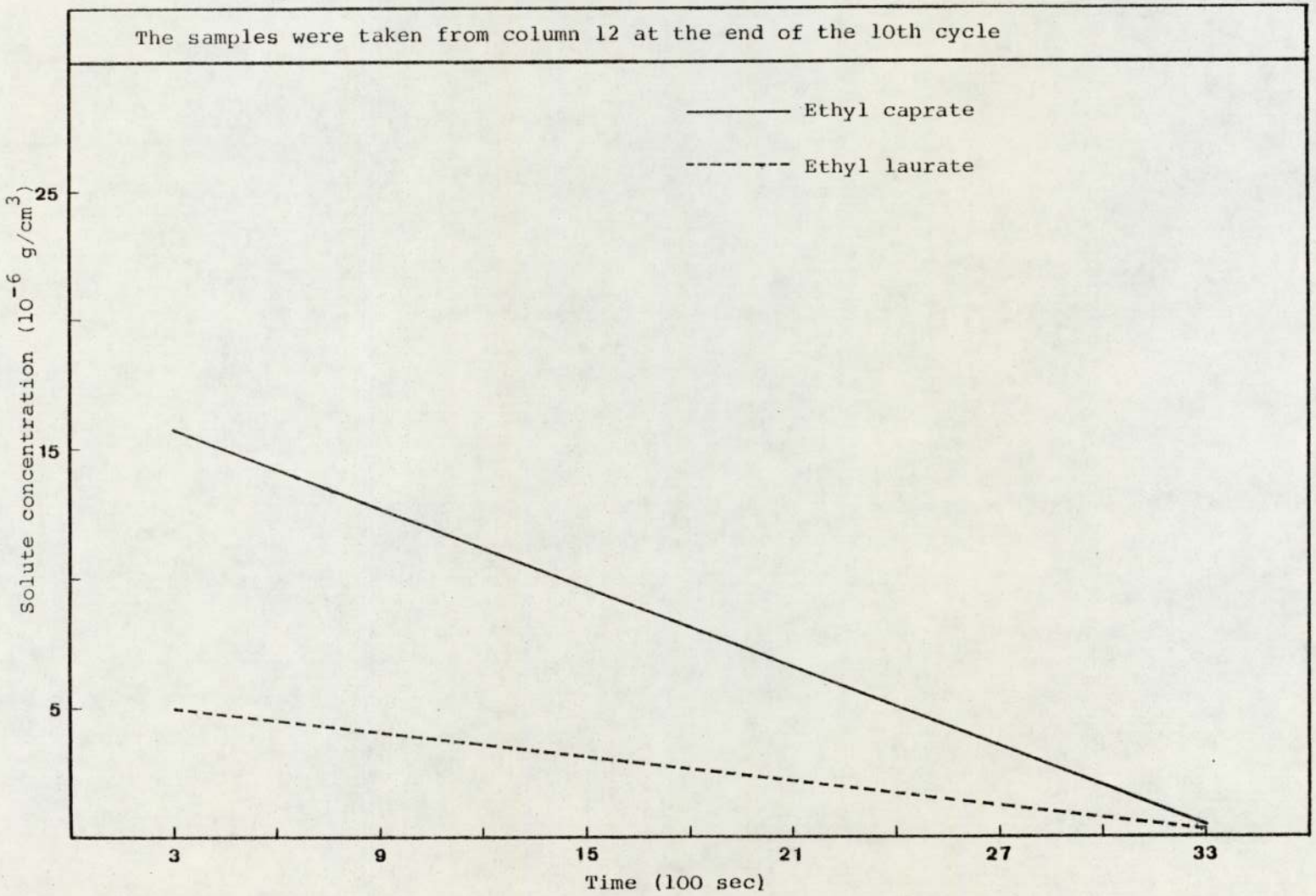

FIG. 7.21 THE EFFICIENCY OF THE PURGE PROCESS FOR RUN 160-50-114-300

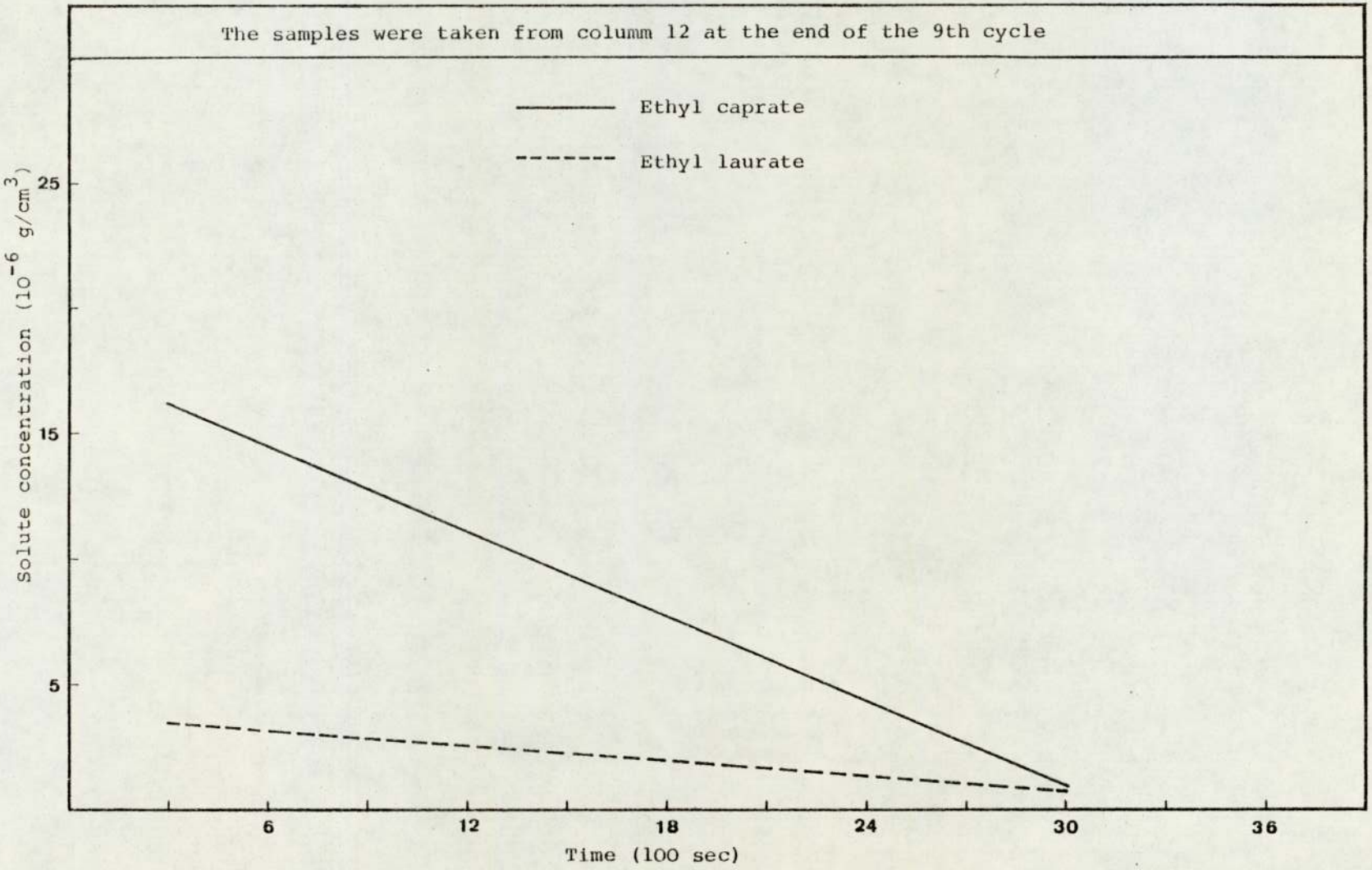

FIG. 7.22 THE EFFICIENCY OF THE PURGE PROCESS FOR RUN 160-75-113-300

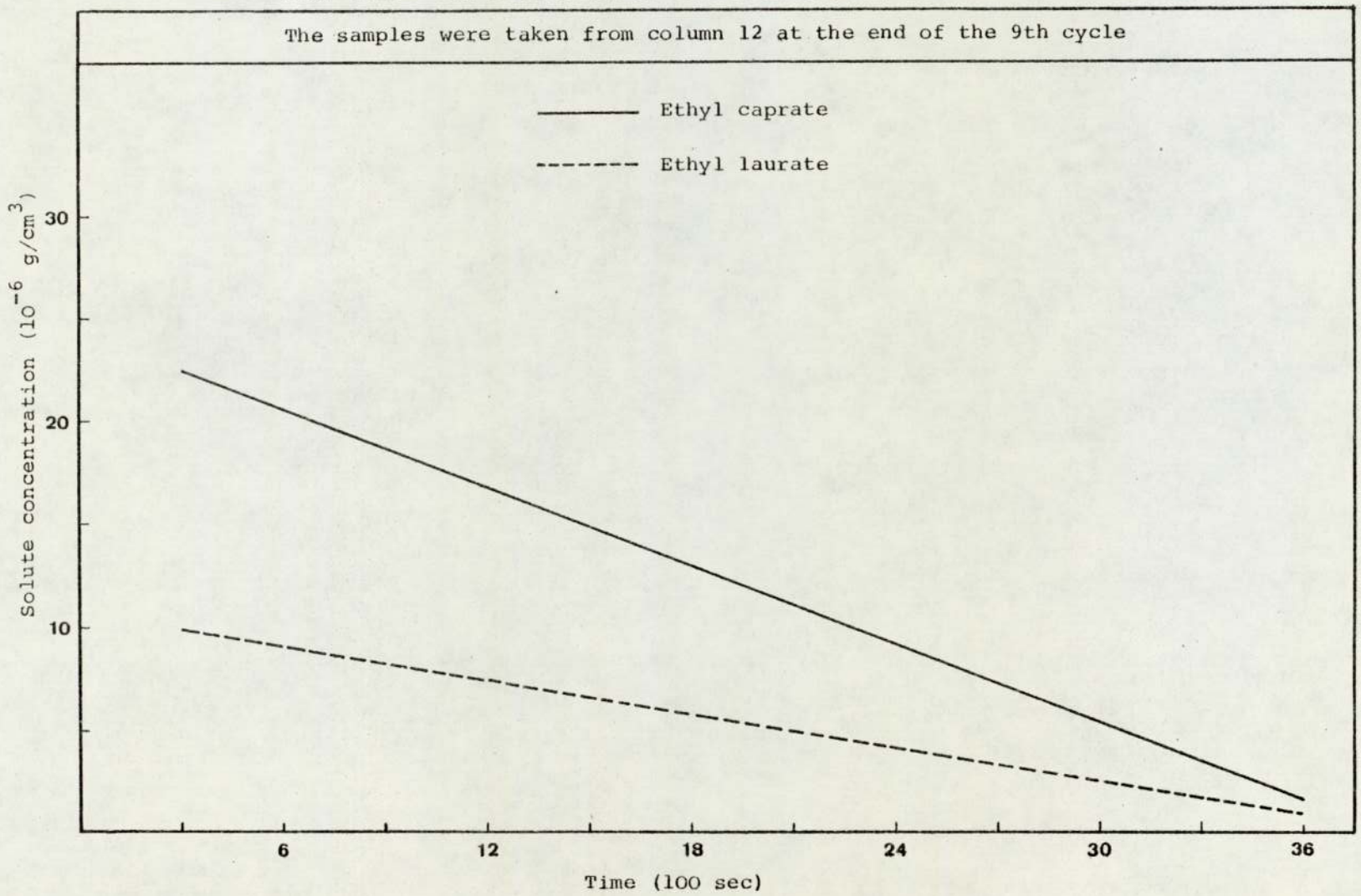

Table 7.6a

Product Purities of Individual Cycles in Run 160-25-114-300

Cycle Number	Product Purities (%)	
	Ethyl caprate	Ethyl laurate
2	50.8	77.0
4	98.9	96.5
6	99.4	98.4
8	99.2	99.1

Table 7.6b

Product Purities of Individual Cycles in Run 160-50-114-300

Cycle Number	Product Purities (%)	
	Ethyl caprate	Ethyl laurate
2	54.2	68.00
4	98.6	95.4
6	99.2	98.7
8	99.6	98.5

Table 7.6c

Product Purities of Individual Cycles in Run 160-75-113-300

Cycle Number	Product Purities (%)	
	Ethyl caprate	Ethyl laurate
2	49.1	56.0
4	93.8	90.7
6	95.2	91.0
8	94.1	92.2

greater than for ethyl laurate, the latter being preferentially retained on the solvent phase. This fact explains why equivolume mixtures of two chemicals of similar densities should give gas phase concentrations at substantially different levels.

A successful separation was defined by Deeble (13) as one giving high purity (in excess of 98%) for both products, in this case ethyl caprate as product 1 and ethyl laurate as product 2. In terms of the concentration profile the requirement means that ethyl laurate should not appear at any time in significant amounts in the section 0-183 cm from the carrier gas outlet (equivalent to columns 1 - 3) while ethyl caprate should not remain in the section equivalent to column 8 (488 - 671 cm) when sequencing occurs.

For the experimental runs of 25 and 50 $cm^3\ h^{-1}$ i.e. run numbers 160 - 25 - 114 - 300 and 160 - 50 - 114 - 300 respectively, the recorded profile for ethyl laurate did not extend beyond column 3 (122 - 183 cm from carrier gas outlet) which indicates a product 1 purity in excess of 99%. However, the purity of product 1 was impaired, particularly at higher solute feed rates of 75 $cm^3\ h^{-1}$.

Inspection of ethyl caprate profile in run 160 - 25 - 114 - 300 suggests that the purity of product 2 (ethyl laurate) was in excess of 99%. The trailing edge of the ethyl caprate profile gradually extends into the fourth

column after the feed point (549 - 610 cm from the carrier gas outlet) in run 160 - 50 - 114 - 300. The maximum ethyl laurate concentration also occurred in that column, while the purity of product 2 was still in excess of 98.4%.

As the feed rate increased to 75 $cm^3 h^{-1}$, the trailing edge of the profiles for both solutes extended toward the isolated column. This observation is consistent with the anti-Langmuir type absorption isotherm; i.e. the preference of the solutes for the solvent phase increases with increasing concentration. The purity of both products is severely affected by increasing the feed rate by 25%. The profile of ethyl laurate did not extend into the fourth column from the feed point (0 - 61 cm from the carrier gas outlet), which suggests a product purity of better than 98% compared with 94.2% which has been experimentally recorded. This may be explained by the fact that the maximum concentration of both solutes for successful separation has been exceeded. Comparison with the run performed at a sequencing interval of 200 seconds i.e. run 160 - 75 - 101 - 200, shows that the slight reduction in ethyl laurate concentration by the use of an increased carrier gas flow rate improved the purity of ethyl laurate by 4% compared with the previous run 160 - 75 - 113 - 300, as detailed in Figs. 7.13 and 7.14. At the same time the purity of ethyl caprate was improved by 1%.

At the slower sequencing rate of 150-seconds in run 160 - 75 - 113 - 150, the reduction in both solute concentrations was even greater than at 200 seconds, i.e. run 160 - 75 -101 - 200, but the purity of the products was again severely affected, as shown in Fig. 7.15.

A comparison of all the column to column concentration profiles (Figs. 7.11 - 7.15), suggests that as the feed rate is increased the concentration profiles extend over the entire length of the separating section, which means that a successful separation is unlikely to be achieved.

Considering the purge section, an indication of the concentration level of the two components within this column on isolation was given by the levels in the preceding column for the sampling time closest to the end of a sequencing interval. The success of the purging could be gauged from the concentration of the solute(s) remaining within the isolated column at the same time. For the SCCR-2 it was decided that the criterion for a successful purging process for the product 2 would be when the inequality in equation 7.2 was met, i.e.

$$S_{min}/L > K_2 \qquad (7.2)$$

From an experimental point of view this criterion was met when incomplete regeneration of the isolated column caused contamination of product 1 as in run 160 - 75 - 114 - 300. Similarly, for the separating section,

contamination of product 2 occurred whether or not the simplified inequality of equation 7.3 was met:

$$K_{(\text{ethyl caprate})} < G_{min}/L' \qquad (7.3)$$

Thus, despite the usefulness of these inequalities in choosing the operating conditions they do not, by themselves indicate that successful purging or separation of the solutes will be achieved.

The most striking observation from the investigation of the purge section was the significance of the solute's hold-up in the column for a period of more than 900-seconds. The results in Figs. 7.20 - 7.22 show that in the time available for purging, i.e. one switching interval, only 90% of the product was being removed. However, in operation this could mean 95 - 99%, since each column is given a total purging time of twice the sequencing interval because of 'double purging', which involves two columns being purged simultaneously by separate gas supplies. In terms of purity this could mean 99% product purities for runs having a feed rate of 25 and 50 $cm^3\ h^{-1}$. In fact these were a little higher than 99%. This could be due to the fact that the pseudo steady state has been disturbed by switching the semi-continuous operational mode to batch mode operation, when studying one column at a time. At a liquid feed rate of 75 $cm^3\ h^{-1}$ as in run 160 - 75 - 113 - 300, complete

purging of the products proved very difficult. In this case both solutes (ethyl caprate and ethyl laurate) were still present in significant concentrations even after one hour of purging. The fact that the purity of both products was severely reduced in the run at 75 $cm^3\ h^{-1}$ can be appreciated by reference to the results given in Fig. 7.22.

Prior to construction of the concentration profile, the sampling procedure (see Section 6.2.2) was tested in every experimental run with this system. The results presented in Fig. 7.16 clearly show that without cooling the sampling tube, significant concentrations (of solutes) were left in the second tube. On cooling the tubes in crushed ice prior to taking samples, the quantity of both solutes left in the second tube dropped significantly (Fig. 7.17). The fact that more material had been trapped in the first tube can be readily appreciated by considering that more material has been condensed under the cooling effect of the tubes. However, using the three tube instead of the two tube system, the solute trapped in the third tube has very little significance compared with the experimental error in handling the three tubes together. (see Figs. 7.18 and 7.19). Therefore the tubes system was adopted thereafter in this research. The results presented in Table 7.6 show that pseudo-steady state (in terms of purity of both solutes) was reached after about

four cycles. The first three cycles could be described as the 'building-up' cycles prior to attainment of pseudo-steady state.

In conclusion, equations 6.7 and 6.8 serve as a reliable guide to the choice of operating conditions and the interpretation of the experimental results. Two factors have been identified as restricting the separating power of the sequential unit. These are, the increase in the respective solute partition coefficient at finite concentrations, and the additional variation of the solute molecule velocity through the separating section caused by both solute concentration and the inevitable pressure gradients. The two factors appear to be of little significance in easy separations like the previous separation of ethyl caprylate and ethyl caprate (Section 7.3). The reason could be the little effect of the pressure fluctuations on the sorption-desorption process in the easy separation, while it is more pronounced when high temperature and difficult separations are involved. The maximum throughput that could be achieved which gave two products of purity in excess of 98.5%, was 80 cm^3 h^{-1}. When the separation difficulty is increased as in the present system (ethyl caprate/ethyl laurate) the throughput had to be substantially reduced to 50 cm^3 hr^{-1} to give product purities in excess of 98.5%. This confirms that the role of the two factors mentioned becomes more significant at higher throughputs. This conclusion raised the question of what would happen if another mixture at higher temper-

ature was investigated ?. To answer this a mixture of two fatty acid esters, ethyl laurate and methyl myristate at 185°C was investigated.

7.6 THE STUDY OF ETHYL LAURATE AND METHYL MYRISTATE SEPARATION AT 185°C

7.6.1 Results

An experimental programme was conducted similar to that illustrated in Section 7.5, with an operating temperature of 185°C, the highest ever recorded so far using this type of machine (SCCR-2).

Using a 70:30 V/V mixture of ethyl laurate and methyl myristate, the feed rate was increased from 25 to 45 $cm^3\ h^{-1}$. This feed mixture was used because of the high price of methyl myristate. A successful separation may be defined as one having reproducible solute concentration profiles with product purities greater than 98%. Based on this definition it appears that the results in Table 7.7 represent unsuccessful separations especially at a feed rate of 45 $cm^3\ h^{-1}$. It must be emphasised however, that the product purities quoted in Table 7.7 were the worst measured value during the run. The fluctuation in the flow caused by changing the traps every other cycle was the major problem. Had the product purities been recorded at steady state during the run, all purities barring those for runs 185 - 25 - 83 - 150 and 185 - 45 - 83 - 150 would probably have been in excess of 99%.

Table 7.7

The Separation of Ethyl Laurate/Methyl Myristate

Run Title	Temperature			Ambient Conditions		Solute Mixture Feedrate	I_s	L'	Separating Section					Purge Section				
	Opera-tion	Carrier Inlet	Purge Inlet	θ_a	P_a				G_a	P_{in}	P_{out}	J_3^2	G_{mc}/L'	S_a	P_{in}	P_{out}	J_3^2	S_{mc}/L'
θ-f-G_{mc}/L'-I_s	°C	°C	°C	°C	KP_a	cm^3h^{-1}	s	cm^3s^{-1}	cm^3s^{-1}	KP_a	KP_a	-	-	cm^3s^{-1}	KP_a	KP_a	-	-
185-25-83-150	185	200	210	22	101	25	150	0.1	10.8	239	152	0.76	83	123	198	122	0.75	1164
185-45-83-150	185	203	205	24	101	45	150	0.1	10.8	239	152	0.76	83	124	199	130	0.78	1140
185-60-83-150	185	200	205	23	101	60	150	0.1	10.8	239	151	0.76	83	123	198	129	0.78	1139
185-60-74-100	185	198	200	25	101	60	100	0.15	10.8	170	123	0.83	74	134	198	122	0.75	839
185-60-85-150	185	200	204	22	101	60	150	0.1	10.8	242	152	0.76	83	112	197	130	0.78	1046

Summary of Results

Run Title	K^∞		Separating Section		Purge Section	Total Time of Run	Total No. of Cycles	Time to Pseudo Steady State	Concentration Profile Analysis			
	Ethyl laurate	Methyl myristate	G_{min}/L'	G_{max}/L'	S_{min}/L'				Time to Analysis	Figure	Product Purities	
θ-f-G_{mc}/L'	-	-	-	-	-	h	-	h	h	-	%E.L.	%M.M.
185-25-83-150	40	63	72	109	1010	8	10	3	8	7.23	98.5	98.0
185-45-83-150	40	63	72	109	1000	8	10	3	8	7.24	97.6	94.8
185-60-83-150	40	63	71	109	997	8	10	3	9	7.25	94.2	90.0
185-60-74-100	40	63	66	89	713	7	10	3	8	7.26	95.0	91.2
185-60-85-150	40	63	71	109	916	8	10	3	7	7.27	95.0	92.3

The ratio of $G_{m.c}/L'$ was fixed at 83 and the switching rate at 150-seconds for the first three runs. The purity of both products was severely reduced in run 185 - 60 - 83 - 150 and an attempt was made to improve these. One method used was that of lowering the sequencing rate to 100 seconds in run 185 - 60 - 77 - 100. In the second attempt the feed mixture was made up to include 20% V/V ethyl acelate. Both attempts resulted in a slight improvement in the purities of both products.

The sampling method was the same as that described in Section 7.4. Since the effectiveness of the sampling method was proved by the results given in Section 7.5, no attempt was made to repeat them in this section. However, the purge column study was again conducted here, as these results were required for the simulation study in Chapter 8.

A summary of experimental and computer results is given in Table 7.7 with the concentration profiles being illustrated in Figs. 7.23 to 7.27. The results of the purge column study are given in Figs. 7.28 to 7.30.

7.6.2 Discussion

The definition of a successful separation for the systems discussed earlier in the study was that (31) product purities should be in excess of 98% and the solute concentration profiles should be reproducible. Based on this definition, at least the first two runs 185 - 25 - 83 -

FIG. 7.23 CONCENTRATION PROFILE FOR RUN 185-25-83-150

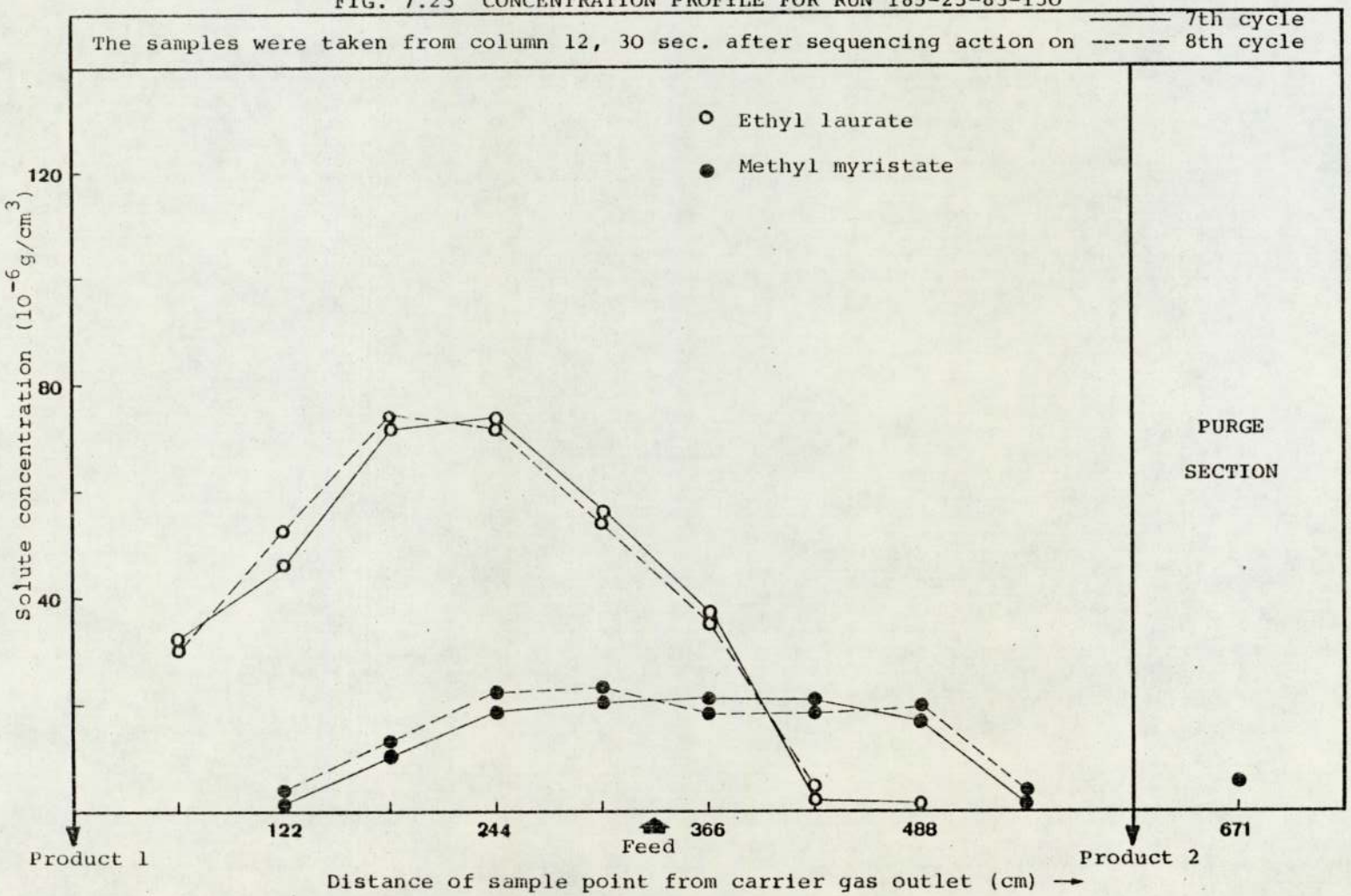

FIG. 7.24 CONCENTRATION PROFILE FOR RUN 185-45-83-150

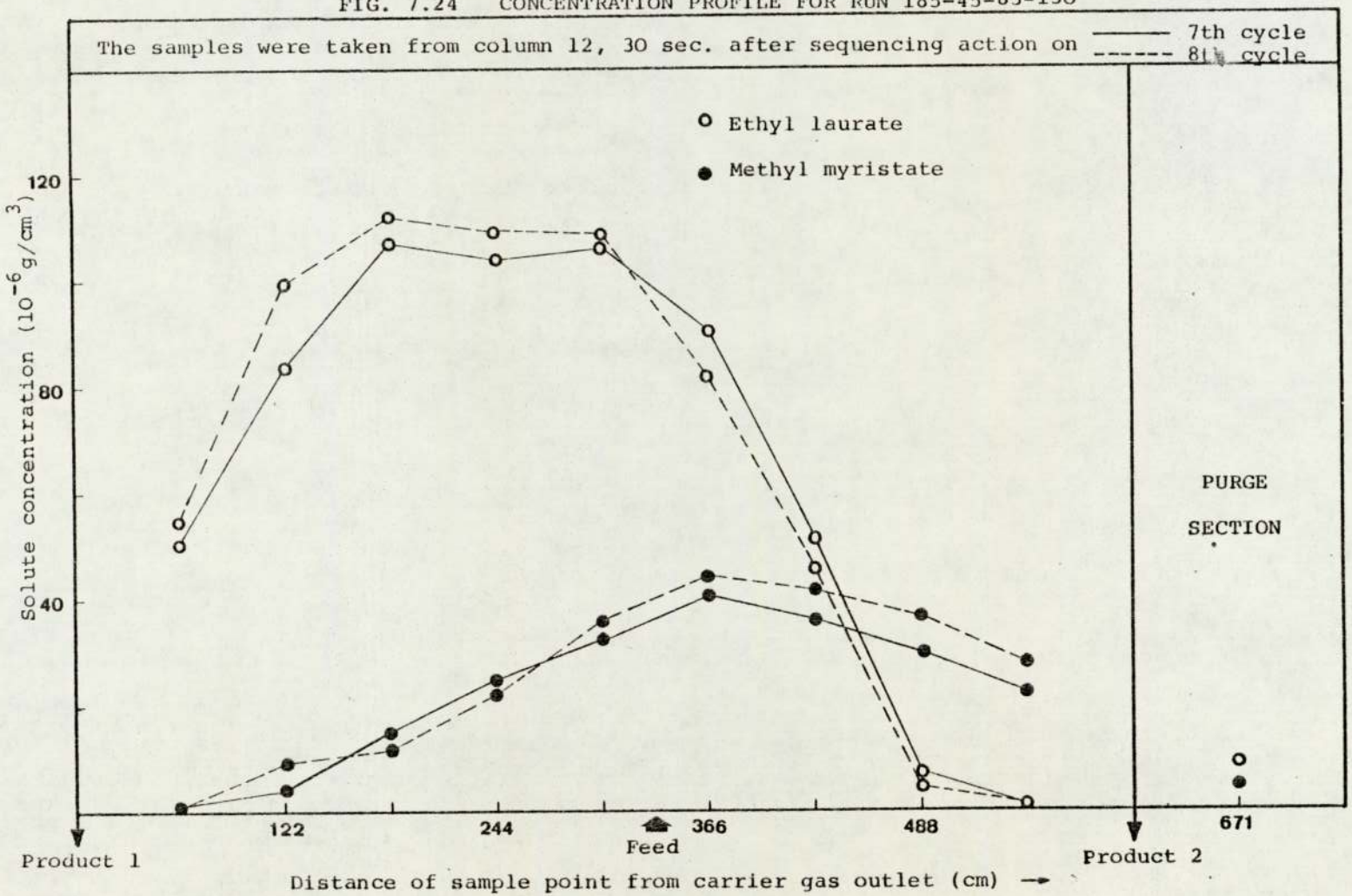

FIG. 7.25 CONCENTRATION PROFILE FOR RUN 185-60-83-150

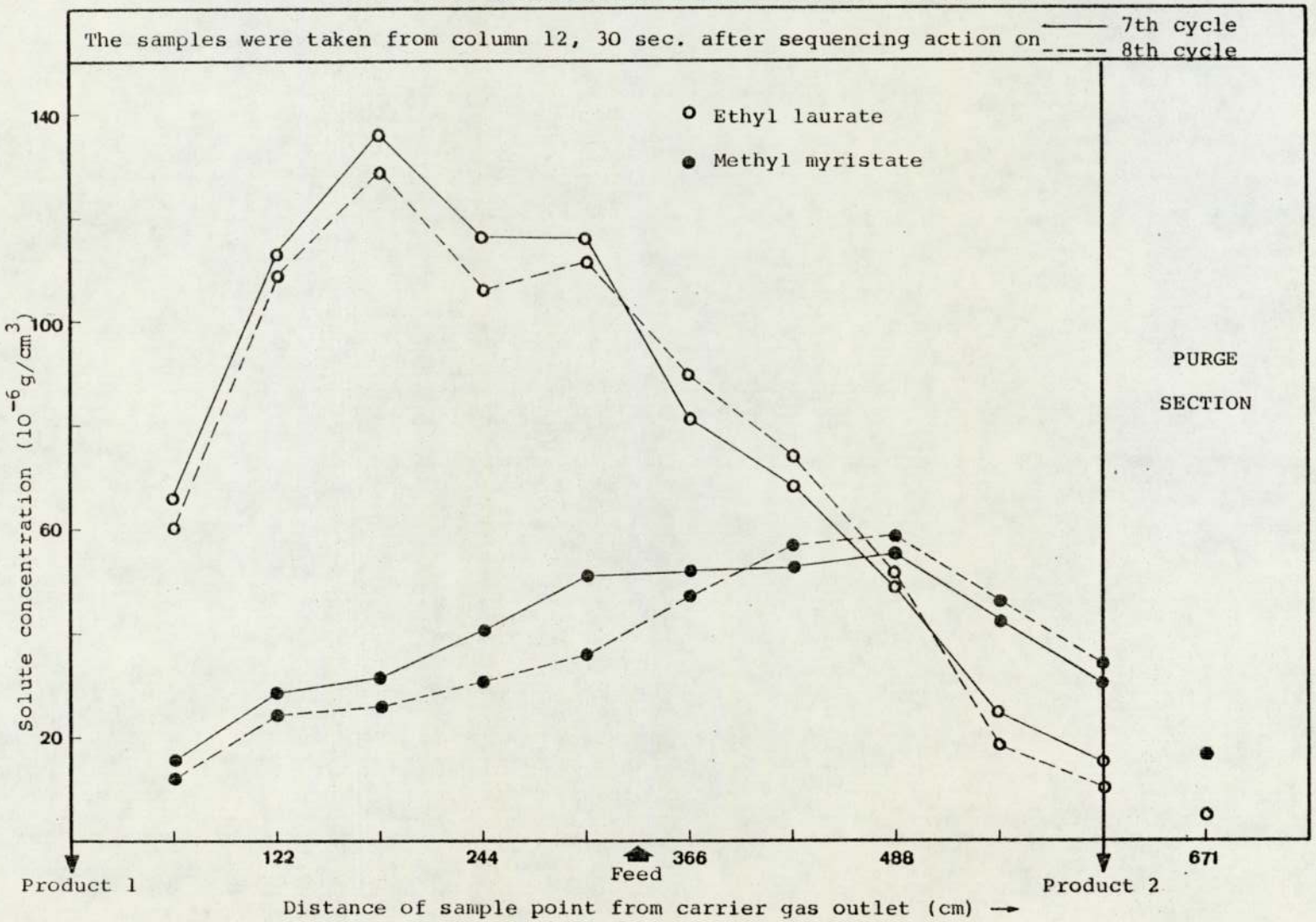

FIG. 7.26 CONCENTRATION PROFILE FOR RUN 185-60-74-100

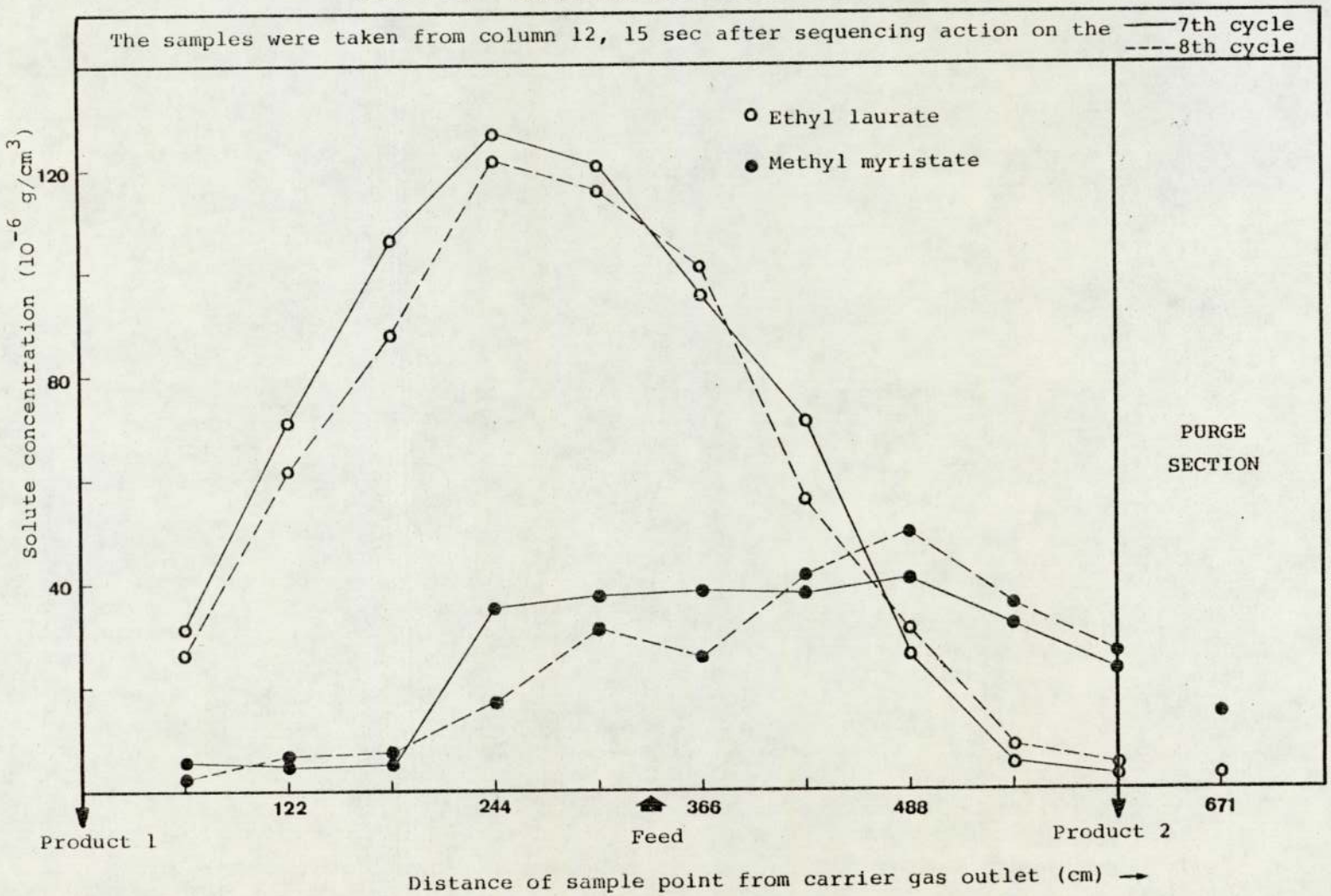

FIG. 7.27 CONCENTRATION PROFILE FOR RUN 185-60-85-150

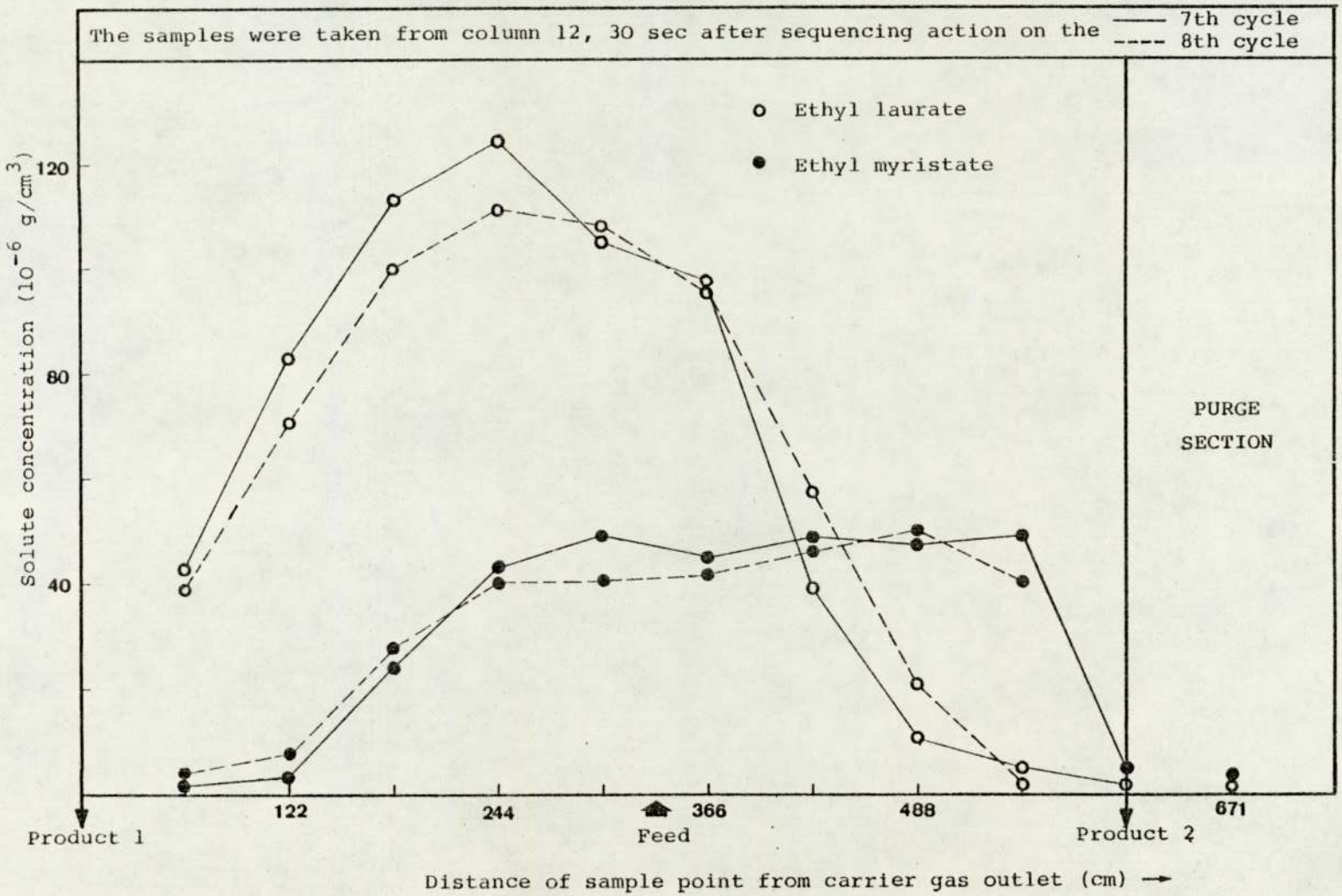

FIG. 7.28 THE EFFICIENCY OF THE PURGE PROCESS FOR RUN 185-25-83-150

The samples were taken from column 12 at the end of the 10th cycle

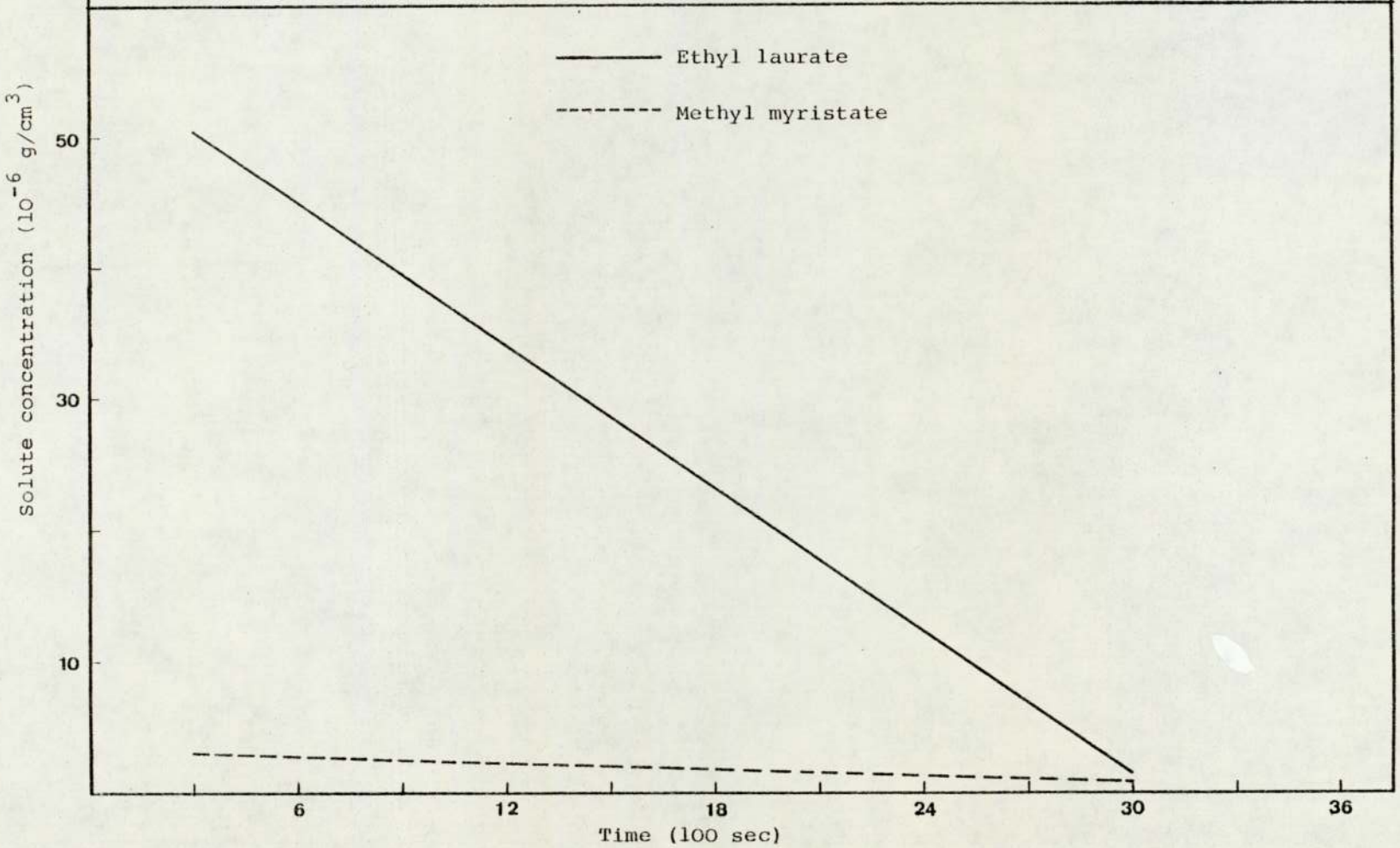

FIG. 7.29 THE EFFICIENCY OF THE PURGE PROCESS FOR RUN 185-45-83-150

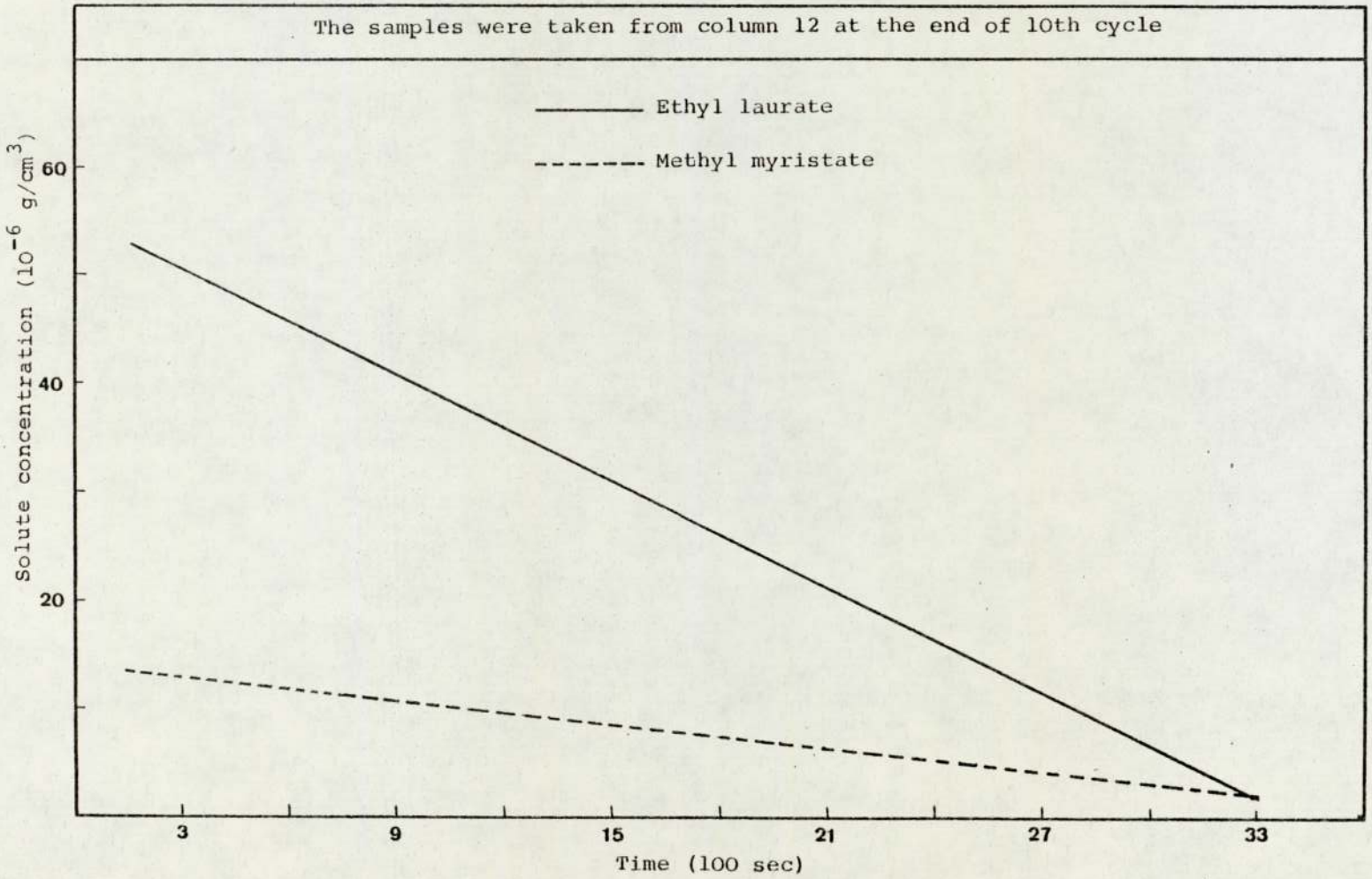

FIG. 7.30 THE EFFICENCY OF THE PURGE PROCESS FOR RUN 185-60-83-150

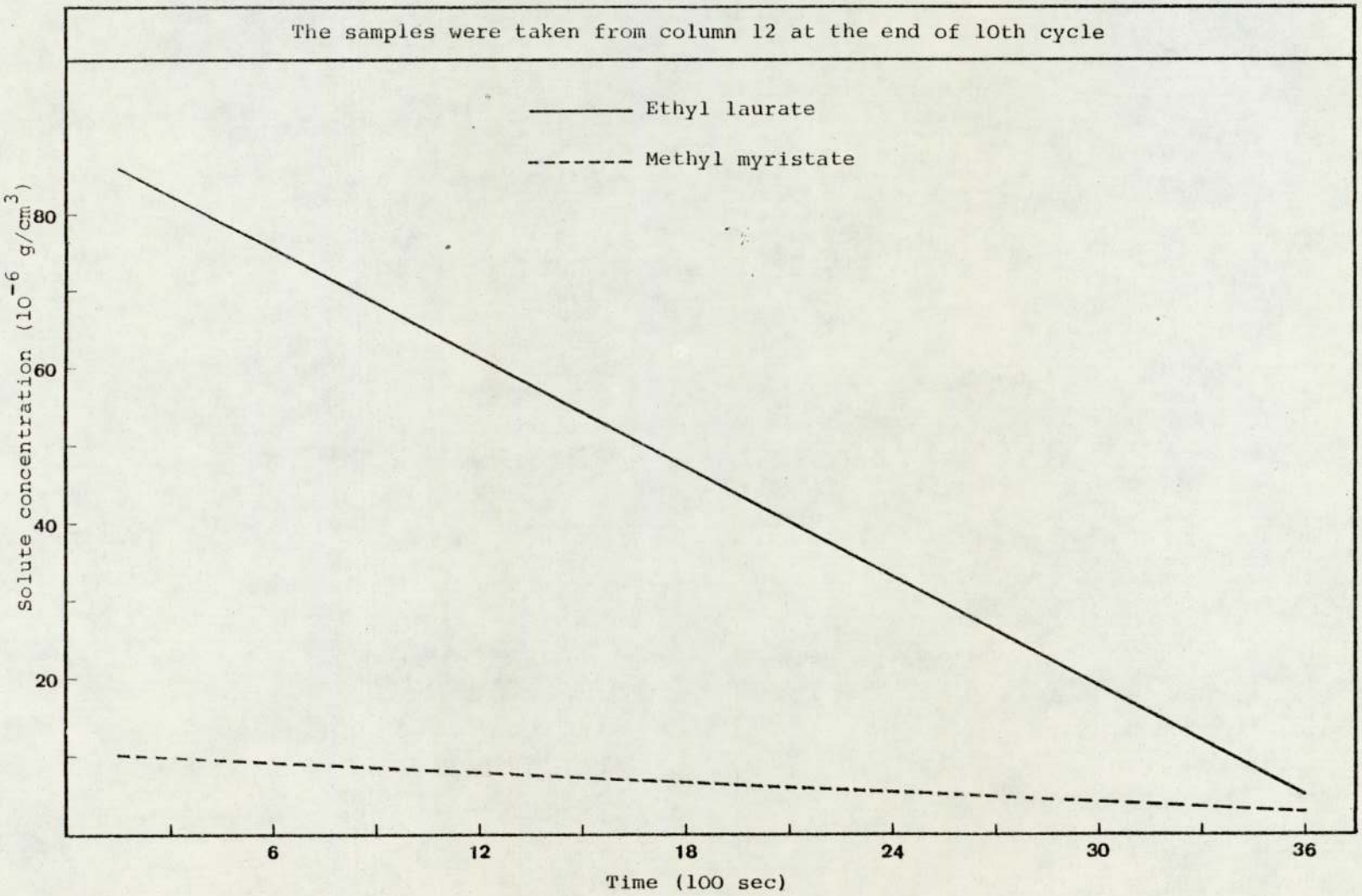

150 and 185 - 45 - 83 - 150 can be considered to be successful separations with purities in excess of 98% and reproducible concentration profiles.

Consideration of Figs. 7.23 to 7.26 shows that the separating section of 10-columns has been used even at lower feed rates of 25 cm^3 h^{-1}. The profile of product 2 (methyl myristate) had advanced three columns in front of the feed point in run 185 - 25 - 83 - 150, (Fig. 7.23), while in run 185 - 45 - 83 - 150 the profile of product 2 had extended to cover the whole available separating column length (Fig. 7.24). In this case very significant contamination of product 1 (ethyl laurate) occurred, and the purity dropped to 97.6%.

The mean level of the gas phase concentration of product 2 (methyl myristate) increased to a significant level in column 1 (61 cm from the carrier gas outlet) with an increase in the feed rate to 60 cm^3 h^{-1} (Fig.7.25). In this case product 1 purity was severly reduced to 94.2%.

The behaviour of the ethyl laurate (product 1) profile during the study was similar to the methyl myristate profile and this should have led to the same product purity. However, this was not the case. The difference in both product purities in run 185 - 25 - 83 - 150 was not significant, but it was in run 185 - 45 - 83 - 150. It

is thought that unsuccessful purging of product 1 from the isolated column was the explanation of this.

As the feed rate was increased, the concentration level of both components increased but this was less appreciable in the case of product 2 than product 1.

In run 185 - 60 - 74 - 100 (see Fig. 7.26) the switching rate was reduced to 100 - seconds, and $G_{m,c}/L'$ to 74 in an attempt to improve on the purities obtained in run 185 - 60 - 83 - 100. This attempt was based upon the fact that if the pressure drop is reduced, the fluctuation in flow will be less. Slight improvements in the purities of both products were noticed (Table 7.7). The resultant profiles of both solutes as shown in Fig. 7.26, were similar to the profiles of run 185 - 60 - 83 - 150 as shown in Fig. 7.25. The exception was that the concentration level of both solutes was lower than for the previous run. This was so because the feed mixture was fed into the column in 100-seconds compared with 150 - seconds.

Ethyl acetate as a third component was introduced with the feed in run 185 - 60 -85 - 150, in another attempt to improve the product purities. However, the purities did not improve or improved only slightly (Table 7.7) and flow fluctuation in the separation and purge sections was experienced. This necessitated frequent adjustment. The phenomenon was not experienced under any other conditions.

The concentration profiles of both solutes as shown in Fig. 7.27 retained the general shape of the other profiles. In addition, the general level of solutes concentration was kept the same as for run 185 - 60 - 83 - 150, as shown in Fig. 7.25.

However, the partition coefficient is specifically related to the migration rate of the mean solute molecule and this is more so at higher temperatures. Giddings (51) noted that the solute zone migration velocity was dependent upon the local column temperature. As the solute concentration is increased the spread of the solute band around the mean solute molecule increases giving a wide variation in the velocity of individual molecules in the direction of gas flow. This variation results from the combined effects of the form of the absorption isotherm, the 'sorption effect' and enthalpic overloading. Resolution of the two species becomes more difficult, since the length of column required to effect the separation increases for low throughputs as is the case in this study. At the limit all of the available separation length is being used (Fig. 7.24 and 7.25). Increasing the throughput levels beyond this value will, for the operating flow rates used in this study, result in contamination of both products even though equation 7.3 is satisfied. Similarly, for the isolated section of fixed length, elimination of the tailing effect needs higher purge gas rates than predicted by equation 7.2.

It was not possible to obtain these with the SCCR-2 unit without the serious consequence of very high fluctuations in the flow which endangered the separation as a whole.

In the discussion so far, isothermal operating conditions have been assumed. This cannot be true in practice with such high temperature separations, because of the combined effects of the heat of solution of the larger samples and the finite rate of heat transfer across large diameter columns. Non-isothermal operation of 10 cm diameter columns has been demonstrated by Hupe et al (57) and of 2.5 cm diameter columns by Peters and Euston (67), Rose (68) and, more recently in a similar unit of 7.6 cm diameters columns (SCCR-1), by Bell (31). Scott (69) has studied the temperature effects resulting from the passage of a solute through a theoretical plate and concludes that the excess heat generated increases with increasing flow rate, sample size, and decreasing partition coefficient values. The above mentioned arguments could highlight what has happened during separation of this system at high temperature and why a lower throughput with degraded purities was experienced in run 185 - 45 - 83 - 150.

The simplified inequality of Equation 7.2, has provided a basis for the selection of the purge gas rate. However, several factors can impose restrictions upon this equation such as; column length, finite concentration effects,

mobile phase compressibility, the effect of temperature fluctuations .... etc., (see Section 6.1). Therefore complete regeneration of the column was not experienced particularly at feed rates of 45 and 60 $cm^3 h^{-1}$.

Comparison of the results of run 185 - 25 - 83 - 150 (Fig. 7.28) with run 185 - 45 - 83 - 150 and 185 - 60 - 83 - 150 (Figs. 7.29 and 7.30), shows several trends. As the feed rate is increased to 45 and 60 $cm^3 h^{-1}$ a successful purging process tends to be extremely difficult to achieve. However, in the time available for purging, i.e. two switching intervals 60-70% was being removed, 30 - 40% of the product remaining behind on the packing to be eluted later.

In such cases, severe contamination of both products has occurred, expecially in runs at feed rates of 45 and 60 $cm^3 h^{-1}$. A study by Bell (31) has revealed that at high feed rates, the temperature in the purge bed could fall 20 - 30 K below ambient. The effect of this fall in temperature has a very significant effect upon the partition of the two solutes in that both thermodynamic theory (167) and experimental results (169), give log K^{∞} as an inverse function of the absolute temperature. At temperatures of 20 - 30 K lower than the ambient temperature more than twice the expected purge gas rate is required. Hence, even with a double purge system, complete removal of the bottom product from the isolated columns is not possible.

In conclusion to this part of the study, it can be said that with regard to the SCCR-2 unit, improved separations will occur at higher temperature with higher throughputs, if an improved design for the purge section can be implemented. Although the mechanical limitations do not allow the unit to be operated at the optimum value of purge flow rates and consequently throughputs, these results were encouraging and it was decided to attempt to separate a mixture at even higher temperature. The maximum temperature of operation, the SCCR-2 unit based on construction materials, is 210° C, because of the P.T.F.E. popette valves. This material starts losing its resiliency at 210-215° C (170) in which case the sealing efficiency will be affected. Hence, a mixture of two fatty acid methyl esters of myristic and stearic acid were chosen for study at an operating temperature of 205° C which is a few degrees less than the maximum temperature the P.T.F.E. can stand without loss of sealing efficiency.

7.7 METHYL MYRISTATE AND METHYL STEARATE AT 205° C

7.7.1 Results

Four experimental runs were performed as shown in Table 7.8. Using a 50:50 w/w mixture of methyl myristate and methyl stearate, the latter dissolved in ethyl acetate as it is a solid at ambient temperature.

The $G_{m.c.}/L'$ was again selected in the range of 78 - 94 and the feed rate was increased from 20 cm^3 h^{-1} to a maximum

Table 7.8

The Separation of Methyl Myristate/Methyl Stearate

	Temperature			Ambient Condtions		Solute Mixture Feedrate	I_s	L'	Separating Section					Purge Section				
	Opera -tion	Carrier Inlet	Purge Inlet	θ_a	P_a				G_a	P_{in}	P_{out}	J_3^2	G_{mc}/L'	S_a	P_{in}	P_{out}	J_3^2	S_{mc}/L'
θ-f-G_{mc}/L'-I_s	°C	°C	°C	°C	KP_a	cm^3h^{-1}	s	cm^3s^{-1}	cm^3s^{-1}	KP_a	KP_a	-	-	cm^3s^{-1}	KP_a	KP_a	-	-
205-20-78-150	205	220	225	23	101.0	20	150	0.1	10.2	267	137	0.65	78	123	198	119	0.74	1219
205-30-87-150	205	228	225	22	101.0	30	150	0.1	11.3	253	157	0.71	87	127	205	125	0.74	1212
205-40-94-150	205	228	225	21	101.0	40	150	0.1	11.8	253	143	0.71	94	127	198	117	0.73	1270
205-30-83-100	205	228	230	21	101.0	30	100	0.15	15.9	205	129	0.76	83	125	205	129	0.76	795

Summary of Results

Run Title	K^∞		Separating Section		Purge Section	Total Time of Run	Total no. of Cycles	Time to Pseudo steady state	Product Purities	
	Methyl myristate	Methyl stearate	G_{min}/L'	G_{max}/L'	S_{min}/L'				% M.M.	% M.S.
θ-f-G_{mc}/L'-I_s	-	-	-	-	-	h	-	h		
205-20-78-150	37	106	63	120	1038	8	10	3	85.5	90.9
205-30-87-150	37	106	75	116	1036	7	9	3	82.0	81.5
205-40-94-150	37	106	79	133	1076	7	9	3	74.0	70.0
205-30-83-100	37	106	65	143	694	8	9	3	82.0	75.0

of 40 cm^3 h^{-1} in steps of 10 cm^3 h^{-1}. The switching rate was kept at 150 - seconds in the first three runs and reduced to 100 - seconds when the purity was impaired in run 205 - 80 - 150.

No column to column concentration profiles was obtained because of a serious condensation problem in the sampling line. Thus, the only record of performance of the sequential unit for these experimental studies was the product purities over different cycles which were taken from the condensing traps (Table 7.9a, b, c, d).

7.7.2 Discussion

Discussion of the results presented in Table 7.8 is difficult in the absence of the concentration profiles, which given an idea of the performance of the SCCR-2 unit. However, there are many possible factors which may have affected the separation at this high temperature and which could explain the poor product purities for this separation.

It was concluded in Section 7.2 that the efficiency of the column in terms of the number of plates is inversely proportional to temperature. With this fact in mind, the low performance of the SCCR-2 unit in the separation of this mixture is not surprising. An increase in plate temperature has the effect of increasing the peak assymmetry for a given solute. This is to be expected because the speed with which the methyl myristate and methyl stearate bands pass, through a column is inversely proportional to their

Table 7.9a

Product Purities of Individual Cycles in Run 205-20-78-150

Cycle Number	Product Purities (%)	
	Methyl myristate	Methyl stearate
2	40.5	38.0
4	89.1	86.0
6	91.2	90.0
8	90.5	89.3
10	92.2	88.3

Table 7.9b

Product Purities of Individual Cycles in Run 205-30-87-150

Cycle Number	Product Purities (%)	
	Methyl myristate	Methyl stearate
2	37.0	43.0
4	74.3	68.2
6	82.4	81.5
8	78.1	80.0
10	83.0	82.0

Table 7.9c

Product Purities of Individual Cycles in Run 205-40-94-150

Cycle Number	Product Purities (%)	
	Methyl myristate	Methyl stearate
2	25.0	23.0
4	61.0	53.0
6	74.0	70.0
8	72.0	70.0
10	74.5	71.0

Table 7.9d

Product Purities of Individual Cycles in Run 205-30-83-100

Cycle Number	Product Purities (%)	
	Methyl myristate	Methyl stearate
2	26.0	31.0
4	51.5	60.0
6	82.0	78.0
8	81.0	79.0
10	82.5	80.2

partition coefficients, which, in turn, decrease exponentially with temperature. It is also possible that the solute(s) velocity profile in the columns has been affected by the transient heat of solution effect in the chromatographic bed. It is worth mentioning that the temperature variations associated with heat transfer across large diameter columns are entirely different from the heat of solution and are caused by the poor heat-transfer characteristics of support materials. Hence the excess plate temperature generated by the passage of the solute will be dissipated more rapidly at the edge of the column than at the centre. This will result in a radial temperature gradient in the column. The radial gradients will give rise to non-uniform cross column solute migration rates, and also contribute to band velocity profile differences. The effect of the radial temperature gradient upon the solute migration rate is still a matter for conjecture. Hupe and co-workers (57) maintain that the centre of the band will be advanced relative to the column wall. Conversely Hyten et al (53) believe that the band centre is retarded relative to the column wall. It is possible that both bodies of opinion may be correct. In investigations of temperature profiles in chromatographic column, diameters ranging from 0.1 to 10 cm have been used and whilst it is questionable to compare results from columns of different diameters, a general trend may be that as the column diameter increases the column tends towards an

adiabatic situation, which could be the case with the SCCR-2 unit. However, in the operation of the SCCR-2 at very high temperature, any variations accompanying the solute band will be lessened by heat conduction through the column packing and column wall. An axial temperature gradient will, however, still exist in which the leading edge of the solute band will be at a higher temperature than ambient giving an increased solute migration rate, whilst the trailing edge of the solute band will be retarded due to the lower temperature being experienced. Therefore, the product 1 profile is more distorted than that eluted later from the column. This case resulted in severe contamination of both products and the lower product purities experienced.

In general, the effect of temperature is also interactive with the flow fluctuation. The change in flow velocity (G), especially in the separating section, caused by gas expansion is the most severe and for typical separations performed by the SCCR-2 at very high temperature (160-205°C), there can be a 100% change in the volumetric gas flow rate. In practical terms this means that should both solute molecules be present in the region close to the carrier gas inlet, the rate of migration will be reduced. Then the solute molecules which should be travelling preferentially with the carrier gas are eventually retarded sufficiently to contaminate product 2. While at the other

end of the separating section the opposite effect is experienced with the rates of migration greatly accelerated. Hence, any component 2 molecules present near to the outlet will have a resultant velocity in the direction of the mobile phase flow, and produce a long leading edge to the concentration profile, with the eventual contamination of the product 1 stream. This explanation is confirmed by the results in Table 7.8. On the other hand the results in Table 7.9 a,b,c,d, confirm that the first four cycles are the building cycles in the establishment of pseudo-steady state conditions. While the variation in the product purities in the subsequent cycles are due to many reasons, including changing the traps every other cycle, and the presence of ethyl acetate as a solvent for methyl stearate. Under the operating conditions for this system at high temperature (205°C), ethyl acetate will vapourise and its vapour can stay in the feed distributor. The presence of the gas phase in the feed distributor will result in non-uniform feeding around the 12-columns and consequently disturb the pseudo-steady state conditions required for a successful separation. A maximum throughput of 20 cm^3 h^{-1} was achieved. This was thought to be governed partly by chromatographic limitations of the SCCR-2 and partly by the combined effects of temperature and non-vaporisation of the liquid feed mixture.

The separating capabilities of the SCCR-2 unit have been further studied using an industrial mixture called

fungal oil at 185° C.

7.8 THE RECOVERY OF γ-LINOLENIC ACID FROM FUNGAL OIL AT 185°C

7.8.1 Introduction

The recommendation made by Liodakis (16) to recover an industrially important fatty acid called γ-linolenic acid from fungal oil was attempted. Fungal oil is a complex industrial mixture of unknown esterified fatty acids in the methyl form containing 20% of γ-linolenic acid (Fig. 7.31). The γ-linolenic acid can be valuable as a dietary supplement for people suffering from multiple sclerosis (blood deficient in fatty acids). The separation of γ-linolenic acid by crystallization or any other conventional separation method can be very costly.

Initial experimental studies (16) on the sequential unit have shown that the recovery of γ-linolenic acid involves many practical difficulties. The reason for these was believed to be the comparatively high partition coefficients (K^{∞}) of γ-linolenic acid and the other fatty acids in the fungal oil on F.F.A.P stationary phase, in addition to their relatively low separation factors.

To overcome this difficulty, the F.F.A.P. had to be replaced by a more specific liquid phase for this kind of separation. The results of Liodakis (16) show that OV-275 liquid phase is the most suitable phase, because it gives comparatively low values for the respective partition

FIG. 7.31 G.L.C. ANALYSIS OF HYDROLYSED-METHYLATED "FUNGAL OIL"

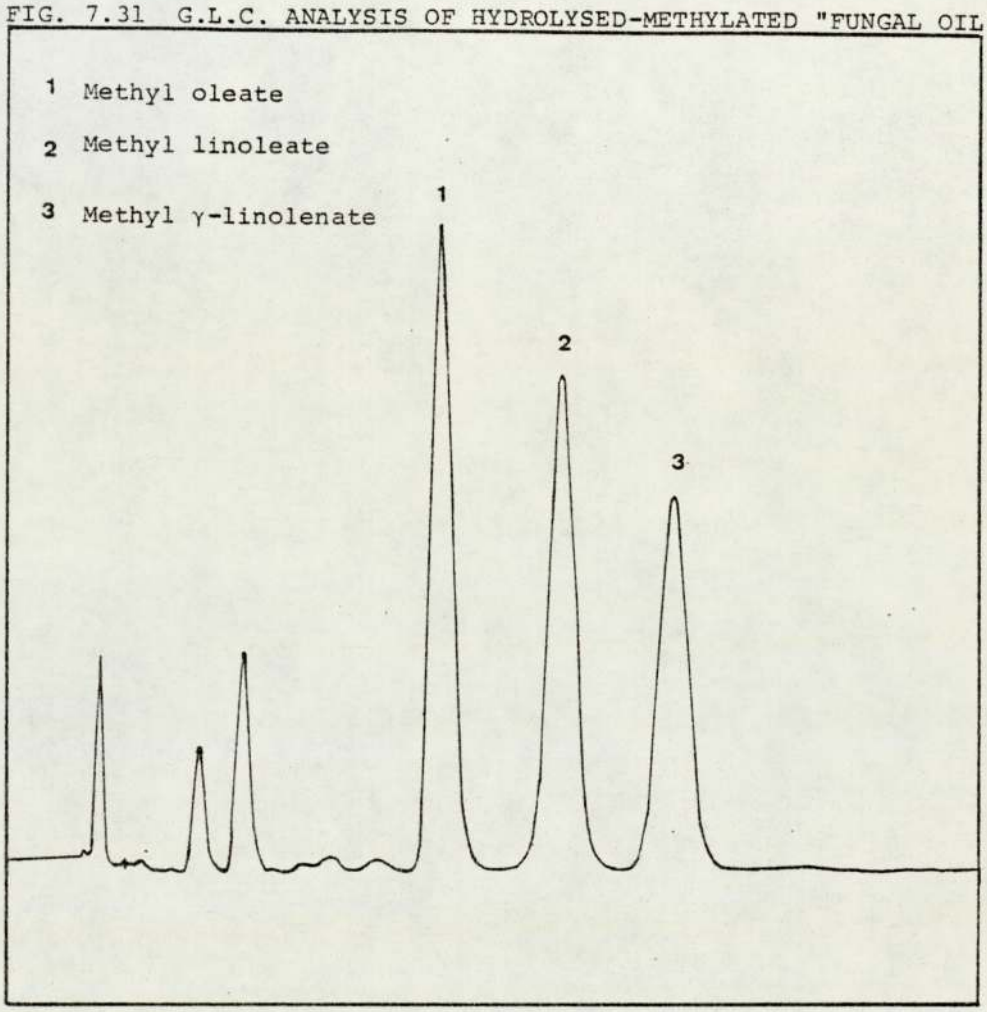

coefficients and has high thermal stability.

Another modification was to introduce the feed fungal oil as a vapour. This was achieved by passing a regulated flow of nitrogen through two feed tanks in series, located inside the SCCR-2 oven. Each feed tank was made out of stainless steel tube 2.5 cm in I.D. and 30.5 cm in length and these were half filled with the "fungal oil" mixture. The carrier gas passed through the two tanks carrying the solute vapours to the feed distributor and then to the chromatographic columns through the energized feed diaphragm valves.

The feed throughputs which could be introduced into the system were very low, i.e 1-3 $cm^3\ h^{-1}$.

7.8.2 Results

The results obtained (Table 7.10) demonstrate the rather unsatisfactory performance of the sequential unit in dealing with low separation factor systems such as the separation of γ-linolenic acid from "fungal oil", which has a separation factor of 1.19 at 185° C. This is mainly due to the $G_{m.c.}/L'$ variations across the separation section, which are very critical in multicomponent separations. Temperature fluctuation is also one of the factors that could affect the separation. However, the lighter components of the "fungal oil" mixture were satisfactorily removed from the product 2, which now contained up to 52% of methyl γ-linolenate compared to the 20% initially present in the

Table 7.10

The Separation of Fungal Oil

Run Title	Temperature			Ambient Conditions		Solute Mixture Feedrate	I_s	L'	Separating Section					Purge Section				
	Opera-tion	Carrier Inlet	Purge Inlet	θ_a	P_a				G_a	P_{in}	P_{out}	J_3^2	G_{mc}/L'	S_a	P_{in}	P_{out}	J_3^2	S_{mc}/L'
θ-f-G_{mc}/L'-I_s	°C	°C	°C	°C	KP_a	cm^3h^{-1}	s	cm^3s^{-1}	cm^3s^{-1}	KP_a	KP_a	-	-	cm^3s^{-1}	KP_a	KP_a	-	-
181-1-411-300	181	185	186	25	101	1.2	300	0.051	28	255	144	0.7	411	153	214	152	0.82	2490
181-1-455-300	181	184	185	22	101	1.2	300	0.051	32	280	135	0.63	455	173	221	159	0.83	2752
183-1-465-300	183	185	186	23	101	1.3	300	0.051	38	322	157	0.63	465	166	235	179	0.86	2433
183-1-415-300	183	185	186	23	101	1.1	300	0.051	36	324	193	0.73	415	164	248	200	0.89	2226
183-1-463-300	183	185	186	24	101	1.0	300	0.051	38	322	157	0.63	463	174	236	181	0.86	2513

Summary of Results

Run Title	K^∞		Separating Section		Purge Section	Total Time of run	Total no. of Cycles	Time to Pseudo Steady State	Product Purities
	Methyl linoleate	Methyl γ-linolenate	G_{min}/L'	G_{max}/L'	S_{min}/L'				% Methyl γ-linolenate in Product II Stream
θ-f-G_{mc}/L'-I_s	-	-	-	-	-	h	-	h	
181-1-411-300	320	398	333	587	2181	8	7	3	36
181-1-455-300	320	398	351	722	2406	8	7	3	47
183-1-465-300	295	363	361	738	2169	8	7	3	50
183-1-415-300	295	363	240	568	2030	8	6	3	52
183-1-463-300	295	363	359	734	2255	8	5	3	49

feed mixture.

7.8.3 Discussion

Consideration of the gas chromatographic analysis of the "fungal oil", Fig. 7.31, shows that the methyl γ-linolenic acid comes at the end of the mixture. Since the SCCR-2 machine is capable of producing only two products for a single-pass operation, the cut position for this purification problem should be between the methyl γ-linolenate and methyl linoleate components, the separation factor being 1.19 at 185° C. Although the temperature is well below the boiling point of the fatty acid ester solutes, it is thought that most of the feed entering the column was retained on the packing without being eluted. Since, the methyl linoleate and the methyl γ-linolenate are isomers of C_{18} highly unsaturated fatty acids (3 double band). It is possible that the tarry material discovered on the valve popettes was the result of polymerisation. This caused the separation study to be abandoned.

7.9 CONCLUDING DISCUSSION OF THE SEPARATION STUDIES

The results presented in this chapter demonstrate the performance of the SCCR-2 unit for the separation of various systems; fatty acid esters over a wide range of temperatures (60-205° C).

For relatively easy systems such as that of ethyl acetate/ethyl butyrate with a separation factor of 2.3 at 60° C

quite successful separations were achieved (Table 7.11). For the more difficult separation of an ethyl caprylate/ethyl caprate mixture, at feed rates of up to 80 cm^3h^{-1}, high purity products were obtained. At a higher temperature of 160°C for the more difficult system of ethyl caprate/ethyl laurate, the maximum throughput to obtain high product purities was reduced to 50 cm^3 h^{-1}. However, at even higher temperature (185°C), a successful separation of ethyl laurate/methyl myristate was performed. The maximum throughput permissible to obtain reasonable product purities was 25 cm^3 h^{-1}.

The separating capabilities of the SCCR-2 unit were further studied using higher temperature of 205°C to separate a mixture of methyl myristate/methyl stearate. A considerably lower throughput (20 cm^3 h^{-1}) than the previous systems was used to give product purities in the range of 85-90%, as shown in Table 7.11.

Furthermore, an industrial mixture at different fatty acids called "fungal oil" was attempted to recover an industrially important fatty acid, γ-linolenic acid, at 185°C. However, unsatisfactory results were obtained.

Five factors have been considered as restricting the separating capabilities of the SCCR-2 unit, namely:

1. The temperature fluctuations during operation caused by many factors such as, variation in the oven temperature, the enthalpic overloading effects,

Table 7.11

Summary of the Chemical Mixtures used in the Separation Studies

Mixture	Comments	Partition Coefficient of Solute on OV-275		Separation Factor	Required Operating Temperature Range For Separation	Throughput $cm^3 h^{-1}$	Product Purities	
		K_1^∞	K_2^∞				Top	Bottom
Ethyl acetate Ethyl butyrate	Equivolume binary mixture	57 at 60°C	135 at 60°C	2.3	60- 70°C	40	99.3	99
Ethyl caprylate Ethyl caprate	"	60 at 105°C	114 at 105°C	1.9	105-110°C	50 80	99.4 98.8	99 98.2
Ethyl caprate Ethyl laurate	"	74 at 160°C	107 at 160°C	1.44	155-175°C	50 75	99.4 95.1	98.4 94.8
Ethyl laurate Methyl myristate	70:30 Binary mixture	40 at 185°C	63 at 185°C	1.57	180-190°C	25 45	98.5 97.6	98.0 94.8
Methyl myristate Methyl stearate	50:50 W/W +25% Ethyl acetate	37 at 205°C	106 at 205°C	2.86	200-210°C	20 30	85.5 82.0	90.9 81.5
Fungal Oil a mixture of the following fatty acids Methyl palmitate Methyl stearate Methyl oleate Methyl linoleate Methyl γ-linolenate	Multicomponent mixture by hydrolysing and methylating "fungal oil" from which the recovery of methyl γ-linolenate was studied on the SCCR-2 unit.	K^∞ m-linoleate =144 at 185°C	K^∞ m-γ-linolenate =172 at 185°C.	1.19	210-280°C	1	-	52

the probable difference in temperature between the carrier gas and the column temperature ..... etc.

2. The increase in the respective solute partition coefficients with finite concentrations.

3. The variation of the solute molecule velocity through the separating section with both solute concentration and the inevitable pressure gradient.

4. The semi-continuous nature of operation.

5. The finite length of the separating section or, to be exact, the finite number of theoretical plates.

Factors 1, 2 and 3 appeared to be the most significant for the comparatively high temperature separations.

Operating the sequential unit at temperatures which gives the lowest partition coefficients was found to be beneficial for the separation, hence the feed mixture was then easily vapourized into the columns. However, for the "fungal oil" mixture operation at such temperatures was not possible because of the high thermal instability of the mixture and the operating limitations of the SCCR-2 equipment.

Finally several possible changes will be suggested in Chapter 9.

CHAPTER 8

THEORETICAL TREATMENT OF THE SCCR-2 UNIT

8.1 INTRODUCTION

For the moving-bed form of continuous chromatography a statistically based model was proposed by Sciance and Crosser (171) to relate the degree of separation, operating conditions and required column length for a binary feed mixture. For components A and B introduced into the mid-point of the column they obtained:

$$\ell n(u_z)_1 = \frac{\ell . K_1''}{2.u} (K_1^{\infty} - \psi) \qquad (8.1)$$

$$\ell n|1-(u_z)_2| = \frac{-\ell K_2''}{2.u} (K_2^{\infty} - \psi) \qquad (8.2)$$

$(u_z)_1$ = bottoms/feed mass flow rate ratio of component A

$(u_z)_2$ = tops/feed mass flow rate ratio of component B

K'' = rate constant of desorption

u = average mobile phase velocity

ψ = operating mobile phase/stationary phase velocity ratio

ℓ = required column length.

Use of the above equations relies on knowing values for K_1'' and K_2''. As published values are scarce and the experimental procedures for their determination are usually difficult, the application of this model is very restricted.

Based on the random walk approach (section 2.3.2.2),

Al-Madfai (26) obtained an expression for predicting plate height in continuous 'moving column' counter-current chromatographs as follows:

$$H = d_p + \frac{2D_m}{u} + \frac{2r'.r''}{u.r''-u_L r'}\left(\frac{u+u_L}{r'+r''}\right)^2 \qquad (8.3)$$

r' = rate of transfer of molecules from gas to liquid

r'' = rate of transfer of molecules from liquid to gas

u_L = stationary phase velocity.

When equation 8.3 is compared to the static column case; in which the plate height

$$H = d_p + \frac{2D_m}{u} + \frac{2.r'.u}{(r'+r'')^2} \qquad (8.4)$$

the inclusion of a term in u_L in equation (8.3) accounts for the extra zone broadening caused by movement of the stationary phase. Al-Madfai (26) using the work of Gluekauf (41) as a basis, related the two plate height definitions through the equation:

$$\frac{N_{CC}}{N} = 3(\alpha-1) \qquad (8.5)$$

where

N_{CC} = number of counter-current theoretical plates or stages

N = number of co-current theoretical plates (elution chromatography)

α = separation factor = K_2/K_1.

The above equation indicates that for systems having a separation factor below 1.33, less theoretical plates are necessary for the continuous case than for the static column. A similar study on the relationship between N_{CC} and N was conducted by Rony (172-174).

Quoting the work of Fitch et al. (88), Barker and Huntington (8, 10, 28) adapted the theory of stage-wise liquid/liquid extraction giving by Alder (175) to develop a relationship for the separation, to an equal degree of purity, of a two component equimolar feed mixture. For a solute mixture feed point at the centre of the separating section:

$$\log \frac{(G/L)_R}{(G/L)_S} = \log\left(\frac{K_2}{K_1}\right) + \frac{2}{N_{CC}}\left|\log\left(1-\frac{E_1}{F_1}\right)+\log\left(\frac{E_2}{F_2}\right)\right| \qquad (8.6)$$

where

$(G/L)_R, (G/L)_S$ = ratio of gas to liquid phase flow rates in the 'rectifying' and 'stripping' sections respectively.

E_1, E_2 = the mass production rates of components 1 and 2 in the top product.

F_1, F_2 = the mass feedrates of components 1 and 2 to the column.

One major disadvantage of equation 8.6 is the inherent assumption of a constant partition coefficient i.e. the infinite dilution value. Tiley (176) overcame this drawback

by developing a computer programme to perform stage-to-stage calculations for a vertical moving-bed column system which allows the introduction of a non-linear absorption isotherm. Tiley (176) who studied the effect of stage number, flow conditions and temperature on the column concentration profiles concluded two significant factors. Firstly, that there was a limiting feed throughput for a given solvent rate, product purity and number of stages, which is dependent on the phase equilibrium characteristics. Secondly, Tiley found an optimum operating temperature below the boiling points of the main components of the feed mixture. In a later paper Pritchard et al. (89) compared the results of a multi-stage computational procedure with experimental results and, provided that an HETP of 13-18 mm was assumed, very approximate agreement was obtained between experiment and theory. Pritchard et al. (89) also argued that a theoretical analysis of the process in terms of the height of a transfer unit (H.T.U.) is the more logical concept for a system involving packed columns, although plate to plate models are more amenable to computation in non-equilibrium systems. Arkenbout and Smith (177), from theoretical considerations, concluded that it is incorrect to assume that the transfer unit analysis will always be more satisfactory than the theoretical plate analysis. Recently, Holland et al. (178) have attempted a synthesis of the two ideas by introducing the concept of

a mass transfer section, thereby enabling the computational procedure for a packed column to be similar to that for a stagewise.

Barker and Lloyd (5, 28) have developed the concepts of H.T.U. for treatment of the counter-current gas/liquid chromatographic process and derived the following equations:

$$(N_{OG})_R = \frac{1}{Q_G/(KQ_L-1)} \ln \left[\frac{M_1/KQ_L - Y_1(Q_G/KQ_L-1)}{M_1/KQ_L - Y_2(Q_G/KQ_L-1)} \right] \qquad (8.7)$$

$$(N_{OG})_S = \frac{1}{(1-Q_G/KQ_L)} \ln \left[\frac{M_2/KQ_L - Y_1(1-Q_G/KQ_L)}{M_2/KQ_L - Y_2(1-Q_G/KQ_L)} \right] \qquad (8.8)$$

Q_G = gas volumetric flow rate.

Q_L = liquid volumetric flow rate.

M_1, M_2 = mass flow rate of solute leaving the column in the product 1 and product 2 streams respectively

$(N_{OG})_R, (N_{OG})_S$ = number of overall gas phase transfer units in 'rectifying' and 'stripping' section respectively.

Barker and Lloyd applied this technique to the vertical moving-bed column and indicated that the main resistance to mass transfer was in the gas phase. Furthermore, a first order relationship was found between the solvent (stationary) phase flow rate and the logarithm of H_{OG}, with H_{OG} values of the order of 10 cm for the systems and conditions studied (3, 4, 28).

All the theoretical treatments of counter-current chromatography discussed in section 8.1 assumed true steady-

state operation, which is only achieved in the original moving-bed systems. An additional variable, time, must be introduced for simulating sequential chromatographic type operations. Sunal (169) developed a digital computer programme for gas/liquid chromatography based on plate-to-plate calculations to describe the operation of the compact circular counter-current chromatograph reported in Chapter 2. A similar approach was also employed by Deeble (13) to simulate the operation of the SCCR-1 gas/liquid chromatographic unit. Bell (31) modified this computer model by introducing other factors, e.g. temperature profiles to improve the accuracy of simulation.

Sakodynskii et al. (179, 180) have developed a plate model of a chromatographic column to include the effects of a non-linear isotherm and interaction between feed components. In a recent publication (181) they have developed a model for calculating the distribution of concentrations at the column outlet based on a semi-continuous chromatographic column model and using as their initial equation a material balance of the form derived by Deeble(13).

In the present work the concept of the plate model, employed by Deeble (13) and Bell (31) for gas/liquid chromatography, has been adapted as a first attempt to simulate the SCCR-2 unit, with the theoretical determination of temperature, pressure and concentration profile. The

HETP has also been determined from a purely theoretical background (see Appendix 4) in an attempt to exclude all experimental results from the model.

However, the accuracy of the simulation was not in good agreement with the experimental results especially at the feed point, (i.e. the computed concentration profiles possessed higher concentration levels than the experimental runs). It was concluded, after these preliminary investigations, that by redefining the mass balance over the feed plate, would greatly enhance the accuracy of the simulation. Bell in his model (31) considered the concentration over the feed plate constant.

8.2 THE MODEL

8.2.1 Mass Balance Over a Theoretical Plate

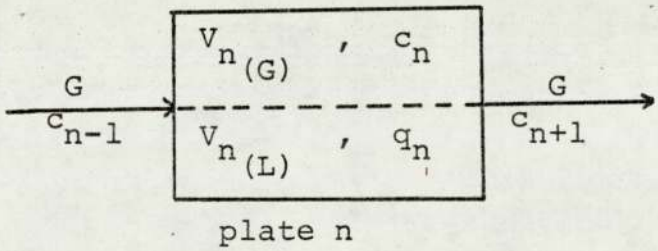

Fig. 8.1

The chromatographic column is considered to consist of a series of idealised mixing stages or theoretical

plates, and a mass balance over plate n gives:

$$G.c_{n-1}=G.c_n+V_{n_{(G)}}.\frac{dc_n}{dt}+V_{n_{(L)}}.\frac{dq_n}{dt} \qquad (8.9)$$

where

G = volumetric gas flow rate

c_n, q_n = solute concentration in gas and liquid phase in plate n over a small time increment Δt

$V_{n_{(G)}}, V_{n_{(L)}}$ = the volumes of gas and liquid phase occupying the nth plate.

Substituting $K = q_n/c_n$, a rearrangement of equation 8.9 gives:

$$G.c_{n-1} = G.c_n + V_n.\frac{dc_n}{dt} \qquad (8.10)$$

where

$V_n = V_{n_{(G)}} + K_n.V_{n_{(L)}}$ is the"effective plate volume". (see Reference (182)).

Assuming that the time increment, Δt, over which equation 8.10 is integrated, is sufficiently small so that C_{n-1} may be considered constant, integration of equation 8.10 gives:

$$c_n = c_{n-1}(1-e^{-\frac{G.\Delta T}{V_n}}) + c_n(0)\, e^{-\frac{G.\Delta T}{V_n}} \qquad (8.11)$$

The first term on the right-hand side of equation 8.11 represents the contribution to c_n from the (n-1)th plate to the nth plate, while the second term represents the

contribution from material present on the nth plate at the beginning of the time increment.

For a feed plate, Bell's (31) model considered the solute concentration on the feed plate to be equal to the theoretical concentration in the feed. Since the physical characteristics (flow, voidage,...etc.) are different from column to column (see section 7.2) this assumption is not valid for the SCCR-2 unit. In the present work, a mass balance over the feed plate similar to equation 8.11 is included in the model. The final mass balance equation for the feed plate is:

$$c_n = \left(\frac{G.c_{n-1} + F_f C_f}{G + F_f}\right)\left(1 - e^{-\frac{G.\Delta T}{V_n}}\right) + c_n(0)\, e^{-\frac{G.\Delta T}{V_n}} \qquad (8.12)$$

where

F_f = feed flow rate

C_f = feed concentration.

8.2.2 The Introduction of Solute Concentration Effects

A correction for the presence of solute molecules in the gas phase needs to be made to the value of the gas flow rate, G.

$$G' = G\left[1 + M_v \left(\frac{c_{n(1)}}{M_1} + \frac{c_{n(2)}}{M_2}\right)\right] \qquad (8.13)$$

where

G' = volumetric flow rate of solute free carrier gas

M_v = molar volume at column operating temperature

M_1, M_2 = respective molecular weights

For solute feedrates below 40 $cm^3.h^{-1}$ the contribution from the solutes may be assumed to be negligible, but at higher throughputs a correction is required. This amounts to a contribution of approximately 3.5% of the total gas flow rate at the maximum feedrate of 80 $cm^3.h^{-1}$.

The effect of gas phase solute(s) concentration on the K value was neglected, and partition coefficient values at infinite dilution were assumed. This was because the partition coefficients at different solute gas phase concentrations were not available and their determination would have involved a separate and long experimental programme.

8.2.3 The Introduction of a Pressure Gradient

For more flexibility in the model a relationship between pressure drop and gas flow rate that was applicable to all types of flow was introduced (183)

$$\frac{\Delta P}{\ell} \cdot g_c = 150 \frac{(1-\varepsilon)^2}{\varepsilon^3} \frac{\mu . u_m}{D_p'^2} + 1.75 \frac{(1-\varepsilon)}{\varepsilon^3} \cdot \frac{G_E . u_m}{D_p'} \qquad (8.14)$$

where

u_m = superficial velocity measured at mean column pressure.

ε = voidage

ℓ = length of column

G_E = mass flow rate of gas

D'_p = effective particle diameter as defined by:

$$D'_p = \frac{6(1-\varepsilon)}{\phi' S_s} \qquad (8.15)$$

where

ϕ' = shape factor for non-sperical particles = 0.65 (184).

S_s = specific surface of particle per unit volume of bed.

However, the type of flow found in the SCCR-2 was laminar, with Reynolds numbers based on the above definition for effective particle diameter, being well below 1.0 (184). The overall pressure drop for a typical experimental separation run has been 130 $KN.m^{-2}$, whereas under identical flow conditions the model will predict a pressure drop of 139 $KN.m^{-2}$.

8.2.4 The Introduction of a Temperature Profile

An expression derived by Scott (69), relating the excess temperature of a plate to the volume of gas flowing through the plate (expressed in terms of plate volume) during a specific time interval was used. The final expression is a standard differential equation of the form:

$$\frac{d\theta}{dV} + \beta_c\theta = \alpha_c \frac{dX_{gn}}{dV} \qquad (8.16)$$

where

α_c, β_c = constants (functions of plate heat capacity and heat losses)

θ = excess temperature of plate above its surroundings

V = volume of gas passed through a plate in terms of plate volumes.

X_{gn} = concentration of solute in the gas phase in plate n.

Solution of equation 8.16 requires the use of statistical tables and is a complex procedure making the solution unsuitable for inclusion in the digital computer simulation. To simplify the solution, $\frac{dX_{gn}}{dV}$ i.e. the change in gas phase concentration during the passage of a certain volume of gas, is not an unknown factor but is calculated by the programme for each time increment. The following assumptions will be made:

(1) linear absorption isotherms

(2) the heat capacity of the gas in the plate is insignificant compared with the heat capacities of the liquid phase and support.

(3) the temperature of the surroundings of the plate is constant

(4) the gas flow rate through the plate is constant

(5) the axial heat conductance is negligible compared with heat conducted radially from the column. Therefore,

$$(V_2\rho_L.S_L+V_1.\rho_p.S_p)\theta = |h_1.K_1\frac{dc_n}{dt}| - A_p.z.dt.\theta \qquad (8.17)$$

where

V_1, V_2 = volumes of liquid phase and solid support

S_L, S_p = specific heats of liquid phase and solid support

ρ_L, ρ_p = densities of liquid phase and solid support

h_1 = heat of solution of component i in the liquid phase

A_p = surface area of theoretical plate

z = composite thermal conductivity of packed bed.

Knowing the change in gas phase concentration over the time increment dt, equation 8.17 may be solved to yield the change in temperature of the plate during the same time interval.

8.2.5 The Programme

A detailed flow chart of the computation is given in Fig. 8.2 with the listing of the programme written in Standard Fortran IV, presented in Appendix 3. A listing of the programme variable names and a sample of the print-out is also given in Appendix 3. The programme is suitable for running on I.C.L. machines, and was computed on a series CDC 7600 machine at the University of Manchester Regional Computer Centre.

FIG. 8.2 FLOWCHART FOR THE COMPUTER SIMULATION OF THE SCCR-2

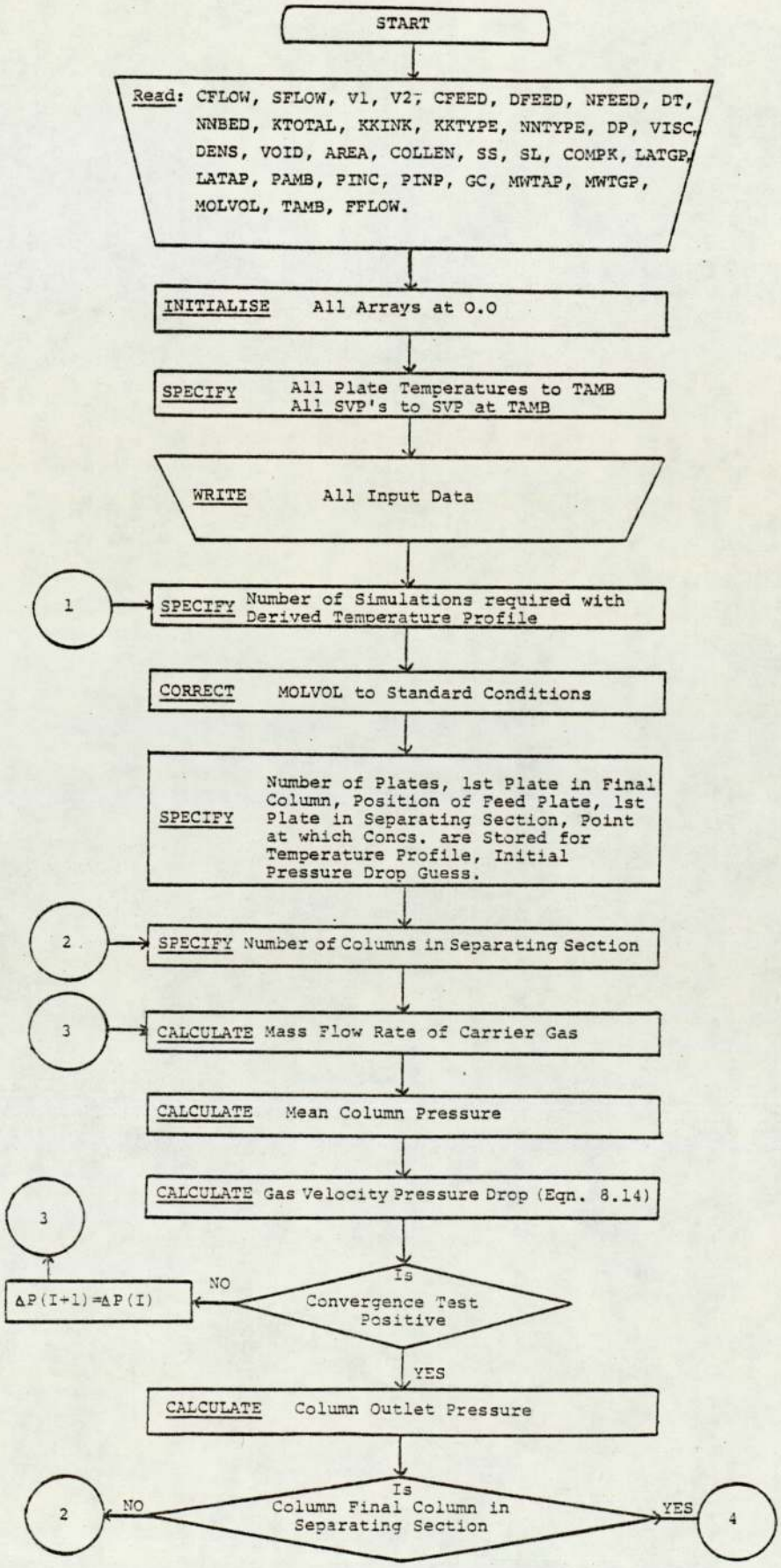

FIG. 8.2 CONTINUED

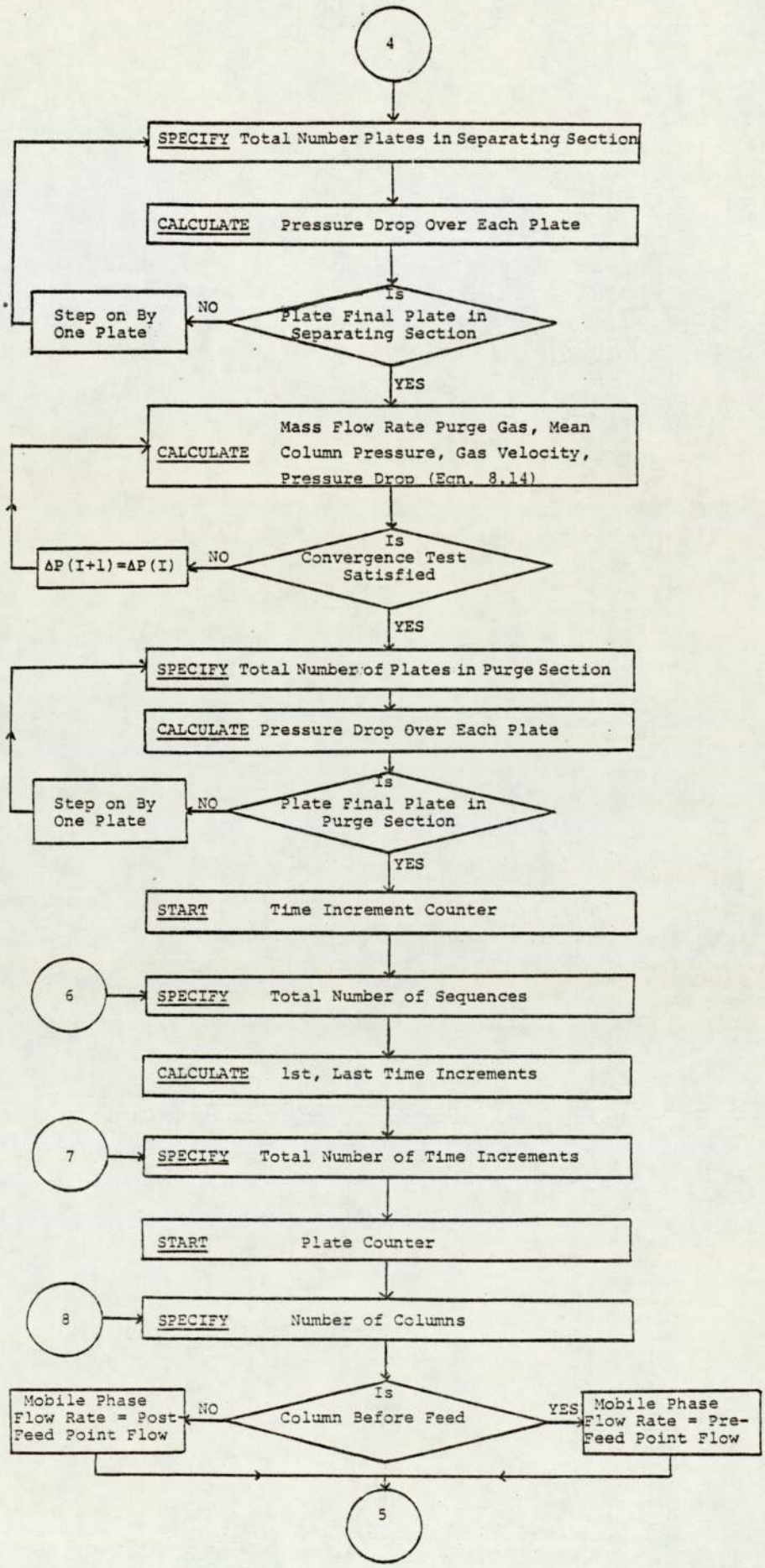

FIG. 8.2 CONTINUED

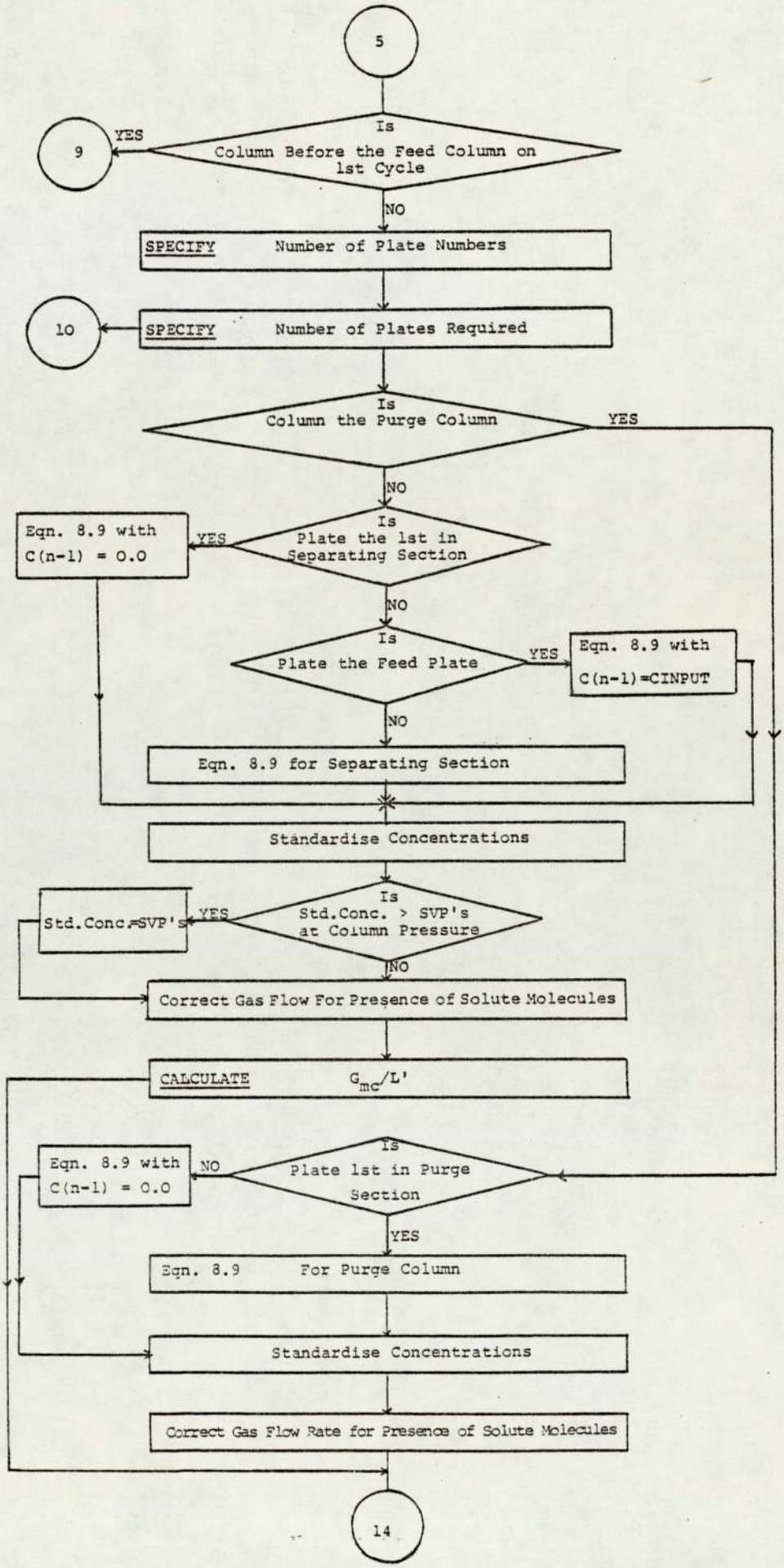

FIG. 8.2 CONTINUED

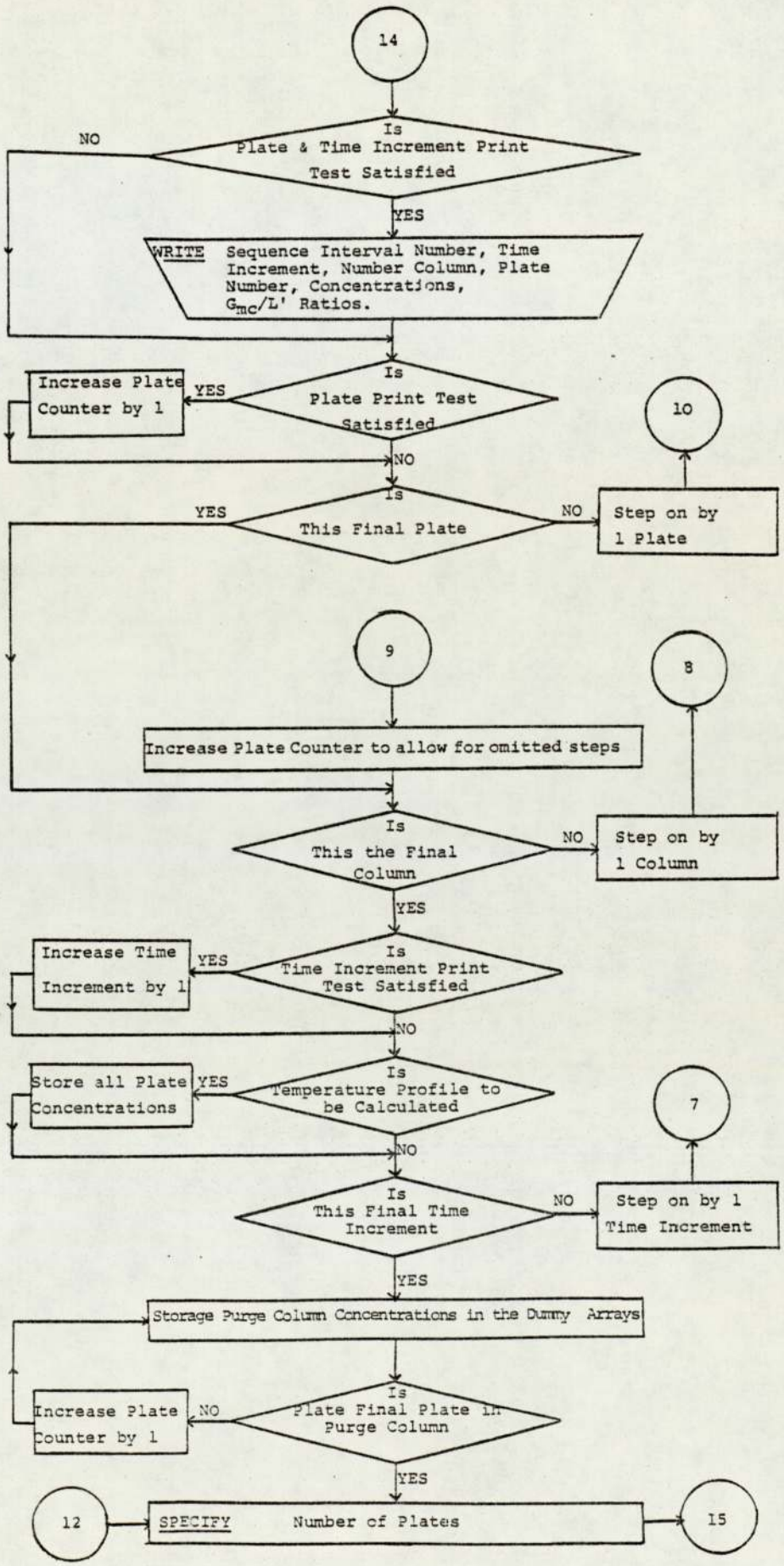

FIG. 8.2 · CONTINUED

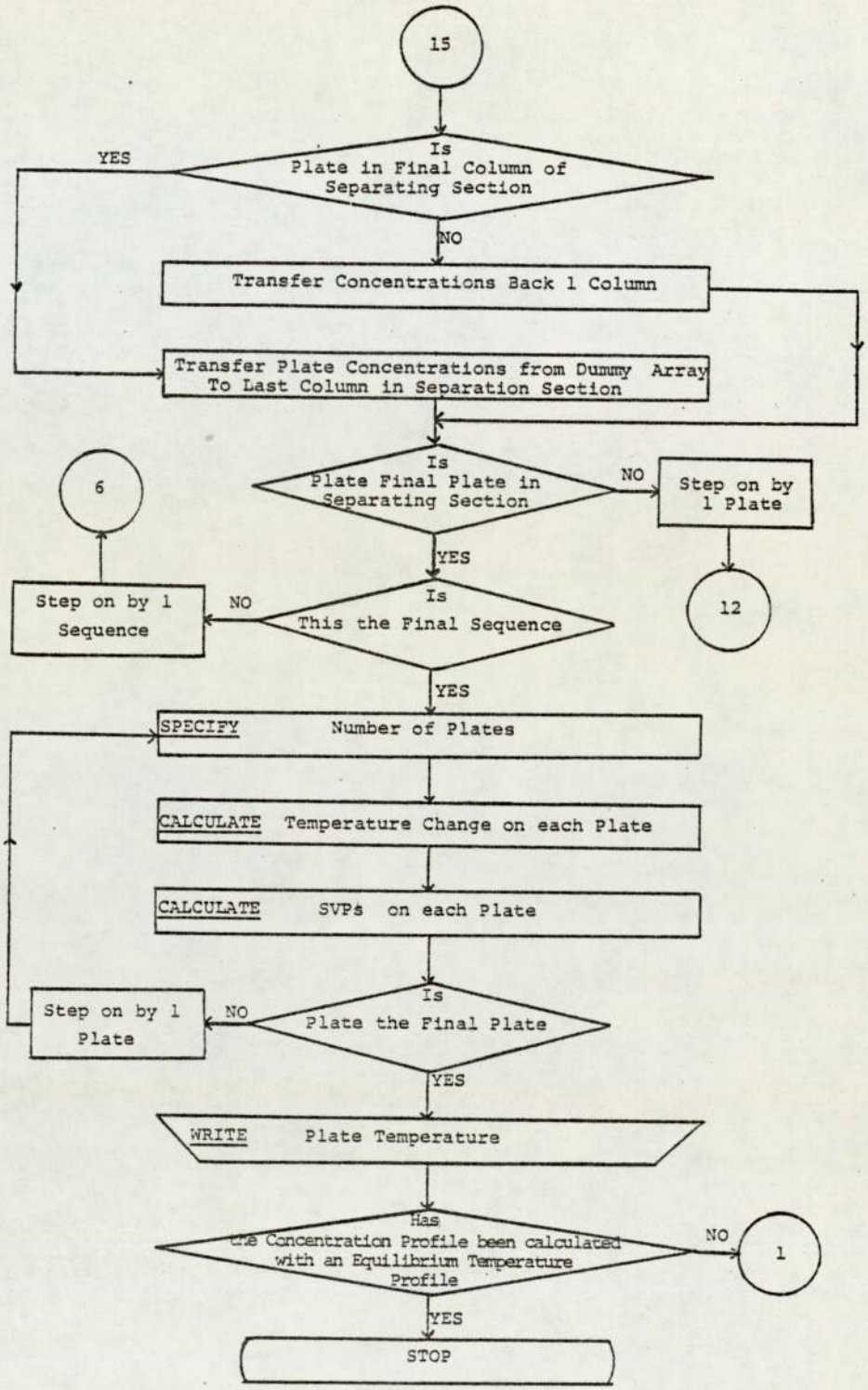

8.3 RESULTS

The experimental results of Arklone.P./Genklene obtained by Liodakis (16) and two more systems ethyl caprate/ethyl laurate and ethyl laurate/methyl myristate at 160°C and 185°C respectively, were simulated using this model. In developing the model to its present state several parameters have had to be optimised with a view to curtailing the execution time of the programme.

The time increment (Δt) over which the column concentrations are assumed to be constant was determined to be 2 seconds. Using a Δt greater than 2 seconds invalidated the constant concentration assumption and resulted in the programme not reaching an equlibrium value. For values of Δt below this value the change in level or form of the respective concentration profiles was minimal and did not warrent the increase in computation time.

The theoretical plate height was estimated to be 0.8916 cm, yielding 68 plates/column (see Appendix 4). It has been shown (13, 31) that for the system Arklone.P./ Genklene with a separation factor of approximately 5, that the number of plates/column is not a major factor in determining a successful separation until either the number of plates/column is reduced to below 15 plates, or the difficulty of separation is increased. As the programme execution time is in direct proportion to the number of

theoretical plates in the model, a compromise was made between accuracy and time, and the number of plates per column was specified as 40 plates in the simulation of Arklone P./Genklene and 50 plates in the other more difficult systems. It must be emphasised however that the above is in agreement with the conclusions drawn by Bell (31), that with a lower separation factor, the number of plates necessary for the separation is higher. Conder (82) working with large scale batch units has also arrived at similar conclusions.

The simulated concentration profiles and their experimental equivalents are given in Figs. 8.3-8.13 with the input data required by the model having the same values as those set experimentally.

8.4 DISCUSSION

A major factor in the computer runs reported in this thesis was found to be the large amount of computing time necessary for each run. This is illustrated by consideration of typical values for the number of plates per column, number of time increments/sequencing interval, and number of sequencing intervals of 40, 150 and 80 respectively. These values necessitate performing the calculation steps of the inner programme loop a total of 4.8×10^6 times for a ten column series in the separation section. Because of the long execution time of the programme, it was necessary

FIG. 8.3 COMPUTER SIMULATION FOR RUN 60-21-43-130

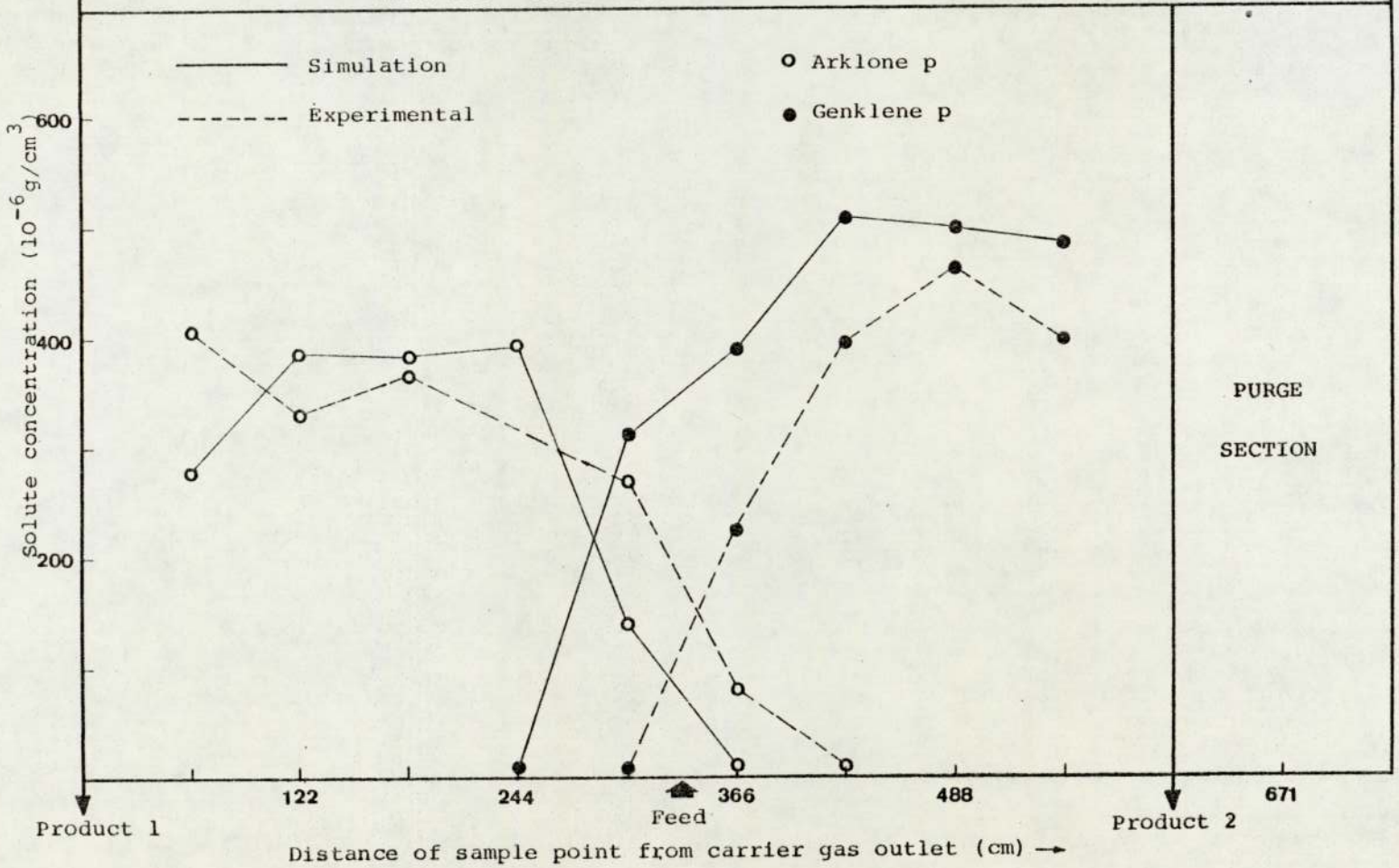

FIG. 8.4 COMPUTER SIMULATION FOR RUN 60-21-38-130

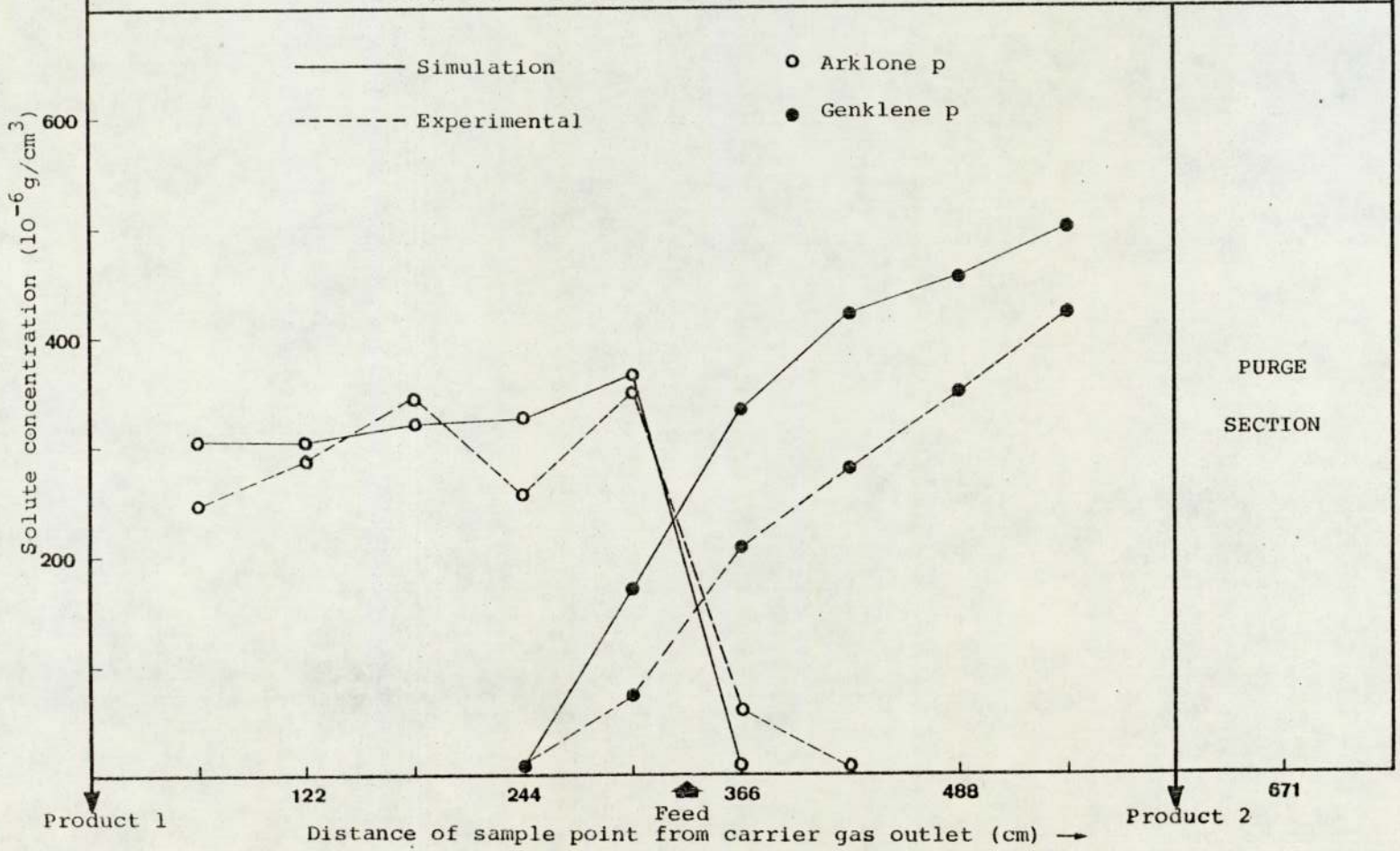

FIG. 8.5 COMPUTER SIMULATION FOR RUN 60-21-43-130

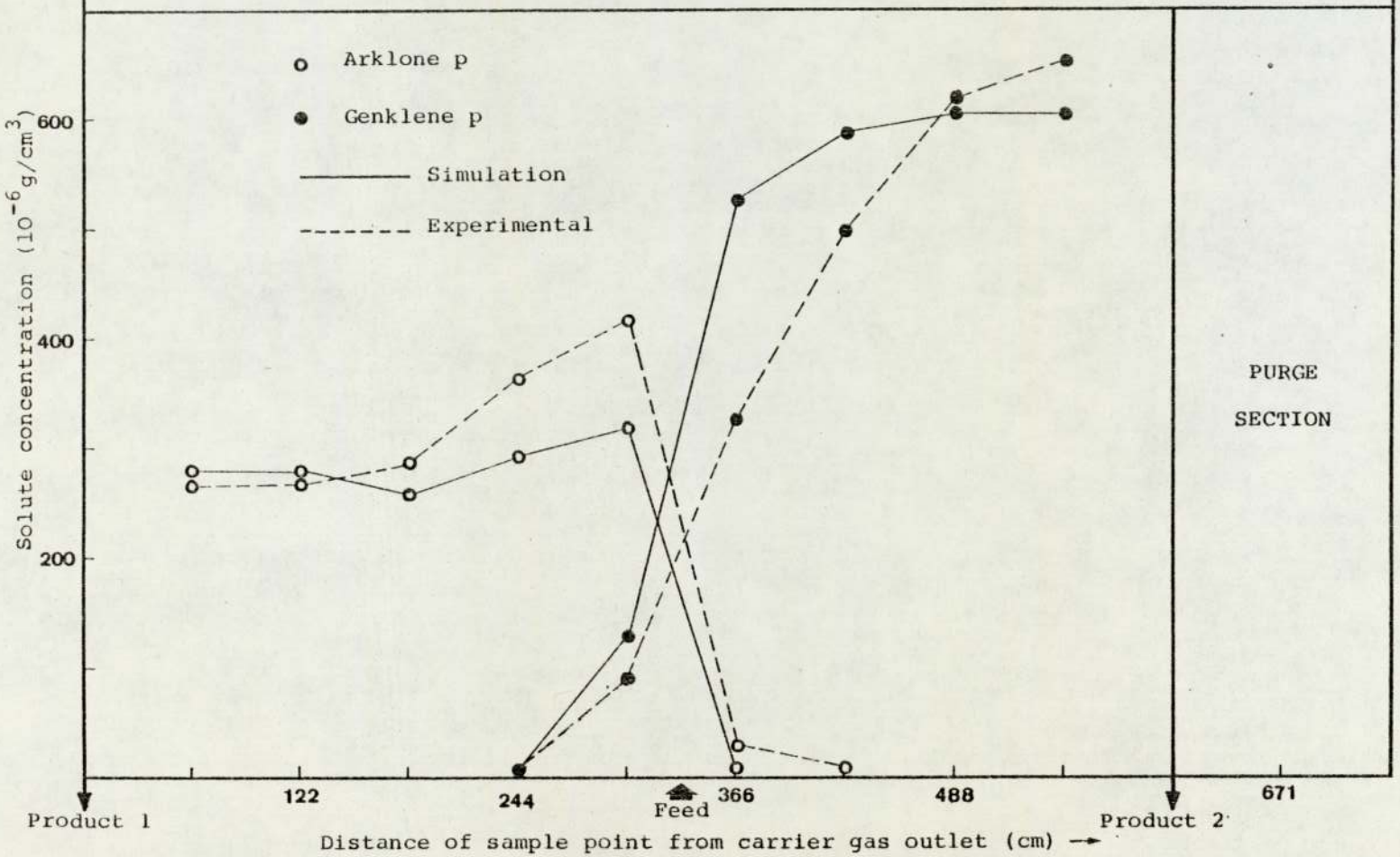

FIG. 8.6 COMPUTER SIMULATION FOR RUN 60-21-58-130

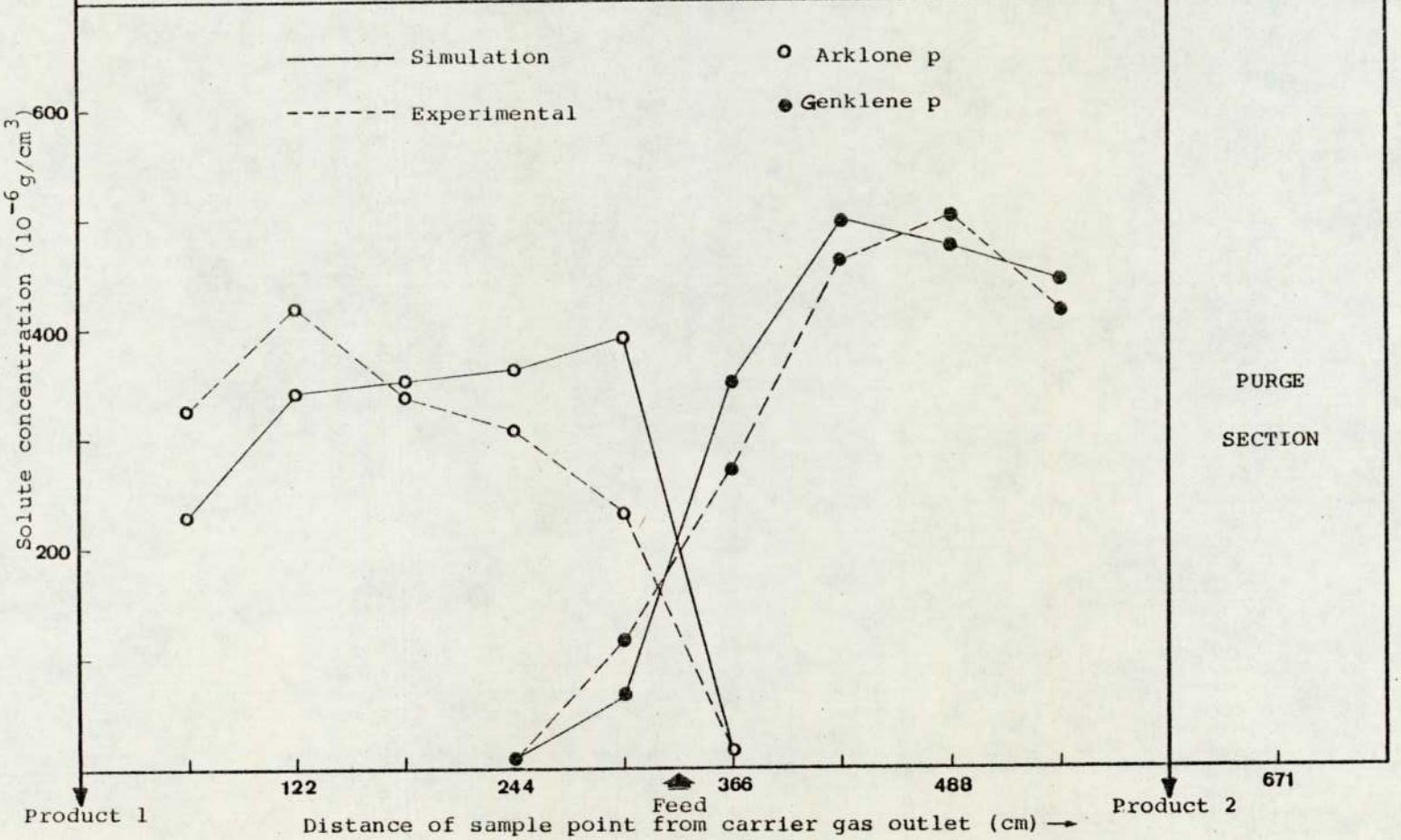

FIG. 8.7 COMPUTER SIMULATION FOR RUN 160-25-114-300

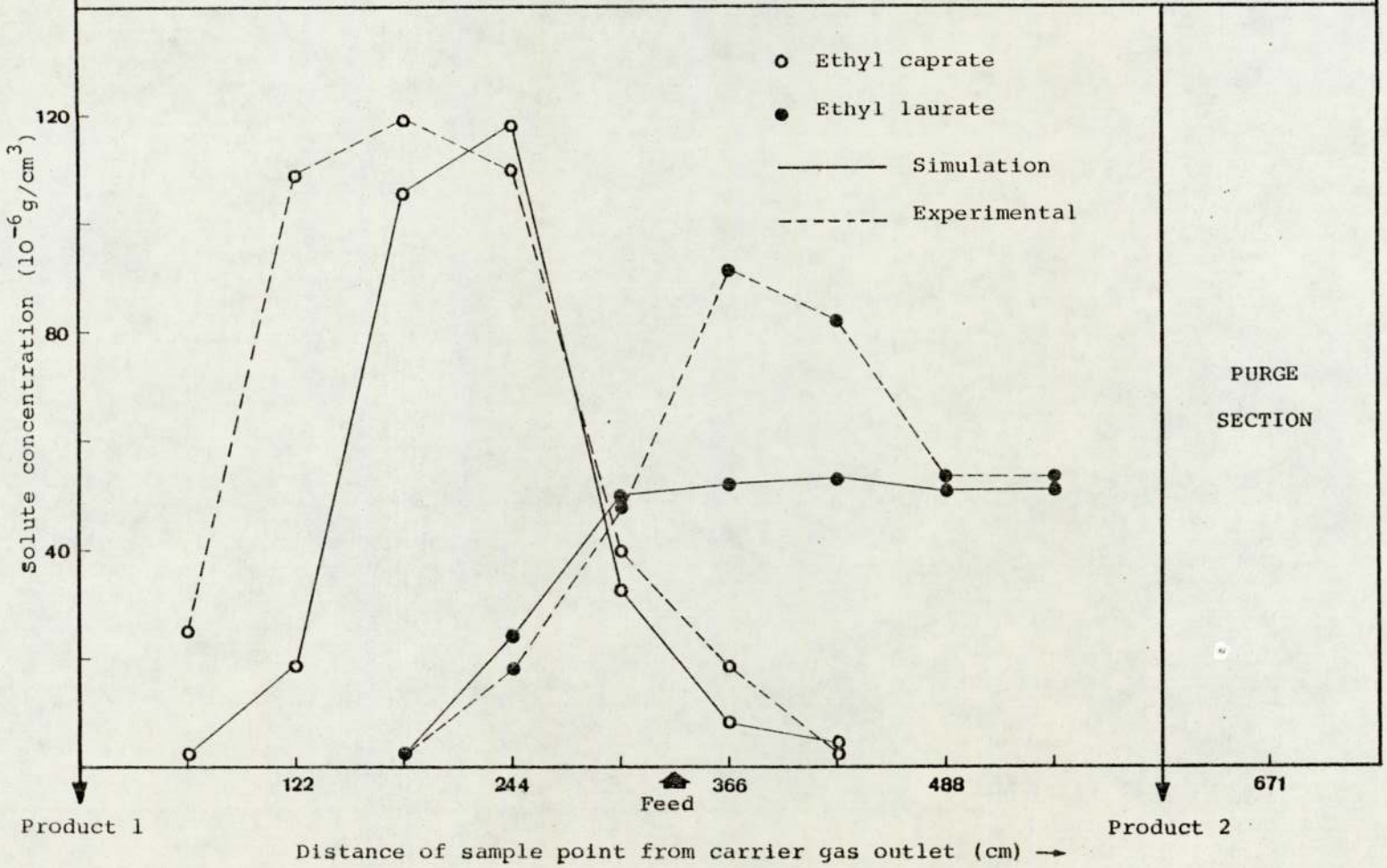

FIG. 8.8 COMPUTER SIMULATION FOR RUN 160-50-114-300

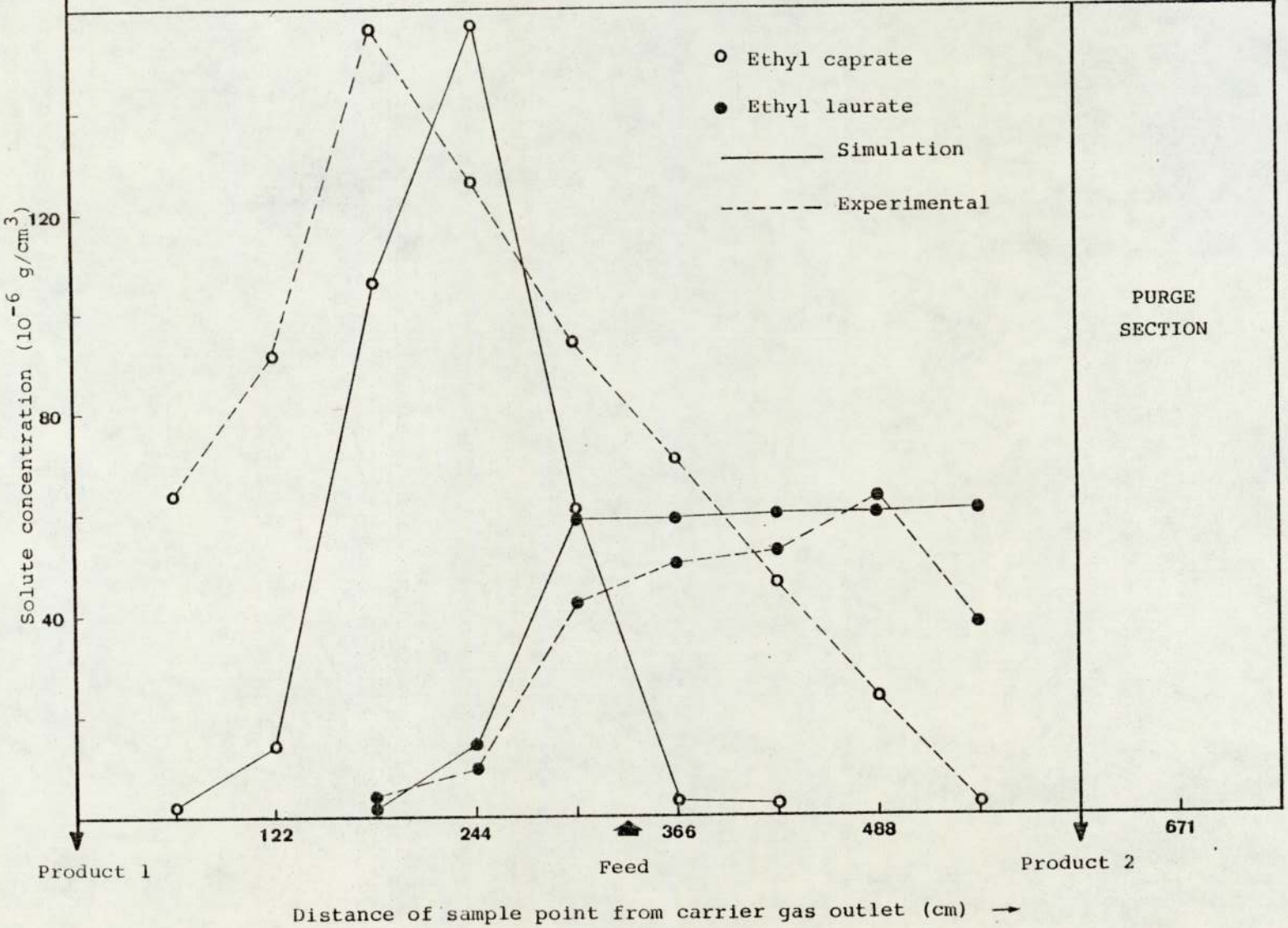

FIG. 8.9 COMPUTER SIMULATION FOR RUN 160-75-113-300

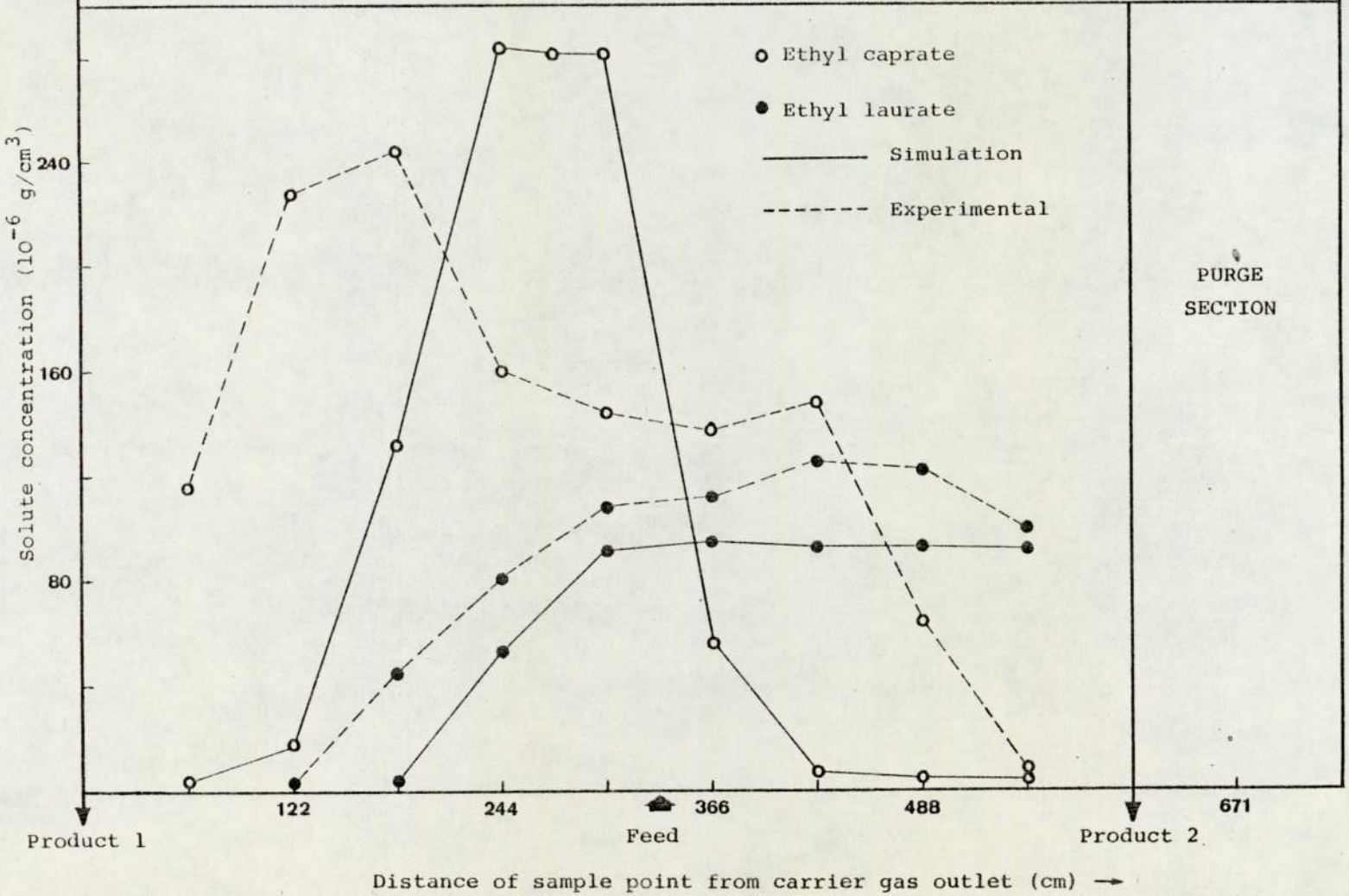

FIG. 8.10 COMPUTER SIMULATION FOR RUN 160-75-101-200

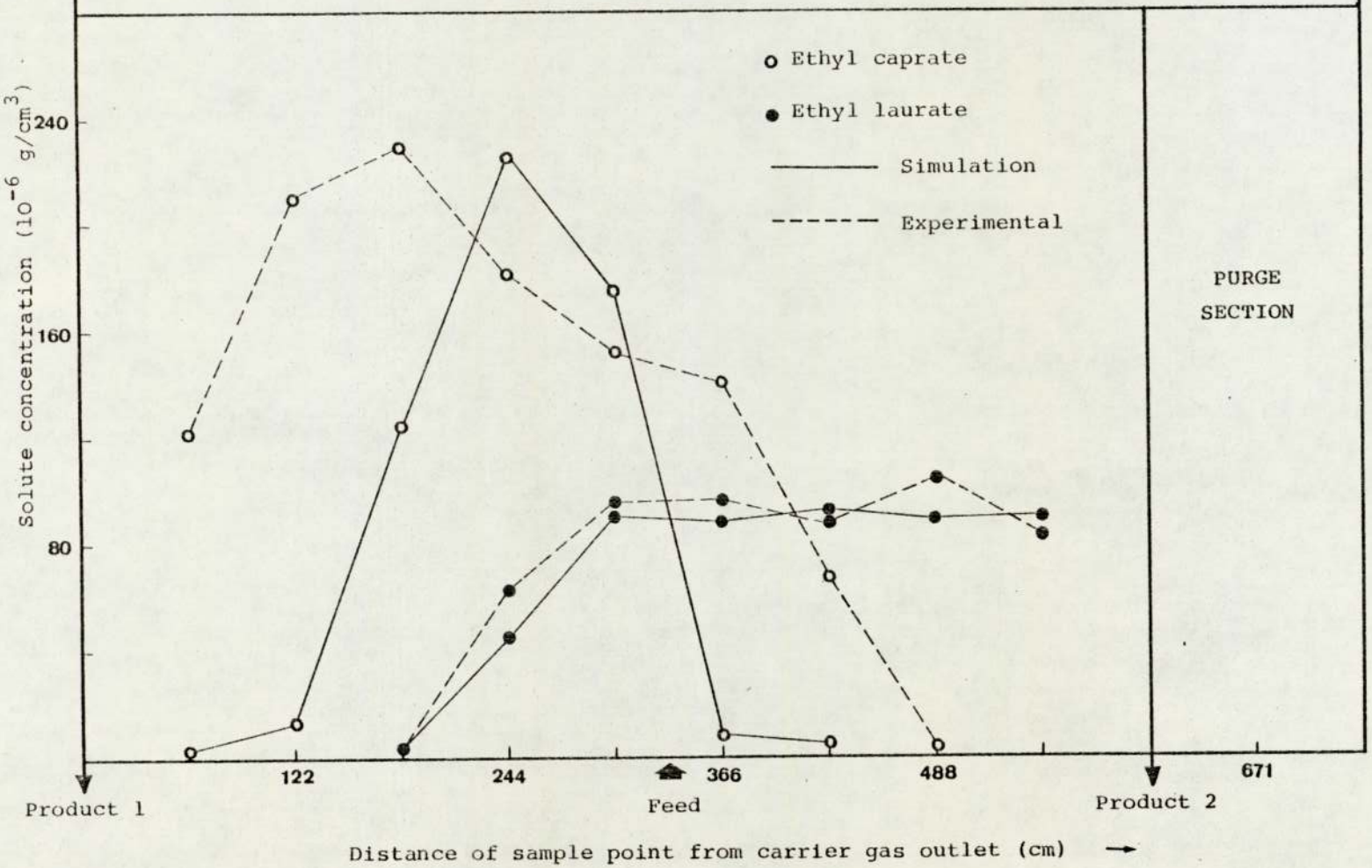

FIG. 8.11 COMPUTER SIMULATION FOR RUN 185-25-83-150

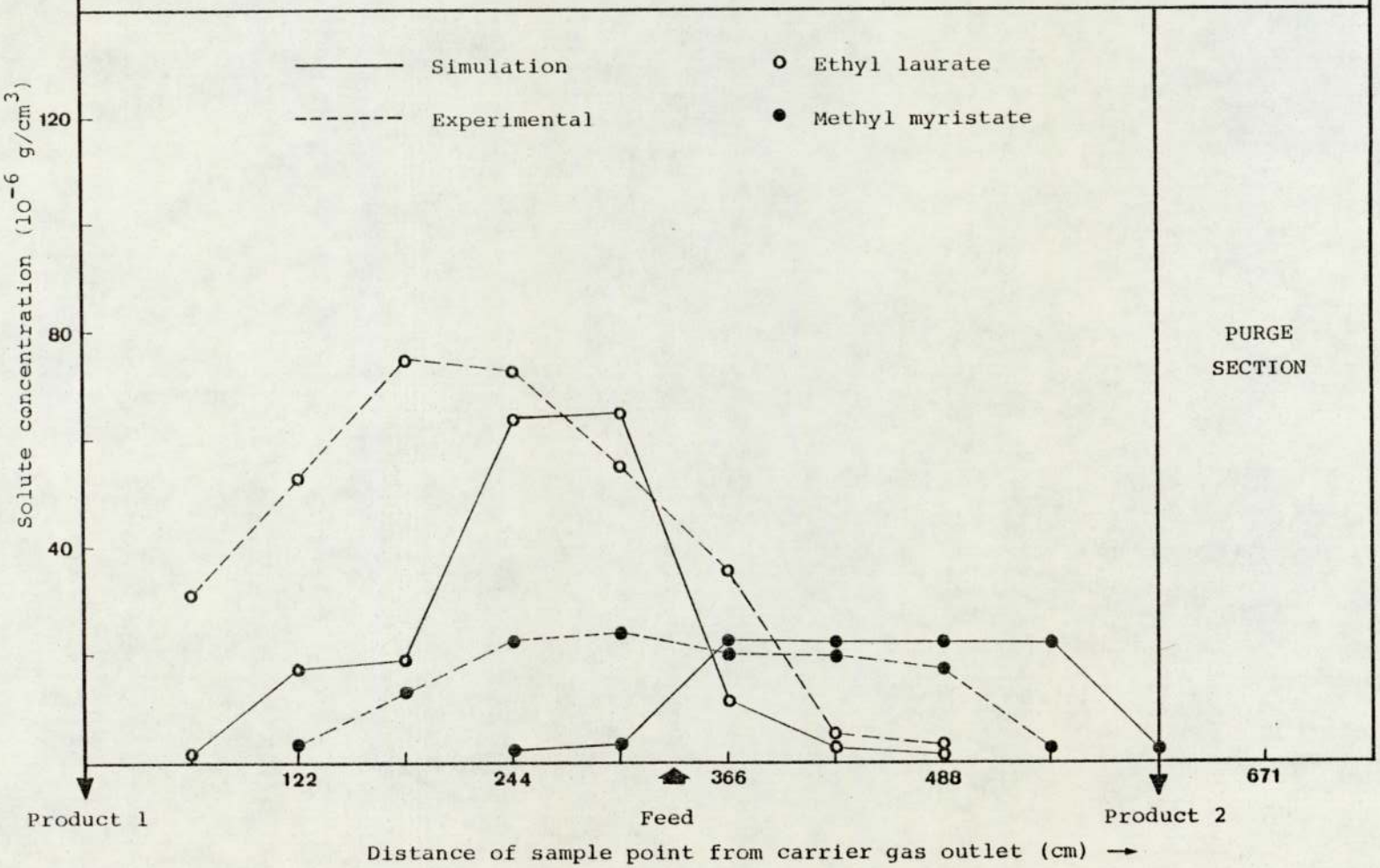

FIG. 8.12 COMPUTER SIMULATION FOR RUN 185-45-83-150

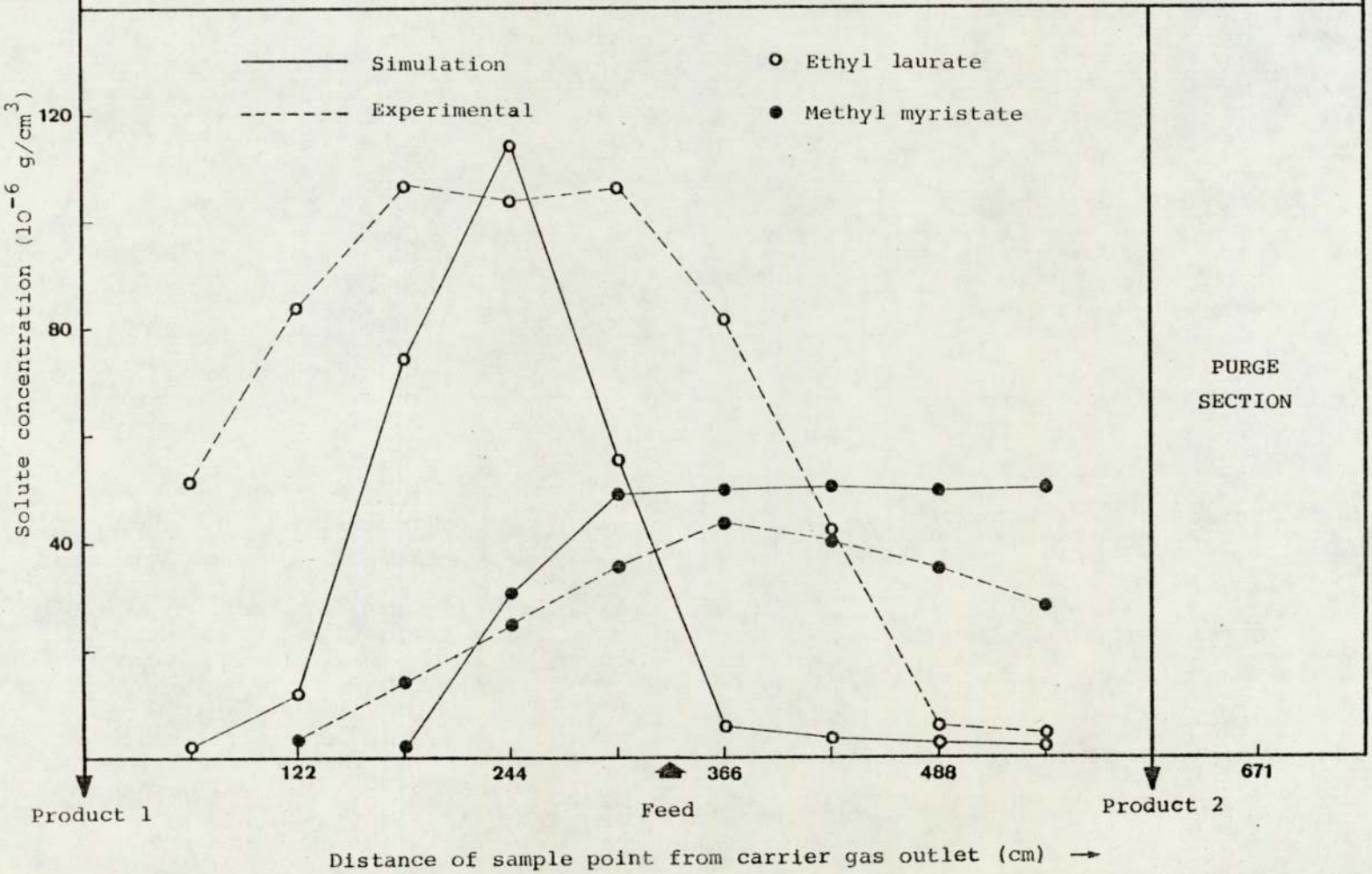

FIG. 8.13 COMPUTER SIMULATION FOR RUN 185-60-74-100

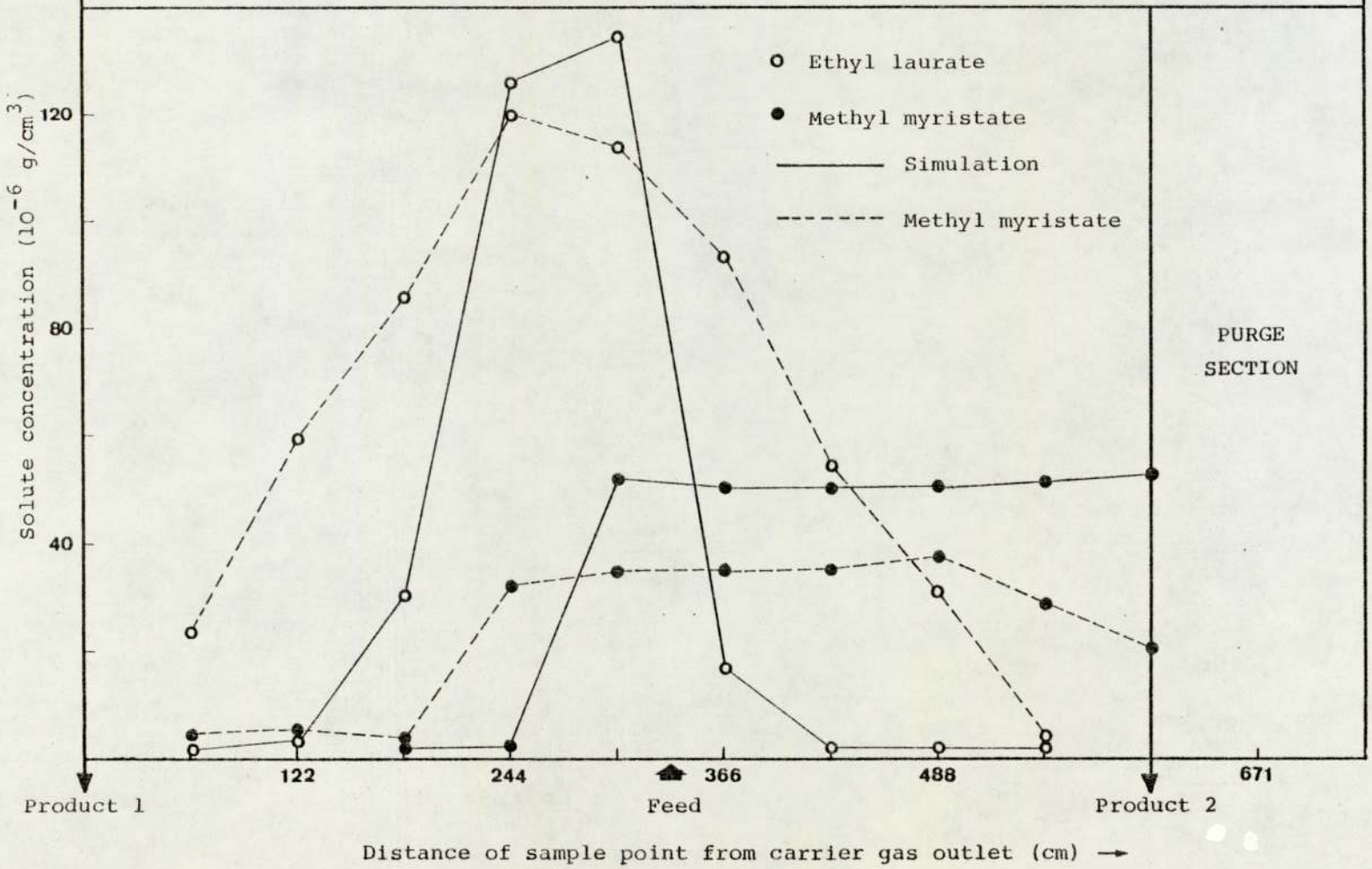

to simulate the existing experimental runs in a limited manner.

In general, good agreement with regard to the location of the "cross-over" point, was found between simulated and experimental profiles in the case of Arklone P./Genklene as shown in Figs. 8.3 - 8.6. The levels of concentration predicted for Arklone P., are in close agreement with experimental values. Regarding the Genklene profile, the predicted values, whilst accurately modelling the profile shape, consistently gave values in excess of those found experimentally. Such discrepancies are probably because the model is not capable of dealing completely with situations where solute condensation from the gas phase may occur. In practice any condensed Genklene will re-vaporise and cool a localised region of the packed bed. Although the model is programmed so that the saturated vapour pressure of Genklene can not be exceeded, it cannot allow for the heating/cooling effect of any condensing/re-vaporising of the solute, and it is this irregularity which may result in the predicted values for Genklene being higher than those measured experimentally. However, condensation of solutes is not a fault of the mathematical simulation but of the experimental equipment and can be prevented by a redesign of the unit, (Chapter 9).

Figs. 8.7 - 8.10 show the simulation of the ethyl caprate/

ethyl laurate system at 160°C. It can be seen that as the difficulty of the separation is increased (S.F. reduced) there is less agreement between the computed profiles and experimental results than for the previous system (Arklone P./Genklene). It will be noticed that the shape of the computed ethyl caprate profile and the "cross-over" point are similar in form to those found experimentally in run 160-25-114-800. The ethyl laurate profile obtained via the model possesses a more pronounced "plateau region" than does the experimental profile. Less accuracy between the computed profiles and the experimental profiles exists at the higher feed rates of 50 and 75 $cm^3.h^{-1}$. This could be due to a high condensation rate from the gas phase. As shown in the computed profiles, given in Figs. 8.8 - 8.10, at the beginning of each simulation, the mobile phase concentration of component 1, the component with least affinity for the stationary phase (ethyl caprate), builds up faster than component 2 (ethyl laurate). The reason could be that ethyl laurate has a larger liquid volume in the column due to its greater affinity for the stationary phase, and its concentration in the mobile phase is consequently less than component 1 (ethyl caprate). The final concentration level of each component, and the time taken to establish this level is not only dependent upon the input concentration and the K values, but also on the column temperature. At present the temperature profile is calculated under equilibrium concentration

conditions, and the concentration profile is then re-calculated with the equilibrium temperature profile superimposed. Ideally, as temperature is a function of the rate of change of concentration within the columns, a non-equilibrium temperature profile could improve the idealistic nature of the present simulation.

The simulated concentration profiles of ethyl caprate/ethyl laurate at 160°C have been shown to be sensitive to temperature. The simulated profile of the more difficult system of ethyl laurate/methyl myristate at 185°C has shown less agreement with the experimental profile shown in Figs. 8.11 - 8.13 especially at feed rates of 45 and 60 $cm^3.h^{-1}$. This could be caused by the combined effect of temperature and the anti-Langmuir absorption isotherm. However, it is interesting to note that the heat balance over a theoretical plate is at present based on the concentration change over the plate during one sequencing interval. Again accuracy may be improved if this calculation were to be based on the concentration change over the plate during one time increment. Programming-wise this may be accomplished by placing the temperature difference equations inside the inner loop of the mathematical simulation. The reason this has not been done is that the time required in the production of the temperature profile then becomes comparable to that required by the concentration profile,

and the programme becomes too lengthy.

However, this agreement between computer and experimental results is not excellent. Reasons for this may be identified as·

1. The assumption of a constant partition coefficient for the components. The variation of K with concentration, observed for the elution of two solutes, would have a marked effect on the migration rates of components in the SCCR-2 unit, and would need to be included in a realistic computer simulation.

2. The assumption that the elution characteristics of the components are independent of each other. The mutual interaction of different solutes and the liquid phase, at finite concentrations, was reported by Sunal (169). This interaction would affect the relative migration rates of molecules in the SCCR-2 unit.

3. The assumption of constant columns characteristics (voidage, weight and packing, and number of plates). This is inconsistent with the experimental observations given in Section 7.2. The column-to-column variations in these variables would result in a variation of component migration rates through each column. Inclusion of these variations in the computer model would, however, have the disadvantage of increasing considerably its complexity.

4. The assumption of a value for the number of plates/column, N of 40 and 50. Ideally a value for N should be calculated from pre-determined data for each column, although the variation of N with packing type, column and packing geometry, component molecular weight and concentration, and mobile phase composition and flow rate would make this extremely complex.

Although these factors would need to be considered for a more detailed and comprehensive simulation programme of the SCCR-2 unit, the present model has served to highlight some of the essential operating features, and should be useful for developing future models of the process. Particularly, the following factors have been observed from results obtained by the model.

1. Reproducible component concentration values obtained for successive cycles, after the attainment of pseudo-equilibrium operation, and the time required to reach these values increases as the time increment (Δt) decreases.

2. The length of column required to achieve complete separation of a two-component mixture increases as the operating temperature is increased.

Summarising, the simulation of the separation of three chemical mixtures with different separation factors and at different temperatures has been investigated, and

CHAPTER 9

CONCLUSIONS AND RECOMMENDATIONS FOR FUTURE WORK

9.1 CONCLUSIONS

1. The sequential counter-current mode of continuous gas chromatography has been successfully applied to the separation of fatty acid esters at temperatures up to 205°C. Economic considerations dictated the design of the SCCR-2 equipment developed for this study which consisted of 12 columns, each 61 cm long and 2.54 cm in diameter. However column dimensions can be varied without increased complexity for higher throughputs.

2. Thermodynamic measurements of various solutes on OV-275 with an analytical scale chromatograph indicated a number of chemical systems suitable for separation studies on the SCCR-2 unit. The selected chemicals provided a combination of mixtures of different separation difficulty and volatility. Hence, a systematic study of the SCCR-2 unit performance at various temperatures (60-205°C) and with different separation difficulty (SF=1.44-2.3^{o}C) could be achieved.

3. Product purities in excess of 99% were obtained for the relatively easy system of ethyl acetate/ethyl butyrate at 60°C with equivalent feeds at rates of up to 40 cm^3h^{-1}. The performance of the SCCR-2 unit for this feed mixture showed very little sensitivity to column conditions within the defined theoretical limits for successful separation (see equation 6.5).

4. At an operating temperature of 105°C, an equivolume mixture of ethyl caprylate/ethyl caprate was separated. Product purities in excess of 99% at feed rates of 80 cm^3h^{-1} were obtained. The finite solute concentration effect was considered to have the most pronounced effect on the deterioration of the product purities.

5. For the more difficult separation of ethyl caprate/ethyl laurate at feed rates of up to 50 cm^3h^{-1} and operating temperatures of 160°C, product purities in excess of 98.5% were obtained. At an even higher temperature (185°C) the successful separation of ethyl laurate/methyl myristate was achieved. The maximum throughput permissible in this case to obtain product purities in excess of 98.0% was 25 cm^3h^{-1}.

The performance of the SCCR-2 unit was further demonstrated at a temperature of 205°C to separate a mixture of methyl myristate/methyl stearate. A considerably lower throughput (20 cm^3h^{-1}) than the previous systems was used to give product purities in the range of 85-90%.

Preliminary studies with a multicomponent mixture of fatty acid esters, called 'fungal oil', at a temperature of 185°C, indicated that the sequential unit had inadequate column length for the isolation of methyl linoleate and methyl-γ-linolenate (SF 1.2) . Also polymerisation of the feed material prevented these studies being pursued.

Seven factors have been identified which restrict the separating capabilities of the SCCR-2 unit:

A- the temperature fluctuations in the column,which are caused by many factors such as; variation in the oven temperature, enthalpic overloading effects, the probable difference in temperature between the carrier gas and the column.

B- the variation of the solute velocity throughout the column cross-section in the separating section.

C- pressure gradient across the columns.

D- the sequencing action

E- the finite length of the separating section.

F- variation in individual column characteristics.

G- the effect of high solute concentrations on the partition coefficients.

6. A digital computer plate model has been developed to simulate the operation of the SCCR-2. This is based on the development of concentration, temperature, and pressure profiles, continuously over a series of theoretical plates. The predicted results have been compared with experimental values. Agreement of the two sets of results becomes less accurate at high feed rates and high temperatures, although methods by which the accuracy of the simulation may be improved have been stated, with the most important recommendation being the inclusion of a variable HETP parameter for each column. This model after such modifications

could be used to investigate the individual effects of key parameters on the overall performance of the SCCR-2 unit.

To improve the separating power of the SCCR-2 system, the following recommendations are made.

9.2 RECOMMENDATIONS

The conclusions as presented above, lead to a number of practical suggestions for improving the SCCR-2 performance. These suggestions are in no way intended as conclusive remedies for the problems of large-scale operation, but should serve to indicate the direction in which possible solutions might be found.

1. The chief source of low performance in large diameter columns in general and in the SCCR-2 in particular, appears to be the consistent increase in zone velocity (probably due to particle size variation) upon passing from the column center to the outer regions. Several approaches can be taken to combat velocity variations.

The effect may be reduced by obtaining more uniform particles and by using the most efficient packing methods available. Alternatively, various techniques to compensate directly for the variations in zone velocity may be employed. Frisone (54) has used saturated rings of filter paper adjacent to the wall to accomplish a selective

retardation. The same effect may also be possible by using a packing mixture containing inert (nonporous) particles which will give the necessary compensation in stationary phase concentration over the tube cross section. Or it may be possible to use a "linked truncated cone" geometry, providing the flow velocity can everywhere be kept reasonably near the optimum. A combination of the latter with mixing tubes, which will themselves contribute a negligible plate height if designed carefully, might provide a more total compensation.

2. It is apparent that the poor separation results at high temperature are not always due to the velocity nonuniformity. Other possibilities are numerous, and the temperature fluctuation within the columns is an important factor. This could be minimised by heating the column interior (perhaps through the resistance heating of an internal element) as well as the exterior.

3. It is sometimes apparent that the loss of component resolution is due more to the scale-up of sample size than of column size. In the case where the physical volume of the injected sample is simply too large to obtain sharp peaks, it might be advisable to use programmed temperature.

4. It is apparent that, in the operation of an isothermal process as in the case of the SCCR-2, the local concentrations of solute(s) may become so high that harmful

nonlinear effects are found. In the case of nonlinear absorption isotherms, it might be possible to find liquid phases with better solution properties. In the case of the apparent nonlinearity arising from the heat of solution, column geometries with more rapid heat exchanging characteristics and column packings with greater heat capacity should be sought.

9.3 FURTHER AREAS OF INVESTIGATION

1. As indicated by this research, continuous gas chromatography has a tremendous potential in separating fatty acid esters. The operation of the SCCR-2 can be further extended to include other derivatives of fatty acids. The main materials of main interest are the long chain amines, diamines, amides and alcohols. There is no reason to believe that continuous gas chromatography will not be developed to separate such materials commercially.

2. Investigation of the effect of changing the feed input position from mid-point to the top of the columns, to enable a more efficient use of the available separating length (31).

3. To convert the SCCR-2 for batch-mode operation. In so doing a useful comparison between batch and continuous gas chromatography can be obtained experimentally rather than theoretically.

APPENDIX 1

CALIBRATION CHARTS

FIG. A.1.1 CALIBRATION OF THE FEED PUMP

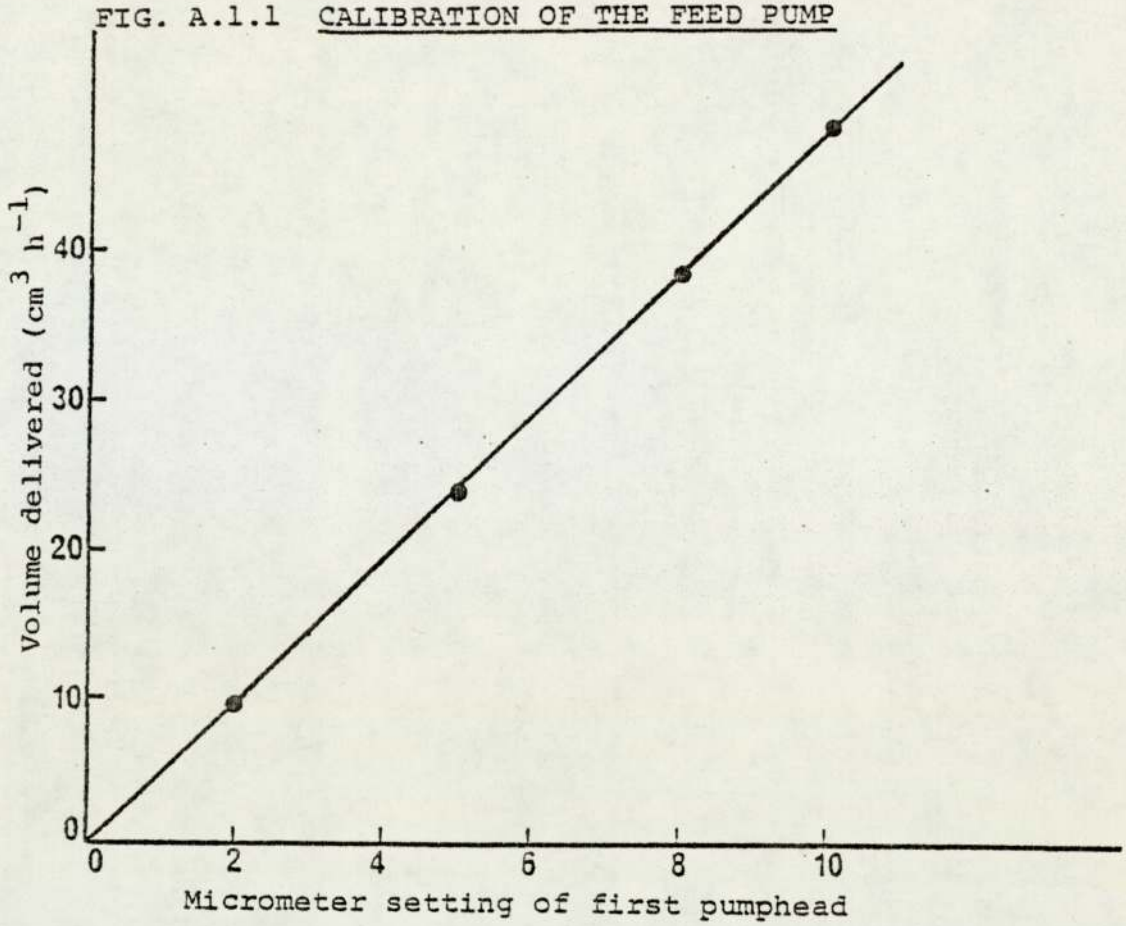

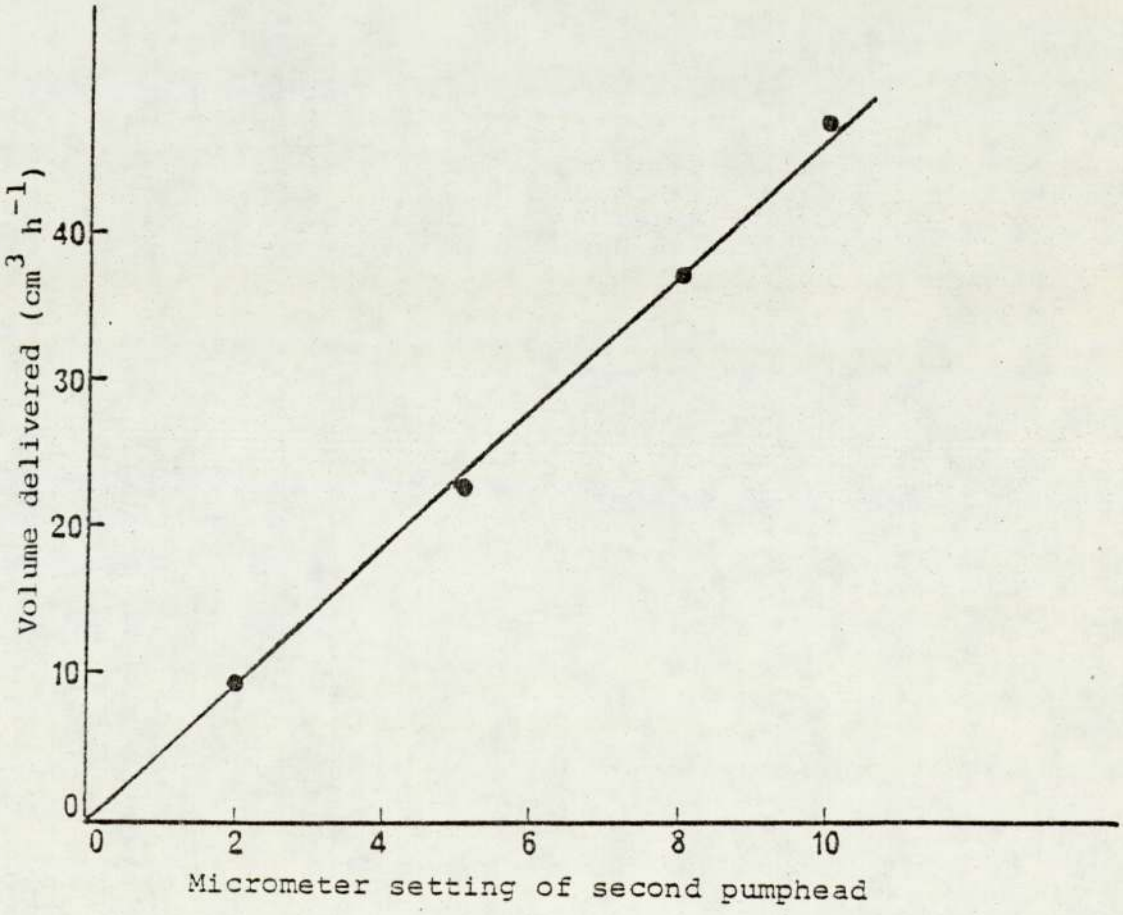

FIG. A.1.2 CALIBRATION OF ROTAMETERS

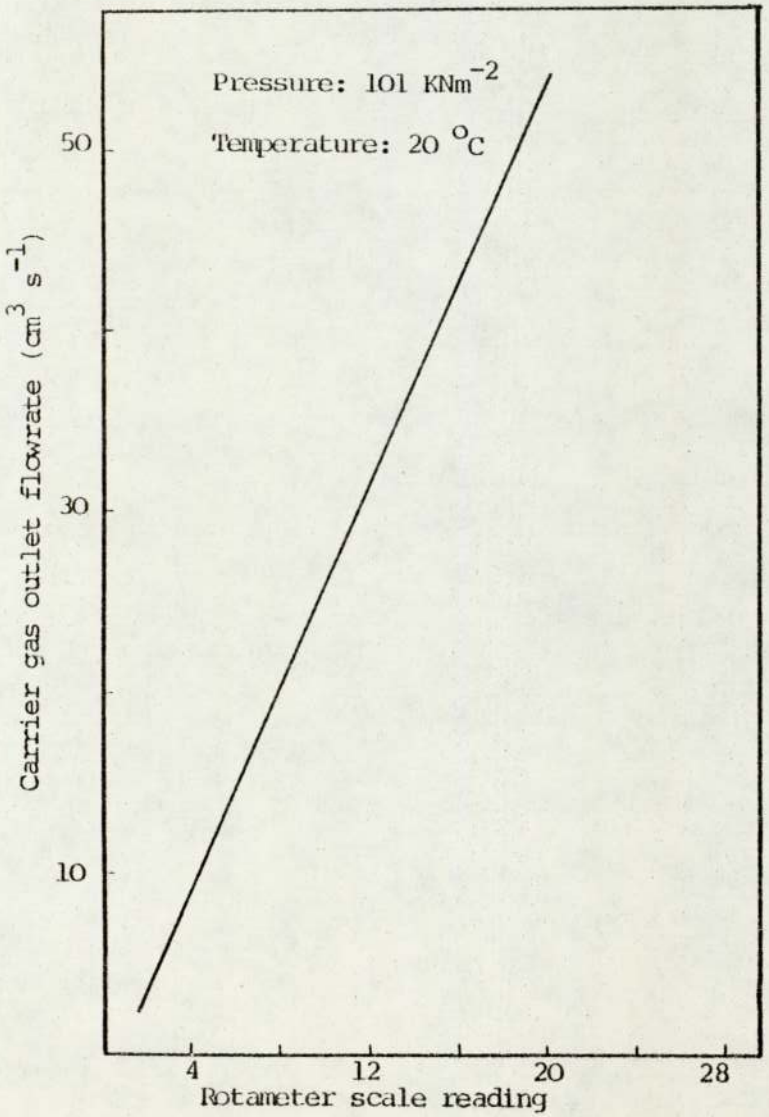

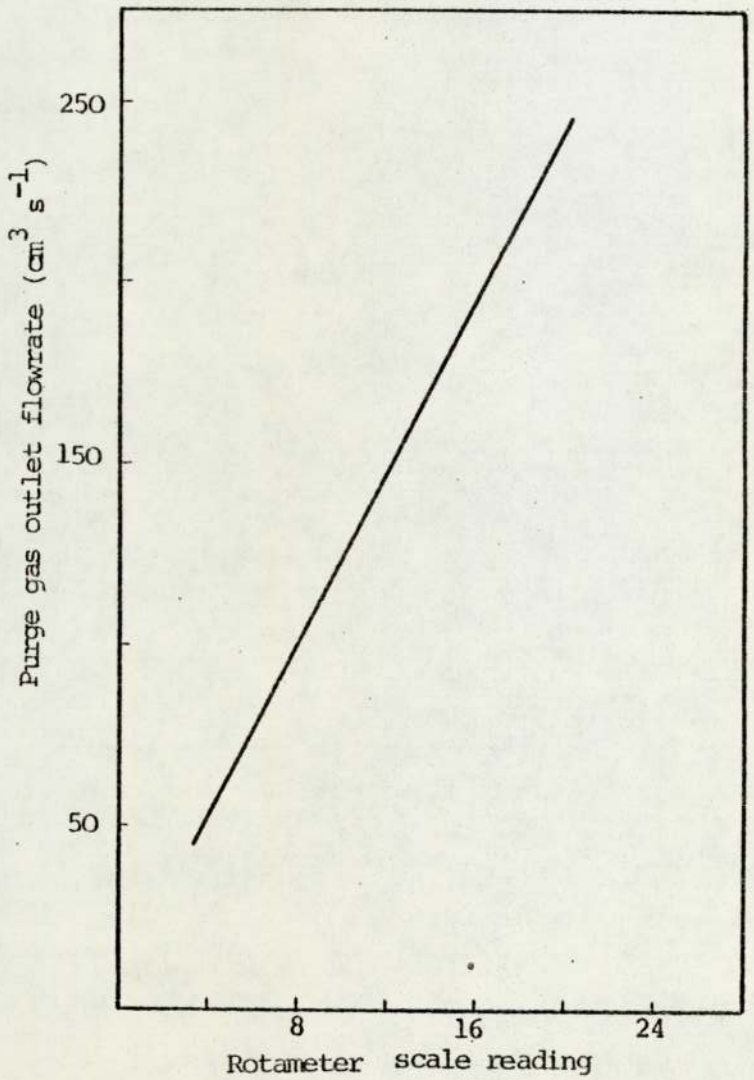

FIG. A.1.3 CALIBRATION OF THERMOCOUPLES

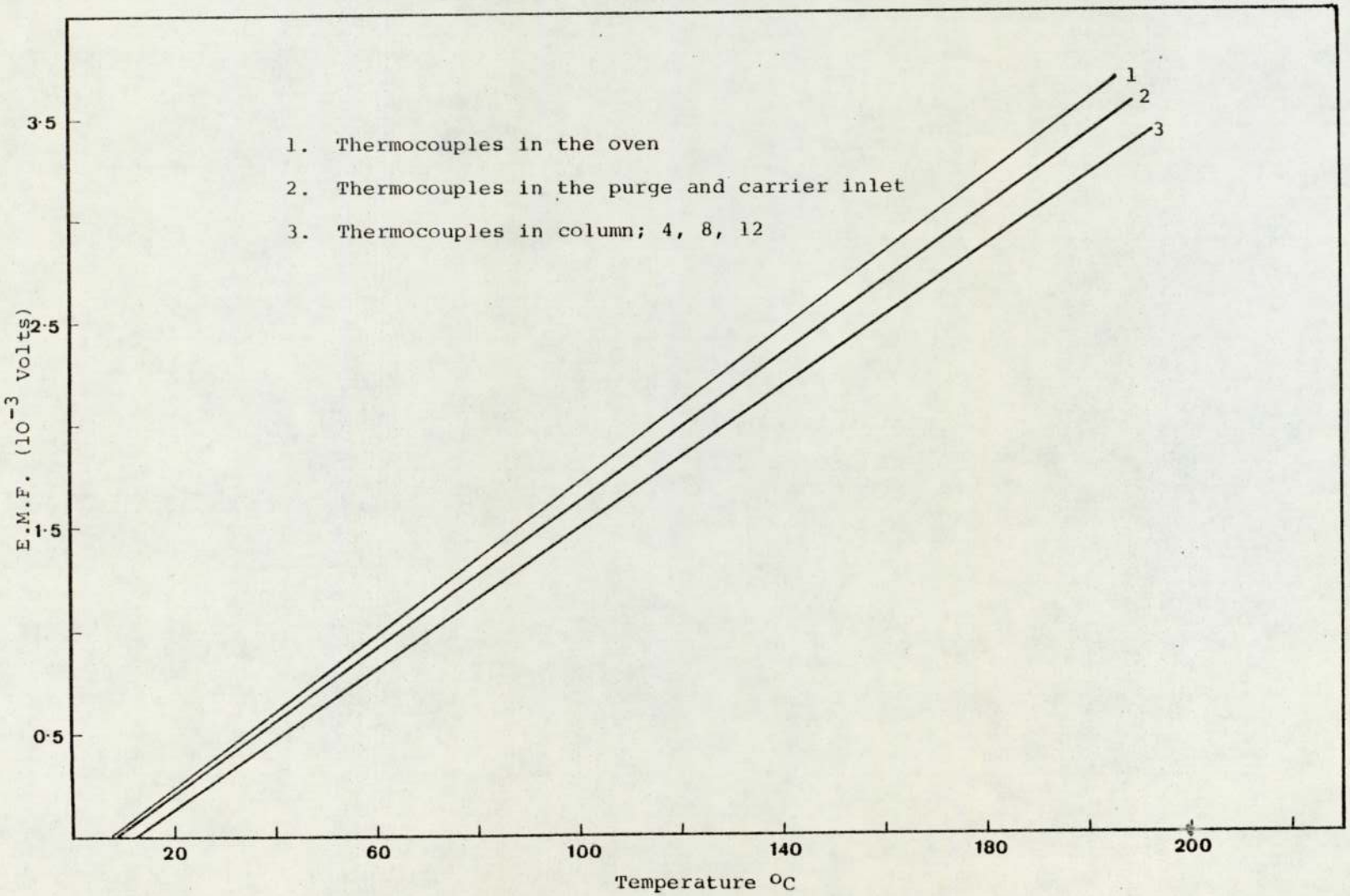

APPENDIX 2

CALCULATION OF $G_{m.c}/L'$

Figure A.2.1

Calculation of $G_{m.c}/L'$ (Run 105-30-95-150)

$$j = \frac{3}{2}\ \frac{(P_{io})^2 - 1}{(P_{io})^3 - 1} = \frac{3}{2}\ \frac{(\frac{274}{177})^2 - 1}{(\frac{274}{177})^3 - 1} = 0.77$$

$$G_{mc} = G_a \times j \times \frac{P_a}{P_o} \times \frac{\theta_o}{\theta_a}$$

$$= 17.2 \times 0.77 \times \frac{101.3}{177} \times \frac{378.16}{297.16} = 9.64\ cm^3 s^{-1}$$

$$L' = \frac{\text{Total volume of solvent in columns}}{\text{Time for 1 cycle}}$$

$$= \frac{183.64}{12 \times 150} = 0.102\ cm^3\ s^{-1}$$

$$\frac{G_{mc}}{L'} = \frac{9.64}{0.102} = 95$$

where

G_a = carrier gas flow rate ($cm^3\ s^{-1}$)

θ_o = operating temperature in k

θ_a = room temperature in k

Similar procedure was used to calculate S_{mc}/L'.

APPENDIX 3

COMPUTER PROGRAMME LISTING

FIG. A.3.1 LISTING OF PROGRAM TO CALCULATE RUN CONDITIONS

```
10  PRINT "PROGRAMME TO CALCULATE RUN CONDITION"
20  PRINT "-------------------------------------"
30  PRINT
40  DIM N$[6]
50  PRINT "FILE NAME"
60  INPUT N$
70  FILES *
80  ASSIGN N$,1,F1
110  Z=1
120  REM Z=NO. OF RUNS
140  REM N=NUMBER OF DATA POINTS
150  P=101.3
160  REM P=AMBIENT PRESSURE IN KN/M**2
170  F=6.2
180  REM F=SLOPE OF CALIBRATION CURVE FOR TOP PRODUCT ROTATOMETER
190  Y=1.38192
200  REM Y=SLOPE OF CALIBRATION CURVE FOR BOTTOM PRODUCT ROTATOMETER
210  W=202
220  REM W=WEIGHT OF LIQUID PHASE IN THE RIG IN GRAM
230  D=1.1
240  REM D=DENSITY OF THE LIQUID PHASE IN GRAM/CM**3
245  PRINT
265  PRINT " RUN DATE=                    "
266  PRINT " -------- "
267  PRINT
269  PRINT "RUN NUMBER [OPER. TEMP. -FEED RATE-SWITCHING RATE-GMC/L]  "
270  PRINT "-----------------------------------------------------------"
271  PRINT
272  PRINT "            [          -          -              -     ]  "
273  PRINT
280  READ #1;P1,P8,S1,S0,T,T1,T2,T3,G,X,I,R
282  PRINT " RUN EXPERIMENTAL CONDITIONS "
283  PRINT "-----------------------------"
285  PRINT
290  PRINT "CAR. INL. PRESS. PSIA= ";P1,"CAR. OUT. PRES. PSIA= ";P8,"PUR. INL. PRES. PSIA= ";S1,"PUR. OUT. PRES. PSIA= ";S0
291  PRINT "AMBIENT. TEMP. C= ";T,"OPERATING TEMP. C= ";T1,"CARRIER TEMP. C=     ";T2,"PUR TEMP. IN C-DEGREE= ";T3
292  PRINT "TOP ROT. READ CM= ";G,"BOT. ROT. READ CM= ";X,"SWIT. RATE(SEC)= ";I,"FEEDING RATE(ML/HR)= ";R
300  REM P1=CARRIER GAS PRESSURE INLET IN PSIA
310  REM P8=CARRIER GAS OUTLET PRESSURE IN PSIA
320  REM S1=PURGE INLET PRESSURE IN PSIA
330  REM S0=PURGE OUTLET PRESSURE IN PSIA
340  REM T=AMBIENT TEMPERATURE IN C-DEGREE
350  REM T1=OPERATING TEMPERATURE
360  REM T2=CARRIER GAS TEMPERATURE IN C-DEGREE
370  REM T3=PURGE GAS TEMPERATURE IN C-DEGREE
380  REM G=TOP PRODUCT ROTATOMETER  IN CM
381  REM X=BOTTOM PRODUCT ROTATOMETER IN CM
390  REM I=SWITCHING RATE IN SECONDES
400  P2=P1+14.7
410  REM P2=CARRIER GAS INLET PRESSURE IN PSIG
420  P3=P8+14.7
430  REM P3=CARRIER GAS OUTLET IN PSIG
```

FIG. A.3.1 CONTINUED

```
440   P4=P2*6.8948
450   REM P4=CARRIER GAS INLET IN KN/M**2
460   P5=P3*6.8948
470   REM P5=CARRIER GAS OUTLET IN KN/M**2 [TOP PRODUCT]
480   S2=S1+14.7
490   REM S2=PURGE INLET PRESSURE IN PSIG
500   S3=S0+14.7
510   REM S3=PURGE OUTLET PRESSURE IN PSIG
520   S4=S2*6.8948
530   REM S4=PURGE INLET PRESSURE IN KN/M**2
540   S5=S3*6.8948
550   REM S5=PURGE OUTLET PRESSURE IN KN/M**2
560   T=T+273.16
570   REM T=ROOM TEMPERATURE IN KELVIN
580   T1=T1+273.16
590   REM T1=OPERATING TEMPERATURE IN KELVIN
600   T2=T2+273.16
610   REM T2=CARRIER GAS TEMPERATURE IN KELVIN
620   T3=T3+273.16
630   REM T3 =PURGE TEMP.  IN KELVIN
640   M=1.5*(((P4/P5) ** 2-1)/((P4/P5) ** 3-1))
650   REM M=J1 CORRECTION FACTOR IN THE SEPARATING SECTION
660   M1=1.5*(((S4/S5) ** 2-1)/((S4/S5) ** 3-1))
670   REM M1=J2 CORRECTION FACTOR IN THE PURGE SECTION
680   G1=(G*1000)/(F*60)
690   REM G1=FLOW OF THE CARRIER GAS IN CM**3/SEC ^GA
700   S=(X*1000)/(Y*60)
710   REM S=FLOW OF THE CARRIER GAS IN CM**3/SEC ^SA
720   G2=(G1*T1*P*M)/(T*P5)
730   REM G2=GM.C VELOCITY OF THE CARRIER GAS CORRECTED IN CM**3/SEC
740   S6=(S*T1*P*M1)/(T*S5)
750   REM S6=SM.C VELOCITY OF PURGE GAS CORRECTED IN CM**3/SEC
760   L=W/(D*12*I)
770   REM L=LIQUID PHASE VELOCITY IN CM**3/SEC
780   G3=(G2*(P5/M)*T2)/(P4*T1)
790   REM G3=G MIN
800   G4=G2/M
900   REM G4=GMAX
1000   S7=(S6*(S5/M1)*T3)/(S4*T1)
1010   REM S7=SMIN
1020   G5=G3/L
1030   REM G5=GMIN/L
1040   G6=G4/L
1050   REM G6=GMAX/L
1060   G7=G2/L
1070   REM G7=GMC/L
1080   S8=S7/L
1090   REM S8=SMIN/L
1100   S9=S6/L
1110   REM S9=SMC/L
1120   PRINT
1121   PRINT "^^^^^^^^^^^^^^^^^^^^^^^^^^^^^^^^^^^^^^^^^^^^^^^^^^^^^^^^^^^^^^"
1125   PRINT
1130   PRINT "OPER. TEMP=    "; T1, "ROOM TEMP=    "; T, "SWIT. RATE=    "; I, "AMB. PRES=   "; P, "FEED RATE=    "; R
1140   PRINT
1150   PRINT
1160   PRINT "FOR SEPARATING SECTION "
1170   PRINT "------------------------"
1180   PRINT
1190   PRINT "P4        P5        G1       G5       G6       G7       M   "
1200   PRINT "---------------------------------------------------------"
1202   PRINT
1210   H=.5
1230   FOR V=1 TO 7
1250   IF H>1 THEN 1280
1260   PRINT  USING 1270; P4, P5, G1, G5, G6, G7, M
1270   IMAGE 3D 5X ,3D 5X, 2D.D 4X, 3D 5X, 3D 5X, 3D 5X, D.DD 3X
1271   GOTO 1350
1280   PRINT  USING 1300; S4, S5, S, S6, S8, S9, M1, L
1300   IMAGE 3D 5X, 3D 5X, 3D 5X, 3D 5X, 4D 5X, 4D 5X, D.DD 3X, D.DD 2X
1320   IF H>1 THEN 1420
1330   PRINT
1340   PRINT
1350   NEXT V
1360   PRINT
1361   PRINT
1370   PRINT "FOR PURGE SECTION"
1380   PRINT "---------------------"
1384   PRINT
1390   H=H+1
1400   PRINT "S4        S5        S       S6       S8         S9       M1      L "
1405   PRINT "----------------------------------------------------------------"
1406   PRINT
1410   GOTO 1230
1420   STOP
1430   END
```

FIG. A.3.2 LISTING OF PROGRAM TO CALCULATE CONCENTRATION PROFILE

```
1   PRINT "PROGRAMME TO CALCULATE COLUMN CONCENTRATION PROFILE"
2   PRINT "-------------------------------------------------------"
3   PRINT
4   DIM N$[6]
5   PRINT "FILE NAME";
6   INPUT N$
7   FILES *
8   ASSIGN N$,1,F1
10   DIM I[200],A[200],G[200],B[200],C[200],D[200],F[200]
20   DIM H[200],K[200],M[200],P[200]
30   X=1
40   REM X=NO. OF SAMPLES PER CYCLE
50   N=12
51   U=1.6785E+10
52   L=2.13636E+10
53   S=5
54   W=.758
55   T=100
56   PRINT
57   PRINT "CYCLE NO. =                    SAMPLING COLUMN =            "
58   PRINT "SAMPLING TIME AFTER THE SEQ. IN SEC =                       "
59   PRINT
60   REM N=TOTAL NO. OF SAMPLES
70   REM U=SLOPE OF FID CALIBRATION CURVE FOR E. LAURATE
73   PRINT "FLOW IN THE CAPILLARY SAMPLING TUBE =                 "
80   REM L=SLOPE OF FID CALIBRATION CURVE FOR M. MYRISTATE
81   REM S=MLS OF SOLVENT IN MLS
82   REM W=FLOW RATE IN CM**3
83   REM T=COLLECTION TIME
84   PRINT LIN(3),"NO";SPA(6);"TOP PRODUCT";SPA(4);"BOTTOM PRODUCT"
85   PRINT LIN(1),"-----------------------------------------------",LIN(1)
90   FOR J=1 TO N
100   READ #1;I[J],A[J],G[J]
105   PRINT I[J],A[J],G[J]
115   REM I(J)=NO. OF ISOLATED COLUMN WHEN SAMPLING COLUMN NO. 12
120   REM A(J)=AREA OF THE E. LAURATE
130   REM G(J)=AREA OF THE M. MYRISTATE
140   B[J]=(A[J]/U)*1000
150   REM B(J)=MASS OF E. LAURATE IN 1 ML SOLVENT
160   C[J]=B[J]*S
170   REM C(J)=MASS COLLECTED IN 5 ML
180   D[J]=C[J]/T
190   REM D(J)=MASS COLLECTED PER SECOND
200   F[J]=D[J]/W
220   H[J]=(G[J]/L)*1000
230   REM H(J)=MASS OF M. MYRISTATE IN 1 ML OF SOLVENT
240   K[J]=H[J]*S
250   REM K(J)=MASS OF M. MYRISTATE IN 5 ML OF SOLVENT
260   M[J]=K[J]/T
270   REM M(J)=MASS COLLECTED FOR ONE SECOND
280   P[J]=M[J]/W
290   REM P(J)=CONCENTRATION OF E. LAURATE IN GM./CM**3
300   NEXT J
310   PRINT LIN(3)," FOR ETHYLE LAURATE "
311   PRINT "----------------------"
312   PRINT
320   PRINT "BED","IN. UN","WT./5ML","WT./SEC","CON. GR./ML"
321   PRINT "---","-----","-------","-------","----------"
322   PRINT
325   PRINT "I(J)","A(J)","C(J)","D(J)","F(J)"
326   PRINT "----","----","----","----","----"
330   Z=.5
340   FOR Y=1 TO X
350   FOR J=Y TO N STEP X
360   IF Z>1 THEN 391
371   PRINT I[J],A[J],C[J],D[J],F[J]
380   GOTO 400
391   PRINT I[J],G[J],K[J],M[J],P[J]
400   NEXT J
405   IF Z>1 THEN 520
410   PRINT
420   PRINT
430   PRINT
450   PRINT
460   NEXT Y
461   PRINT
470   PRINT " FOR METHYLE MYRISTATE "
471   PRINT "----------------------"
500   Z=Z+1
505   PRINT "I(J)","G(J)","K(J)","M(J)","P(J)"
506   PRINT "----","----","----","----","----"
510   GOTO 340
520   STOP
530   END
```

FIG. A.3.3 LISTING OF PROGRAM FOR THE SIMULATION OF THE SCCR-2

```
      PROGRAM PLATES2(INPUT,OUTPUT,TAPE1=INPUT,TAPE2=OUTPUT)
      DIMENSION C(720),D(720),X(60),Y(60),DT(20)
      DIMENSION DELT(720),TEMP(720),T(720),P(720),SVP(720)
      DIMENSION DDF(720),DDL(720),CCF(720),CCL(720),DELD(720),DELC(720)
      DIMENSION PINCAR(20)
      REAL MOLVOL,MWTAP,MWTGP
      REAL ML,MS,LATGP,LATAP,LRATE,MASSF
C     READ INPUT DATA
      READ(1,13)L
      READ(1,888)(DT(J),J=1,L)
      READ(1,3) CFLOW,SFLOW,V1,V2,CFEED,DFEED,FFLOW
      READ(1,4) NFEED,NNBED,KTOTAL,KKINK,KKTYPE,NNTYPE
      READ(1,715) DP,VISC,DENS,VOID,AREA,COLLEN
      READ(1,88)N1,N2,N3,N4,N5,N6,N7
      READ(1,99)N8,N9,N10,N11,N12
      READ(1,794)SS,SL,COMPK,LATGP,LATAP
      READ(1,5)PAMB,PINC,PINP,GC
      READ(1,14)MWTAP,MWTGP,MOLVOL,TAMB
C     SET DUMMY ARRAYS EQUAL TO ZERO
      DO 999 J=1,L
      DO 1 NN=1,720
      T(NN)=TAMB
      SVP(NN)=0.321E-03
    1 CONTINUE
C     OUTPUT DATA
      WRITE(2,22)
      WRITE(2,23)
      WRITE(2,24)
      WRITE(2,25)
      WRITE(2,25)
      WRITE(2,26)
      WRITE(2,25)
      WRITE(2,27)
      WRITE(2,25)
      WRITE(2,28)
      WRITE(2,25)
      WRITE(2,25)
      WRITE(2,31)
      WRITE(2,25)
      WRITE(2,7)CFLOW,SFLOW,V1,V2
      WRITE(2,25)
      WRITE(2,8)CFEED,DFEED,DT
      WRITE(2,25)
      WRITE(2,9)NFEED,NNBED,KTOTAL,KKINK,KKTYPE,NNTYPE
      WRITE(2,25)
      WRITE(2,10)PAMB,PINC,PINP
      WRITE(2,25)
      WRITE(2,720) DP,VISC,DENS,VOID,AREA,COLLEN
      WRITE(2,25)
      WRITE(2,19)MWTAP,MWTGP,MOLVOL,TAMB
      WRITE(2,25)
      WRITE(2,1095)SS,SL,COMPK,LATGP,LATAP
      WRITE(2,25)
      WRITE(2,22)
C     DEFINE PROGRAM PARAMETERS
      XX=1.0
      GO TO 466
  467 XX=XX+1.0
  466 CONTINUE
      DO 937 NN=1,720
      C(NN)=0.0
      D(NN)=0.0
      P(NN)=0.0
  937 CONTINUE
      DO 2 NN=1,60
      X(NN)=0.0
      Y(NN)=0.0
    2 CONTINUE
      MOLVOL=MOLVOL*(TAMB/273.2)*(101.3/PAMB)
      NNTOT=N1+N2+N3+N4+N5+N6+N7+N8+N9+N10+N11+N12
      NNBTEN=(N1+N2+N3+N4+N5+N6+N7+N8+N9+N10)+1
      NNFEED=(N1+N2+N3+N4)+1
      NNBED1=N1+1
      KKKK=(KTOTAL*KKINK)-(KKINK-1)
```

FIG. A.3.3 CONTINUED (1)

```
      KKK=KTOTAL*KKINK-1
      PINCAR(1)=PINC
C     START PRESSURE DROP CALCULATIONS
      DELP1=1.0
      DO 712 I=1,10
      MASSF=DENS*CFLOW
  711 PMEAN=PINCAR(I)-(DELP1/2.0)
      VEL=(CFLOW*PAMB)/(AREA*PMEAN)
      A1=150.0*((1-VOID)**2)*VISC*VEL/((VOID**3)*(DP**2))
      A2=1.75*(1-VOID)*MASSF*VEL/((VOID**3)*DP)
      DELP=(A1+A2)*COLLEN/(GC*10000.0)
      IF(ABS(DELP1-DELP).LE.0.1)GO TO 710
      DELP1=DELP
      GO TO 711
  710 CONTINUE
      PINCAR(I+1)=PINCAR(I)-DELP
  712 CONTINUE
      PINPUR=PINP
      DELP1=1.0
      MASSF=DENS*CFLOW
  714 PMEAN=PINPUR-DELP1/2.0
      VEL=(SFLOW*PAMB)/(AREA*PMEAN)
      A1=150.0*((1-VOID)**2)*VISC*VEL/((VOID**3)*(DP**2))
      A2=1.75*(1-VOID)*MASSF*VEL/((VOID**3)*DP)
      DELP=(A1+A2)*COLLEN/(GC*10000.0)
      IF(ABS(DELP1-DELP).LE.0.5) GO TO 716
      DELP1=DELP
      GO TO 714
  716 CONTINUE
      POPUR=PINPUR-DELP
      NNBED2=(N1+N2)+1
      NNBED3=(N1+N2+N3)+1
      NNBED4=(N1+N2+N3+N4)+1
      NNBED5=(N1+N2+N3+N4+N5)+1
      NNBED6=(N1+N2+N3+N4+N5+N6)+1
      NNBED7=(N1+N2+N3+N4+N5+N6+N7)+1
      NNBED8=(N1+N2+N3+N4+N5+N6+N7+N8)+1
      NNBED9=(N1+N2+N3+N4+N5+N6+N7+N8+N9)+1
      NNELEV=(N1+N2+N3+N4+N5+N6+N7+N8+N9+N10+N11)+1
      K1=N1+N2
      K2=K1+N3
      K3=K2+N4
      K4=K3+N5
      K5=K4+N6
      K6=K5+N7
      K7=K6+N8
      K8=K7+N9
      K9=K8+N10
      K10=K9+N11
      K11=K10+N12
      NDUM1=K1
      NDUM2=K2
      NDUM3=K3
      NDUM4=K4
      NDUM5=K5
      NDUM6=K6
      NDUM7=K7
      NDUM8=K8
      NDUM9=K9
      NDUM10=K10
      NDUM11=K11
      DO 210 NN=NNBED1,NDUM1
      P(NN)=(PINCAR(1)-(((PINCAR(1)-PINCAR(2))/(N1))*(NN-N1)))
     1/PAMB
  210 CONTINUE
      DO 220 NN=NNBED2,NDUM2
      P(NN)=(PINCAR(2)-(((PINCAR(2)-PINCAR(3))/(N2))*(NN-NDUM1)))
     1/PAMB
  220 CONTINUE
      DO 230 NN=NNBED3,NDUM3
      P(NN)=(PINCAR(3)-(((PINCAR(3)-PINCAR(4))/(N3))*(NN-NDUM2)))
     1/PAMB
  230 CONTINUE
      DO 240 NN=NNBED4,NDUM4
      P(NN)=(PINCAR(4)-(((PINCAR(4)-PINCAR(5))/(N4))*(NN-NDUM3)))
     1/PAMB
  240 CONTINUE
      DO 250 NN=NNBED5,NDUM5
```

FIG. A.3.3 CONTINUED (2)

```
      P(NN)=(PINCAR(5)-(((PINCAR(5)-PINCAR(6))/(N5))*(NN-NDUM4)))
     1/PAMB
  250 CONTINUE
      DO 260 NN=NNBED6,NDUM6
      P(NN)=(PINCAR(6)-(((PINCAR(6)-PINCAR(7))/(N6))*(NN-NDUM5)))
     1/PAMB
  260 CONTINUE
      DO 270 NN=NNBED7,NDUM7
      P(NN)=(PINCAR(7)-(((PINCAR(7)-PINCAR(8))/(N7))*(NN-NDUM6)))
     1/PAMB
  270 CONTINUE
      DO 280 NN=NNBED8,NDUM8
      P(NN)=(PINCAR(8)-(((PINCAR(8)-PINCAR(9))/(N8))*(NN-NDUM7)))
     1/PAMB
  280 CONTINUE
      DO 290 NN=NNBED9,NDUM9
      P(NN)=(PINCAR(9)-(((PINCAR(9)-PINCAR(10))/(N9))*(NN-NDUM8)))
     1/PAMB
  290 CONTINUE
      DO 310 NN=NNBTEN,NDUM10
      P(NN)=(PINCAR(10)-(((PINCAR(10)-PINCAR(11))/(N10))*(NN-NDUM9)))
     1/PAMB
  310 CONTINUE
      DO 320 NN=NNELEV,NDUM11
      P(NN)=(PINPUR-(((PINPUR-POPUR)/(N11))*(NN)))/PAMB
  320 CONTINUE
      DO 330 NN=1,NNBED
      P(NN)=(PINPUR-(((PINPUR-POPUR)/(N12))*(NN)))/PAMB
  330 CONTINUE
      WRITE(2,12)
      KKSUM=1
C     START SCCR1 SIMULATION
C     SWITCHING LOOP
      DO 100 K=1,KTOTAL
      ISTKK=KKINK*(K-1)+1
      LSTKK=KKINK*K
      DO 200 KK=ISTKK,LSTKK
      NNSUM=1
C     N LOOP,FOR TOTAL NUMBER OF COLUMNS USED
      DO 300 N=1,12
      IF(N.LE.(NFEED-K)) GO TO 500
      NNFST=NNBED*(N-1)+1
      NNLST=NNBED*N
C     NN LOOP FOR TOTAL NUMBER OF PLATES IN UNIT
      DO 400 NN=NNFST,NNLST
  465 CONTINUE
      IF(N.EQ.11)GO TO 80
      IF(N.EQ.12)GO TO 80
      IF((N.EQ.1).AND.(NN.EQ.NNFST)) GO TO 40
      IF(NN.EQ.NNFEED)GO TO 50
      CCON=C(NN-1)
      DCON=D(NN-1)
      CINPUT=0.0
      DINPUT=0.0
      GO TO 60
   40 C(NN-1)=0.0
      D(NN-1)=0.0
      CCON=C(NN)
      DCON=D(NN)
      GO TO 70
   50 CCON=C(NN-1)
      DCON=D(NN-1)
      CFLOWC=CFLOW*(1.+MOLVOL*(CCON/MWTGP+DCON/MWTAP))
      A=CFLOWC*DT(J)/P(NN)
      LRATE=147.0/(12*KKINK)
      ZZ=A/LRATE
      AA=EXP(-A/(V1+V2*46.0))
      GG=EXP(-A/(V1+V2*74.7))
      IF(C(NN-1).LT.0.1E-10)C(NN-1)=0.0
      IF(D(NN-1).LT.0.1E-10)D(NN-1)=0.0
      C(NN)=(1.0-GG)*((CFLOWC*C(NN-1)+FFLOW*CFEED)/CFLOWC)+GG*C(NN)
      D(NN)=(1.0-AA)*((CFLOWC*D(NN-1)+FFLOW*DFEED)/CFLOWC)+AA*D(NN)
      GO TO 150
   60 IF(C(NN-1).LT.0.1E-10)C(NN-1)=0.0
      IF(D(NN-1).LT.0.1E-10)D(NN-1)=0.0
   70 CCOL=CCON*P(NN)
      DCOL=DCON*P(NN)
      IF(DCOL.GE.SVP(NN))DCOL=SVP(NN)
```

FIG. A.3.3 CONTINUED (3)

```
      CFLOWC=CFLOW*(1.+MOLVOL*(CCON/MWTGP+DCON/MWTAP))
      A=CFLOWC*DT(J)/P(NN)
      LRATE=147.0/(12*KKINK)
      ZZ=A/LRATE
      AA=EXP(-A/(V1+V2*46.0))
      GG=EXP(-A/(V1+V2*74.7))
      C(NN)=(1.-GG)*(C(NN-1)+CINPUT)+GG*C(NN)
      D(NN)=(1.-AA)*(D(NN-1)+DINPUT)+AA*D(NN)
      GO TO 150
   80 IF(NN.EQ.NNFST)GO TO 90
      IF(C(NN-1).LT.0.1E-10)C(NN-1)=0.0
      IF(D(NN-1).LT.0.1E-10)D(NN-1)=0.0
      CCON=C(NN-1)
      DCON=D(NN-1)
      GO TO 95
   90 C(NN-1)=0.0
      D(NN-1)=0.0
      CCON=C(NN)
      DCON=D(NN)
   95 CCOL=CCON*P(NN)
      DCOL=DCON*P(NN)
      IF(DCOL.GE.SVP(NN))DCOL=SVP(NN)
      SFLOWC=SFLOW*(1.+MOLVOL*(CCON/MWTGP+DCON/MWTAP))
      A=SFLOWC*DT(J)/P(NN)
      LRATE=147.0/(12*KKINK)
      ZZ=A/LRATE
      AA=EXP(-A/(V1+V2*46.0))
      GG=EXP(-A/(V1+V2*74.7))
      C(NN)=(1.-GG)*C(NN-1)+GG*C(NN)
      D(NN)=(1.-AA)*D(NN-1)+AA*D(NN)
  150 IF((NN.EQ.(NNTYPE*NNSUM)).AND.(KK.EQ.(KKTYPE*KKSUM)))GO TO 160
      GO TO 170
  160 WRITE(2,161)K,KK,N,NN,C(NN),D(NN),ZZ
  170 IF(NN.EQ.(NNTYPE*NNSUM))NNSUM=NNSUM+1
  400 CONTINUE
      GO TO 300
  500 NNSUM=NNSUM+NNBED/NNTYPE
  300 CONTINUE
      IF(KK.EQ.(KKTYPE*KKSUM)) GO TO 180
      GO TO 212
  180 KKSUM=KKSUM+1
      WRITE(2,185)
      GO TO 200
  212 CONTINUE
      IF(KK.NE.KKKK) GO TO 778
      DO 779 I=1,NNTOT
      CCF(I)=C(I)
      DDF(I)=D(I)
  779 CONTINUE
  778 CONTINUE
      IF(KK.NE.KKK) GO TO 200
      DO 781 I=1,NNTOT
      CCL(I)=C(I)
      DDL(I)=D(I)
  781 CONTINUE
  200 CONTINUE
      WRITE(2,190)
      WRITE(2,195)
      DO 1500 NN=1,NNBED
      X(NN)=C(NN)
      Y(NN)=D(NN)
 1500 CONTINUE
      DO 2000 NN=1,NNTOT
      IF(NN.GE.NNBTEN)GO TO 2010
      NNADJ=NN+NNBED
      C(NN)=C(NNADJ)
      D(NN)=D(NNADJ)
      GO TO 2000
 2010 NNADJ=NN+1-NNELEV
      C(NN)=X(NNADJ)
      D(NN)=Y(NNADJ)
 2000 CONTINUE
  100 CONTINUE
      WRITE(2,25)
      WRITE(2,25)
C     TEMPERATURE CALCULATION
      DO 803 I=1,NNTOT
      DELC(I)=CCL(I)-CCF(I)
```

FIG. A.3.3 CONTINUED (4)

```
      DELD(I)=DDL(I)-DDF(I)
  803 CONTINUE
      ML=204.4/(NNBED*12)
      MS=1362.9/(NNBED*12)
      SURAR=486.76/NNBED
      HTCP=(MS*SS)+(ML+SL)
      XXXX=KKINK
      HTLOSS=COMPK*SURAR*XXXX
      DO 901 I=1,NNTOT
      DELT(I)=((LATAP*46.0*V2*DELC(I))+(LATGP*76.7*DELD(I)*V2
     1))/(HTCP+HTLOSS)
      T(I)=TAMB+DELT(I)
      IF(T(I).GE.433.2)SVP(I)=0.321E-03
      IF((T(I).LE.458.2).AND.(T(I).GE.456.2))SVP(I)=0.31E-03
      IF((T(I).LE.456.2).AND.(T(I).GE.454.2))SVP(I)=0.3E-03
      IF(T(I).LE.454.2)SVP(I)=0.295E-03
  901 CONTINUE
      IF(XX.EQ.1.0)GO TO 468
      GO TO 467
  468 CONTINUE
  999 CONTINUE
    3 FORMAT(7F10.0)
    4 FORMAT(6I4)
    5 FORMAT(4F10.0)
    6 FORMAT(4E13.5)
    7 FORMAT(1H ,7HCFLOW= ,F8.3,4X,7HSFLOW= ,F8.3,4X,4HV1= ,F10.5,
     14X,4HV2= ,F10.5)
    8 FORMAT(1H ,7HCFEED= ,E13.6,4X,7HDFEED= ,E13.6,4X,4HDT= ,F10.5)
    9 FORMAT(1H ,7HNFEED= ,I2,1X,7HNNBED= ,I3,1X,8HKTOTAL= ,I3,
     11X,7HKKINK= ,I4,1X,8HKKTYPE= ,I3,1X,8HNNTYPE= ,I3)
   10 FORMAT(1H ,6HPAMB= ,F6.1,1X,6HPINC= ,F6.1,1X,6HPINP= ,F6.1)
   12 FORMAT(1H ,2H K,5X,5H  KK ,5X,3H N ,5X,5H  NN ,5X,
     114H      C(NN)     ,5X,14H      D(NN)     )
   13 FORMAT(I2)
   14 FORMAT(4F10.0)
   15 FORMAT(4E13.6)
   19 FORMAT(1H ,7HMWTAP= ,F6.2,2X,8HMWTGP=  ,F6.2,2X,8HMCLVOL= ,
     1 F6.0,2X,6HTAMB= ,F5.1)
   21 FORMAT(20X,E13.6,10X,E13.6,10X,E13.6,10X,E13.6)
   22 FORMAT(1H1)
   23 FORMAT(10X,' SCCR2 COMPUTER SIMULATION ')
   24 FORMAT(10X,' ************************* ')
   25 FORMAT(1H0)
   26 FORMAT(10X,'RUN NUMBER 1A,PRODUCED ON 27/6/78,CONDITIONS FOR
     1EL/ML AT APPROX G/L=83  AMB TEMB SET AT 21 DEG C')
   27 FORMAT(10X,'SYSTEM ETHYL LAURATE AND METYLE MYRISTETE')
   28 FORMAT(10X,'FEED RATE=25MLS/HRS')
   31 FORMAT(1X,'INPUT DATA ')
   88 FORMAT(7I5)
   99 FORMAT(5I5)
  161 FORMAT(1H,I2,5X,I5,5X,I3,5X,I5,5X,E14.6,5X,E14.6,5X,F10.4)
  185 FORMAT(1H ,32HNEXT TIME INTERVAL FOR PRINT OUT)
  190 FORMAT(1H ,23HNEXT SWITCHING INTERVAL)
  195 FORMAT(1H ,2H K,5X,5H  KK ,5X,3H N ,5X,5H  NN ,5X,
     114H      C(NN)     ,5X,14H      D(NN)     )
  715 FORMAT(6F10.0)
  794 FORMAT(5F10.0)
  720 FORMAT(1H ,4HDP= ,E11.4,3X,6HVISC= ,E11.4,3X,6HDENS= ,E11.4,
     13X,6HVOID= ,E11.4,3X,6HAREA= ,F10.4,3X,8HCOLLEN= ,F8.4)
  777 FORMAT(10X,E15.6,10X,E15.6)
  888 FORMAT(F10.0)
 1095 FORMAT(1H ,4HSS= ,F10.4,4HSL= ,F10.4,7HCOMPK= ,F10.6,7HLATGP= ,
     1F10.4,7HLATAP= ,F10.4)
      STOP
      END
```

FIG. A.3.4 EXAMPLE OF SCCR-2 SIMULATION OUTPUT

K	KK	N	NN	C(NN)	D(NN)	ZZ(G_{mc}/L')
23	6612	11	420	0.	0.	1038.0695
23	6612	11	440	0.	0.	1040.8605
23	6612	12	460	0.	0.	1937.9800
23	6612	12	480	0.	0.	1764.6021
NEXT TIME INTERVAL FØR PRINT OUT						
23	6699	1	20	0.	0.	136.5714
23	6699	1	40	.467362E-07	0.	149.1915
23	6699	2	60	.773147E-05	0.	81.2080
23	6699	2	80	.259625E-04	0.	81.5652
23	6699	3	100	.695923E-04	0.	82.1215
23	6699	3	120	.147500E-03	0.	82.9799
23	6699	4	140	.265854E-03	.421349E-05	84.2515
23	6699	4	160	.251851E-03	.233285E-04	84.6123
23	6699	5	180	.107169E-03	.529806E-04	83.8944
23	6699	5	200	.228593E-04	.482858E-04	83.2661
23	6699	6	220	.384691E-05	.492768E-04	83.3123
23	6699	6	240	.528523E-06	.492233E-04	83.4903
23	6699	7	260	.533255E-07	.491823E-04	83.7009
23	6699	7	280	.472854E-08	.493573E-04	83.9175
23	6699	8	300	0.	.493474E-04	84.1355
23	6699	8	320	0.	.494553E-04	84.3557
23	6699	9	340	0.	.494982E-04	84.5776
23	6699	9	360	0.	.495755E-04	84.8010
23	6699	10	380	0.	.381914E-04	84.9380
23	6699	10	400	0.	.687626E-07	84.7496
23	6699	11	420	0.	0.	1038.0695
23	6699	11	440	0.	0.	1040.8605
23	6699	12	460	0.	0.	1937.9800
23	6699	12	480	0.	0.	1764.6021
NEXT TIME INTERVAL FØR PRINT OUT						
23	6786	1	20	0.	0.	136.5714
23	6786	1	40	.232529E-10	0.	149.1909

FIG. A.3.5 VARIABLE PARAMETERS IN SCCR-2 MODEL

LOCAL VARIABLES IN SUBROUTINE PLATES2

NAME	TYPE	CURRENT VALUE	
C	REAL	ARRAY (720)	Standardised Conc.
D	REAL	ARRAY (720)	" "
X	REAL	ARRAY (60)	Dummy variable
Y	REAL	ARRAY (60)	" "
DT	REAL	ARRAY (20)	Time increment
DELT	REAL	ARRAY (720)	ΔT over plate
T	REAL	ARRAY (720)	Absolute Temp.
P	REAL	ARRAY (720)	Absolute pressure
SVP	REAL	ARRAY (720)	SAT' VAP' pressure
DDF	REAL	ARRAY (720)	Standardised Conc.
DDL	REAL	ARRAY (720)	" "
CCF	REAL	ARRAY (720)	" "
CCL	REAL	ARRAY (720)	" "
DELD	REAL	ARRAY (720)	" "
DELC	REAL	ARRAY (720)	" "
PINCAR	REAL	ARRAY (20)	Carrier inlet pressure
MOLVOL	REAL	28843.5247799	Molecular volume
MWTAP	REAL	200.330000000	Molecular weight
MWTGP	REAL	228.380000000	" "
ML	REAL	.335416666667	Wt. 'Liquid Phase'
MS	REAL	2.47083333333	Wt. Packing
LATGP	REAL	92.000000000	Latent Heat
LATAP	REAL	69.000000000	" "
LRATE	REAL	.612500000000E-01	L'
MASSF	REAL	.921888000000E-02	Mass flow rate
L	INTEGER	4	Counter
J	INTEGER	3	Counter
CFLOW	REAL	8.730000000000	Carrier gas flow rate
SFLOW	REAL	70.600000000	Purge flow rate
V1	REAL	3.918500000000	Plate volume
V2	REAL	.310000000000	" "
CFEED	REAL	.225500000000E-04	Feed Conc.
DFEED	REAL	.480600000000E-04	" "
NFEED	INTEGER	5	Feed Bed
NNBED	INTEGER	40	Number plates/bed
KTOTAL	INTEGER	24	Total number sequences
KKINK	INTEGER	200	Sequencing interval
KKTYPE	INTEGER	87	Printing interval
NNTYPE	INTEGER	20	Plate print interval
DP	REAL	.158600000000E-03	Particle diameter
VISC	REAL	.188300000000E-03	Gas viscosity
DENS	REAL	.105600000000E-02	Gas density
VOID	REAL	.667000000000	Voidage
AREA	REAL	3.836000000000	Plate area
COLLEN	REAL	61.000000000	Column length
N1	INTEGER	40	Number plates/column 1
N2	INTEGER	40	Number plates/column 2
N3	INTEGER	40	Number plates/column 3
N4	INTEGER	40	Number plates/column 4
N5	INTEGER	40	Number plates/column 5
N6	INTEGER	40	Number plates/column 6
N7	INTEGER	40	Number plates/column 7

FIG. A.3.5 CONTINUED (1)

N8	INTEGER	40	Number plates/column 8
N9	INTEGER	40	Number plates/column 9
N10	INTEGER	40	Number plates/column 10
N11	INTEGER	40	Number plates/column 11
N12	INTEGER	40	Number plates/column 12
SS	REAL	.200000000000	Specific heat
SL	REAL	.200000000000	" "
COMPK	REAL	.342000000000E-03	Thermal conductivity
PAMB	REAL	101.300000000	Ambient pressure
PINC	REAL	308.000000000	Carrier pressure
PINP	REAL	184.000000000	Purge pressure
GC	REAL	981.000000000	Gas constant
TAMB	REAL	297.160000000	Ambient Temperature
NN	INTEGER	480	Counter
XX	REAL	1.000000000000	Constant
NNTOT	INTEGER	480	Total Number plates
NNBTEN	INTEGER	401	Last bed, 1st plate
NNFEED	INTEGER	161	Feed plate
NNBED1	INTEGER	41	Sep. Sect., 1st plate
KKKK	INTEGER	4601	Counter
KKK	INTEGER	4799	"
DELP1	REAL	28.4984742010	ΔP in Purge bed
I	INTEGER	11	Counter
PMEAN	REAL	169.750762899	Mean pressure
VEL	REAL	10.9830715572	Gas velocity
A1	REAL	4608610.35717	Dummy
A2	REAL	1253.72871379	"
DELP	REAL	28.6648021650	Corrected ΔP
PINPUR	REAL	184.000000000	Purge pressure IN
POPUR	REAL	155.335197835	Purge pressure OUT
NNBED2	INTEGER	81	1st plate in bed
NNBED3	INTEGER	121	" " " "
NNBED4	INTEGER	161	" " " "
NNBED5	INTEGER	201	" " " "
NNBED6	INTEGER	241	" " " "
NNBED7	INTEGER	281	" " " "
NNBED8	INTEGER	321	" " " "
NNBED9	INTEGER	361	" " " "
NNELEV	INTEGER	401	" " " "
K1	INTEGER	80	Last plate in bed
K2	INTEGER	120	" " " "
K3	INTEGER	160	" " " "
K4	INTEGER	200	" " " "
K5	INTEGER	240	" " " "
K6	INTEGER	280	" " " "
K7	INTEGER	320	" " " "
K8	INTEGER	360	" " " "
K9	INTEGER	400	" " " "
K10	INTEGER	440	" " " "
K11	INTEGER	480	" " " "
NDUM1	INTEGER	80	Counter
NDUM2	INTEGER	120	"
NDUM3	INTEGER	160	"
NDUM4	INTEGER	200	"
NDUM5	INTEGER	240	"
NDUM6	INTEGER	280	"
NDUM7	INTEGER	320	"
NDUM8	INTEGER	360	"

FIG. A.3.5 CONTINUED (2)

NDUM9	INTEGER	400	Dummy.
NDUM10	INTEGER	440	"
NDUM11	INTEGER	480	"
KKSUM	INTEGER	21	Counter
K	INTEGER	10	"
ISTKK	INTEGER	1801	"
LSTKK	INTEGER	2000	"
KK	INTEGER	1812	"
NNSUM	INTEGER	24	"
N	INTEGER	12	"
NNFST	INTEGER	441	"
NNLST	INTEGER	480	"
CCON	REAL	2,92727846085	Plate Conc.
DCON	REAL	0.	" "
CINPUT	REAL	0.	Plate N Feed Conc.
DINPUT	REAL	0.	" " " "
CFLOWC	REAL	8,73000000000	Corrected flow rate
AA	REAL	37,01485385 30	Dummy
GG	REAL	7,58956893063	"
SFLOWC	REAL	2617·17114586	Purge flow rate
NNADJ	INTEGER	40	Dummy
SURAR	REAL	12,16900000000	Surface area
HTCP	REAL	1,02958333333	Heat capacity
XXXX	REAL	200,00000000	Counter
HTLOSS	REAL	0.	Heat loss

APPENDIX 4

CALCULATION OF HETP

A.4.1 ESTIMATION OF THE HEIGHT OF A THEORETICAL PLATE

Chapter 2 presented several theories which describes the behaviour of a chromatographic column in terms of HETP. Giddings (36) developed the non-equilibrium theory in which the mass transfer or non-equilibrium terms were expressed as functions of diffusivity, particle diameter, stationary phase dimensions, etc., and obtained the following definition of the theoretical plate height.

$$H = \frac{2\gamma' D_m}{u} + q'R(1-R)\frac{d_f^2.u}{D_s} + \left[\frac{1}{2\lambda d_p} + \frac{D_m}{w.d_p^2.u}\right]^{-1} \qquad (2.17)$$

In the application of the above equation to the SCCR-2 unit it is necessary to evaluate many physical parameters, many of which are specific to the individual solute components, e.g. molar volumes and collision diameters. The evaluation of certain parameters in equation 2.17 relating to the individual solutes is a complex problem and therefore it has been simplified by assuming that, in the cases where parameters vary for the individual solutes, the mean value may be used.

Individual terms from equation 2.17 are discussed below with an estimation of their physical value.

1. Labyrinth Factor γ'

The structural parameter γ' is a function of the independent terms for tortuosity and constriction and has

been evaluated as 0.46 for crushed firebrick (186).

2. Configuration Factor q'

The above factor is to allow for the shape of the stationary phase layer, and Giddings (36) has given a typical value of 0.25 for preparative gas chromatographic column.

3. Retention Ratio R

The fraction of solute in the mobile phase (R) (187) is given by

$$R = \frac{V_m}{V_m + \sum_i K_i V_s} \qquad (A.4.1)$$

which for the solutes Arklone. P and Genklene is 9.057×10^{-3}.

4. Stationary Phase Film Thickness d_f

Giddings (36) related the film thickness to the particle diameter via $\frac{d_f}{d_p} \leqslant 0.03$. For the solid support in question $d_p = 0.0305$ which makes $d_f \leqslant 0.03 \times 0.0305 = 9.15 \times 10^{-4}$cm.

5. Particle Diameter d_p

The size range of Chromosorb P, used as packing in the SCCR-2 was 358-251 microns, giving a mean particle diameter of 3.05×10^{-2}cm.

6. Flow Velocity

The mean flow velocity changes as the carrier gas expands during its passage through the SCCR-2. The variation in HETP with mobile phase velocity has been discussed in

section 2.3.2.1 and therefore it is necessary to define a mean column velocity, u_{mc}, for use in equation 2.17. u_{mc} is defined (184) as follows:

$$u_{mc} = \frac{F}{A} \qquad (A.4.2)$$

where

F = column carrier gas flowrate cm^3/sec connected to outlet pressure.

A = inter-particle volume of the bed.

7. Mobile and Stationary Phase Molecular Diffusion Coefficients D_m, D_s

The mobile phase diffusion coefficient may be calculated from the Hirschfelder-Bird-Spot 2 equation (188).

$$D_m = \frac{0.00186\ T^{\frac{1}{2}}\left(\frac{1}{M_1} + \frac{1}{M_2}\right)^{\frac{1}{2}}}{p.\sigma_{12}^2 \cdot r_{12}} \qquad (A.4.3)$$

where

M_1 = molecular weight of solvent (carrier gas)

M_2 = molecular weight of solute

p = absolute pressure in atmosphere

r_{12} = mean collision diameter

$$= \frac{(r_o)_1 + (r_o)_2}{2} \qquad (A.4.4)$$

$(r_o)_1 (r_o)_2$ =individual solvent, solute, collision diameters

σ_{12} = collision integral for diffusion

The collision diameters may be calculated directly from viscosity measurements, or from the empirical equation (184) given below

$$r_o = 1.18\ V_b^{\frac{1}{3}} \qquad (A.4.5)$$

where V_b is the molar volume of the fluid at the normal boiling point determined by the method of addition. For nitrogen, this was found to be 3.7 cm^3, and for a 50:50 mixture of Arklone.P/Genklene, V_b was evaluated as 122.1.

The collision integral, σ_{12}, is a function of $K_b.T/\varepsilon_{12}$ where K_b is Boltzmann's constant and ε_{12} is the energy of molecular interaction. Values of, σ_{12} are tabulated in reference (184).

Substitution into equation A.4.3 yields a value for D_m at 60°C of 0.00239 $cm^2.s^{-1}$. It must be emphasised that this value is an average value for the two solutes, Arklone.P/ Genklene evaluated at a mean column pressure of 1.86 atmospheres.

A recommended relation (184) for estimation of diffusivities of non-electrolytes in liquids at low concentration of the diffusing component is the Wilke and Chang equation (189):

$$\frac{D_s.\mu}{T} = 7.4\times10^{-8}\ \frac{(X.M_L)^{\frac{1}{2}}}{V_b^{0.6}} \qquad (A.4.6)$$

where

μ = viscosity of liquid phase

X = association parameter (1.0 for non-associated liquids)

M_L = molecular weight of liquid phase

The above equation shows that D_s depends on the solvent through reciprocal viscosity, $\frac{1}{\mu}$, but this effect is tempered somewhat by the fact that D_s increases with the square root of solvent molecular weight. It can be seriously questioned whether the inverse viscosity relationship holds for the long snake-like molecules used as solvents in gas chromatography (190) and therefore it is perhaps fortunate that the plate height terms containing D_s terms contribute very little to the overall plate height. The absolute value for the viscosity of the OV-275 solvent has not been determined and it is not possible to calculate it. Alternatively a supplied value for a similar liquid phase (OV-225) from the manufacturer is given as 2010 Cp, resulting in a stationary phase molecular diffusion coefficient of the order of 1×10^{-6} $cm^2.s^{-1}$. Whilst this value can be no more than an estimate it is reinforced by the opinion of Giddings (36) who states that for gas chromatography the ratio of liquid to gas diffusion coefficients, is about 10^{-5}.

8. Eddy Diffusion Factor λ

The above factor, present in the coupled part of equation 2.17 may be defined as

$$\lambda_i = W_\beta^2 . W_\lambda / 2 \qquad \text{A.4.7}$$

where $W_\beta^2 . W_\lambda$ is evaluated for each of five categories of the velocity in equality highlighted in section 2.3.2.2. Giddings (36) has estimated the individual contributions to λ_i as;

$$\lambda_1 = 0.5;\ \lambda_2 = 10^4;\ \lambda_3 = 0.5;\ \lambda_4 = 0.1;\ \lambda_5 = 0.02\left(\frac{d_c}{d_p}\right)^2$$

giving

$$\lambda_i = 1.01 \times 10^4$$

This value for λ can only be a very approximate value, however, as the term for eddy diffusion, $\frac{1}{2.\lambda.d_p}$, in the coupled expression given by equation 2.17, is not the dominant term, contributing less than 1.2% for SCCR-2 conditions. Further accuracy in the estimation of λ is not thought necessary.

9. Diffusional Flow Parameter W

In a similar manner to evaluating λ, the parameter W may be defined (36) as

$$W_i = W_\alpha^2 . W_\beta^2 / 2 \qquad \text{(A.4.8)}$$

evaluated again for the five types of velocity inequality occuring within the packed columns. The non-equilibrium approach to evaluating W requires specific information regarding the velocity, which for the SCCR-2 is not available. However Giddings (36) has also used W in the 'random walk' method of determining H, and has reported that the numerical results so obtained were not inferior to those developed from the non-equilibrium theory. The approximate magnitude of the velocity inequalities are as follows:

Transchannel, $W_1 = 0.01$

Transparticle, $W_2 = 0.10$

Short-range interchannel, $W_3 = 0.5$

Long-range interchannel, $W_4 = 2.0$

Transcolumn, $W_5 = 0.001(\frac{d_c}{d_p})^2$

It is the final velocity inequality for the transcolumn effects that is of particular importance to large diameter columns and from the above definition it becomes apparent that the plate height becomes a function of the column diameter squared for a constant particle diameter. Contrary to this definition, Pretorius and de Clerk (63) indicate that plate height increases with d_c at constant $\frac{d_p}{d_c}$, reaches a maximum at $\frac{d_p}{d_c} = 0.05$ and then decreases with increasing d_c. Support for this theory is given by Spencer and Kucharski (64) and Knox (65). The value of W_5 which gives

maximum contribution to plate height is 0.4. The overall summed value for W_i then becomes 3.01.

Having defined and estimated all the parameter in equation 2.17 the theoretical plate height is given by:

$$\frac{2\times0.46\times0.00239}{1.255} + \frac{0.25\times0.00957(1-0.00957)(9.15\times10^{-4})^2\ 1.255}{1.0\times10^{-6}}$$

$$+\left[\frac{1}{2\times1.01\times10^{4}\times0.0305} + \frac{0.239\times10^{-2}}{3.01\times(0.305)^{2}\times1.255}\right]^{-1} = 1.471 \text{ cm}$$

A.4.2 ADDITIONAL FACTORS WHICH CONTRIBUTES TO HETP

In section 2.4.1 mechanisms leading to zone broadening were discussed. Of particular importance to the SCCR-2 were two additional plate height contributions resulting from cross-column temperature fluctuations, H_t, and the uneveness of the flow velocity, H_c. The contribution from these terms must be evaluated and added to the overall plate height.

H_t, has previously been defined in section 2.4.1.2 and is given by

$$H_t = \alpha_t.(\Delta T)^2 \frac{r_c^2 \cdot u}{900 \cdot D_m} \qquad (2.24)$$

ΔT in the above equation is the temperature difference between the column axis and wall, which will have a specific

value for each axial point within the SCCR-2. As the HETP defined by equation 2.17 is not a point value but an average value for conditions within the SCCR-2, the average temperature difference between the axis and wall for the ten separating columns is required. This was measured by inserting thermocouples at the wall and the axis, and the average temperature difference was found to be approximately 4.0°C, giving a contribution from H_t of 0.045 cm.

Many approaches have been suggested for theoretically formulating the term, H_c, (51,59,61,63). Hupe (59) using a statistical treatment generated the following expression

$$H_c = \frac{2.83 \cdot r_c^{0.58}}{u^{1.886}} \qquad (2.20)$$

and whilst the cross-sectional velocity profile corresponding to this relationship was an unusual shape, the fit to a variety of experimental results on columns between 1.3 and 10 cm diameter was very good. For SCCR-2 conditions the contribution from H_c makes to the overall plate height is 1.953 cm.

The final height equivalent to a theoretical plate expression becomes

$$H = \frac{2\gamma D_m}{u} + q'R(1-R)\frac{d_f^2 u}{D_s} + \left[\frac{1}{2.\lambda.d_p} + \frac{D_m}{W.d_p^2.u}\right]^{-1} + H_c + H_t$$

$$= 3.469 \text{ cm} \qquad (A.4.9)$$

The above figure gives an average of 17 plates/column in the SCCR-2, but from the experimental determination of HETP, this cannot be true. It is the opinion of the author that the above equation may be re-written to include the term H_c as a coupled parameter. H_c is included in the Van Deemter equation to allow for cross column velocity fluctuations and will therefore include the transcolumn velocity inequality defined by Giddings as W_5. The addition of separate contributions to plate height is only valid if those contributions are independent from each other (c.f. addition of variances in the random-walk theory). Therefore if the term H_c includes a contribution for the transcolumn velocity inequality it will not be independent from the other velocity correction terms (W_1-W_4) and may be included in the coupled part of equation A.4.9 to give

$$H = \frac{2\gamma' D_m}{u} + q'R(1-R)\frac{d_f^2.u}{D_s} + \left|\frac{1}{2.\lambda.d_p} + \frac{D_m}{W'.d_p^2.u} + \frac{1}{H_c}\right|^{-1} + H_t$$

$$= 0.8196 \text{ cm} \qquad \text{(A.4.10)}$$

Where W' does not include a contribution from W_5, the transcolumn effect. This gives 74 plates/column in the SCCR-2 and is in agreement with the experimental determination.

NOMENCLATURE

NOMENCLATURE

A	term accounting for eddy diffusion in chromatographic theoretical plate height equation
A_p	surface area of theoretical plate
B	term accounting for longitudinal diffusion in chromatographic theoretical plate height equation
C_m	term accounting for mobile phase resistance to mass transfer in chromatographic theoretical plate height equation
C_s	term accounting for mobile phase resistance to mass transfer in chromatographic theoretical plate height equation
c	solute concentration in mobile phase
c_f	feed concentration
D_m	mobile phase molecular diffusivity
d_p	mean particle diameter
D_p'	effective diameter of particles, as defined by equation 8.15
d_f	thickness of stationary phase liquid film

d_r	radial diffusion coefficient
D_s	stationary phase molecular diffusivity
d_c	internal column diameter
d_{pc}	ratio of particle to column diameter
E	eddy diffusivity
E_1, E_2	mass production rates of component 1 and 2 at the top of a column
$F_{1,2}$	feed rate of component 1 and 2 to the column
F	carrier gas volumetric flow rate measured at ambient conditions
F_f	feed flow rate
F_m	fractional volume of mobile phase in a chromatographic column
F_s	fractional volume of stationary phase in a chromatographic column
f	feed rate
f'	factor to allow for the effect on column length of increasing the mole fraction of solute in the liquid phase

G	Gas phase volumetric flow rate in the main separating section of the sequential unit, solute free
G'	volumetric flow rate of solute free carrier gas
G_a	gas phase volumetric flow rate measured at ambient conditions
G_E	mass flow rate of gas
G_{mc}	gas phase volumetric flow rate measured at mean column pressure
G_{min}, G_{max}	the volumetric mobile phase flow rates at the column inlet and outlet respectively
G_2	constant in the plate height equation for large diameter columns
g_c	gravitational constant
$(G/L)_R, (G/L)_S$	ratio of gas to liquid flow rates in the rectifying and stripping sections of the columns
H	height equivalent to a (chromatographic) theoretical plate, H.E.T.P.
H_c	contribution to H in large diameter columns caused by non-uniformity of the velocity profile

H_t	contribution to H, caused by thermal fluctuations across the column
h_i	heat of solution of component 1 in the liquid phase
I'	Aris integral describing the velocity profile gradient in the chromatographic plate height equation for large diameter columns
I	the length of a sequencing interval
j	James and Martin gas phase compressibility factor
K	partition coefficient of solute bewteen mobile and stationary phases
K_b	Boltzmann's constant
K^∞	partition coefficient at infinite dilution
ΔK	change in K^∞ with increasing solute concentration
$\Delta K'$	change in K^∞ with change in temperature
K'	mass distribution ratio = $F_m/K.F_s$
K"	rate constant of desorption
L	liquid solvent volumetric flow rate

L'	apparent liquid solvent flow rate in the sequential unit
L_M	distance migrated by the centre of a component zone
ℓ	column length
ℓ'	root mean square step length in random walk model
M_1, M_2	mass flow rate of solute leaving the column as product 1 and 2, H.T.U. model
M_f	molecular weight of feed component
M_L	molecular weight of liquid phase
M_v	solute molar volume at column operating temperature
N	number of theoretical co-current chromatographic plates within a column
N_{cc}	number of counter-current theoretical plates or stages
$(N_{OG})_R$	number of overall gas phase transfer units in the rectifying section of a column, H.T.U. model

$(N_{OG})_S$	number of overall gas phase transfer units in the stripping section of a column, H.T.U. model
n'	number of steps in random walk model
P_a	ambient pressure
P_a^o	vapour pressure of component
P_i	pressure inlet
P_o	pressure outlet
P	absolute pressure in atmosphere
Q_G	gas volumetric flow rate from H.T.U. model
Q_L	liquid volumetric flow rate from H.T.U. model
q	solute concentration in stationary phase
q'	configuration factor dependent on shape of stationary phase layer
R	retention ratio = elution volume/total bed volume
R_g	gas constant
r'	rate of transfer of molecules from gas to liquid phase in random walk model for continuous chromatography

r''	rate of transfer of molecules from liquid to gas phase in random walk model for continuous chromatography
r_c	column radius
r_o	individual molecular collision diameter
r_{12}	mean molecular collision diameter for component 1 and 2
S	volumetric gas flow rate in the purge section of the sequential unit
S_1, S_2	factors to account for the effect of the sequential nature of operation
S_L	specific heat of liquid phase
S_{mc}	volumetric gas flow rate measured at mean purge column pressure
SF	separation factor, K_1/K_2
S_p	specific heat of packing
S_s	specific surface of particle per unit volume of bed
T	absolute temperature
ΔT	temperature difference between column axis and wall

T_a	ambient temperature
T_c	column temperature
t	time
t_m	elution or retention time of unretained component
t_R	elution or retention time of retained component
t'_R	adjusted retention time, $t_R - t_m$
t_w	width of an eluted peak (time units)
t_{ric}, t_{roc}	time from injection to the commencement of the recording of the inlet and outlet profiles
$\bar{t}_{ri}, \bar{t}_{ro}$	peak mean or first moment in time units for the recorded inlet and outlet profiles
u	average interstitial gas phase velocity
u_L	stationary phase velocity in random walk model for continuous chromatography
u_{mc}	interstitial gas phase velocity at mean column pressure
u_m	superficial column velocity
$(u_s)_l$	bottoms/feed mass flow rate ratio of component, l, in probabilistic model

$(u_z)_2$	tops/feed mass flow rate ratio of component 2, in probabilistic model
v_b	molar volume at boiling point
V_G	volume of gas phase in a column corrected for gas compressibility = $j.V_m$
V_L	volume of liquid phase impregnated on the solid support
V_M	mobile phase volume of column
$V_{n(G)}$	gas phase volume in plate n of a chromatographic model
$V_{n(L)}$	liquid phase volume in plate n of a chromatographic model
V_R	elution or retention volume of component
V_S	stationary phase volume in column
V_1	volume of packing per theoretical plate
V_2	volume of liquid phase per theoretical plate
V	volumetric gas flow rate expressed in terms of plate volumes
$W, W_\alpha, W_\beta, W_\lambda$	factors in chromatographic theoretical plate height equation to allow for non-uniformity of the velocity profile

X	association parameter in Wilke and Chang equation
X_{gn}	concentration of solute in gas phase over the nth plate of theoretical model proposed by Scott
Y_o	mole fraction of solute in the gas phase
Y_1, Y_2	gas phase solute concentrations at points 1 and 2 in the column
z	composite thermal conductivity of packed bed

GREEK SYMBOLS

α	separation factor
α'	packing geometry factor in chromatographic plate height equation for large diameter columns
α_c	constant in the excess plate temperature equation
α_t	constant of value 0.004 in the theoretical plate height equation for heating rate
β_c	constant in excess plate temperature equation
γ'	labyrinth factor

γ_s	obstructive factor within solid particles
δ_1, δ_1'	series of factors to correct theoretical operating (G/L) limits of the SCCR-2 unit
ε	void fraction of a packed bed
ε_{12}	energy of molecular interaction
θ	excess temperature of plate above its surroundings
λ	eddy diffusion factor
μ	dynamic viscosity
ν	reduced velocity = $u\ d_p/D_M$
ℓ'	step length in random walk model
ρ	density
ρ_L	density of liquid phase
ρ_p	density of solid support
σ	standard deviation
σ^2	variance
$(\sigma_t)^2_{r.i}$	time based variance of the eluted peak recorded at the column inlet

$(\sigma_t)^2_{r,o}$	time based variance of the eluted peak recorded at the column outlet
σ_{12}	collision integral for diffusion
ϕ	shape factor
ψ	operating mobile phase/stationary phase velocity ratio in probabilistic model

REFERENCES

REFERENCES

1. P. E. Barker and D. Critcher, Chem. Eng. Sci., 13, 82, 1960.

2. D. Critcher, Ph.D. Thesis, University of Birmingham, 1963.

3. P. E. Barker, and D. Lloyd, Symposium on the less common means of separation, Inst. Chem. Eng., London, p.68, 1964.

4. D. Lloyd, Ph.D. Thesis, University of Birmingham, 1963.

5. P. E. Barker and D. Lloyd, U.S. Patent, 3, 338, 031.

6. P. E. Barker and Universal Fisher Engineering Co. Ltd., British Patent Applications 33630/65, 43629/65, 5764/681, 44375/68.

7. P. E. Barker and D. H. Huntington, J. Gas. Chromatog., 4, 59, 1966.

8. D. H. Huntington, Ph.D. Thesis, University of Birmingham, 1967.

9. P. E. Barker and D. H. Huntington, "Gas Chromatography", A. B. Littlewood, Ed. Inst. of Petroleum, p. 135, 1967.

10. P. E. Barker and D. H. Huntington, Declema Monograph, 62, 153, 1969.

11. P. E. Barker and R. E. Deeble, Anal. Chem., 45, 1121, 1973.

12. P. E. Barker and R. E. Deeble, British Patent, 1,418,503,

U.S. Patent 4, 001, 112.

13. R. E. Deeble, Ph.D. Thesis, University of Aston in Birmingham, 1974.

14. P. E. Barker and R. E. Deeble, Chromatographia, 8 (2), 67, 1975.

15. P. E. Barker and S. E. Liodakis, Chromatographia, 11 (12), 703, 1978.

16. S. Liodakis, Ph.D. Thesis, University of Aston in Birmingham, 1977.

17. P. E. Barker, J. F. Ellison and B. W. Hatt, "Advances In Chromatographic Fractionation of Macromolecules", Chem. Soc., London, 1976.

18. J. F. Ellison, Ph.D. Thesis, University of Aston in Birmingham, 1976.

19. H. Purnell, "Gas Chromatography", John Willey and Son Inc., New York, 1962.

20. J. W. Amy, L. Brand and W. Baitinger, "Progress in Industrial Gas Chromatography", H. A. Szymanski, H. A., Ed., p. 147, Plenum Press, New York, 1961.

21. M. J. E. Golay, "Gas Chromatography", H. J. Noebles, N. Brenner and R. F. Wall, Eds. Academic Press, New York, p. 1., 1961.

22. U. S. Patent, 3, 250, 058, 1966, 3, 491, 512, 1968.

23. J. J. Kirland, "Gas Chromatography", H. J. Noebles, N. Brenner and R. F. Wall, Eds. Academic Press, New York, p. 1, 1961.

24. A. B. Carel, R. E. Clement and G. Perkins, "Advances in Chromatography", A. Zlatkis Ed., Preston Tech., Abstracts Co., Evanston, Illonois, p. 133, 1969.

25. P. Valentin, G. Hagenhach, B. Roz and G. Guiochon, "Gas Chromatography", S. G. Perry, Ed., Applied Science publishers, London, p. 157, 1973.

26. P. E. Barker and S. Al-Madfai, J. Chromatogr. Sci., 1, 425, 1969.

27. S. Al-Madfai, Ph.D. Thesis, University of Birmingham, 1969.

28. P. E. Barker, "Preparative Gas Chromatography", A. Zlatkis, Ed., Wiley-Interscience, London, p. 135, 1971.

29. P. E. Barker, "Progress In Separation", Perry and Van Oss, Eds., John-Wiley and Sons, p. 325, 1971.

30. P. E. Barker, "Development In Chromatography", Applied Science publishers Ltd., p. 41, 1977.

31. D. M. Bell, Ph.D. Thesis, University of Aston in Birmingham, 1977.

32. P. E. Barker and S. Al-Madfai, "Advances in Chromatography", Preston Tech. Abstracts, Las Vegas, p. 123, 1969.

33. P. E. Barker, S. E. Liodakis and M. I. Howari, Can. J. Chem.Eng., 57, Feb., 42, 1979.

34. C. B. Ching, Ph.D. Thesis, University of Aston in Birmingham, 1978.

35. A. T. James and A. J. P. Martin, Biochem. J., 50, 679, 1952.

36. J. C. Giddings, "Dynamics of Chromatography", Part I, Principles and Theory, Marcel Dekker, New York, p. 323, 1965.

37. J. H. Purnell, "Gas Chromatography", John Wiley and Sons, London, 1962.

38. A. B. Littlewood, "Gas Chromatography", Academic Press, New York, 1962.

39. A. J. P. Martin and R. L. M. Synge, Biochem. J., 35, 1358, 1941.

40. S. W. Mayer and E. R. Tompkins, J. Am. Chem. Soc., 69, 2866, 1947.

41. E. Glueckauf, Trans. Farad. Soc., 51, 34, 1955.

42. J. C. Giddings, J. Chromatogr., 2, 44, 1959.

43. L. Lapidus and N. R. Ammundson, J. Phys. Chem., 56, 984, 1952.

44. J. J. Van Deemeter, F. J. Zuiderweg, and A. Klinkenberg, Chem. Eng. Sci., 5, 271, 1956.

45. E. Kucera, J. Chromatogr., 19, 237, 1965.

46. O. Grubner, "Advances in Chromatography Vol. 6", R. A. Keller and J. C. Giddings, Eds., Marcel Dekker Inc., New York, p. 173, 1968.

47. E. Grushka, J. Phys. Chem., 76, 2586, 1972.

48. M. Golay, "Gas Chromatography", D. H. Destry, Ed., Butterworths, London, p. 36, 1958.

49. J. C. Giddings, J. Chem. Ed., 35, 588, 1958.

50. A. Einstein, Ann. der. Physik, 17, 549, 1905.

51. J. C. Giddings, J. Gas Chromatogr., 1(1), 12, 1963.

52. J. C. Giddings and G. E. Jensen, J. Gas Chromatogr., 2(9), 290, 1964.

53. F. H. Huyten, W. Van Beersum and G. W. A. Rijnders, "Gas Chromatography", R. P. W. Scott, Ed., Butterworths, London, p. 224, 1960.

54. G. J. Friscone,J. Chromatogr., 6, 97, 1961.

55. G. M. C. Higgins and J. F. Smith, "Gas Chromatography", A. Gold, Ed., p. 94, 1965.

56. G. W. A. Rijnders, "Advances in Chromatography", Vol. 3, Marcel Dekker, Ed., New York, p. 215, 1966.

57. K. P. Hupe, U. Busch and K. Winder, J. Chromatogr. Sci., 7, 1, 1969.

58. S. A. Volkov, V. Y. Zel. Venskii, K. I. Sakodynskii and F. Ya. Fvolov, J. Chromatogr., 77, 97, 1973.

59. E. Bayer, K. P. Hupe and H. Mack, Anal. Chem., 35, 492, 1963.

60. A. B. Littlewood, Anal. Chem., 38, 2, 1966.

61. S. T. Sie and G. W. A. Rijnders, Anal. Chem. Acta., 38, 3, 1967.

62. A. Aris, Proc. Roy. Soc., Ser. A., 252, 538, 1959.

63. V. Pretorius and K. de Clark, "Preparative Gas Chromatography", A. Zlatkis and V. Pretorius, Eds., Wiley -Interscience, London, P. 1, 1971.

64. S. F. Spencer and Kucharski, Facts and Methods, 7(4), 8, 1966.

65. J. H. Knox, "Advances in Gas Chromatography", A. Zlatkis and L. Ettre, Eds., Preston Technical Abstracts Co., Illinois, 1966.

66. J. Knox and J. F. Parcher, Anal. Chem., 41, 1599, 1959.

67. J. Peters and C. B. Euston, Anal. Chem., 37, 657, 1965.

68. A. Rose, D. J. Rogers and R. S. Henly, Separation Sci., 2, 229, 1967.

69. R. P. W. Scott, Anal. Chem., 35, 481, 1963.

70. M. Verzele, J. Chromatogr., 15, 482, 1964.

71. M. Verzele, Planta. Medica. Suppl.,38, 1967.

72. G. Guichon and L. Jacob, Chromatogr. Rev., 14, 77, 1971.

73. F. Helferich, J. Chem. Educ., 41, 410, 1964.

74. C. H. Bosanquet and G. D. Morgan, "Vapour Phase Chromatography", D. H. Desty, Ed., Butterworths, London, p. 35, 1957.

75. C. H. Bosanquet, "Gas Chromatography", D. H. Desty, Ed., Butterworths, London, p. 107, 1958.

76. J. R. Conder and J. H. Purnell, Trans. Farad. Soc., 64, 13, 1968.

77. J. R. Conder and J. H. Purnell, Trans. Farad. Soc., 65, 824, 1969.

78. G. J. Krige and V. Pretorious, Anal. Chem., 37, 1186, 1965.

79. S. M. Gordon, G. J. Kring and V. Pretorious, J. Gas Chromatogr., 2, 241, 1964.

80. J. M. Gordon, G. J. Kring and V. Pretorious, J. Gas Chromatogr., 2, 285, 1964.

81. J. M. Gordon, G. J. Kring and V. Pretorious, J. Gas Chromatogr., 3, 87, 1965.

82. J. R. Conder, "New Developments in Gas Chromatography", J. H. Purnell, Ed., Wiley-Interscience, New York, p. 137, 1973.

83. J. R. Conder and M. K. Shingari, J. Chromatogr. Sci., 11, 525, 1973.

84. J. M. Ryan, Chem. Eng., May, 19, 170, 1969.

85. A. B. Carel, R. E. Clement and G. Perkins, J. Chromatogr. Sci., 7, 218, 1969.

86. ELF, Petroleum Company Brochure, France, 1970.

87. P. Valentin in "Separation of Components by GLC", in Symposium Alternative to Distillation, Manchester, 1979.

88. G. R. Fitch, M. E. Probert and P. F. Tiley, J. Chem. Soc., 4875, 1962.

89. D. W. Pritchard, M. E. Probert and P. F. Tiley, Chem. Eng. Sci., 26, 2063, 1971.

90. R. P. W. Scott, "Gas Chromatography", D. H. Desty, Ed., Butterworths, London, p. 189, 1958.

91. H. Schultz, "Gas Chromatography", M. Van Swaay, Ed., Butterworths, London, p. 225, 1963.

92. A. Clayer, L. Agneray, G. Vandenbussche, and P. Petel, Z. Anal. Chem., 236, 240, 1968.

93. A. Clayer, L. Agneray, G. Vanderbussche, and M. Bruni, Z. Anal. Chem., 236, 250, 1968.

94. U. S. Patent, 2, 869, 672, 1958.

95. C. Berg, Chem. Eng. Progr., 47, 585, 1951.

96. M. V. Sussman, CHEMTECH, 6, April, 260, 1976.

97. H. Pichler and H. Schultz, Brennstoff Chem., 39, 48, 1958.

98. U. S. Patent, 2, 893, 995, 1959.

99. U. S. Patent, 3, 016, 107, 1962.

100. D. Glasser, "Gas Chromatography", A. B. Littlewood, Ed., Inst. of Petroleum, London, p. 119, 1967.

101. C. L. Guillemin, J. Chromatogr., 30, 222, 1967.

102. D. B. Broughton, Chem. Eng. Prog., 64, 60, 1968.

103. D. B. Broughton, R. W. Nenzil, J. M. Phasris and C. S. Brearly, Chem. Eng. Prog., 66(a), 70, 1970.

104. D. P. Thornton, Hydrocarbon Process, 49(11), 151, 1970.

105. L. Szepesy, S. Z. Sebestyen, I. Feher and Z. Nagy, J. Chromatogr., 108, 285, 1975.

106. V. P. Chizhkov, G. A. Yushina, L. A. Sinitzina and B. A. R. Rudenko, J. Chromatogr., 120, 35, 1970.

107. P. E. Barker and R. E. Deeble, Symposium on Less Common Means of Separation, Inst. of Chem. Eng., London, 1972.

108. K. England, Ph.D. Thesis, University of Aston in Birmingham, 1979.

109. A. Knoechelmann, Unpublished work, University of Aston in Birmingham, 1979.

110. A. J. P. Martin, Discussions, Farad Soc., 7, 332, 1949.

111. D. Dinelli, M. Taramasso and S. Polezzo, J. Chromatogr., 7, 477, 1962.

112. D. Dinelli, M. Taramasso, , S. Polezzo, U. S. Patent, 3, 187, 488, 1965.

113. J. B. Fox, J. Chromatogr., 43, 55, 1969.

114. S. Polezzo and M. Taramasso, J. Chromatogr., 11, 19, 1963.

115. M. Taramasso, J. Chromatogr., 49, 27, 1970.

116. L. D. Mosier, U. S. Patent, 3, 078, 647, 1963.

117. M. V. Sussman, K. N. Astill, R. Rombach, A. Cernllo and S. S. Chen, Ind. Eng. Chem. Fund, 11, 181, 1972.

118. M. V. Sussman, K. N. Astill and R. N. S. Rathore, J. Chromatogr. Sci., 12, 91, 1974.

119. F. R. Cropper and A. Heywood, Nature, 172, 1101, 1953.

120. A. I. M. Keulemans, "Gas Chromatography", Second Ed., Reinhold Publishers, p. 243, New York, London, 1959.

121. R. L. Pecsok, Principles and Practice of Gas Chromatography, London, Chapman and Hall, p. 226, New York, John Wiley and Sons, 1959.

122. A. T. James, in "Methods of Biochemical Analysis", Ed. D. Glick, Interscience, Vol. 8, p. 1-59, New York, 1960.

123. R. K. Beerthuis, G. Dijkstra, J. G. Keppler and J. H. Recourt, Ann. New York Acad. Sci., 72, 616, 1959.

124. C. H. Orr and J. E. Callen, J. Am. Chem. Soc., 80, 249, 1958.

125. C. H. Orr and J. E. Callen, Ann. New York Acad. Sci., 72, 649, 1959.

126. S. R. Lipsky and R. A. Landowne, Biochem. Biophy. Acta., 27, 666, 1958.

127. S. R. Lipsky and R. A. Landowne, Ann. New York Acad. Sci., 72, 666, 1959.

128. B. M. Craig and N. L. Murty, Can. J. Chem., 36, 1297, 1958.

129. R. R. Condon, Anal. Chem. 31, 1717, 1959.

130. S. R. Lipsky, J. E. Lovelock and R. A. Landowne, J. Am. Chem. Soc., 81, 1010, 1959.

131. S. R. Lipsky, R. A. Landowne and J. Lovelock, Anal. Chem., 31, 852, 1959.

132. S. R. Lipsky, R. A. Landowne and M. R. Godet, Biochem. Biophy. Acta., 31, 336, 1959.

133. J. K. Haken, J. Chromatogr. Sci., 13, 430, 1975.

134. G. C. Cochrane, J. Chromatogr. Sci., 13, 440, 1975.

135. D. M. Otternstein and D. A. Bartley, Anal. Chem., 43, 952, 1971.

136. D. M. Otternstein, "Advances in Chromatography", Giddings and Keller, Eds., Marcel Dekker, Vol. 3, p. 137, New York, 1966.

137. R. G. Ackmann, J. Chromatogr. Sci., 10, 560, 1972.

138. G. C. Analysis of Fatty Acids, Special report prepared by L. S. Ettre, W. Averill and F. J. Kabot, Perkin Elmer, No. GC.AP-001.

139. A. T. James and A. J. P. Martin, Analyst 77, 915, 1952.

140. A. T. James and A. J. P. Martin, J. Chromatogr., 2, 552, 1959.

141. F. R. Cropper and A. Heywood, Nature, 171, 1101, 1953.

142. F. R. Cropper and A. Heywood, Nature, 172, 1063, 1954.

143. A. T. James and A. J. P. Martin, Biochem. J., 63, 144, 1956.

144. W. Stoffel and E. H. Ahrens, J. Am. Chem. Soc., 80, 6604, 1958.

145. J. W. Farquhar, Nutrition Rev., 17, Supplement, 1959.

146. B. M. Craig and N. L. Murty, Can. J. Chem., 36, 1297, 1958.

147. C. Litchfield, R. Reiser, A. F. Isbell and G. L. Feldman, J. AM. Oil Chem. Soc., 41, 52, 1964.

148. C. R. Scholfield and H. J. Dutton, J. Am. Oil Chem. Soc., 47, 1, 1970.

149. W. R. Supina, U. S. Patent, 3, 263, 401.

150. D. M. Ottenstein, D. A. Bartley and W. R. Supina, J. Chromatogr., 119, 401, 1976.

151. K. E. Murray, Prog. Chem. Fats Lipids, 3, 243, 1955.

152. K. S. Markley, "Fatty Acids", Second Edn. Part 3, p. 1983, Interscience, New York, 1964.

153. V. J. Muckerheide, Fats and Oils Series, K. S. Markley, Ed., Part 4, p. 2679, Interscience, New York, 1967.

154. F. D. Gunstone, "An Introduction to the Chemistry and Biochemistry Fatty Acids and their Glycerides", Second Edn, Chapman and Hall Limited, 1967.

155. E. S. Pattison (Ed.), "Fatty Acids and their Industrial Applications", Marcel Dekker, Inc., New York, 1968.

156. J. B. Brown, D. K. Kolb, Prog. Chem. Fats Lipids, 3, 57, 1955.

157. F. D. Collins, "New Biochemical Separations", A. T. James and J. L. Morris, Eds., p. 379, Van Nostrand, New York, 1964.

158. J. M. M. Moerno and A. V. Roncero, "Analysis and Characterisation of Oils, Fats and Fat Product", H. A. Boekenoogen, Ed., Vol. 1, Interscience, New York, 1964.

159. A. Rose, D. J. Royer and R. S. Henley, Separation Sci., 2, 211, 1967.

160. A. Rose, D. J. Royer and R. S. Henley, Separation Sci., 2, 257, 1967.

161. C. R. Scholfield, Presented in Am. Chem. Soc. Meeting, Atlantic City, New Jersey, Sept., 1974.

162. C. L. Gillemin, J. Chromatogr., 4, 104, 1966.

163. J. Albrecht and M. Verzele, J. Chromatogr. Sci., 8, 586, 1970.

164. B. Jones, Mechanical Engineering Department, University of Birmingham, Private communication.

165. J. C. D. Brand and A. I. Scott, in "Elucidation of Structures by Physical and Chemical Methods", Part I, K. W. Bently, Ed., p. 61, Interscience, New York, 1963.

166. P. E. Barker, and D. I. Lloyd, J. Inst. Petrol., 49, 73, 1963.

167. K. Denbigh, "The Principle of Chemical Equilibrium", p. 276, Cambridge University Press, 1964.

168. J. C. Sternberg, "Advances in Chromatography", J. C. Giddings and R. A. Keller, Eds., Vol. 2, p. 205, Edward Arnold, New York, 1966.

169. A. B. Sunal, Ph.D. Thesis, University of Aston in Birmingham, 1973.

170. G. H. Bloore Co. Ltd., Birmingham, Private communications.

171. C. T. Sciance and O. K. Crosser, A.I.Ch.E. Journal, 12(1), 100, 1966.

172. P. Rony, Separation Science, 3, 239, 1968.

173. P. Rony, Separation Science, 3, 357, 1968.

174. P. Rony, Separation Science, 5, 121, 1970.

175. L. Alder, "Liquid-Liquid Extraction", Elsevier, Amsterdam, Second Edn., 1959.

176. P. Tiley, J. Appl.Chem., 17(5), 131, 1967.

177. G. J. Arkenbout and W. M. Smith, Separation Science, 2, 575, 1967.

178. R. E. Rubac, R. McDaniel and C. D. Holland, A.I.Ch.E. Journal, 15, 568, 1969.

179. K. I. Sakodynskii, L. V. Streltzov, V. Yu Zelvenski, S. A. Volkov and I. N. Rozheko, Anal. Chem., 45, 1557, 1973.

180. I. N. Rozhenko, V. Yu. Zelvenskii, S. A. Volkov and K. I. Sakodynskii, Theor. Osn. Khim. Tekhnol., 9, 3, 1975.

181. I. N. Rozhenko, A. G. Zyskin, V. Yu. Zelvenskii, and K. I. Sakodynskii, Chromatographia, 10(1), 25, 1977.

182. J. J. Van Deemter, F. J. Zuiderwerg and A. Klinkenberg, Chem. Eng. Sci., 5, 271, 1955.

183. S. Ergun, Chem. Eng. Prog., 48(2), 89, 1952.

184. "Chemical Engineers Handbook", J. H. Perry, Ed., McGraw-Hill, New York, 1963.

185. J. Fletcher, Private communication, Aston University in Birmingham.

186. J. H. Knox and L. McLaren, Anal. Chem., 36, 1477, 1964.

187. L. K. Barry and L. R. Synder, "An Introduction to Separation Science", John Wiley, New York, 1970.

188 J. O. Hirschfelder, R. B. Bird, and S. Spotz, Trans. Am. Soc., Mech. Engnrs., 71, 921, 1949.

189. C. R. Wilke, and P. Chang, Am. Inst. Chem. Engnrs., 1, 264, 1955.

190. S. Glasstone, K. J. Laidler and H. Eyring,"The Theory of Rate Processes", McGraw-Hill, New York, 1941.

SUPPORTING PUBLICATION

Separation of Organic Mixtures by Sequential Gas-Liquid Chromatography

P. E. BARKER, S. E. LIODAKIS and M. I. HOWARI

Chemical Engineering Department, University of Aston in Birmingham, England

A new sequential continuous chromatographic refiner (SCCR-2) for high temperature production scale G.L.C. (gas-liquid chromatographic) separations is described. In this equipment the counter-current movement between the gas and liquid phase is simulated by sequencing a system of inlet and outlet port functions around twelve static 2.54 cm internal diameter and 61 cm long stainless steel columns. The versatility of the equipment has been demonstrated by the separation of equivolume mixtures of the halocarbons arklone P/genklene P, methylchloroacetate/ethyl lactate and ethyl caprate/ethyl laurate at temperatures of 60°, 105° and 160°C respectively. Throughputs between 21-75 cm^3h^{-1} have been explored with product purities in excess of 99.8% achieved under certain process conditions.

On décrit un nouveau dispositif de chromatographie préparative continue (SCCR-2 Refiner) utilisant la chromatographie gaz-liquide séquentielle, à des températures élevées et à l'échelle d'une production. Dans cete équipement, on simule le mouvement à contre-courant, qui se produit entre les phases gazeuse et liquide, en mettant en séquence un système d'orifices d'entrée et de sortie autour de 12 colonnes statiques en acier inoxydable de diamètre intérieur de 2.54 centimètres et de longueur de 61 centimètres. On a démontré la souplesse d'emploi de cet équipement en séparant des mélanges de volumes égaux des produits suivants: (1) hydrocarbures halogénés (halocarbons) Arklone P et Genklene P; (2) chloroacétate de méthyle et lactate d'éthyle; (3) caprate d'éthyle et laurate d'éthyle. La séparation s'est faite respectivement à des températures de 60°C, 105°C et 160°C. On a examiné des productions variant entre 21 et 75 $c.c.h^{-1}$ et l'on a obtenu une pureté de produit excédant 99.8% dans certaines conditions de séparation.

G.L.C. is known for its superior separating capabilities and near universal applicability, although scale-up problems have still to be overcome before becoming a well-established large-scale separation technique. Various attempts have been made over the past thirty years to increase the throughput capabilities of a G.L.C. system using either batch or continuous operation[1-4]. Amongst them the "repetitive injection" batch operated systems and the continuous counter-current systems have found the most success.

Since the latter seems to give a greater column packing utilization[5], considerable effort has been directed towards the development of G.L.C. systems based on the counter-current mode. With this technique, the gas and liquid phase flows are moved counter-currently, while the binary mixture to be separated is fed continuously into the middle of the column. The relative flowrates of the two phases are adjusted so that the less soluble component of the feed mixture travels in the direction of the gas flow and the other is carried with the liquid phase. The more soluble component is then stripped off the liquid phase in a different section of the column assisted by heat and/or a high gas flowrate.

The technological development of chromatographic systems operating under counter-current flow conditions has undergone three main stages:

i) moving-packing systems
ii) moving-column systems
iii) moving port systems

The moving-packing systems usually involve a vertical column in which the mobile phase flows upwards, the packing moves downwards under its own gravity and the feed mixture is introduced continuously somewhere near the middle of the column. Barker and co-workers[1,7-9] have extensively studied the above method on G.L.C. systems, and high separated product purities were reported for volatile organic mixture separations at feed throughputs of about 30 cm^3h^{-1} when using a column diameter of 2.5 cm. Other publications on similarly operated G.L.C. equipments are those given by Scott[10], Fitch et al[11] and Schultz[12]. Also industrially the technique has been applied to gas/solid chromatographic systems[13,14]. In general, moving-packing systems suffer from the disadvantage of solid handling problems, the resulting attrition necessitating re-sieving and replenishement of expensive packing. The chromatographic efficiency of the columns is also less due to the low uneven packed densities.

To avoid the packing attrition experienced in the moving packing chromatographs, the moving-column systems have been developed. In the latest scheme, the packing is packed into a tubular bundle of 44 stainless steel tubes which is rotated in the opposite direction to the mobile phase flow past fixed inlet and outlet ports. This type of chromatograph for laboratory scale separations has been extensively studied over a period of about 10 years by Barker and co-workers[1-2,15-18], a wide range of successful separations being reported in the literature for both gas-liquid and liquid-liquid chromatographic systems. However, equipments operating on this basis are in general mechanically complex, requiring seals between moving parts, which impose limitations on their scale-up to industrial sizes.

The above disadvantages have led to the development of the moving port system for production scale chromatographic purposes. With this equipment the chromatographic beds are held stationary and the counter-current flow conditions are simulated by simply changing the inlet and outlet port locations around the chromatographic beds. The sequencing of port operations takes place in the same general direction as mobile phase flow. The sequential type of chromatographs proposed by Barker and Deeble[2,6,19-21] are based on the above principle.

Other continuous chromatographic systems include amongst others the one developed by Szepesy et al[22] for liquid-liquid chromatographic separations, while industrially the "Parex", "Olex" and "Molex" processes[23,24], which are pseudo-moving packing processes developed by the Universal Oil Products Com-

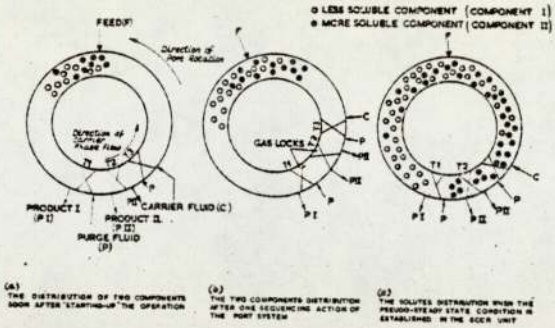

Figure 1 – Diagrammatic representation of the principle of of the SCCR operation.

pany, find current application for the recovery of p-xylene, olefin and n-paraffin separations.

Development of the new high temperature sequential chromatographic equipment

The principle of operation of the sequential continuous chromatographic refiner (SCCR) is illustrated in Figure 1, using a binary feed mixture for separation.

Figure 1a. schematically shows the distribution of two components within the system soon after "starting-up" the equipment. Feed enters the system at port F, while the carrier fluid is introduced at port C which then flows through the chromatographic packed column. Component I, the component with less affinity for the stationary phase on the packing, travels with the carrier fluid moving towards the product I offtake, port, *PI*. In contrast, component II which has greater affinity for the stationary phase is retained preferentially on the stationary phase. Two sections of the closed loop are isolated by gas locks T1, T2 and T3 (double purge operation) in which independent fluid streams (purge streams) enter at ports P and exit from ports *PII*. The double purge operation was thought essential for the operation of the SCCR-2 equipment, presently described. This was because the latter unit was mainly intended for the separation of fatty acids and essential oils, which have normally high absorption properties, their removal from the liquid phase being relatively difficult.

Figure 1b. shows the two component distribution soon after all the port functions have been advanced one position around the static chromatographic column. The movement of the ports has the same general direction as the carrier fluid, therefore simulating the counter-current movement between chromatographic packing and carrier phase flow.

Figure 1c. represents the fully established operating condition of the system. The less soluble component is now issuing from port PI, as pure product I. Meanwhile, the more soluble component is contained in the isolated sections which are purged at such a rate as to ensure the complete removal of pure product II.

The above described chromatographic system is normally used to produce two products, but obviously for a multi-component feed mixture, the products may be collected and re-run, if more than two fractions are required. Side streams can be taken between the feed and normal product ports, but such side streams are less pure than those taken from the normal product ports. In general, the sequential chromatographic system seems a very promising approach towards production scale continuous chromatography, since it does not involve moving beds or any moving seal, and are expected to be more mechanically reliable; also they are adaptable to any column dimensions to facilitate their scale-up.

The first SCCR unit (SCCR-1), designed and constructed by Barker and Deeble[20,21], consisted of 12 discrete sections linked together to form a closed symmetrical ring. Each section was a 61 cm long and 7.6 cm in diameter chromatographic column, provided with the necessary port functions (feed inlet, carrier gas inlet and outlet, purge gas inlet and outlet and gas lock) by six solenoid valves. The SCCR-1 unit has been successfully used by Barker, Deeble and Bell [6,25,36] to separate binary halocarbon mixtures at feed rates of up to 1500 cm^3h^{-1}, with typical purities in excess of 99.7% for both products.

The construction of the SCCR-1 unit was limited by economic considerations such as:

1) Its materials of construction (brass) which can corrode and act as decomposition sites for many organic chemicals.

2) The use of air as carrier gas, so many organic substances are either oxidized or degraded in this atmosphere. In addition the use of highly flammable chemicals were not possible for safety reasons.

3) The lack of heating facilities, hence the SCCR-1 could only be used to separate substances which were easily volatilized at ambient temperature.

These limitations have led to the development of a new sequential continuous chromatographic refiner (SCCR-2) described in this paper, to work at temperatures of up to 200°C, using nitrogen as the carrier gas and being constructed of 316 stainless steel and P.T.F.E. (see Figure 2). In general, the SCCR-2 unit was constructed for high temperature separations of low-volatile organic compounds and is mainly intended for industrially based problems such as the separation of fatty acids and essential oils.

Description of the SCCR-2 equipment

The SCCR-2 unit consisted of 12 chromatographic columns connected alternatively at top and bottom to form a closed symmeterical ring. Each of the 12 columns made from stainless steel, was 61 cm long, 2.54 cm in internal diameter and was packed with 16.67% F.F.A.P. (free fatty acid phase) on 500-353μm chromosorb W, AW-DMCS, chromatographic packing material, when separating arklone *P*/genklene *P* mixtures and methyl chloroacetate/ethyl lactate mixtures. For the separation of ethyl caprate/ethyl laurate mixtures 15% of OV-275 (a cyno silicone) coated on chromosorb-P-AW-DMCS as a solid support was used instead of *F.F.A.P.* This is because of the higher heat thermal stability and selectivity of the OV-275 for the separation of fatty acids at higher temperatures. The diameter of the columns was chosen as 2.54 cm, only one third the diameter of the SCCR-1 unit, because of the high cost of building an all stainless steel/P.T.F.E. unit and the necessity of keeping carrier gas costs down when using nitrogen.

Six pneumatically operated, normally closed, diaphragm valves were arranged around each column to give the required operating functions: feed inlet (*F*), carrier gas inlet (*C*), product I outlet (*PI*), purge gas inlet (*P*), product II outlet (*PII*) and gas lock (*T*) as shown in Figure 1. These valves were specially designed[27] to fulfil the following operating requirements:

1) Be capable of operation at temperatures of up to 200°C. This high temperature is necessary for the

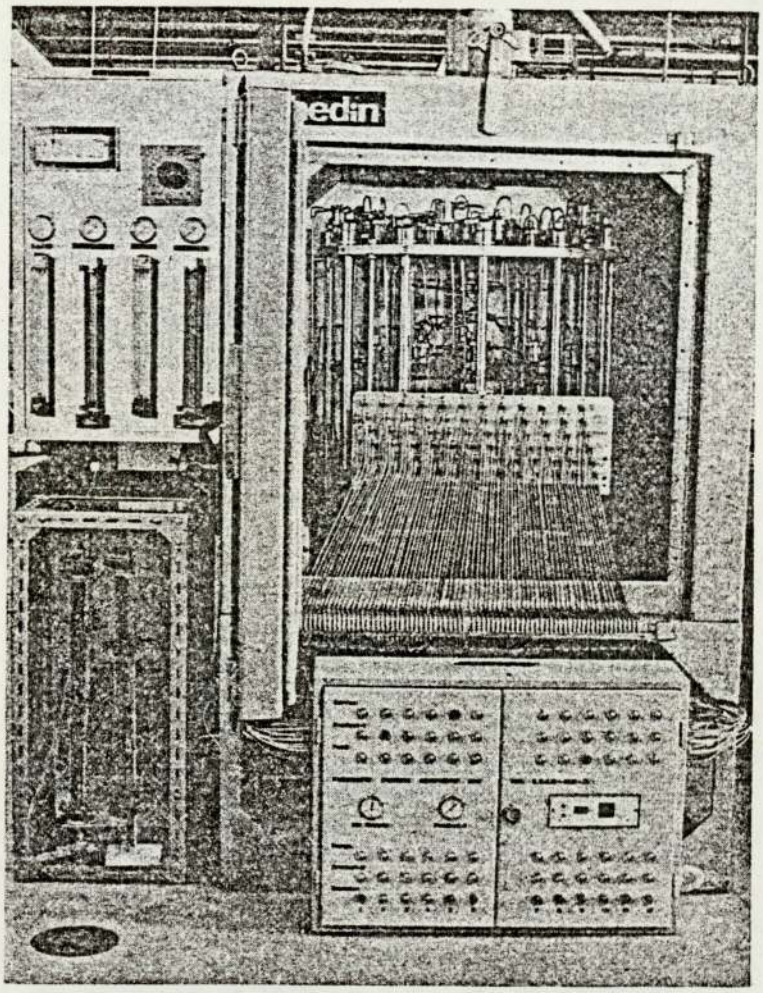

Figure 2 — Sequential continuous chromatographic refiner equipment. (SCCR-2).

chromatographic separation of some fatty acids and essential oils.

2) All materials of construction in contact with the working fluids to be resistant to most organic chemicals, to increase the range of possible separations by the sequential unit.

3) Capable of withstanding a differential forward or back pressure in excess of 446 kPa.

Figure 3 shows diagrammatically the relative position of diaphragm valves on four consecutive columns, with the numbers 1 to 12 assigned to the individual columns. The 12 gas locks (transfer valves), being situated in the transfer line between each pair of columns, were used to form the purge section in the unit, by isolating two consecutive columns (double column purge operation). Isolation of an individual column was achieved by closing two consecutive transfer valves. The other 12 valves of each type (*F,C,PI,P,PII*), were connected via stainless steel tubing to an independent, centrally situated, distributor system. Lines from the gas distributors then passed to the relevant control and measuring devices, while the feed distributor was connected to a positive displacement pump.

The system of the 12 chromatographic columns with their respective valves, pipe and distribution networks was housed in an oven, supplied by Hedinair Ltd., capable of operating at temperatures of up to 200°C.

The port rotation required for this sequential type of equipment, was achieved by a pneumatic control unit, supplied by Festo Pneumatic Ltd., which sequenced the position of the energized valves around the unit in the required pattern, at the desired time interval.

During the SCCR-2 operation and within a particular sequencing interval, the carrier gas enters the system via the energized to open valve *C* on column 1, travels through 10 columns and exits with the less soluble component from column 10, where the valve PI is energized to open (see Figure 3). The 11 and 12 columns meanwhile are isolated by having closed ~~(de-energized)~~ the valves *T* on the transfer lines 10/11, 11/12 and 12/1. Also the valves *P* and *PII* on columns 11 and 12 are energized to open, effecting purging of the more soluble component. Finally the feed mixture is introduced into column 5 through the energized to open *F* valve. In the next sequencing action of the valves, column 12 and 1 are isolated. Purge gas enters column 12 and 1 to remove product II. Carrier flows from column 2 round the unit to exit from column 11 with the product I. Feed is now entering column 6. Twelve sequencings complete the cycle, which continues automatically.

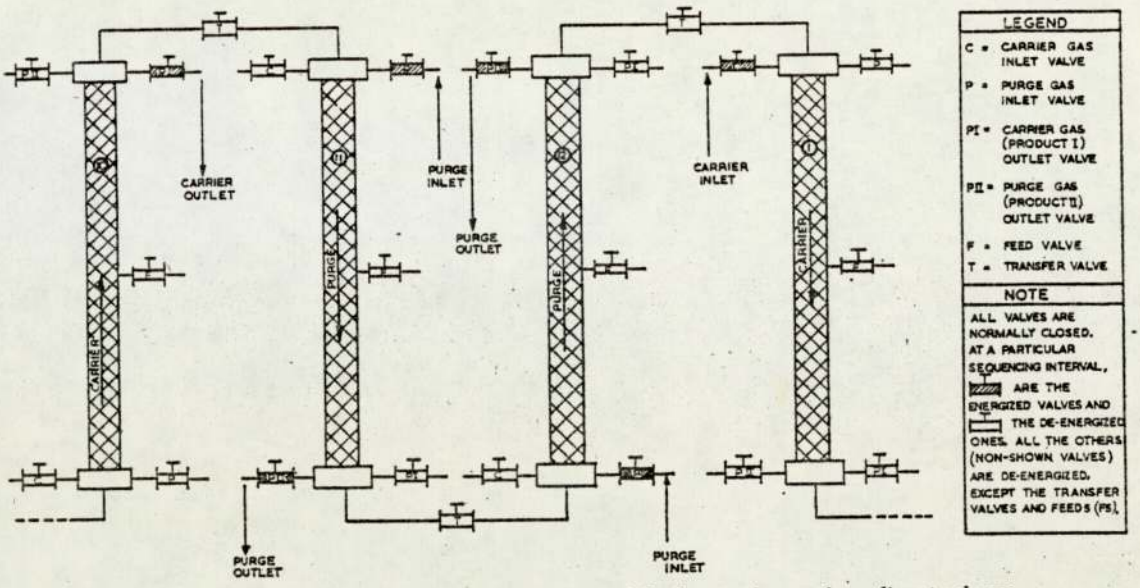

Figure 3 – Schematic diagram showing the position of diaphragm valves on four adjacent columns.

As is shown in Figure 4 (the overall flow diagram of the SCCR-2 equipment) the nitrogen, supplied in cylinders, is initially regulated to a pressure of 515 kPa (60 psig) and then passes through a silica gel bed, 5.5 cm I.D. and 51 cm long for drying, before being split into the respective carrier and purge streams. Both the carrier and purge streams are controlled by pressure regulators. The individual gas flowrates were monitored by two rotameters. After leaving the rotameters, the nitrogen streams enter the SCCR-2 oven and pass through the respective preheating and distribution systems, entering the chromatographic columns through diaphram valves.

Product streams leaving the unit (see Figure 4) are collected by the appropriate distribution systems and then pass out of the oven, the solute being substantially condensed in a series of cold traps. Final clean-up of the outlet nitrogen streams is achieved by passing each stream through a charcoal adsorption bed, 2.5 cm in I.D. and 57 cm long. The flowrates of both product streams are then regulated and finally measured by rotameters before being vented to the atmosphere.

Experimental

The selection of operating conditions for the separation of a binary feed mixture with the SCCR-2 machine, was based on the theory outlined by Barker and Lloyd[1] for counter-current chromatographic systems. Thus, the following approximate relations were used[27] as a guide to the selection of experimental settings for the operation of the SCCR-2 unit:

$$K_i^{\infty} < G_{mc}/L' < K_i^{\infty}\eta \quad \text{(1)}$$

$$S_{mc}/L' > K_i^{\infty}\eta \quad \text{(2)}$$

where,

G_{mc}, S_{mc} = the mean carrier and purge gas volumetric flowrate, respectively

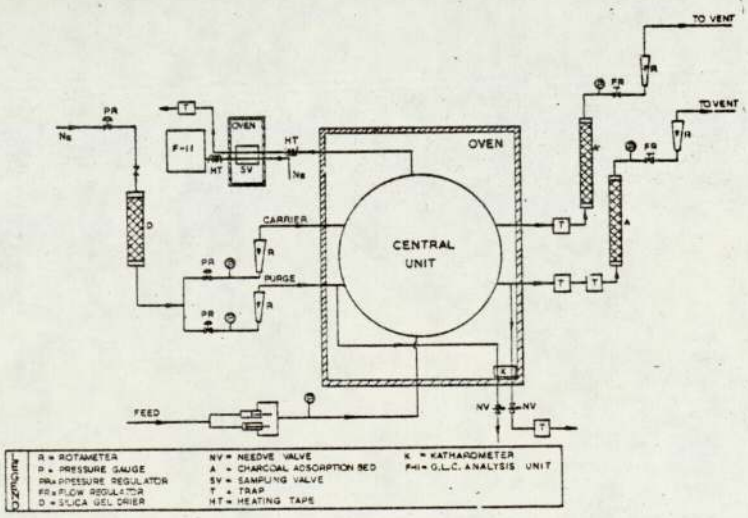

Figure 4 – Flow diagram of the SCCR-2 unit.

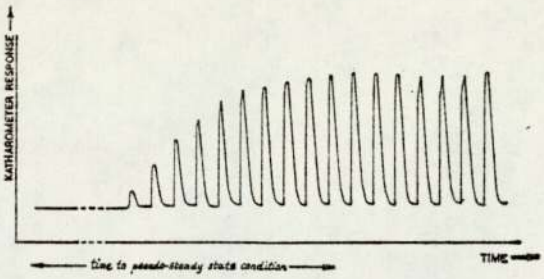

Figure 5 – An example of a Product II katharometer response with time.

L' = total volume of liquid phase in columns/cycle time.
= the apparent stationary phase volumetric flowrate in the sequential unit.
$K_l^{\infty}, K_l^{\infty}$ = the partition coefficients of solutes at infinite dilution, determined experimentally by an analytical scale G.L.C.[27].

The above inequalities were found adequate to give the preliminary experimental settings required for the operation of the SCCR-2 unit. However, the more precise relationships are given in reference[6].

In the SCCR-2 unit during an experimental run a reproducible state condition was eventually reached. This was not a true steady state condition due to the sequential nature of operation, the separation being in fact semi-continuous. However, the reproducible state condition was generally established in the system, usually after two sequencing cycles whereby, although the solute concentration profiles within the columns and outlets changed with time during a sequencing interval, the concentration profiles were reproduced from one cycle to the next. The approach to this pseudo-steady state condition was determined during a run by monitoring one product stream of the SCCR-2 unit with a Katharometer (see Figure 4). Consequently, the product concentration level could be continuously observed by the Katharometer traces, which became reasonably consistent once the pseudo-steady condition was established in the unit, as shown in the example given in Figure 5.

Once the pseudo-steady condition was achieved, the symmetry of the sequential unit permitted determination of the column to column concentration profile and the main record of performance of the SCCR-2 unit under varying operating conditions was this solute concentration profile around the 12-columns. A column to column concentration profile was obtained experimentally by analysing gas samples taken from a fixed sample point in the 12-column arrangement

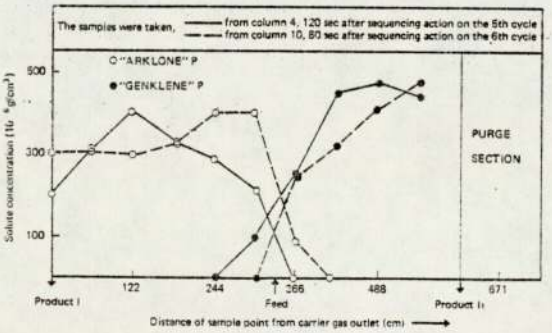

Figure 6b – Concentration profile for run 60-21-43-130.

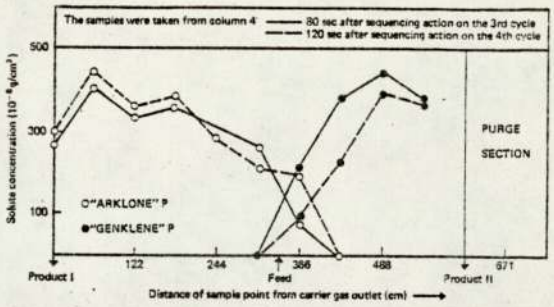

Figure 6a – Concentration profile for run 60-21-29-130.

during a complete sequencing cycle, at a constant time after each sequencing action of the valves. The basis of the column to column concentration profile analysis is that the sample point although in a fixed position in one column, essentially changes its position relative to the input and output functions as the unit sequences around the closed cycle. Therefore, the resultant profile is equivalent to sampling all twelve columns simultaneously at a constant time after the sequencing of valves.

Gas samples were automatically withdrawn from the sample point by using a sampling valve, connected to a timer and housed in an oven (see Figure 4). On actuation of this sampling valve, samples were taken from the sequential unit into a Perkin-Elmer F-11 chromatograph for quantitative analysis. This method proved unsuitable when separating ethyl caprate/ethyl laurate mixtures at 160°C because of condensation problems through the sampling lines from the column to the sampling valve. An alternative method was used by having a short sampling line and absorbing the gas streams in two glass tubes in series containing ethyl acetate maintained at 4°C.

From the recorded analysis data, the column to column concentration profiles were plotted as shown in Figures 6-9. To plot the concentration profile the distance of the sample point from the carrier gas outlet after each sequencing action was required. This was determined by ignoring the unpacked column to column transfer line length and considering each packed column length equal to 61 cm. An experimental study for testing the reproducibility of the concentration profiles obtained from different sequencing cycles or from differing sample points was made and the derived results are presented.

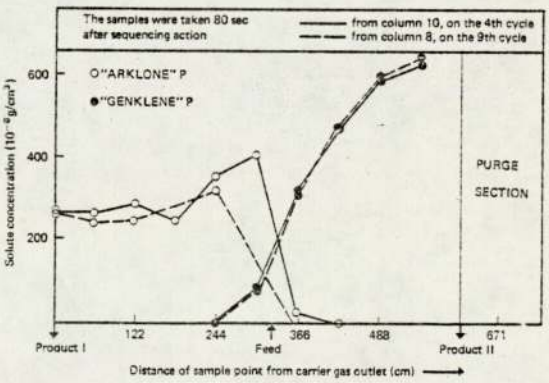

Figure 6c – Concentration profile for run 60-21-58-130.

TABLE 1

THE SEPARATION OF ARKLONE P/GENKLENE P. SUMMARY OF OPERATING CONDITIONS

Run Title	Temperature			Ambient conditions		Solute mixture feedrate	I_s	L'	Separating Section					Purge Section				
	Operation	Carrier inlet	Purge inlet	θ_a	P_a				G_a	P_{in}	P_{out}	J_3^2	G_{mc}/L'	S_a	P_{in}	P_{out}	J_3^2	S_{mc}/L'
θ-f-G_{mc}/L'-I_s	°C	°C	°C	°C	*kPa*	cm^3h^{-1}	*s*	cm^3s^{-1}	cm^3s^{-1}	kPa	kPa			cm^3s^{-1}	kPa	kPa		
60-21-29-130	60	61	80	20	101	21	130	0.087	4.2	198	184	0.96	28.9	188	184	158	0.93	1460
60-21-43-130	60	62	80	21	102	21	130	0.087	6.2	198	181	0.95	43.1	212	184	153	0.91	1674
60-21-58-130	60	62	80	19	101	21	130	0.087	8.3	198	177	0.94	58.4	212	184	153	0.91	1670
60-21-44-60	60	62	80	21	101	21	60	0.189	13.3	198	167	0.91	43.8	188	184	158	0.92	662
60-21-43-80	60	63	80	20	100	21	80	0.142	10.0	198	172	0.93	43.3	190	184	159	0.93	889

Summary of Results

Run Title	K^∞		Separating section		Purge section	Total time of run	Total no. of cycles	Time to pseudo steady state	Concentration profile analysis			
	A.P.	G.P.	G_{min}/L'	G_{max}/L'	S_{min}/L'				Time to analysis	Figure	Product Purities	
θ-f-G_{mc}/L'-I_s						h		min	min		%A.P.	%G.P.
60-21-29-130	30	174	28.0	30.1	1348	3.03	7	52.0	58.0	6a	>99.9	>99.6
60-21-43-130	30	174	41.6	45.5	1530	2.60	6	52.0	104.0	6b, 7c	>99.9	>99.8
60-21-58-130	30	174	55.1	52.1	1525	7.37	17	52.0	104.0	6c	>99.9	>99.9
60-21-44-60	30	174	40.6	48.2	618	1.60	8	24	48	7a	>99.6	>99
60-21-43-80	30	174	40.4	46.5	826	3.20	12	32	64	7b	>99.8	>99.2

TABLE 2

THE SEPARATION OF METHYL CHLOROACETATE/ETHYL LACTATE

Run Title	Temperature			Ambient condtions		Solute mixture feedrate	I_s	L'	Separating Section					Purge Section				
	Operation	Carrier inlet	Purge inlet	θ_a	P_a				G_a	P_{in}	P_{out}	J_3^2	G_{mc}/L'	S_a	P_{in}	P_{out}	J_3^2	S_{mc}/L'
θ-f-G_{mc}/L'-I_s	°C	°C	°C	°C	kPa	cm^2h^{-1}	s	cm^3s^{-1}	cm^3s^{-1}	kPa	kPa			c^3ms^{-1}	kPa	kPa		
105-21-378-300	105	108	135	26	100	21	300	0.041	21.3	198	146	0.84	378	232	184	136	0.84	4418
105-21-413-300	105	108	135	25	102	21	300	0.041	23.0	205	144	0.82	413	248	198	143	0.83	4597
105-21-444-300	105	108	135	28	102	21	300	0.041	25.0	205	146	0.83	444	245	191	139	0.84	4625

Summary of Results

Run Title	K^∞		Separating section		Purge section	Total time of run	Total no. of cycles	Time to pseudo steady state	Concentration profile analysis			
	M.C.	E.L.	G_{min}/L'	G_{max}/L'	S_{min}/L'				Time to analysis	Figure	Product Purities	
θ-f-G_{mc}/L-I_s						h		h	h		% M.C.	% E.L.
105-21-378-300	302	457	332	450	3387	5.00	5	2.00	3.00	8a	>99.8	>99.2
105-21-413-300	302	457	354	504	3952	3.00	3	2.00	2.00	8b	>99.8	>99.5
105-21-444-300	302	457	381	535	4007	5.00	5	2.00	3.00	8c	>99.3	>99.7

TABLE 3

THE SEPARATION OF ETHYL CAPRATE/ETHYL LAURATE

Run Title	Temperature			Ambient conditions		Solute mixture feedrate	I_s	L'	Separating Section					Purge Section				
	Operation	Carrier inlet	Purge inlet	θ_a	P_a				G_a	P_{in}	P_{out}	J_s^2	G_{mc}/L'	S_a	P_{in}	P_{out}	J	S_{mc}/L'
θ-f-G_{mc}/L'-I_s	°C	°C	°C	°C	*kPa*	cm^3h^{-1}	*s*	cm^3s^{-1}	cm^3s^{-1}	*kPa*	*kPa*	—	—	cm^3s^{-1}	*kPa*	*kPa*	—	—
160-25-114-300	160	166	170	21	101.3	25	300	0.051	10.8	308	239	0.87	114	137	198	129	0.78	2425
160-50-114-300	160	167	174	21	101.3	50	300	0.051	10.8	308	239	0.87	114	134	198	129	0.78	2361
160-75-113-300	160	168	171	24	101.3	75	300	0.051	10.8	308	239	0.87	113	131	205	130	0.77	2235
160-75-101-200	160	190	195	22	101.3	75	200	0.08	14.8	308	256	0.91	101	121	184	125	0.80	1496
160-75-113-150	160	185	192	22	101.3	75	150	0.10	21.5	308	242	0.88	113	154	198	129	0.78	1351

Summary of Results

Run Title	K^∞		Separating section		Purge section	Total time of run	Total no. of cycles	Time to pseudo steady state	Concentration Profile Analysis			
	Ethyl caprate	Ethyl laurate	G_{min}/L'	G_{max}/L'	S_{min}/L'				Time to analysis	Figure	Product Purities	
θ-f-G_{mc}/L'-I_s						h		h	h		% E.C.	% E.L.
160-25-114-300	74	107	103	131	2079	12	10	3	7	9a	99.4	99.3
160-50-114-300	74	107	103	131	2042	11	9	3.5	5	9b	99.4	98.4
160-75-113-300	74	107	103	130	1910	11	9	4	6	9c	94.2	91.2
160-75-101-200	74	107	100	112	1376	10	9	3	5		95.1	94.8
160-75-113-150	74	107	108	129	1211	10	9	3	4		93.7	92.8

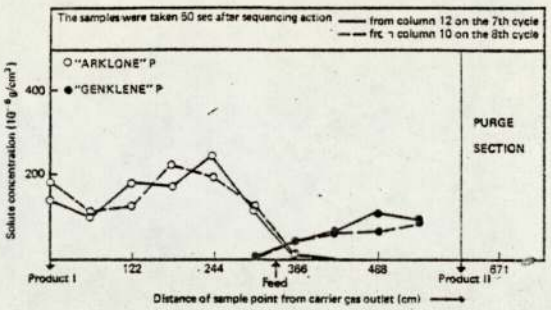

Figure 7a — Concentration profile for run 60-21-44-60

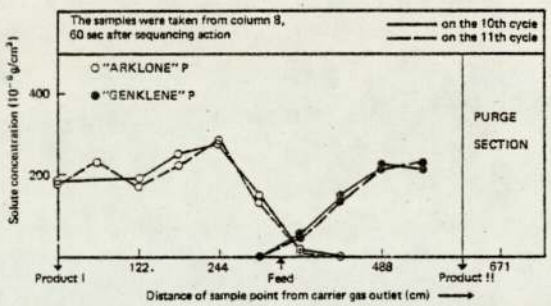

Figure 7b — Concentration profile for run 60-21-43-80

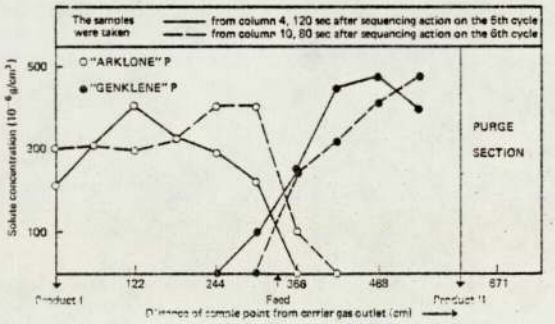

Figure 7c — Concentration profile for run 60-21-43-130

From the recorded column to column concentration profiles during a run a products purity level could be determined. In addition when volatile feed mixtures were involved for separation, gas samples were withdrawn from the product outlet lines by a gas tight syringe to determine their purity. However, for less volatile components liquid samples were collected from the condensing traps into marked sample bottles which were analysed at the end of the run[27].

Results and Discussion

Several separations were performed on the SCCR-2 unit. The objectives of these experimental studies were to determine the separating capabilities of the unit and its separating limits. For this reason the separation of chemical mixtures which had different separation difficulty and volatility was studied on

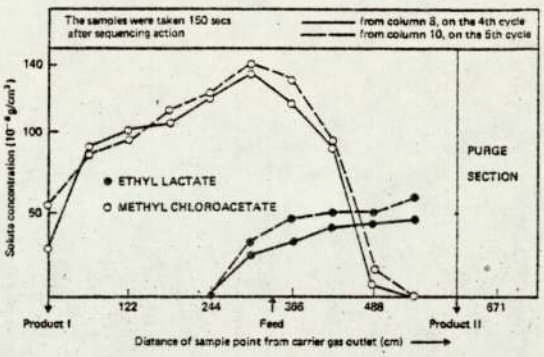

Figure 8a — Concentration profile for run 105-21-379-300

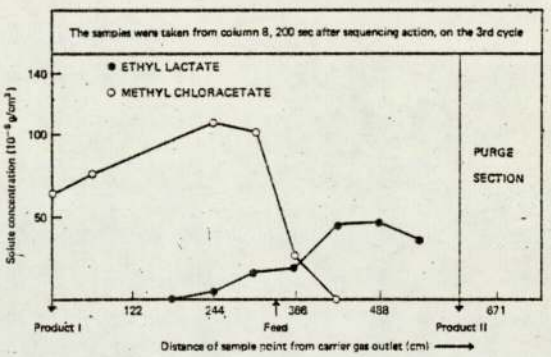

Figure 8b — Concentration profile for run 105-21-413-300

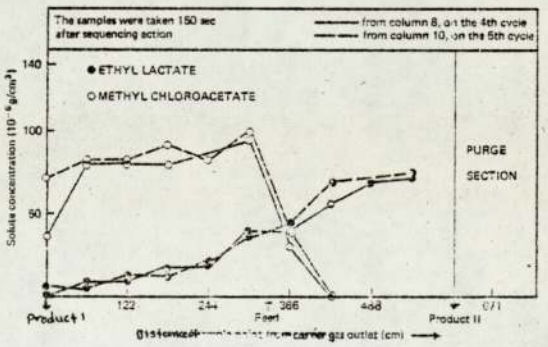

Figure 8c — Concentration profile for run 105-21-444-300

the SCCR-2 equipment. The systems selected had separation factors in the range of 1.44-5.8 and required equipment operation in the range 60°-160°C. In addition the effect of the operating variables such as feed throughput, temperature, ratio of the mean gas flowrate to the liquid rate, and sequencing rate, on the SCCR-2 performance was studied. Finally, the efficiency of the sequential unit in terms of the number of theoretical plates was experimentally determined[27].

In this paper details of five experimental runs for the separation of the equivolume halocarbon mixture of arklone P/genklene P are presented in Table 1.

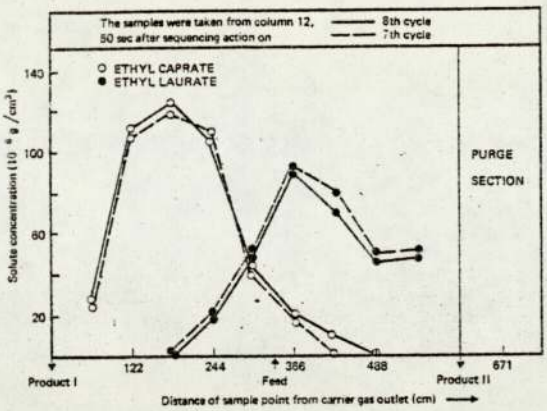

Figure 9a – Concentration profile for run 160-25-114-300

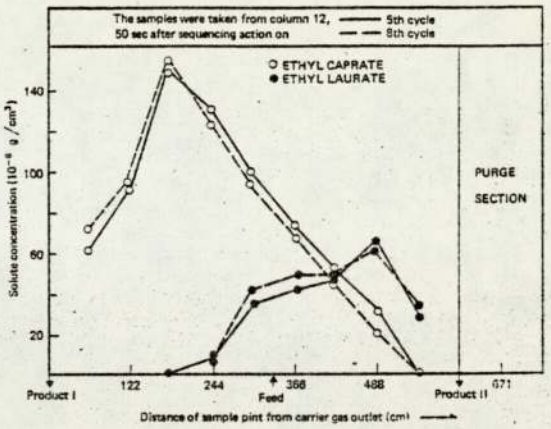

Figure 9b – Concentration profile for run 160-50-114-300

The results of the separation of 50/50 v/v mixtures of methyl chloroacetate/ethyl lactate are given in Table 2, and those for the separation of ethyl caprate/ethyl laurate in Table 3. Each experimental run is denoted by a combination of the four main operating variables; the operating temperatures (°C), the feed rate (cm^3h^{-1}), the ratio of the mean column gas flowrate to the apparent liquid rate, and the sequencing rate (s).

In Table 1 the runs 60-21-29-130, 60-21-43-130 and 60-21-58-130 show the effect of increasing the apparent gas to liquid rate ratio, G_{me}/L', while maintaining constant the operating temperature, feedrate and sequencing rate. This was achieved by increasing the carrier gas outlet flowrate, G_a, from 4.2 cm^3s^{-1} to 8.3 cm^3s^{-1}. The performance of the sequential unit under these experimental conditions has shown very little sensitivity to changes in G_{me}/L' as shown in the concentration profiles plotted in Figures 6a, 6b, and 6c. This was expected because of the large differences between the partition coefficients of the feed components (separation factor 5.8 at 60°C) and therefore the wide range of G_{me}/L' values for which the successful separation is effected (see inequalities equation 1.2). The ease of separation of the arklone P/genklene P system is also indicated from the shape of the solute concentration profiles, which have sharp leading and trailing edges. In addition, as is shown in the column to column concentration profile plots, only two to three chromatographic columns were used for this separation, the remaining being partially served to improve the purity of both products. This resulted in high product purities (see Table 1).

The experimental runs 60-21-44-60, 60-21-43-80 and 60-21-43-130 (see Table 1) show the effect of increasing the sequencing rate, while maintaining the value of G_{em}/L' approximately constant by proportionately reducing the carrier gas flowrate. As the sequencing interval was extended from 60 to 130, with a corresponding reduction in the carrier gas flowrate, G_a, from 13.3 to 6.2 cm^3s^{-1}, the concentration of Arklone P and Genklene P more than doubled (see Figures 7a, 7b, 7c). However, these solute concentration changes were not severe enough to affect the performance of the sequential unit. Thus, the shape of the concentration profiles remained the same throughout these runs, with sharp leading and trailing edges, while the degree of overlap of the two solute profiles was always retained within two or three column-lengths around the feed point.

The separating capabilities of the SCCR-2 unit have been further examined by selecting the more difficult system methyl chloroacetate/ethyl lactate (separation factor about 1.5). Three experimental runs were performed to show the effect of apparent gas to liquid rate ratio on the performance of the sequential unit for the separation of this mixture. Details of these experimental runs are given in Table 2 and Figures 8a, 8b, 8c.

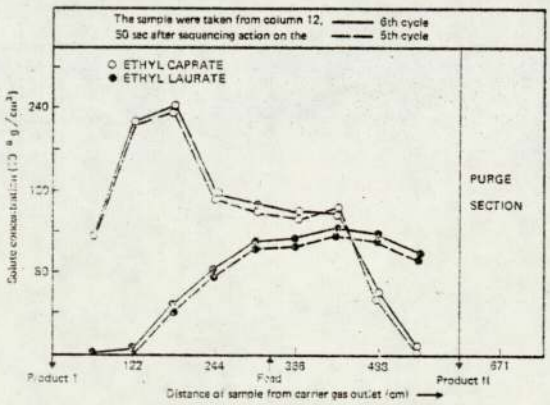

Figure 9c – Concentration profile for run 160-75-113-300

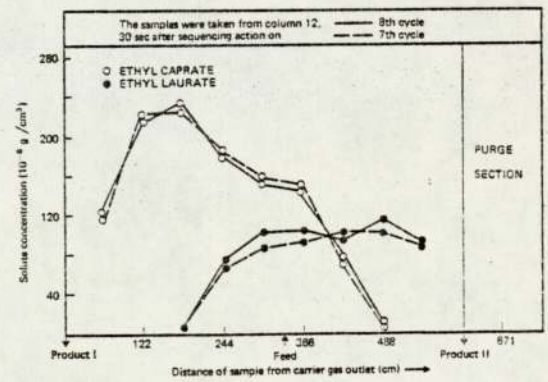

Figures 9d – Concentration profile for run 160-75-101-200.

Increasing the G_{mc}/L' ratio from 378 to 444 by proportionately increasing the carrier gas flowrate, Ga, from 21.3 to 25.0 cm^3s^{-1}, permitted observation of the concentration profiles from one extreme (loss of purity of product II) to the other (product I impure), see Table 2 and Figures 8a, 8b, 8c. For run 105-21-378-300, the values of G_{mc}/L' and G_{min}/L' being quite close to the partition coefficient, K , of methyl chloroacetate, resulted in severe loss of product II purity, the methyl chloroacetate profile covering the entire length of the separating section. Increasing the value of G_{mc}/L' leads to the two components exhibiting a greater preference to move in the direction of the flowing carrier gas stream towards the product I exit port. This resulted in a general reduction in the concentration level of methyl chloroacetate, while that for ethyl lactate increased. Consequently, as run 105-21-413-300 demonstrates the expected increase in product II purity occurs without any loss of product I purity. Further increases of the G_{mc}/L' *ratio*, however results in some loss of product I purity. Thus at a G_{mc}/L' ratio of 444 the ethyl lactate had developed a long leading edge which contaminated the methyl chloroacetate exiting as product I.

Experiments with the fatty acid derivative mixture ethyl caprate/ethyl laurate demonstrated the capability of the SCCR-2 equipment to operate at a temperature of 160°C while achieving product purities of around 99% at throughputs of 50 cm^3h^{-1}. On incheasing the throughput to 75 cm^3h^{-1} product purities declined to beteween 91-94%, (see Table 3). Some of the concentration profiles for this system are shown in Figures 9a, 9b, 9c and they indicate that as the feed throughput was increased from 25-75 cm^3h^{-1} the number of active columns required to produce the separation was increased from 5 to 8. Reducing the switch time from 300 to 200 s and the G_{mc}/L' ratio from 113 to 101 helped to improve the purity of both products.

For each of the above experimental runs, two concentration profiles have been plotted to show the reproducibility of the separation. Thus, column to column concentration profiles at different sequencing cycles, from varying sample points and at a different time after the sequencing action, were recorded for both the arklone P/genklene P and methyl chloroacetaete/ethyl lactate systems (Figures 6c, 7a, 7b, 8a, 8c). In particular, Figure 7b shows that the profiles determined from the same sample point are quite reproducible. This establishes the fact that the pseudo-steady state condition is achieved in the sequential unit. However, one should bear in mind that this column to column concentration profile changes with time during a sequencing interval, due to the semi-continuous nature of operation. Reasonably reproducible profiles were also obtained from differing sample points (see Figures 6c, 7a, 8a and 8c), which suggests well matched chromatographic columns in the sequential unit. However, it is expected, owing to the column to column variations in bed packing characteristics, that when the unit is operataed at conditions close to its separating limits the concentration profiles obtained from differing sample points would be less reproducible.

Conclusions

The sequential counter-current mode of continuous chromatography has been successfully applied to G.L.C. separations at temperatures of up to 160°C. Economic considerations dictated the design of the SCCR-2 equipment developed for this study which consisted of 12 columns, each 61 cm long and 2.54 cm in internal diameter. Higher throughputs could be achieved by using columns of larger diameter, while an increase in the separating capabilities of the unit can be achieved by simply increasing the length of the columns and/or the number of columns.

For the separation of Arklone P/Genklene P, product purities in excess of 99.8% were obtained at feed-rates of 21 cm^3h^{-1} under various operating conditions. The performance of the SCCR-2 unit for this feed mixture has shown very little sensitivity to column conditions within the defined theoretical limits for sucessful separation (see inequalities Equations (1) (2).

The initial separation studies with the more difficult system of methyl chloroacetate/ethyl lactate demonstrate the capability of the sequential unit to separate the mixture into two pure products at feed rates of 21 cm^3h^{-1} and an operating temperature of 105°C.

The continuous separation of ethyl caprate/ethyl lauratee (separation factor (1.44)) at 160°C is the highest temperature recorded so far at which successful separations have been achieved with this equipment. At throughputs of 50 cm^3h^{-1} product purities were around 99% while at 75 cm^3h^{-1} purities decreased to about 94%.

Acknowledgment

Dr. B. Jones of the Mechanical Engineering Department, Birmingham University for assistance in the design of the pneumatic valves used on the equipment.

Nomenclature

f = solute mixture feedrate.
G = gas phase volumetric flowrate in the main separating section of the sequential unit.
G_a = gas phase volumetric flowrate measured at ambient conditions.
G_{mc} = gas phase volumetric flowrate measured at mean column pressure.
G_{min} = gas phase volumetric flowrate at the column inlet
G_{max} = gas phase volumetric flowrate at the column outlet.
I_s = the length of a sequencing interval.
J_3^2 = correction factor for gas phase compressibility.
K^∞ = partition coefficient at infinite dilution.
L' = apparent liquid phase volumetric flowrate in the sequential unit.
P = pressure
P_a = ambient pressure.
S = volumetric gas flowrate in the purge section of the sequential unit.
S_a = volumetric purge gas flowrate measured at ambient conditions.
S_{mc} = volumetric purge gas flowrate measured at mean purge column pressure.

θ = temperature in °C
θ_a = ambient temperature in °C

References

(1) Barker, P.E., "Preparative Gas Chromatography", Zlatkis, A., Ed., Wiley-Interscience, London, 1971, p. 325.
(2) Barker, P.E., Knapman, C.H. (Editor), Developments in Chromatography, Applied Science Publishers, London (1978).
(3) Conder, J.R., "New Developments in Gas Chromatography", Purnell, J.H. Ed., Wiley-Interscience, New York, 1973, p. 137.
(4) Sussman, M.V. and Rathore, R.S., Chromatographia 8, 55 (1975).
(5) Rendell, M., Process Eng., 66 (April 1975).
(6) Barker, P.E. and Deeble, R.E., Chromatographia 8, 67 (1975).
(7) Barker, P.E., and Critcher, D., Chem. Eng. Sci. 13, 82 (1960).

(8) Barker, P.E., and Lloyd, D., Symposium on "The Less Common Means of Separation", 1963, Inst. Chem. Eng., London, 1964, p. 68.
(9) Barker, P.E. and Huntington, D.H., J. Gas Chromatogr. 4, 59 (1966).
(10) Scott, R.P.W., "Gas Chromatography 1958", Desty, D.H. Ed., Butterworths, London, 1958, p. 189.
(11) Fitch, G.R., Probert, M.E. and Tiley, P.F., J. Chem. Soc., 4875 (1962).
(12) Schultz, H., "Gas Chromatography 1962", Van Swaay, M. Ed., Butterworths, London, 1963, p. 225.
(13) Berg, C., Chem. Eng. Prog. 47 585 (1951).
(14) Sussman, M.V., CHEMTECH, 260 (Apr. 1976).
(15) Barker, P.E. and Huntington, D.H., Dechema Monographien, 62 153 (1969).
(16) Barker, P.E. and Al-Madfai, S., J. Chromatogr. Sci. 7, 425 (1969).
(17) Barker, P.E., Barker, S.A., Hatt, B.W. and Somers, P.J., Chem. Proc. Eng. (London) (1), 52, 64 (1971).
(18) Barker, P.E., Hatt, B.W. and Williams, A.N., Chromatographia 7, 377 (1977).
(19) Barker, P.E. and Deeble, R.E., British Patent 1,418,503 and U.S. Patent 4,001,112.
(20) Barker, P.E. and Deeble, R.E., Anal. Chem. 45, 1121 (1973).
(21) Deeble, R.E., Ph.D. Thesis, Univ. Aston, Birmingham (1974).
(22) Szepesy, L., Sebestyen, Sz., Feher, I. and Nagy, Z., J. Chromatogr. 108, 285 (1975).
(23) Broughton, D.B., Chem. Eng. Prog. 64, 60 (1968).
(24) Broughton, D.B., Nenzil, R.W., Phasris, J.M. and Brearly, C.S., Chem. Eng. Prog. 66, 70 (1970).
(25) Bell, D.M., Ph.D. Thesis, Univ. Aston, Birmingham (1977).
(26) Barker, P.E. and Bell, D.M., paper submitted for publication.
(27) Liodakis, S.E., Ph.D. Thesis, Univ. Aston, Birmingham (1977).

Manuscript received January 30, 1978; accepted for publication November 3, 1978.

★ ★ ★